Experimental myocardial infarction : a proteomics point of view

Experimental Myocardial Infarction:

A Proteomics Point of View

Experimental Myocardial Infarction: A Proteomics Point of View

Thesis, Universiteit Maastricht, Maastricht, The Netherlands
ISBN-10: 90-9019992-6
ISBN-13: 9789090199924

Printed by Claes Printing
Cover designed by Bruno Vermeulen

Experimental Myocardial Infarction:

A Proteomics Point of View

PROEFSCHRIFT

ter verkrijging van de graad van doctor
aan de Universiteit Maastricht,
op gezag van de Rector Magnificus,
Prof. mr. G.P.M.F. Mols
volgens het besluit van het College van Decanen,
in het openbaar te verdedigen
op woensdag 7 december 2005 om 16.00 uur

door

Tijl De Celle

geboren op 16 mei 1974 te Asse (België)

Promotor:

Prof. dr. J.F.M. Smits

Copromotor:

Dr. B.J.A. Janssen

Beoordelingscommissie:

Prof. dr. E.C.M. Mariman (voorzitter)
Prof. dr. W.A. Buurman
Prof. dr. H.J.G.M. Crijns
Prof. dr. M.J.A.P. Daemen
Prof. dr. D.J.G.M. Duncker (Universitair Medisch Centrum Rotterdam)

Financial support by Pfizer Belgium for the publication of this thesis is gratefully acknowledged.

Table of contents

Abbreviations

AAR: area at risk
ACE: angiotensin-converting enzyme
ADH: alcohol dehydrogenase
AK: adenylate kinase
AM(D)(T)P: adenosine mono-(di-)(tri-) phosphate
ANOVA: analysis of variance
AW: anterior wall
AWTd(s): anterior wall thickness in diastole (systole)
AZAN: azocarmine anilineblue

BPV: blood pressure variability
BrdU: 5-bromo-2-deoxyuridine
BW: body weight

CHAPS: 3-(3-(cholamidopropyl)-dimethylammonio)-1-propanesulfonate
CID: collision-induced dissociation
COMT: catechol-O-methyltransferase
C(P)K: creatine (phospho) kinase
CX: circumflex

DCM: dilated cardiomyopathy
2-DE: 2-dimensional gel electrophoresis
DIGE: 2-D difference gel electrophoresis
DMTU: dimethylthiourea
DNA: deoxyribonucleic acid
DP: developed pressure
DSP: dual specificity phosphatase
DTT: dithiothreitol

Ec: extracellular
ECG: elektrocardiogram
EDP: end diastolic pressure
ED(S)V: end diastolic (systolic) volume
EF: ejection fraction
ER: endoplasmic reticulum
ESI: electrospray ionisation

$FADH_2$: flavin adenine dinucleotide, reduced form
FS: fractional shortening

GAPDH: glyceraldehyde phosphate dehydrogenase
dGM(T)P: dihydroxyguanosine mono(tri)phosphate
GSH: reduced glutathione

GSK: glycogen synthase kinase
GR: glutathione reductase
GSSG: oxidized glutathione

HIF: hypoxia inducible factor
Hint: histidine triad nucleotide binding protein
HNE: hydroxynonenal
hnRNP: heterogeneous nuclear ribonucleoprotein
HPLC: high performance liquid chromatography
HR(V): heart rate (variability)
HSA: human serum albumin
HSP: heat shock protein

ICAM: intracellular adhesion molecule
IEF: isoelectric focusing
i.m.: intramuscularly
IPG: immobilised pH gradients
i.p.: intraperitoneally
IR: ischaemia-reperfusion
IS: infarct size
ISLAND: Infarct Size Limitation: Acute N-acetylcyteine Defense
i.v.: intravenously

JNK: jun-kinase

LA: left atrium
LAD: left anterior descending coronary artery
LC: liquid chromatography
LDH: lactate dehydrogenase
LDL: low density lipoprotein
LOX: lipoxygenase
LVAd(s): left ventricular area in diastole (systole)
LV((E)D(S)P): left ventricle ((end) diastolic (systolic) pressure)
LVIDd(s): left ventricular internal cavity diameter in diastole (systole)
LW: lung weight

MALDI: matrix assisted laser desorption ionisation
MAP: mean arterial pressure
5-MCA-NAT: 5-methoxy-carbonylamino-N-acetyl-tryptamine
MCP: monocyte chemoattractant protein
MDA: malondialdehyde
MHC: myosin heavy chain
MI: myocardial infarction
MIP: macrophage inflammatory protein
MLC: myosin-regulatory light chain

MMP: matrix metalloproteinase
monoHER: 7-monohydroxyethylrutoside
MPG: N-(2-mercaptopropionyl)-glycine
MPO: myeloperoxidase
M_r: molecular weight
MS: mass spectrometry
MS/MS: tandem mass spectrometry

NAC: N-acetylcysteine
NAD(P): nicotinamide adenine dinucleotide (phosphate)
NCBI: National Center for Biotechnology Information
NF-κB: nuclear factor-κB
(e-)/(h-)/(i-)/(mt-)/(n-)NO(S): (endothelial-)/(human-) (inducible-)/ (mitochondrial-) nitric oxide (synthase)

PDH: pyruvate dehydrogenase
PE(G): polyethylene glycol
PARP: poly-(ADP-ribose) polymerase
PI: permanent ischaemia
pI: isoelectric point
PKC: protein kinase-C
PMN: polymorphonuclear neutrophils
PTCA: percutaneous transluminal coronary angioplasty
PTM: post translational modifications
PUFA: poly unsaturated fatty acids
PW: posterior wall
PWTd(s): posterior wall thickness in diastole (systole)

(m)RNA: (messenger) ribonucleic acid
ROS: reactive oxygen species
RPP: rate pressure product

SAP: serum amyloid P-component precursor
s.c.: subcutaneously
SD: standard deviation
SDS(-PAGE): sodium dodecyl sulphate (-polyacrylamide gel electrophoresis)
S.E.M.: standard error of mean
(ec-)(h-)/(r-)SOD: (extracellular-) (human-)/(recombinant-) superoxide dismutase
SV: stroke volume

TAC: transverse aortic constriction
TFA: trifluoracetate
TIMP: tissue inhibitor matrix metalloproteinase
(c)Tn: (cardiac) troponin
TOF: time of flight

tPA: tissue plasminogen activator
TTC: triphenyltetrazoliumchloride
TUNEL: terminal transferase dUTP (deoxyuridine triphosphate) nick-end labeling

UCH: ubiquitin carboxyl-terminal hydrolase

VCAM: vascular cell adhesion molecule
VW: ventricular weight

Wnt: Wint

Chapter 1

General introduction

The general introduction of this thesis is divided into four separate parts. The first part discusses the structural and functional adaptations of the heart after myocardial infarction in the mouse (published in the handbook "The Physiological Genomics of the Critically Ill Mouse" [1]). In the second part the focus will be on oxidative stress and antioxidant therapy related to cardiac ischaemia and reperfusion. In the third part, the application of proteomics particularly in the field of cardiovascular research will be discussed. Finally, in the fourth part, the aims of the present thesis are outlined.

1. Structural and functional adaptations of the heart after coronary artery ligation in the mouse

1.1. Introduction

Despite advances in the treatment of myocardial infarction (MI), congestive heart failure secondary to infarction continues to be a major complication. In Western societies heart failure is becoming a pandemic disease for which the current treatment is still symptomatic rather than curative [2]. Developing an effective therapy for heart failure is a challenging assignment for many research groups. Mouse models are increasingly used in this research quest, because modification of the genome is relatively easier than in any other mammal. However, due to the small size of the mouse, many techniques had to be scaled down and refined. In the past 5 years, this process has been largely concluded. Sophisticated tools, including non-invasive echocardiography [3-10] and magnetic resonance imaging [11, 12] are available now to examine the molecular mechanisms underlying heart failure in mouse models or to test the efficacy of novel interventions.

With exception of some inbred strains [13, 14], mouse strains do not develop heart failure spontaneously. Murine cardiac dysfunction is usually experimentally induced by toxic or pharmacological agents [15, 16], viral infections [17], surgical interventions [18], and genetic modifications. In these genetic models one or more genes that are crucial for cardiac performance are disrupted [19-21]. Alternatively, cardiac function is altered by overexpressing genes that are placed under control of cardiac specific promoters [15, 22]. There is a variable degree to which these genetic models reflect the pathogenesis and pathophysiological characteristics of human heart failure. Some interfere dramatically with cardiac growth and development and cause the death of the animal *in utero* or soon after birth. In other models the genetic modification does not lead to any obvious cardiac malfunctioning under normal conditions. However, cardiac dysfunction becomes apparent when the heart is challenged to increase its work load [23, 24]. Cardiac stress is often imposed by a surgical procedure in which the aortic arch between the carotid arteries is narrowed, the so-called TAC (transverse aortic constriction) procedure. The progression of left ventricular hypertrophy following TAC has been described in detail by Liao *et al.* [5]. However the TAC model is only to a minor extent associated with cardiac ischaemia. To mimic the predominant ischaemic nature of human heart failure, many research groups make use of the so-called MI (myocardial infarction) model. In this model

ischaemia is induced by permanent ligation of the left anterior descending (LAD) coronary artery of the mouse heart.

The aim of this section is to describe some general and technical aspects of the development of the mouse MI model (section 1.2.). In addition, we will summarize the structural and functional changes that occur over time after ligation of the LAD in the mouse (section 1.3. and 1.4.). Finally it is discussed to which extent this mouse MI model is suitable for studying heart failure in humans (section 1.5.).

1.2. General and technical aspects

To our knowledge the mouse MI model has been described first by Kogan *et al.* in 1977 [25]. In this paper the authors describe also the TAC procedure as well as the banding of the apex of the heart to produce cardiac aneurysms. Because the paper is written in the Russian language and the mouse model was not popular at that time, this publication did not receive much attention. Ten years later Japanese researchers reported the occurrence of spontaneous infarctions in male F1 hybrid mice of the NZW x BXSB strain [13, 14]. The incidence of spontaneous MI was 45 % at the age of 24 weeks and in a few cases dilated cardiomyopathy was observed. However, in such affected animals, the infarct size was generally smaller than 10 % of the ventricular area. As we will discuss later, the size of the infarcted area is probably too small to affect cardiac output and the development of obvious heart failure. This particular mouse model proved to be lupus-prone and is currently used to study the involvement of auto-immune factors in this disease.

Paralleling developments in genomic research, the mouse MI model was rediscovered in the early nineties and in 1993 the first non-invasive echocardiographic description of murine cardiac function following MI appeared [6]. From then on the number of publications on this model has been ever increasing, rendering about 200 publications in the year 2004. (To achieve the latter number PubMed was searched using the keywords "myocardial ischaemia" or "myocardial infarction" and (mice or mouse)). About 2/3 of the studies that make use of this model focussed on mechanisms of ischaemia-reperfusion, while about 1/3 examined cardiac remodelling following permanent occlusion of the LAD.

Figure 1 depicts the *in vivo* murine coronary vasculature after loading the blood with a fluorochrome. Both the LAD and circumflex (CX) are clearly visible. When the thoracic cavity is opened one can usually, under microscopic view, identify the LAD on the anterior epicardial side. The branching point of the LAD and CX arteries, however, is not directly visible because it is mostly covered by the left atrium. In our experience mice do not survive the coronary occlusion when the ligature is placed too high and includes both the LAD and CX. When the LAD is ligated below the location where the CX branches, the average survival rate is about 60-70 %.

In our experience the outcome of the surgical intervention does not depend upon the type of anaesthesia that is used. We have performed the ligation of the LAD under pentobarbital [18, 20, 26], ketamine/xylazine [23, 26], or isoflurane.

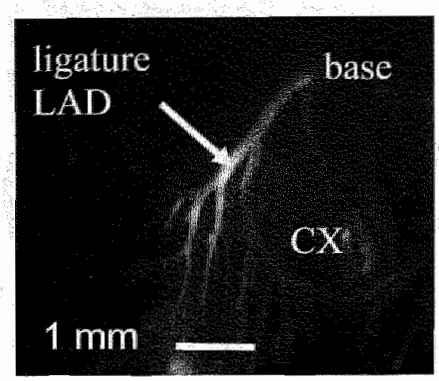

Figure 1: Photograph of the coronary arteries of a mouse heart after injection of a fluorochrome. The left anterior descending (LAD) and circumflex (CX) are indicated. Myocardial infarction is induced by ligation of the LAD under its branching point with the CX artery.

Following the surgical intervention under isoflurane, mice wake up within minutes after the volatile anaesthetic is withdrawn. With pentobarbital, mice may remain sedated for prolonged periods (up to 3-4 hours). Generally, the recovery from surgery improves when the anaesthetic period is kept to a minimum. However, in this particular case, the prolonged sedative period may prevent the occurrence of cardiac arrhythmias or other complications that may arise from this intervention. After surgery mice are kept for 24 hours in a special recovery room with the ambient temperature set at 30 °C. They are inspected regularly and positive pressure respiration is applied if necessary. When needed additional oxygen is added and a two-lead surface ECG is made for continuous inspection. In our hands, i.v. injection of local anaesthetics such as lidocaine does not seem to improve survival. Analgaesic agents such as buprenorphine should be administered with care after coronary artery ligation. In our experience, s.c. injections of buprenorphine (at recommended doses of 2 mg/kg) at the time the mice are still deeply anaesthetized, depresses breathing, worsens their condition and decreases survival rate. Therefore additional analgaesic treatment is started when mice begin awaking from anaesthesia.

When the LAD is ligated at the indicated place about 40-60 % of the left ventricular area becomes ischaemic. If reperfusion follows after 30 minutes of ischaemia, part of the area at risk (AAR) will recover spontaneously. However, about 20 % of the left ventricular area is affected chronically [27]. The longer the ischaemic period, the larger the infarcted area will become, reaching up to 50 % of the left ventricle following permanent ischaemia. In ischaemia-reperfusion protocols, the infarct size is not only dependent upon the architecture of the coronary arteries and duration of the ischaemic period, but also upon many experimental factors. One of these is body temperature. If body temperature is not maintained during surgery the hypothermia may protect against ischaemic damage and remaining infarct sizes will be much smaller [28]. Besides temperature, many more factors have been described that act as a preconditioning factor and limit infarct size [29].

1.3. Structural and histological aspects

An acute occlusion of a mouse coronary artery leads to rapid apoptosis and necrosis in the infarcted part of the heart [30]. This evokes a wound healing process which starts with an early inflammatory response, in which neutrophylic granulocytes migrate into the infarcted area [27]. Hence, the inflammatory response is followed by the formation of granulation tissue, which is rich in inflammatory cells, (myo-) fibroblasts and small blood vessels [19]. This process starts at the border zone of the infarcted area as early as 3 days after MI and is associated with an increase of DNA synthesis, measured as nuclear BrdU incorporation. The enhanced DNA synthesis is mainly detected in non-myocytes (>90 %) and occurs also in non-infarcted areas [18]. During the first two weeks of the wound healing process, cells from the granulation tissue migrate into the infarcted area where necrotic debris is removed by macrophages and replaced by (myo-) fibroblasts and blood vessels. Eventually, the granulation tissue matures into a scar, a process characterized by extensive extracellular matrix deposition and significant cell loss. Enhanced collagen disposition has also been demonstrated in the non-infarcted area [18, 20]. In contrast to the content of the final scar that develops after a dermal wound, the intriguing feature of a cardiac scar is that it still contains myofibroblasts even years after MI [31], possibly to cope with the rhythmic stretch to which the scar is subjected.

The phenotypic result of the wound healing process is depicted in figure 2. Representative sections through murine hearts are shown in comparison to a non-infarcted heart (panel A) to illustrate the gross histological remodelling of the heart at 7 (panel B) and 14 (panel C) days after MI. Note that the infarcts are transmural, located mainly antero-apically and that the septum and right ventricle are spared [18, 32].

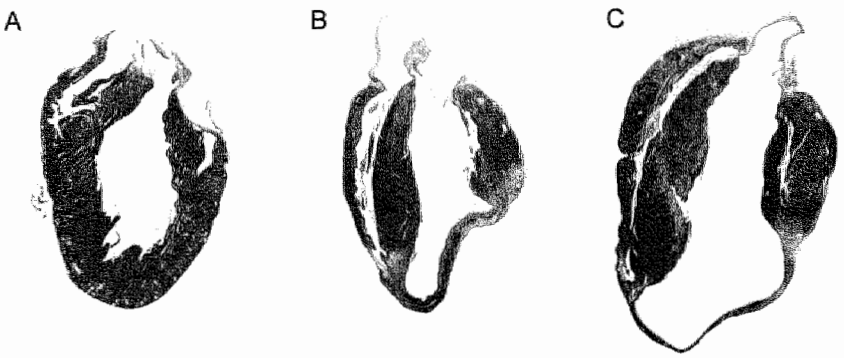

Figure 2: Histological sections of a murine hearts. Panel A shows a non-infarcted control heart. Panel B and C are sections taken 7 and 14 days after ligation of the left anterior descending coronary artery, respectively. Note that during the remodelling process the left ventricular cavity dilates progressively and the spared myocardium hypertrophies. This process is associated with remarkable thinning of the infarcted area. The histological changes are explained in more detail in the text.

The remodelling of the heart leads to enlargement of the left ventricular volume and thickening of the remaining healthy tissue, which is already visible at two weeks after MI. Septal mass was found to be linearly related to the expansion ratio defined as the length of thinned ventricular wall divided by the total endocardial surface [32]. As indicated by echocardiographic measurements the dilatation is nearly completed at 4 weeks after MI [33, 34] but additional dilatation can occur at later stages [3].

The study of the process of infarct healing in animal models allows the monitoring of the effects of either genetic or pharmacological interventions. This has yielded new information regarding the role of matrix metalloproteinases (MMPs), which are involved in the degradation of the preexisting extracellular matrix scaffold and in the migration of the cells into the area of infarction. MMPs form a large family of endoproteinases that can degrade components of the extracellular matrix. Their activity is fine-tuned by endogenous inhibitors, the so-called tissue inhibitors of metalloproteinases (TIMPs). MMPs are present in the normal heart but mainly in their latent form, and are activated in pathological conditions by proteolytic cleavage. The most potent activator of MMPs is plasmin, the activated form of plasminogen. The generation of plasmin is controlled by the balance between plasminogen activators and plasminogen activator inhibitors [24].

Several studies have demonstrated the importance of the plasminogen system in infarct healing. In mice lacking the plasminogen gene, infarct healing was virtually abolished. Inflammatory cells were found to be unable to migrate into the infarcted myocardium and no dilatation of the infarct area was observed. The gelatinolytic activity of MMP-2 and MMP-9 was depressed in the plasminogen-deficient hearts, suggesting a role of MMPs in this remarkable model [35]. Impaired cardiac healing after MI was also observed in mice lacking urokinase plasminogen activator [36]. Creemers *et al.* found that in mice deficient for TIMP-1 infarct dilatation was augmented and associated with a pronounced hypertrophic response of the viable myocardium [20]. Together, these observations underscore the importance of a balanced activation of the MMP system during infarct healing.

Another aspect of infarct healing that so far has received little attention is the control of cell migration in both space and time, the so-called architectural control of infarct healing. We have identified members of the Wnt/frizzled signal transduction system, known to be involved in the architectural control of the developing Drosophila, to be overexpressed during infarct healing. The overexpression of the frizzled-2 turned out to be confined to the phase of infarct healing where cells migrate in the infarcted area and align parallel with the epi- and endocardial plane. In contrast, no frizzled-2 expression was observed in stationary myofibroblasts [37]. In the mean time, we have observed attenuated infarct healing in mice that were immunized with a peptide fragment of the frizzled-2 receptor [38]. Moreover, overexpression of a soluble frizzled-related protein, which can act as a scavenger for Wnt protein ligands, reduced infarct size and improved cardiac function after MI [39]. Recent data indicate that overexpression of the enzyme glycogen synthase kinase 3-ß (GSK3-ß), involved in the intracellular signaling of frizzled-receptors, can inhibit the development of cardiac hypertrophy [15]. Finally, the involvement of the Wnt/frizzled signaling

transduction system in the neovascularization of the infarcted area has been suggested [40].
The combined findings of these studies suggest a functional role for the Wnt/frizzled cascade in diverse aspects of cardiac remodelling after MI.

1.4. Physiological aspects

Myocardial function has been examined at several time points after infarction using a variety of methods. The findings of these physiological measurements are largely in agreement with what would be expected on the basis of the cardiac structures as depicted in figure 2. Using myocardial contrast echocardiography, hypo- and akinetic ventricular wall segments can already be demonstrated at 30 min and 24 h after MI and are associated with a reduction of the fractional shortening from 45 to 24 % [8, 9]. The magnitude of this effect (of permanent ligation) is comparable to values induced by 30 min of cardiac ischaemia (and 24 h reperfusion) [11, 41]. Scherrer-Crosbie *et al.* found that LV dimensions were already enlarged 24 h after MI when compared to values before surgery. End-diastolic volumes increased from 24 to 33 μl and end-systolic volumes from 10 to 24 μl [8]. Thus, it is not surprising that derived parameters such as stroke volume, ejection fraction, and cardiac output are considerably reduced early after MI [32, 42]. Later after MI when wound healing progresses, cardiac function may somewhat recover. Probably due to dilation of the left ventricle and hypertrophy of the remaining viable cardiomyocytes, stroke volume and cardiac inotropy may somewhat recover. In this respect, Michael *et al.* found that 2 weeks after MI the decrease in ejection fraction was only 25 % whereas the initial decline was 47 % [32]. Four weeks after MI and later, when the dilatation process is more or less completed, cardiac function assessed serially by echocardiography remains however depressed [3, 33, 34]. Values on remaining cardiac function vary considerably. Six weeks after MI or later, the observed decline in fractional shortening ranged from 30 % [7] to 50 % [33] or even more. Reduction in ejection fractions up to 75 % of preoperative values have been reported too [34]. As recently demonstrated part of this variation may be strain- [43] and age-dependent [44].

Functional measurements do not always parallel the histopathological observations after MI in the mouse. For instance Creemers *et al.* found that, despite a 42 % infarct size, the ejection fraction was not reduced 2 weeks after MI [20]. Among the explanations that were given was the remark that the MI procedure may also affect the papillary muscle and lead to mitral regurgitation, which would cause a pseudo-normalization of the left ventricular ejection fraction. The incidence of this phenomenon, however, is currently unknown and should be verified by ultrasound Doppler measurements. In our experience, as verified from histological sections, papillary muscles are largely preserved. In a recent paper, Nemoto *et al.* suggested that pressure volume loops are among the most sensitive methods to document small changes in left ventricular function in mice [45]. In our lab we found that 1 and 3 weeks after MI left ventricular systolic pressure and pressure development (+dP/dt) as measured under basal conditions were reduced by 20-30 % [18]. However, such a reduction in baseline +dP/dt is not consistently found. In some studies that were

conducted in our lab the difference in pressure development became discernible only during stimulation of the heart either with dobutamine or during volume loading [20, 23]. On the one hand, these observations suggest that the mouse heart is apt to compensating large infarcts under basal conditions but fails when it is challenged to increase its working load. On the other hand variations in experimental conditions and variations in genetic background may contribute to the divergent degrees of cardiac dysfunction that are observed in mice.

Although direct left ventricular pressure and volume measurements may belong to the most sensitive techniques that are available, they have the disadvantage that they can only be performed once (terminal measurement) and require the use of anaesthetics. To overcome these hampering factors, we have pursued and validated the feasibility of chronic cardiac output measurements in conscious mice. Using electromagnetic as well as transit time flow probes, which are chronically implanted around the ascending aorta, we are able now to measure ascending aortic blood flow in conscious conditions over prolonged periods of time [26]. For skilled surgeons, the success rate of the procedure is about 70 % in control mice. After MI the success rate is lower and seems to depend more on the physical condition of the mouse rather than on technical aspects. Thus, as is applicable for any intervention after MI, the procedure is associated with some bias towards eliminating mice in which cardiac function is inferior.

Despite this we were able to demonstrate that ascending aortic blood flow was reduced after MI in the mouse. As exemplified in figure 3, peak aortic blood flow reached up to 100 ml/min in an adult intact mouse, but was severely depressed after MI. Neglecting coronary blood flow, the average basal stroke volume determined as the average aortic blood flow per beat, was significantly reduced (in sham-operated mice: 31±7 µl versus 25±4 µl after MI, values are means ±SD, see [26]). Because heart rates were not altered after infarction, average differences in basal cardiac output paralleled those of stroke volume, being 20±4 ml/min in sham-operated and 16±3 ml/min in MI mice (means ±SD). Cardiac work can be increased in conscious mice by volume loading. This is accomplished by constructing a Frank-Starling curve by rapidly infusing i.v. a warmed Ringer's solution (2.5 ml/min during one minute), thereby doubling the blood volume of the mouse [46]. As shown in figure 3, this results in a rise in peak and average aortic blood flow.

The average increase in stroke volume was significantly (P=0.03) greater in sham-operated than in MI mice (10.4±4.5 µl versus 6.1±3.5 µl, see [26]). Surprisingly, heart rate does not increase with volume loading in mice. In the given example even a small reduction is observed, suggesting that the Bainbridge reflex does not play a dominant role in this condition. An alternative method to stimulate cardiac output in conscious mice is the i.v. infusion of dobutamine. Using this tool we observed that heart rate rather than stroke volume increased [46]. At high heart rates above 600 beats/min filling times are probably rate limiting. Georgakoupolus *et al.* demonstrated recently that end-diastolic volumes declined with increasing heart rates [47]. From these observations we learn that the mouse, at least in comparison to humans, who can increase cardiac output by a factor 4, has a limited cardiac reserve (+30 % to 50 %).

Yet, with the chronically implanted flow probes, reductions in stroke volume and cardiac output due to MI can be measured reliably.

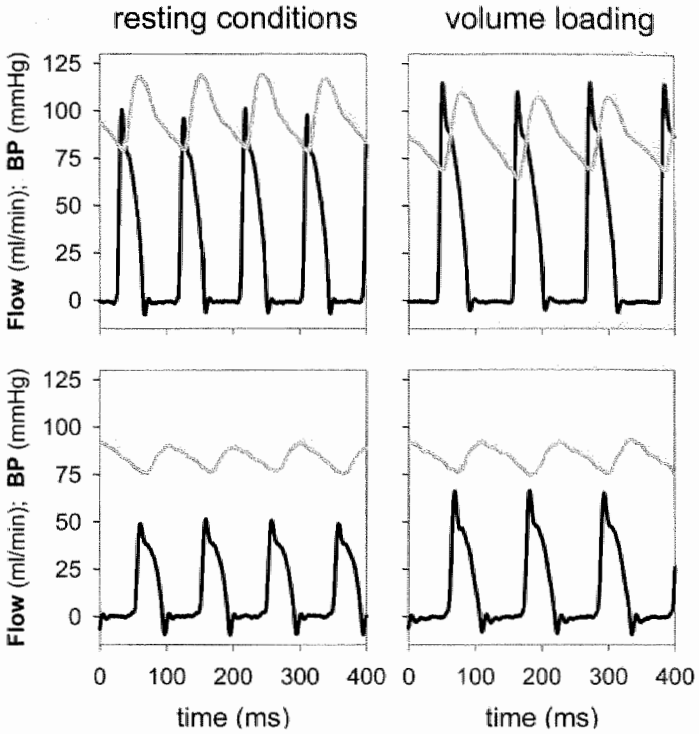

Figure 3: Original tracings of ascending aortic blood flow (thick line) and arterial blood pressure (thin line) in conscious unrestrained mice. The upper two panels show tracings obtained in a control mouse under basic (resting, not moving) as well as stimulated (volume loading) conditions. In the lower two panels the tracings are shown as obtained in a mouse, 5 weeks after MI. Note that average and peak aortic blood flows are reduced in comparison to the control mouse. More details are given in the text.

1.5. Does the mouse MI model reflect human heart failure?

The above mentioned studies clearly demonstrate that the mouse MI model is suitable to study molecular alterations involved in cardiac remodelling and left ventricular dysfunction after ischaemic damage. But, does the MI mouse model reflect human heart failure? For this, in our view, the physiological derangement should include more than left ventricular dysfunction only. However, in our experience relevant characteristics such as congestion and cachexia are only observed occasionally after MI in the mouse and exercise intolerance is difficult to measure. In many studies lung and liver weights after MI are not given or were reported to be unaltered [3, 33, 34]. This suggests that the mouse seems to tolerate a reduced cardiac output over prolonged periods of time. One of the explanations may be that mice are able to

reduce metabolic rate and slip into a torpor-like state to preserve energy during the day. This adaptive mechanism is evoked in mice when homeostasis is threatened by fasting or cold exposure [48] and is associated with very low heart rates (< 200/min) and decreased oxygen consumption. It may be that after MI, mice are more prone to go into such a state of hibernation preserving energy for the remaining periods of activity. Long-term telemetric studies are necessary to validate this hypothesis.

Recently, Gould *et al.* showed that age is an important factor [44]. In most studies MI is induced in relatively young (2-4 months old) mice. However, when coronary artery ligation was performed in 14 months old mice, death rate during a 60 days follow-up period was dramatically higher. Only 9 out of 25 of these older mice survived this follow up period, despite the observation that infarct size was smaller (18 %) than in young (28 %) mice. These observations suggest that additional factors than only left ventricular dysfunction play an important role. The extent of neurohumoral activation as judged from plasma hormones or direct sympathetic nerve measurements is positively correlated to the degree of heart failure in humans. In mice, however, due to the limited volume of blood, neurohormones can not be determined repeatedly after MI. To circumvent this problem we have examined potential alterations in blood pressure variability (BPV) and heart rate variability (HRV) after MI in the mouse. We and others recently validated that also in mice frequency-dependent changes in BPV and HRV are related to altered autonomic control [49, 50].

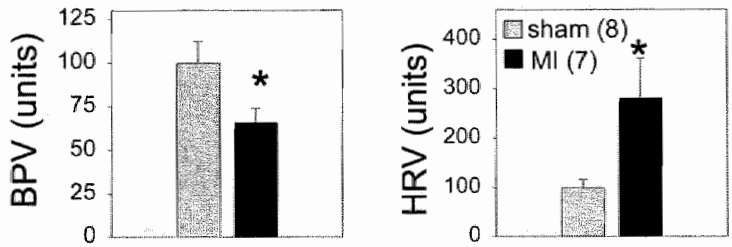

Figure 4: Comparison of indices of blood pressure variability (BPV) and heart rate variability (HRV) in sham-operated and mice 5 weeks after MI. BPV and HRV were determined as cumulative spectral density power obtained in a 0.1-1 Hz frequency band. For comparison, values BPV and HRV were normalized to those obtained in sham-operated controls (100 units).

As shown in figure 4, the index of BPV was significantly lower in MI than in sham-operated mice [51]. This finding corresponds to observations made in heart failure patients. In mice and in patients, the reduction in BPV may be attributed to a declining influence of sympathetic nerves on blood vessel contractions [52], possibly caused by sympathetic desensitization. In contrast, the HRV index increased significantly after MI in the mouse. In heart failure patients, however, HRV is decreased. This apparent discrepancy can be explained by the fact that heart rate

control in the mouse, unlike in humans, is predominantly sympathetically mediated. We have shown before that in intact mice both β-adrenergic blockade as well as ganglionic blockade increase HRV [49]. Thus the increase in HRV after MI may also point to a declining influence of sympathetic nerves on HR control. Because sympathetic desensitization is a manifestation of heart failure in humans, these findings suggest that analysis of BPV and HRV may be useful to monitor changes in autonomic control over time in the mouse after MI.

1.6. Conclusion

Taken together, data suggest that the MI mouse model is suitable to study the molecular aspects of wound healing evoked by cardiac ischaemic damage and that the model has similar characteristics of left ventricular dysfunction and autonomic dysfunction as observed in patients with heart failure. On the other hand, despite the fact that infarct size and dilatation are more pronounced in mice than in patients, other symptoms of heart failure such as congestion, dyspnea or cachexia do not always accompany severe left ventricular dysfunction in mice. This suggests that additional factors make men more prone to developing heart failure after MI, and that the mouse MI model may be less suitable in this respect.

2. Oxidative stress and antioxidant therapy in cardiac ischaemia and reperfusion

2.1. Introduction

Coronary artery occlusion, resulting from atherosclerotic plaques, plaque rupture, or vasospasms, reduces myocardial blood flow. When this is sufficiently prolonged or severe it results in myocardial cell injury, necrosis and apoptosis, ultimately leading to deterioration of cardiac function.

The treatment of coronary artery occlusion involves the use of thrombolytic agents (i.e., tissue plasminogen activator, streptokinase), percutaneous transluminal coronary angioplasty or coronary artery bypass surgery, in order to restore blood flow to the ischaemic myocardium. Reperfusion of an occluded human coronary artery is known to reduce infarct size, to limit deterioration of left ventricular function, and to reduce overall mortality [53, 54]. However, it is recognized that the readmission of oxygenated blood into previously ischaemic myocardium can initiate a cascade of events that will paradoxically produce additional myocardial cell dysfunction and cell necrosis [55-57]. This phenomenon is termed "ischaemia-reperfusion (IR) injury", and has been proposed to be caused mainly by the generation of reactive oxygen species (ROS).

Evidence supporting the role of ROS in myocardial IR injury is fourfold. First, an association has been recognized by demonstrating the generation, accumulation, and release of various ROS and simultaneous changes in the levels and/or activity of endogenous antioxidants [58-66]. Second, exposure of myocardium to exogenous ROS results in myocardial dysfunction that is comparable to that elicited by IR [67]. Third, indirect evidence is derived from studies that have demonstrated *in vivo* or *in vitro* cardioprotective effects of antioxidants following IR (section 2.6). Fourth, the role of ROS in IR injury is directly supported by genetic approaches whereby overexpression or deficiency of genes participating in the antioxidant defence alters the outcome of IR injury (section 2.6).

The following sections will discuss the chemistry of these ROS (section 2.2), their cellular and enzymatic sources (section 2.3), their interactions with biomolecules and the subsequent damage they cause (section 2.4). In addition, the endogenous antioxidant system and its responses to oxidative stress during cardiac IR will be discussed (section 2.5). Furthermore, we will give a detailed overview of the antioxidant interventions in experimental models of cardiac IR (section 2.6). Finally, attention will be paid on the results of antioxidant treatment in the clinical setting of cardiac IR (section 2.7).

2.2. Definition and chemistry of reactive oxygen species and free radicals

Reactive oxygen species and oxygen free radicals, i.e. atoms or molecules with unpaired electrons in their outer orbit, are generated and degraded by all aerobic organisms. They include a number of chemically reactive molecules derived from

oxygen. The cellular production of oxygen free radicals occurs from both enzymatic and non-enzymatic sources. In this case, any electron-transferring protein or enzymatic system can give rise to the formation of ROS as "by-products" of electron transfer reactions (see further section 2.3.).
The superoxide anion $O_2^{\cdot-}$ resulting from molecular oxygen (O_2) by addition of an electron is, in spite of being a free radical, not highly reactive. Catalyzed by superoxide dismutase (SOD), two molecules of $O_2^{\cdot-}$ dismutate to hydrogen peroxide (H_2O_2) and molecular oxygen (table 1).
In a reaction catalyzed by metal ions (Fe^{2+} and Cu^{2+}), the hydroxyl radical ($OH^{\cdot}$) is formed from H_2O_2 (table 1). Hydroxyl radicals are very reactive and interact with almost all molecules found in the cell. Attack of $OH^{\cdot}$ upon biological compounds (lipids, proteins, DNA) induces the formation of carbon-centred radicals that can react with O_2 to give peroxyl radicals ($RO_2^{\cdot}$). Reaction of $OH^{\cdot}$ with thiols can also produce thiyl radicals ($RS^{\cdot}$).
Peroxyl radicals are the main chain-propagating species in the process of lipid peroxidation in membranes. The reactions lead to the generation of lipid hydroperoxides (LOOH) and in the presence of trace amounts of iron to alkoxyl radicals ($RO^{\cdot}$) [68].
Free radicals also include nitric oxide ($NO^{\cdot}$) which is synthesized enzymatically from L-arginine by nitric oxide synthase (NOS). Nitric oxide functions as an intracellular messenger stimulating guanylate cyclase, thereby relaxing smooth muscles e.g. those in blood vessels. Membrane-bound proteins are especially important targets for NO and nitrosylation of proteins is known to regulate enzymatic activity [69]. Peroxinitrite ($ONOO^-$), is formed by the biradical reaction between nitric oxide ($NO^{\cdot}$) and superoxide anion $O_2^{\cdot-}$ (table 1).

Table 1: Free radical formation reactions

$O_2^{\cdot-} + O_2^{\cdot-} + 2H^+ \rightarrow H_2O_2 + O_2$
$O_2^{\cdot-} + H_2O_2 \rightarrow O_2 + OH^{\cdot} + OH^-$ (Haber-Weiss reaction)
$Fe^{3+}/Cu^{2+} + O_2^{\cdot-} \rightarrow O_2 + Fe^{2+}/Cu^{+}$
$Fe^{2+}/Cu^{+} + H_2O_2 \rightarrow Fe^{3+}/Cu^{2+} + OH^- + OH^{\cdot}$ (iron-catalyzed Fenton reaction)
$O_2^{\cdot-} + NO^{\cdot} \rightarrow ONOO^-$

2.3. Sources of reactive oxygen species and free radicals

As mentioned before, the cellular production of ROS occurs from both enzymatic and non-enzymatic sources. In this section we will give a complete overview of these sources and explain the mechanisms of ROS production.

2.3.1. Mitochondria

Within a cell, mitochondria largely contribute to the production of free radicals via the respiratory chain. During normal cellular metabolism the free energy necessary to generate ATP is extracted from the oxidation of NADH and $FADH_2$ by the electron

transport chain (figure 5). Normally the end product of oxygen in this process is water, when oxygen accepts 4 electrons at the cytochrome c oxidase complex (complex IV) (figure 5). However, part of the oxygen is incompletely, i.e. 1 electron instead of 4 electrons, reduced to $O_2^{\cdot-}$ (figure 5).
The major sites for free radical production are at the NADH-coenzyme Q reductase (complex I) and cytochrome c oxidase (complex III) components of the mitochondrial electron transport chain [71-81] (figure 5).
During ischaemia when oxygen is absent to accept electrons, there is an increased ratio of reduced to oxidized components of the electron transport chain. In addition to this, declines in the activities of electron transport complexes I, III, IV, ATP synthase, and adenine nucleotide translocase have been observed during ischaemia and/or reperfusion [82-89].
After reperfusion, when oxygen reaches the mitochondria, it reacts directly with the reduced complexes and consequently generation of reactive oxygen radicals is promoted.

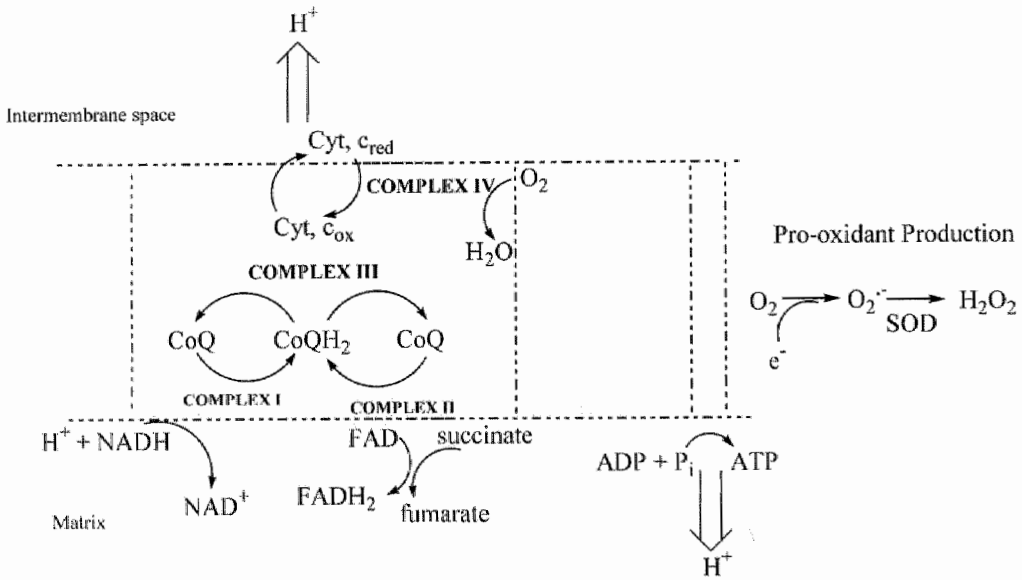

Figure 5: Mitochondrial electron transport and pro-oxidant generation (modified from Sadek *et al.* [70]). Reducing equivalents in the form of NADH and $FADH_2$ produced through the function of the Krebs cycle enter the electron transport chain through complex I and complex II, respectively. Electrons are then transferred through a series of redox couples with the final electron acceptor being O_2, leading to the formation of H_2O. The energy that is liberated in the process of passing electrons to successively lower reduction potentials is utilized to pump protons from the mitochondrial matrix into the mitochondrial intermembrane space. The proton gradient so established is then utilized by ATP synthase to convert ADP and P_i to ATP. By virtue of the redox reactions carried out during electron transport, it is not surprising that this process is a potential source of oxygen derived radicals during normal physiological processes and during disturbances in metabolic homeostasis such as IR.

2.3.2. Xanthine oxidoreductase

Xanthine oxidoreductase has two interconvertable forms. Xanthine oxidase reduces oxygen only. Xanthine dehydrogenase reduces either oxygen or NAD^+, but has greater affinity for the latter. Both forms catalyse the conversion of hypoxanthine to xanthine and xanthine to uric acid, the terminal two reactions of the purine degradation pathway in humans. Tissue damage caused by xanthine-oxidoreductase generated ROS during reperfusion was first hypothesized by Granger *et al.* as shown in figure 6 [90].

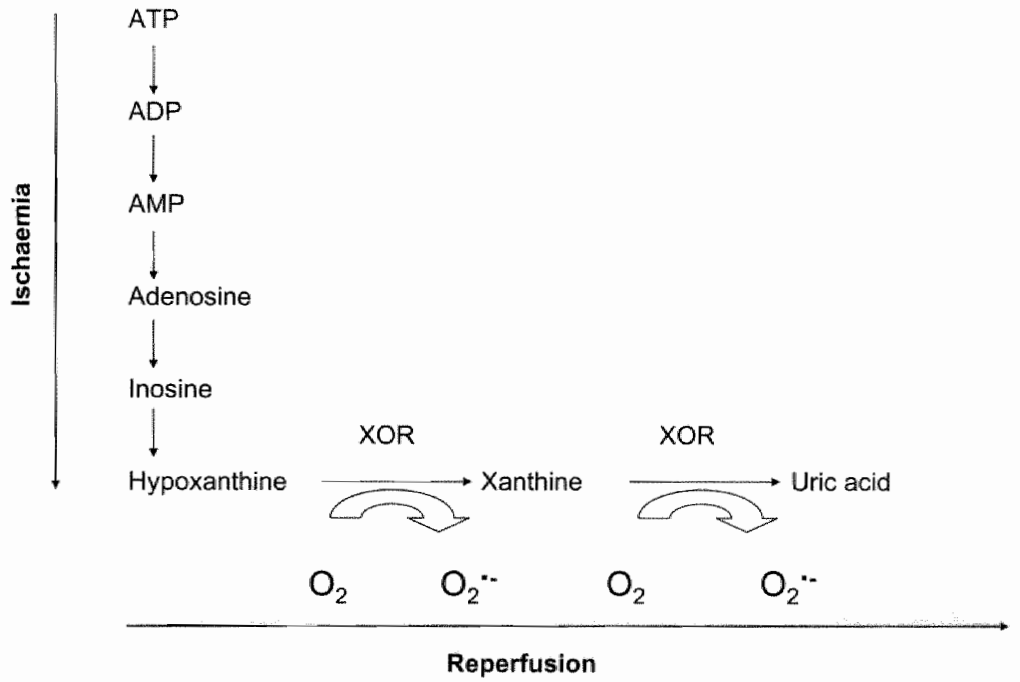

Figure 6: Xanthine-oxidoreductase-generated ROS due to ATP catabolism during ischaemia and increased electron availability on reperfusion (modified from Berry *et al.* [91]).

Xanthine oxidoreductase activity can be found in mammalian liver and small intestine [92] and in other mammalian tissues, including bovine heart [93, 94] and rat heart [94, 95]. The abundance of xanthine oxidoreductase is relatively low in human tissue, but it has been consistently identified in liver, small intestine, endothelial cells and mammary glands [96-98]. Furthermore, most [95, 99-101] but not all [96, 102] studies have identified xanthine oxidoreductase protein and/or activity in the human heart. Subcellular localization methods have demonstrated the presence of xanthine oxidoreductase both in the cytosol and on cell membranes [103].

2.3.3. NADPH oxidase

Neutrophils are involved in the inflammatory response related to the wound healing process after IR and myocardial infarction (section 1.3.). Neutrophils are a primary source of ROS [104, 105], including superoxide anions ($O_2^{\cdot-}$), generated by the activity of the membrane-associated multisubunit NADPH oxidase [106]. The superoxide anion thus formed is rapidly broken down to hydrogen peroxide (H_2O_2) by superoxide dismutase, and then to hydroxyl radicals ($OH^{\cdot}$). The NADPH oxidase system is also present in vascular smooth muscle cells, endothelial cells, and fibroblasts where it is responsive to a variety of neurohormonal stimuli, including angiotensin II, tumor necrosis factor-α, and growth factors [107].
Another source of ROS in neutrophils is the heme-containing enzyme myeloperoxidase, found in azurophilic granules. It converts H_2O_2 to hypochlorous acid (HOCl) in the presence of halides, such as chloride. The bactericidal HOCl oxidizes various amines to toxic chloramines.

2.3.4. Nitric oxide synthase

Nitric oxide (NO) is synthesized endogenously by a family of enzymes called nitric oxide synthases (NOS) which exists in three major isoforms. While neuronal NOS (nNOS, NOS1) and endothelial NOS (eNOS, NOS3) are Ca^{2+}/calmodulin-dependent and constitutively expressed in a wide variety of cells, inducible NOS (iNOS, NOS2) is Ca^{2+} independent and is expressed in cells of the immune system and other cells in response to various stimuli [108].
The ability of some cells to regulate the expression of iNOS allows them to produce large amounts of nitric oxide on demand. Neuronal NOS, eNOS and iNOS are all present in the cytosol. Another NOS, mitochondrial NOS (mtNOS), is exclusively present in the mitochondria [109, 110]. Co-stimulation of superoxide production and mtNOS can result in the formation of high concentrations of the highly reactive and damaging peroxinitrite ($ONOO^-$) [111, 112]. All NOS enzymes function as homodimers. They generate nitric oxide (NO) by a two-step oxidation of the amino acid L-arginine to citrulline and NO via the intermediate compound N-hydroxy-L-arginine [113].

2.3.5. Remaining sources

The endoplasmatic reticulum (ER) is a membrane-bound intracellular organelle that is primarily involved in lipid and protein biosynthesis. Smooth ER, which is devoid of ribosomes, contains enzymes that catalyze a series of reactions to detoxify lipid-soluble drugs and other harmful metabolic products. These include cytochrome P450 and b_5 families of enzymes that can oxidize unsaturated fatty acids and xenobiotics and reduce molecular O_2 to produce $O_2^{\cdot-}$ and/or H_2O_2 [114-116]. Nuclear membranes contain cytochrome oxidases and electron transport systems that resemble those of the ER [116]. It has been postulated that electrons "leaking" from these latter enzymatic systems may give rise to ROS that can damage nuclear DNA *in vivo* [117].

Peroxisomes are membrane-enclosed organelles and are an important source of total cellular H_2O_2 production [118]. They contain a number of H_2O_2 -generating enzymes including glycolate oxidase, D-amino acid reductase, urate oxidase, L-α-hydroxyacid oxidase, and fatty acetyl-CoA oxidase [118]. Peroxisomal catalase utilizes H_2O_2 produced by these oxidases to oxidize a variety of other substrates in "peroxidative" reactions [119]. These types of oxidative reactions are particularly important in liver and kidney cells in which peroxisomes detoxify a variety of toxic molecules (including ethanol) that enter the circulation.
Auto-oxidation of small molecules such as dopamine, adrenaline, flavins, and hydroquinones can also be an important source of intracellular ROS production [116]. In most cases, the direct product of such autooxidation reactions is $O_2^{\cdot-}$.
Phospholipase A_2 hydrolyzes phospholipids to generate arachidonic acid which is a substrate for cycloxygenase-and lipoxygenase (LOX)-dependent synthesis of the four major classes of eicosanoids: prostaglandins, prostacyclins, thromboxanes, and leukotrienes. These synthetic pathways involve a series of oxidation steps that involve a number of free radical intermediates [116]. Arachidonic acid metabolism, particularly involving the LOX pathway, which leads to leukotriene synthesis, has been reported to generate ROS [120-123].

2.4. Oxidative modifications of biomolecules: proteins, lipids and DNA

As mentioned before, ROS increase in concentration upon reperfusion of ischaemic cardiac tissue [124-132]. It is well established that these reactive species can interact with and damage various cellular components, such as proteins, lipids, DNA and consequently contribute to cardiac IR injury. In this section we give an overview of these oxidative modifications and shortly illustrate them, as far as available, with examples in the setting of cardiac IR.

2.4.1. Proteins

As explained in figure 7, oxygen free radicals as for example hydroxyl radicals ($OH^{\cdot}$), induce oxidation of amino acid residue side chains.
Table 2 lists the products formed during oxidation of amino acids that are most susceptible to oxidation.
Even under mild conditions of oxidative stress, particularly induced by peroxinitrite, cysteine residues are targets for S-glutathiolation or disulfide formation and methionine residues are converted to methionine sulfoxide residues [133] (table 2). Several studies have shown oxidation of thiol groups of proteins caused by oxidative stress during cardiac IR [134-136]. For example, glyceraldehyde phosphate dehydrogenase (GAPDH) is a target for S-glutathiolation during IR [135]. GAPDH oxidation is associated with a loss in reduced cysteine status that correlates with the inactivation of this enzyme during IR [135].

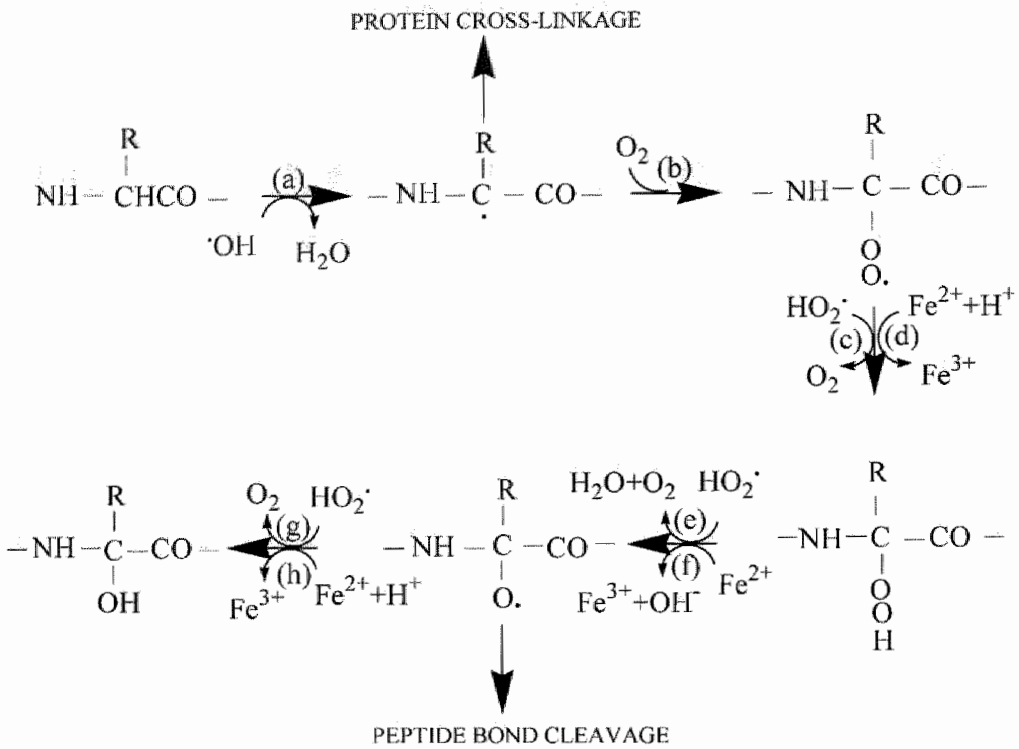

Figure 7: Oxidative attack of the polypeptide backbone (modified from Berlett *et al.*[133]). Reactions are initiated by the $OH^{\cdot}$-dependent abstraction of the α-hydrogen atom of an amino acid residue to form a carbon-centered radical (reaction a). The carbon-centered radical thus formed reacts rapidly with O_2 to form an alkylperoxyl radical intermediate (reaction b), which can give rise to the alkylperoxide (reaction c), followed by formation of an alkoxyl radical (reaction e), which can be converted to a hydroxyl protein derivative (reaction g). Many of the steps in this pathway that are mediated by interactions with $HO_2^{\cdot}$ can be catalyzed also by Fe^{2+} (reactions d, f, h) or by Cu^{2+} (not shown). The alkyl, alkylperoxyl, and alkoxyl radical intermediates in this pathway may undergo side reactions with other amino acid residues in the same or a different protein molecule to generate a new carbon-centered radical capable of undergoing similar reactions. Moreover, in the absence of oxygen, when reaction b is prevented, the carbon-centered radical may react with another carbon-centered radical to form a protein-protein cross-linked derivative. The generation of alkoxyl radicals (reactions e, f) sets the stage for cleavage of the peptide bond by either the diamide or α-amidation pathways [133].

Furthermore, more proteins are substrates for S-thiolation during *in vitro* reperfusion of the ischaemic rat heart. To these belong actin, HSP-27, protein-tyrosine phosphatase 1B, protein kinase Cα, the small G-protein ras, triose phosphate isomerase, aconitate hydratase, M-protein nucleoside diphosphate kinase B, and myoglobin [134-136]. Unfortunately no further implications for cardiac function were investigated in these studies [134-136].

Table 2: Amino acids most susceptible to oxidation (modified from Berlett *et al.*[133]).

Amino acids	Oxidation products
Cysteine	Disulfides, cysteic acid
Methionine	Methionine sulfoxide, methionine sulfone
Tryptophan	2-,4-,5-,6-, and 7-Hydroxytryptophan, nitrotryptophan, kynurenine, 3-hydroxykynurenine, formylkynurenine
Phenylalanine	2-,3-Dihydroxyphenylalanine, 2-,3-, and 4-hydroxyphenylalanine
Tyrosine	3,4- Dihydroxyphenylalanine, tyrosine-tyrosine cross-linkages, Tyr-*O*-Tyr, cross-linked nitrotyrosine
Histidine	2-oxohistidine, asparagine, aspartic acid
Arginine	Glatamic semialdehyde
Lysine	α-Aminoadipic semialdehyde
Proline	2-Pyrrolidone, 4-,5-hydroxyproline pyroglutamic acid, glutamic semialdehyde
Threonine	2-Amino-3-ketobutyric acid
Glutamyl	Oxalic acid, pyruvic acid

Aromatic amino acid residues are among the preferred targets for oxygen radical attack [133]. For example tryptophan residues are readily oxidized to formylkynurenine, kynurenine, and to various hydroxy derivatives; phenylalanine and tyrosine residues yield a number of hydroxy derivatives; histidine residues are converted to 2-oxohistidine, asparagines, and aspartic acid residues [133] (table 2). Additionally tyrosine and tryptophan residues are selective targets for peroxinitrite-dependent nitration [133].

As shown in table 2, direct oxidation of lysine, arginine, proline, and threonine residues may also yield carbonyl derivatives [133]. In addition, carbonyl groups may be introduced into proteins by reactions with aldehydes (4-hydroxy-2-nonenal or malondialdehyde) produced during lipid peroxidation (see section 2.4.2.) [137, 138] or with reactive carbonyl derivatives (ketoamines or ketoaldehydes) generated as a consequence of the reaction of reducing sugars or their oxidation products with lysine residues [139].

The presence of carbonyl groups in proteins has been used as a marker of ROS-mediated protein oxidation. Several sensitive methods for the detection and quantitation of protein carbonyl groups have been developed [140]. For example, it was demonstrated that the cardiac myofibrillar protein actin was oxidized during cardiac IR in an *in vitro* rat model [141, 142]. Antioxidant treatment reduced myofibrillar protein oxidation and subsequently increased the degree of cardiac contractility recovery after IR significantly [142].

As shown in figure 7, oxidative stress also results in the formation of protein-protein cross-linkages. A recent study for example, reported interprotein disulfide interactions between highly abundant cardiac proteins (actin and tropomyosin) following cardiac IR [142].

Furthermore, oxidation of the protein backbone may result in protein fragmentation (figure 7). For example, cleavage of myosin-regulatory light chain (MLC-2) in its functionally important N-terminal site occurred in stunned rabbit myocardium [143]. Treatment with a hydroxyl radical scavenger, *N*-(2-mercaptopropionyl) glycine, prevented this proteolytic truncation of MLC-2 and was associated with preservation of contractile function [143]. Therefore, proteolytic damage to MLC-2, related to the presence of hydroxyl radicals during reperfusion, correlates with myocardial stunning and may contribute to impaired contractility [143].

It has been described that the accumulation of oxidized proteins depends not only on the rate of protein oxidation but also on the activity of the proteasome, a major intracellular proteolytic system which degrades oxidized forms of proteins [144]. It was shown that free radical-derived modifications of the proteasome during *in vivo* cardiac IR inactivated this system and consequently resulted in intracellular accumulation of oxidized proteins which may further impact the outcome of IR [145].

2.4.2. Lipids

Polyunsaturated fatty acids (PUFA) of cell membrane lipids are highly susceptible to peroxidation by oxygen radicals [137]. Not surprisingly, increases in the level of free radicals are paralleled by elevated rates of lipid peroxidation during myocardial ischaemia [146] and reperfusion [147-153]. As shown in figure 8, peroxidation of membrane lipids results in the fragmentation of polyunsaturated fatty acids giving rise to various aldehydes, alkenals, and hydroxyalkenals such as malonaldehyde and 4-hydroxy-2-nonenal (HNE) [137].
Many of these products are cytotoxic when introduced into cells in culture or experimental animals; effects to be mediated in large part by their reactivity towards proteins [137].

HNE, a major product of lipid peroxidation, is thought to be the most reactive of these compounds and is, therefore, an important mediator of free radical damage [137]. HNE reacts with proteins at the sulfhydryl group of cysteine, the imidazole nitrogen(s) of histidine, and/or the ε-amine of lysine [137, 154-157], resulting in enzyme inactivation [137, 138, 158, 159]. For example, formation of HNE-modified proteins was increased by >50-fold after 30 min of ischaemia in rat heart [160]. Furthermore, the concentration of HNE in the perfusate increased upon reperfusion of rat ischaemic myocardium [151].
Mitochondria, a source of free radicals during reperfusion [161, 162], are likely targets of lipid peroxidation and HNE-mediated dysfunction. In an *in vitro* rat model of cardiac IR, Lucas *et al.* demonstrated that the degree of mitochondrial dysfunction during reperfusion was positively correlated with the level of HNE-modified proteins, and, moreover, also with the age of the animals [163]. Furthermore, treatment of intact cardiac mitochondria with HNE reduces NADH-linked respiration [164] mainly via inactivation of α-ketoglutarate dehydrogenase [165]. In addition, adduct formation of HNE with cytochrome-c oxidase during cardiac reperfusion resulted in dysfunction of this respiratory enzyme [88]. Finally, HNE was also shown to contribute to the reduction of β-adrenoceptor function in the heart by oxidative stress [166].

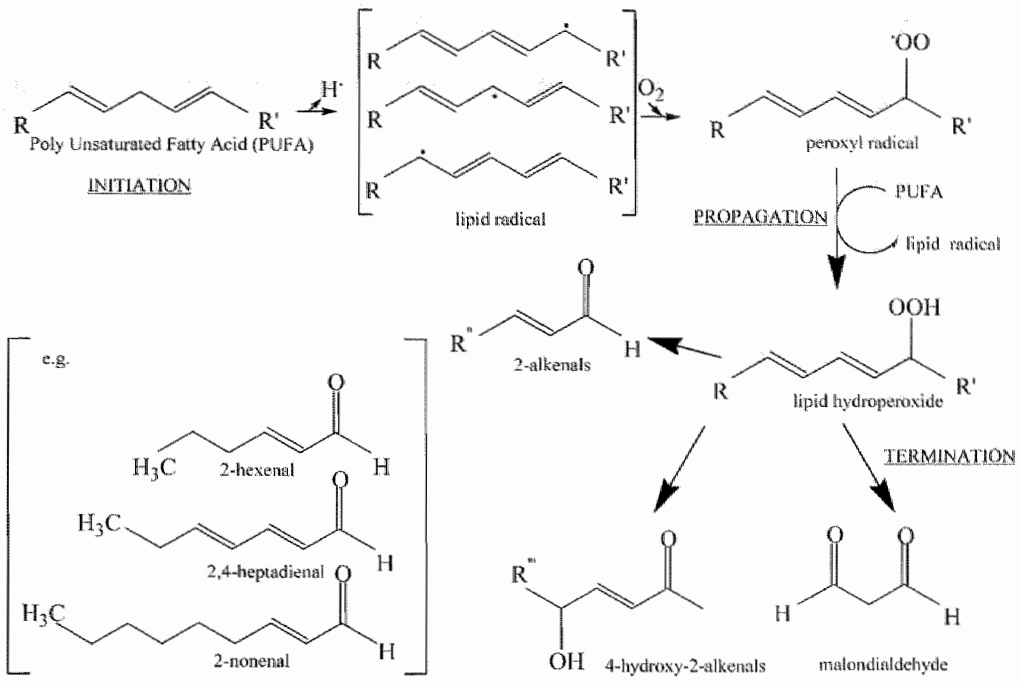

Figure 8: Process of lipid peroxidation and formation of toxic radicals (modified from Berlett *et al.* [133]).

2.4.3. DNA

Reactive oxygen species can also cause oxidative modifications of nucleotides. Specifically, ROS produce 8-oxo-7,8-dihydroxyguanosine triphosphate (8-oxo-dGTP), which modifies the bases in DNA and generates 8-oxo-7,8-dihydro-2'-deoxyguanosine (8-oxo-dG) [167]. As a result, 8-oxo-dGTP is considered a potent mutagenic substrate for DNA replication [168]. Oxidative DNA damage has been detected in cancer and neurodegenerative diseases [167]. However, limited data are available regarding heart diseases, except for an increased level of 8-oxo-dG formation in aged hearts [169] and in superoxide dismutase 2 mutant mice [170].

Increased generation of ROS has been associated with mitochondrial DNA damage and dysfunction in failing hearts after myocardial infarction [171]. The incorporation of 8-oxo-dGTP into DNA is prevented by 8-oxo-dGTPase, which hydrolyzes 8-oxo-dGTP into 8-oxo-dGMP. It was shown that the level of 8-oxo-dGTPase was increased in the mitochondria isolated from post-MI mice hearts as oxidative stress increased. This suggests a preventive mechanism activated against ROS-induced DNA damage in failing hearts [172].

Single-strand DNA breaks, caused by ROS can also activate the nuclear enzyme poly-(ADP-ribose) polymerase (PARP). This initiates an energy-consuming, inefficient cellular metabolic cycle with transfer of the ADP-ribosyl moiety of NAD^+ to protein acceptors and subsequent depletion of NAD^+ and ATP pools [173-178].

Activation of PARP has been demonstrated in *in vitro* and *in vivo* models of cardiac IR [179, 180]. Inactivation of the enzyme significantly limited additional ROS production [181], reduced myocardial necroses and inflammation and preserved ATP pools, restoring myocardial function after IR [182-184].

2.5. Responses of the endogenous antioxidant system during IR

Endogenous antioxidants are present in tissues to minimize injury by ROS. This endogenous antioxidant system is composed of both, antioxidant enzymes, including superoxide dismutase (SOD), catalase and glutathione peroxidase, and non-enzymatic antioxidants including α-tocopherol (vitamin E), ubiquinonone (coenzyme Q10), ascorbate (vitamin C), and glutathione (GSH). The major endogenous antioxidants and their sites of action in cardiomyocytes are presented in table 3.

Table 3: The major endogenous antioxidants and their sites of action in cardiomyocytes (modified from Dhalla *et al.* [185])

Name	Site	Action
Cu,Zn- SOD (SOD1)	cytoplasm	SOD $2\,O_2^{\cdot-} + 2H^+ \rightarrow H_2O_2 + O_2$
Mn- SOD (SOD2)	mitochondria	
Catalase	peroxisomes and mitochondrial membrane	Catalase $H_2O_2 \rightarrow 2\,H_2O + O_2$
Glutathione peroxidase	cytoplasm	Glutathione peroxidase $H_2O_2 + 2GSH \rightarrow 2H_2O +$ GSSG
Glutathione	intracellular	cellular reductant
Coenzyme Q10 (ubiquinone)	cell membrane	redox active electron carrier
Vitamin E (α-tocopherol)	cytoplasm and plasma	breaks lipid peroxidation chain and LDL reaction
β-Carotene (pro-vitamin A)	plasma	inhibits oxidation of LDL
Vitamin C (ascorbic acid)	cytoplasm and plasma	directly as an antioxidant or as a cofactor for vitamin E

In parallel to studies that have investigated the generation of ROS in ischaemic and reperfused hearts, reports have also described the time-dependent changes in levels of endogenous myocardial antioxidants following cardiac IR [186-194]. However, inconsistent results were found in those studies. Upon oxidative stress, some studies reported increased activities of myocardial enzymatic antioxidants [190], while other studies reported decreased activities [186-189, 193]. In addition, both increased content of myocardial non-enzymatic antioxidants [191], and decreased content of myocardial non-enzymatic antioxidants have been reported [149, 186-188, 190, 191, 194].

These contradictions may be due to differences in experimental design of these studies. Therefore, when antioxidant systems are evaluated in the same model, one may arrive at a comprehensive understanding of how the cardiac tissue endogenous antioxidant system operates as an integrated system against free radical injury.

In a series of experiments, Haramaki *et al.* took an integrative approach to study systematic changes in the myocardial endogenous antioxidant defences in the

isolated rat heart during IR [195]. They found that myocardial hydrophilic antioxidants such as ascorbate (vitamin C) and glutathione were easily oxidized to dehydroascorbate and glutathione disulfide, and were released from the myocardium. In contrast, antioxidant enzymes and lipophilic antioxidants remained unchanged under conditions of IR. At the moment of severe oxidative challenge induced by reperfusion with exogenous H_2O_2, the decrease in the hydrophilic antioxidants exacerbated further and was under these conditions also associated with a reduction of the lipophilic antioxidants. These results demonstrate that antioxidants are gradually utilized in a certain order and support the idea that they are hierarchically organized during cardiac IR. These observations can have therapeutic implications in that they lend support to rationalization of combined treatment with different antioxidants for conditions associated with different degrees of oxidative stress.

There is also increasing evidence for the involvement of an antioxidant network during cardiac IR in human. For instance, many studies have demonstrated oxidative modification and release of the myocardial hydrophilic antioxidants in patients undergoing coronary bypass surgery utilizing aortic cross-clamping [196-205]. Ferrari *et al.* were the first to report the formation and release of oxidized glutathione (GSSG) in the coronary sinus following human myocardial IR [205]. The coronary sinus concentration of GSSG was related to the duration of the ischaemic period providing evidence for consumption of GSH in humans subjected to heart surgery [205]. They also found a positive correlation between reduced glutathione levels and delay in postoperative recovery of cardiac function [205].
Data from myocardial biopsies indicate that the cross-clamp period produces also a massive loss of myocardial glutathione [202]. Moreover, reperfusion results in oxidative damage, as evidenced by release of the oxidized form of glutathione (GSSG) in the coronary sinus [202]. These authors have described a relationship between myocardial glutathione and baseline LV function [202].

In patients, Barsacchi *et al.* observed a large variability in basal atrial vitamin E content and a reproducible and substantial decrease in vitamin E content after cardiopulmonary bypass surgery [197]. This was directly related to the aorta cross-clamping duration. Also the net myocardial loss of vitamin E in the first 5 minutes of reperfusion was positively correlated with the total cross-clamp time [199]. Similar observations have been made in humans even following short episodes of myocardial ischaemia as for example during angioplasty [206-208].

We can conclude that in animal models as well as in various clinical settings consumption of endogenous antioxidants occurs during myocardial IR. However, more research is needed to identify the types and time course of this consumption of endogenous antioxidants in order to optimize antioxidant treatment.

2.6. Antioxidant interventions in experimental models of cardiac IR

2.6.1. Antioxidant enzyme interventions

The evidence implicating ROS in the pathogenesis of myocardial IR injury is in part based on *in vitro* and *in vivo* experiments that have examined the ability of free radical

scavengers to alter the injury response. Superoxide dismutase (SOD) and catalase have received most attention in this regard. Table 4 gives an overview of animal studies in which *in vivo* and *in vitro* (Langendorff model) approaches as well as animal cardiomyocytes in culture were used to test for protective effects of antioxidant enzymes against cardiac IR injury induced by ROS. Around 40 publications were found in literature.

The first evaluation of antioxidant enzyme therapy in myocardial reperfusion injury was performed by Jolly *et al.* in an *in vivo* dog model [209]. This study, published in 1984, revealed that the combined administration of SOD and catalase significantly reduced infarct size after 24 hours of reperfusion. Since this report, there have been a number of studies that have also demonstrated a beneficial effect of combined SOD and catalase treatment in experimental models of myocardial IR injury [209-212]. However, an equal amount of studies could not prove such favourable effects of combined treatment on cardiac recovery after IR [213-216].

Also mono-therapy with SOD led to conflicting results with several studies in support of protective effects [213, 217-224] and several studies that could not show protective effects in cardiac IR [225-230].

So far, only two studies have tested effects of mono-therapy with catalase. However they failed to prove protective effects [224, 230].

Two separate groups compared the effects of single therapy with SOD or catalase on cardiac IR injury together in one single study [220, 230]. The study of Werns *et al.* [220] could prove beneficial effects with SOD compared to catalase in a dog model of IR, while the study of Gallagher *et al.* in the same animal model could not show an effect with either substance [230].

The reasons for the discrepancy in results with SOD and/or catalase among these studies are unclear. Among the experimental variables that have been postulated to explain these conflicting results are: 1/ animal species; 2/ general features of the experimental model (e.g. anaesthetized or awake model, open- or closed- chest model); 3/ the presence or absence of critical stenosis; 4/ duration of ischaemia; 5/ duration of reperfusion; 6/ pharmacokinetic considerations; 7/ method used to quantitate infarct size; 8/ inclusion or omission of measurements to control for baseline predictors of infarct size (e.g. collateral blood flow). However, up to now, there is no study available in literature that really proved that one of these factors or a combination is the cause for this discrepancy.

Several studies have tried to increase the plasma half-life of SOD by conjugation with polyethylene glycol (PEG). Also these studies revealed positive [232, 234] and negative [233, 234] results. In the latter studies it has been suggested that PEG-SOD may in fact be too large to gain access into cells, and therefore unable to scavenge the superoxide radicals derived from intracellular sources.

In contrast to PEG-SOD, synthetic low molecular weight SOD-mimetic molecules such as M40403 [235] and SC-52608 [236] have yielded positive results in an *in vivo* rat model and an *in vitro* rabbit model of IR, respectively. This underscores the need to further test the protective effects of low molecular weight SOD mimetics in the setting of cardiac IR.

Intracellular concentrations of SOD have been raised by gene therapy also. With this technique, protective effects of extracellular SOD and Mn-SOD were proven in an *in vivo* rabbit [237] and *in vitro* mouse model [238], respectively. These results may have significant clinical implications for the development of novel cardioprotective strategies in the setting of cardiac IR.

Another experimental strategy that has been used to study the role of ROS in myocardial IR injury is to assess the injury response in mutant mice in which the gene encoding a specific antioxidant enzyme has been either deleted or overexpressed. Transgenic mice in which various isoforms of SOD have been overexpressed [239-242, 244] or deleted [243-245], as well as mice that lack or overexpress glutathione peroxidase [248, 249] or haeme-oxygenase [246, 247] and glutathione peroxidase [248] have been developed and tested in the context of cardiac IR. The relative contribution of the endogenous enzymes, i.e. cytosolic Cu, Zn-SOD versus mitochondrial Mn-SOD, in protecting the heart from oxidative injury after IR was tested *in vitro* by Asimaki *et al.* [245]. They found that Mn-SOD (+/-) mice had a deficit in post-ischaemic myocardial function. Cardiac tissue from these animals showed a higher level of lipid peroxidation compared with wild type mice and Cu, Zn-SOD (+/-) mice. This implies a major role for Mn-SOD compared to Cu, Zn-SOD in protecting the heart against *in vitro* IR injury. However, *in vitro* studies in which Cu, Zn-SOD was overexpressed [241, 242] or deleted [243] showed improved or impaired functional recovery, respectively. This suggests that cytosolic Cu, Zn-SOD might also be involved in the protection against *in vitro* cardiac IR injury. The *in vivo* effect of mitochondrial Mn-SOD was investigated by Jones *et al.* [244]. They demonstrated that cytoprotection resulting from Mn-SOD overexpression in transgenic mice was associated with the preservation of cardiac output and fractional shortening at 7 days after IR. In addition, an *in vivo* protective role for extracellular SOD (Ec-SOD) was proven by Dewald *et al.* who showed less inflammation, less fibrosis and no ventricular dysfunction up to 7 days after IR [240].

Both, glutathione peroxidase and heme-oxygenase protect against IR injury. Transgenic mice that overexpress glutathione peroxidase are resistant to myocardial IR injury [248], whereas glutathione peroxidase knockout mice are more susceptible to myocardial reperfusion injury compared with their wild-type counterparts [249].

Haeme-oxygenase overexpression has a protective *in vitro* and *in vivo* role during reperfusion [246, 247].

Table 4: Overview of effects of antioxidant enzymes on cardiac ischaemia-reperfusion. Several parameters were tested using *in vitro* (Langendorff model) and *in vivo* animal models as well as cardiac cell cultures.

Antioxidant	Species	Model	Time/ Route	Effects	Ref
Antioxidant enzyme application					
1/ Cu,ZnSOD 2/ unmodified SOD	rat	24 h Ischaemia *in vivo*	30 min before Ischaemia i.v. bolus	1/ Cu,Zn- SOD: high tissue concentration, no effect on mortality rate, significant lower IS/LV (dose dependent), attenuated apoptosis ("TUNEL", DNA laddering) 2/ unmodified SOD: low tissue concentration, no effect	[225]
1/ Cu, Zn-SOD 2/ unmodified SOD	rat	72 h Ischaemia cardiomyocytes	time: ?	1/ Cu, Zn-SOD: high uptake in cells, suppressed cell death (24 h), reduced cell damage (LDH release), suppressed apoptosis (nuclear fragmentation, DNA laddering, temporally retained bcl-2 protein level); 2/ unmodified SOD: no uptake, no effect	[226]
Cu,Zn-SOD	pig	30- 90 min Ischaemia/ 24 h Reperfusion *in vivo*	5 min before Reperfusion (for 1h)/ Route: ?	reduction in IS/AAR (not in 90 min Ischaemia/ 24 h Reperfusion group)	[231]
1/ tPA alone 2/ tPA + SOD	dog	acute coronary thrombosis *in vivo*	during Ischaemia (for 20 min)/ i.v.	SOD: no effect on mean time of reflow & reperfusion rate; improved myocardial segmental shortening; significant fewer premature ventricular contractions; preserved relaxation response in coronary arterial rings; reduced platelet aggregation	[217]
SOD	rat	3h Ischaemia/ 2h Reperfusion cardiomyocytes	during Ischaemia and Reperfusion	preservation of cell membrane integrity (LDH concentration) (dose dependent)	[218]
SOD	rabbit	1h Ischaemia/ 1h Reperfusion *in vitro*	15 min before Ischaemia-end of Reperfusion	significant improved contractile performance (developed and resting tension); protection of myocardial ultrastructure	[219]
SOD	rabbit	30min Ischaemia/ 24h Reperfusion *in vivo*	20min before Ischaemia (for 20 min)/ i.v.	no effect on IS/AAR	[227]
SOD	dog	40 min Ischaemia/ 4 days Reperfusion *in vivo*	25 min before Reperfusion- 35 min after Reperfusion intra-atrial	no cardioprotective effect: no influence on IS/LV, lower rate-pressure product	[228]
SOD	dog	90 min Ischaemia/ 6-24 Reperfusion *in vivo*	15 min before Ischaemia- 15 min after Reperfusion intra-atrial/ i.v.	reduced IS/AAR (6 h and 24 h); no difference in leukocyte accumulation	[220]

(continued)

Antioxidant	Species	Model	Time/ Route	Effects	Ref
SOD	pig	60 min Ischaemia /3 h Reperfusion *in vivo*	A/ cardiac vein: 15 min before Ischaemia (for 30 min) B/ intra-atrial: idem	protective effect dependent on route of administration A/ reduction in IS/AAR and IS/LV: significant higher +dp/dt during reperfusion compared to control group, no recovery of ischaemic zone function B/ no reduction in IS/AAR and IS/LV, slight recovery of +dp/dt, no recovery of ischaemic zone function	[221]
Human-SOD	dog	A/ 2 h Ischaemia/ 4 h Reperfusion B/ 2 h Ischaemia /48 h Reperfusion *in vivo*	2 min before Reperfusion (for 45 min) i.v.	no protective effect (both early (4 h) and late (48 h)); no reduction of IS and no improvement of myocardial function (systolic thickening fraction)	[229]
Human-SOD	dog	90 min Ischaemia/ 48 h Reperfusion *in vivo*	at initiation of Reperfusion (for 1h)/ intra-atrial	reduction in IS/LV and IS/AAR, only patchy areas of necrosis, smaller extent of apoptosis ("TUNEL" staining)	[222, 223]
1/ SOD/catalase 2/ rSOD	dog	90 min Ischaemia/ 1 week Reperfusion *in vivo*	5 min before Reperfusion- 1h after Reperfusion intra-atrial	decrease in number of arrhythmic beats/min in the rSOD group (not at later time-points), no reduction IS/AAR, no reduction in the amount of necrosis, no improvement in regional myocardial dysfunction	[213]
1/ SOD 2/ catalase	dog	3 h Ischaemia/ 24 h Reperfusion *in vivo*	15 min before Reperfusion (for 1h)/ Route:?	1/,2/: no reduction of IS/AAR and IS/LV	[230]
1/ SOD 2/ catalase	dog	90 min Ischaemia/ 6 h Reperfusion *in vivo*	15 min before Ischaemia-15min after Reperfusion intra-atrial	1/ SOD: protective effect: reduced IS/LV and IS/AAR 2/ catalase: no protective effect: no reduced IS	[224]
SOD/catalase	rat	30 min Ischaemia/ 120 min Reperfusion *in vitro*	15 min before Ischaemia (for 15min)	reduction of apoptosis (DNA laddering, microscopically), reduced lipid peroxidation (MDA), improved recovery of cardiac function (aortic flow, +dp/dt)	[210]
SOD/catalase	pig	60 min Ischaemia/ 5h Reperfusion *in vivo*	3 min before Reperfusion-1h after Reperfusion intra-atrial	reduced IS/AAR	[211]

(continued)

Antioxidant	Species	Model	Time/ Route	Effects	Ref
SOD/catalase	baboon	2 h Ischaemia/ 22 h Reperfusion *in vivo*	A/ low dose: 1 h (15 min before Reperfusion)/ i.v. B/ high dose: 1 h (15 s before Reperfusion)/ intra-atrial, i.v.	no cardioprotective effect: no influence on IS/LV, no influence on heart rate, mean arterial pressure, left atrial pressure, cardiac output, +dp/dt	[214]
SOD/catalase	dog	90 min Ischaemia /4 h Reperfusion *in vivo*	25 min before Reperfusion, for 60 min/intra-atrial	no reduction of IS/LV or IS/AAR	[215]
SOD/catalase	dog	A/ 6 h Ischaemia/ 6 h Reperfusion B/ 6 h Ischaemia/ 30-48 h Reperfusion *in vivo*	A/ 15 min before Ischaemia- end of Ischaemia B/ idem as (1)-10 min after Reperfusion intra-atrial	A/ reduction IS/LV and IS/AAR; reduced foci of necrosis B/ no reduction in IS/LV and IS/AAR; transmural, confluent area of necrosis, no reduction in inflammation (granulocytes)	[212]
SOD/catalase	dog	90 min Ischaemia/ 4 days Reperfusion *in vivo*	25 min before Reperfusion (for 1 h) intra-atrial	no reduction in IS/LV or IS/AAR	[216]
SOD/catalase	dog	90 min Ischaemia/ 24 h Reperfusion *in vivo*	A/ 15 min before Ischaemia (for 2h) B/ 15 min before Reperfusion (for 1 h) C/ 40 min after Reperfusion (1 h) intra-atrial	A/, B/: reduction of IS/AAR; only patchy distributed necrotic areas C/: no reduction of IS/AAR; transmural extent of myocardial ischaemic injury	[209]
PEG-SOD	dog	A/ 90 min Ischaemia/ 6 h Reperfusion B/90 min Ischaemia/ 4days Reperfusion *in vivo*	A/ 15 min before Ischaemia (for 1 h) B/ 15 min before Reperfusion (during Reperfusion)	A/ reduced IS/AAR; sustained plasma SOD activity for 6 hours B/ reduced IS/AAR; sustained plasma SOD activity for 4 days	[232]

(continued)

Antioxidant	Species	Model	Time/ Route	Effects	Ref
PEG-SOD/ catalase	dog	90 min Ischaemia/ 4 days Reperfusion /*in vivo*	30 min before Reperfusion (for 30 min) intra-atrial	no reduction in IS/LV and IS/AAR; no change in hemodynamic parameters (heart rate, blood pressure, rate-pressure product)	[233]
1/ Lecithinized Cu, Zn-SOD 2/ PEG-SOD 3/ SOD	rat	45 min Ischaemia/ 120 min Reperfusion *in vivo*	5 min before Reperfusion i.v.	similar serum SOD levels in group 1&2 and significant higher than in group 3; significant higher heart SOD tissue level in group 1 compared to group 2&3 1/: reduction in IS/AAR; 2/,3/: no reduction in IS/AAR	[234]
SOD mimetic application					
M40403	rat	30 min Ischaemia/ 60 min Reperfusion *in vivo*	15 min before Ischaemia i.v. bolus	protective effect (reduced IS/AAR, ventricular arrhythmias, mast cell degranulation, lipid peroxidation (MDA), calcium overload, nitrotyrosine, inflammation (MPO activity, ICAM-1, P-selectin)	[235]
SC-52608	rabbit	30 min Ischaemia /45 min Reperfusion /*in vitro*	5 min before Ischaemia- end of Reperfusion	protective effect is dose-dependent; high dose: improved cardiac function (EDP), reduced cell injury (creatine kinase and K^+ release, morphological)	[236]
Gene therapy					
Ec-SOD vector	rabbit	30 min Ischaemia/ 3 days Reperfusion *in vivo*	vector: 3 days before Ischaemia, i.v.; induction: 2h before Ischaemia	reduction of IS/LV and IS/AAR ratio	[237]
Mn- SOD vector and catalase vector	mouse neonatal	5 min Ischaemia/15 min Reperfusion *in vitro*	day -3 before Ischaemia intrapericardial	elevated cardiac SOD and catalase protein levels and activity, reduced contractile dysfunction (peak force, rate of force generation)	[238]
Genetically modified mice					
Mn-SOD overexpression	mouse	*in vitro*: 35 min Ischaemia/45 min Reperfusion *in vivo*: 50 min Ischaemia/ 4 h Reperfusion	not relevant	increased SOD activity in heart tissue; no changes in other antioxidant enzymes (CuZnSOD, catalase, GSH, GR); staining for MnSOD in mitochondria (and cytosol); *in vitro*: higher functional recovery (+dp/dt, LVDP, LVDPxHR), lower tissue damage (LDH release); *in vivo*: reduced IS/LV and IS/AAR	[239]

(continued)

Antioxidant	Species	Model	Time/ Route	Effects	Ref
Ec-SOD overexpression	mouse	15 min Ischaemia/ Reperfusion daily for 3, 5, 7 days/ *in vivo*	not relevant	less chemokine induction (MCP-1, MIP-1β mRNA); less macrophage infiltration; less fibrosis; reduced myofibroblast deposition; no ventricular dysfunction (fractional shortening, anterior wall thickening)	[240]
Human Cu,Zn-SOD overexpression	mouse	30 min- 45 min Ischaemia/ 2 min- 2 h Reperfusion *in vitro*	not relevant	increased expression in both myocytes and endothelial cells; SOD abolished the burst of radical production; 2-fold recovery of contractile function (rate-pressure product); decreased IS/LV; improved recovery of high energy phosphates (ATP, phospho-creatine)	[241]
Human Cu,Zn-SOD overexpression	mouse	35 min Ischaemia/ 45 min Reperfusion *in vitro*	not relevant	increased SOD activity in heart tissue, no change in activity of other antioxidant enzymes (MnSOD,catalase, GSH, GR) or HSP-70,-25, increased staining for SOD in cytosol of endothelial and smooth muscle cells (no increase in cardiomyocytes); improved functional recovery (dp/dt, LVDP(xHR), LVEDP), reduced tissue damage (LDH release)	[242]
1/ Cu,Zn-SOD (-/-) 2/ Cu,Zn-SOD (+/-)	mouse	30 min Ischaemia/ 2 h Reperfusion *in vitro*	not relevant	1/ lower functional recovery (developed force, +dp/dt); no significant difference in coronary flow; higher IS/AAR, tissue damage (CK release) and oxidative stress (hydroxyl radical,MDA) 2/ functional recovery, protective effect (reduced IS/AAR, CK release and oxidative stress)	[243]
1/ MnSOD overexpression 2/ Cu,Zn-SOD (-/-) 3/ Cu,Zn-SOD overexpression 4/ GPx overexpression	mouse	30 min Ischaemia/ 24 h or 7 days Reperfusion *in vivo*	not relevant	1/ MnSOD overexpression: significantly reduced IS/AAR (24 h); improved functional recovery (fractional shortening, cardiac output, anterior wall motion (7 days)) 2/, 3/, 4/: Cu,Zn-SOD -/-, Cu,Zn-SOD overexpression, GPx overexpression: no influence on IS/AAR (24 h), no echocardiographic data available	[244]
1/ SOD1 (+/-) 2/ SOD2 (+/-)	mouse	30 min Ischaemia/ 60 min Reperfusion *in vitro*	not relevant	no compensatory increase in the other SOD isoforms; SOD1 (+/-) group: higher functional recovery (HRx developed pressure, EDP), higher lipid peroxidation compared with SOD2 (+/-) group	[245]

(continued)

Antioxidant	Species	Model	Time/ Route	Effects	Ref
Heme oxygenase-1 overexpression	mouse	*in vitro*: 40 min Ischaemia/ 45 min Reperfusion *in vivo*: 30 min Ischaemia/ 3 h Reperfusion	not relevant	high expression in the heart, labelling in cardiomyocytes; in vitro: higher functional recovery (dp/dt, LVDP(xHR), LVEDP); reduced LDH release; in vivo: reduced apoptosis ("TUNEL")	[246]
Heme oxygenase-1 overexpression	mouse	*in vitro*: 30 min Ischaemia/ 40 min Reperfusion/ *in vivo*: 1 h Ischaemia/24 h Reperfusion	not relevant	increased protein levels of HO-1 in the heart; *in vitro*: improved recovery of contractile performance (LVEDP, left ventricle developed pressure, RPP); *in vivo*: reduced inflammatory response (CD-45 staining), reduced IS/AAR, lower oxidative damage (MAL-2)	[247]
Glutathione peroxidase overexpression	mouse	30 min Ischaemia/20min Reperfusion *in vitro*	not relevant	increased glutathione peroxidase activity in the heart, reduced IS/AAR, lower tissue damage (CK release), higher myocardial contractile recovery (developed force, dF/dt_{max})	[248]
Glutahione peroxidase (-/-)	mouse	30 min Ischaemia/ 2 h Reperfusion *in vitro*	not relevant	lower contractile recovery (developed force, +dp/dt), reduced coronary flow, higher tissue damage (creatine kinase release) and IS/LV ratio in the glutahione peroxidase (-/-) group compared to wild type	[249]

Overall we can conclude that studies with transgenic mice in which endogenous levels of antioxidant enzymes are altered yield more consistent results in support of a role for ROS in myocardial IR injury than animal studies in which antioxidant enzymes were exogenously administrated. This difference may reflect a need for substantial elevations in intracellular antioxidant enzyme levels for protection against cardiac IR, achieved by exogenous administration of antioxidant enzymes.

2.6.2. Interventions with antioxidant agents

Many studies have examined the role of less specific antioxidant interventions in reducing cardiac IR injury. Around 50 publications were found in literature and are listed in table 5. These antioxidants can be grouped into nine different classes, i.e. vitamin C- and E-like antioxidants; polyphenolic compounds; melatonin or structural analogues; cytochrome P_{450}; lipid peroxidation inhibitors; xanthine oxidase inhibitors; glutathione analogues; derivatives of thiourea and pyruvate; and miscellaneous. Their effects are discussed in separate sections below.

Vitamin C- and E-like antioxidants

Vitamin E (α-tocopherol) is a lipid-soluble vitamin which resides in cell membranes and acts physiologically as a free radical scavenger by breaking peroxyradical chain reactions of membrane lipids [250]. Using a model of saline-perfused rabbit heart muscle, Guarnier *et al.* were the first to describe protective effects of α-tocopherol against IR injury [251]. The protection was shown in three ways, including reduced rates of enzyme leakage, some preservation of the endogenous energy-rich phosphate reserves, and the maintenance of mitochondrial respiratory function to near control levels. These *in vitro* protective effects of α-tocopherol were confirmed by Massey *et al.* [252] and Chen *et al.* [253].
Protective effects of α-tocopherol were less obvious *in vivo*. One study proved protective effects [254] while two studies could not [255, 256]. An explanation for these conflicting *in vivo* results is not evident. The achieved myocardial vitamin E levels may be different between studies and depend on the duration, dose, time point or route of administration [255].
In this regard, acute administration of α-tocopherol is not feasible due to its high lipophilicity and slow tissue incorporation [252, 257]. Consequently, vitamin E analogues such as IRFI 042 [258], MDL analogues [259-262] and Raxofelast [263], with less lipophilic character have been developed. These agents showed *in vivo* protective effects in a rat model of cardiac IR. In the case of MDL-73404, reduced infarct size and improved recovery of cardiac output were demonstrated 8 days after reperfusion [259].

Vitamin C was not tested as mono-therapy but only in combination with vitamin E [257]. On this basis no conclusions can be drawn about possible protective effects of vitamin C in cardiac IR.

Polyphenolic compounds

Epidemiological evidence indicates that the consumption of red wine is beneficial in the prevention of coronary heart disease [301, 302]. This beneficial effect has been attributed to the antioxidants present in the polyphenolic fraction of red wine which include phenolic acids, trihydroxy stilbenes, oligomeric proanthocyanidins, and the flavonoids [303-305].
Polyphenols i.e flavonoids (quercetin, flavones, baicalein, purpurogallin, proanthocyanidin) and the trihydroxy-stilbenes (resveratrol and astringinin) have been tested for their ability to reduce cardiac IR injury. The polyphenolic compounds have *in vitro* [264-266, 269-271] as well as *in vivo* [267, 268, 272] cardioprotective effects.
Wu *et al.* found *in vivo* protective effects of the flavonoid purpurogallin which were superior in regard to infarct size compared to the protective effects of Trolox, a vitamin E analogue [267].

Melatonin

Melatonin (n-acetyl-5-methoxytryptamine) is a hormonal product of the pineal gland with a highly lipophilic nature. It has the ability to directly scavenge free radicals and has also been reported to alter the activities of enzymes (as superoxide dismutase and nitric oxide synthase) which improve the antioxidant defence capacity of the organism [306, 307].
During cardiac IR, melatonin has proven *in vitro* protective effects [274-276]. However, *in vivo* protective effects of melatonin as tested in mice and rats, were only present shortly after initiation of reperfusion (2 h) but not at a longer term (6 h and 24 h) [273]. This may be explained by the short half-life reported for melatonin [308]. In addition, these *in vivo* protective effects were dose dependent and not present when melatonin was administered intraperitoneally (i.p.) during reperfusion [273].
In contrast, injection of melatonin directly into the left ventricle right before reperfusion conferred cardioprotection [273]. Therefore, to obtain a protective effect, a certain time is necessary for sufficient uptake of melatonin into the blood circulation after i.p. administration [273].

Cytochrome P_{450} inhibitors

Granville *et al.* demonstrated *in vitro* as well as *in vivo* protective effects of cytochrome P_{450} inhibitors [277]. Chloramphenicol, cimetidine and sulfaphenazole reduced superoxide production and consequently reduced infarct size after IR [277]. This suggests a role for cytochrome P_{450} in the generation of oxidative stress during myocardial IR.

Lipid peroxidation inhibitors

As described before (section 2.4.2.), lipid peroxidation importantly contributes to tissue damage during cardiac IR [309-311]. The experimental compounds U74389G

and U74006F are members of the group of 21-aminosteroids lacking classical glucocorticoid or mineralocorticoid activity. These agents have been termed "lazaroids" [312, 313] and are known as potent *in vitro* inhibitors of lipid peroxidation in a manner similar to vitamin E [279, 312, 313]. They act protective during *in vitro* IR [280]. *In vivo* protective effects for U74389G during IR have been obtained in a heart transplantation model [278] but not in a model of transient coronary artery occlusion [279]. Another lipid peroxidation inhibitor, indenoindole H290/51, diminished infarct size and improved recovery after *in vivo* IR.

Xanthine oxidase inhibitors

As mentioned before (section 2.3), xanthine oxidase is a major potential source of superoxide radicals and plays an important role in the genesis of IR injury. The xanthine oxidase inhibitors allopurinol and its active metabolite oxypurinol were tested in rat and dog models of IR, respectively. Beneficial effects, being a reduction in cardiac tissue damage [283], improved recovery of ventricular function [265, 283], and reduced incidence of arrhythmias were demonstrated shortly after initiation of reperfusion (10-30min). However, long-term protective effects for oxypurinol could not be demonstrated [216].

Glutathione analogues

N-(2-mercaptopropionyl)-glycine (MPG) is a low molecular weight synthetic analogue of glutathione, an important endogenous antioxidant. Studies on potential *in vivo* protective effects of MPG during ischaemia and reperfusion yielded conflicting results. Mitsos *et al.* [104] could prove protective effects after 6 h of reperfusion while others did not [284, 285]. In another study only short-term (3 h) but no long-term protective effects (72 h) [287] of MPG were found. From another set of studies it appeared that protection was dependent on the time point of drug administration [286, 288, 289] and on the duration of the ischaemic period [290]. This may suggest that MPG has only a short duration of action [290].

Table 5: Overview of studies on cardiac ischaemia-reperfusion, in which the effects of antioxidant agents on several parameters were tested using *in vitro* (Langendorff model) and *in vivo* animal models or cardiac cell cultures.

Antioxidant	Species	Model	Time/ Route	Effects	Ref
Vitamin C and E-like antioxidants					
α-tocopherol	rabbit	30 min Ischaemia/ 40 min Reperfusion *in vitro*	20 min before Ischaemia- end of Reperfusion	protective effect (attenuation in: hypoxic-induced rise in resting tension, depletion of ATP/ CP stores, deterioration of mitochondrial function and release in LDH, CPK, lactate)	[251]
α-tocopherol	pig	45 min Ischaemia/ 3 days Reperfusion *in vivo*	for 4 weeks before Ischaemia; oral	increased myocardial vitamin E content; no reduction of IS/AAR; no recovery of cardiac function (dp/dt, regional systolic shortening)	[255]
α-tocopherol	rabbit	60 or 180 min Ischaemia/ 6 h Reperfusion *in vivo*	for 10 days before Ischaemia; oral	reduction of IS/AAR	[254]
α-tocopherol	rat	25 min Ischaemia/ 30 min Reperfusion *in vitro*	for 14 days before Ischaemia; oral	increased myocardial vitamin E content, improved recovery of cardiac function (developed pressure,+/-dp/dt), reduced tissue damage (lower unesterified fatty acid content, reduced increase in tissue Ca^{2+} level, release of LDH)	[252]
α-tocopherol analogs	rabbit	30 min Ischaemia/ 72 h Reperfusion *in vivo*	15 min before Ischaemia/ 5 min before Reperfusion; i.v.	no reduction in IS/AAR	[256]
IRFI 042 (α-tocopherol)	rat	45 min Ischaemia/ 5 h Reperfusion *in vivo*	5 min after Reperfusion; i.p.	reduced myocardial necrosis, improved cardiac output, limited membrane lipid peroxidation, restored endogenous vitamin E and SOD, inhibition of hydroxyl radical formation, reduced inflammatory response (NF-κβ, leucocytes)	[258]
Vitamin E and C	pig	45 min Ischaemia/ 3 days Reperfusion *in vivo*	A/ chronic vit. E before Ischaemia/ acute vitamin C before Reperfusion B/ acute vitamin C and E during Ischaemia; i.v.	A/ reduction in IS/AAR, improved regional systolic function B/ reduction in IS/AAR, no improvement of regional systolic function	[257]

(continued)

Antioxidant	Species	Model	Time/ Route	Effects	Ref
1/α-tocopherol 2/ α-,γ-,-δ-tocopherols	rat	24 h Ischaemia/ 3 h Reperfusion cardiomyocytes	pre-treatment for 30 min	reduced myocyte injury (LDH release), attenuated decrease in SOD activity, reduced upregulation of iNOS expression/activity; mixed tocopherol preparation (α-, -γ, -δ-tocopherol) was much superior to α-tocopherol in myocyte protection	[253]
MDL 73404 (α-tocopherol)	rat	60 min Ischaemia/ 8 days Reperfusion *in vivo*	10 min before Ischaemia (for 90 min)/ i.v.	reduced IS/AAR, recovery of cardiac function (cardiac output, HR), lower mortality during Reperfusion, decreased lipid peroxidation, reduced plasma phosphokinase activity; *in vitro*: recovery of cardiac function (LVSP, +/-dp/dt, coronary flow)	[259]
MDL 73404 (α-tocopherol)	rat	A/ *in vivo*: 1 h Ischaemia/ 30 min Reperfusion B/ *in vitro*: 30 min Ischaemia/ 30 min Reperfusion	A/ *in vivo*: 10 min before Ischaemia- end of Reperfusion/ 30 min before Reperfusion- end of Reperfusion/ i.v. B/ *in vitro*: 20 min before Ischaemia (for 20 min)	A/ reduction in IS/AAR B/ better recovery of ventricular function (+/-dp/dt, HR, LVSP, LVDP)	[260]
MDL 74270 (α-tocopherol)	rat	1 h Ischaemia/ 30 min Reperfusion *in vivo*	10 min before Ischaemia- end of Reperfusion; i.v.	reduced IS/LV, reduced plasma CPK activity	[261]
1/ MDL 74270 2/ MDL 73954 (α-tocopherol)	rat	60 min Ischaemia/ 30 min Reperfusion *in vivo*	10 min before Ischaemia- end of Reperfusion; i.v.	reduced IS/AAR, reduction in tissue damage (CPK release, only at highest dose)	[262]
Raxofelast (α-tocopherol)	rat	1 h Ischaemia/ 6 h Reperfusion *in vivo*	5 min after Ischaemia Route: ?	protective effect (reduced tissue necrosis, neutrophil infiltration, lipid peroxidation), restored endogenous antioxidants (vitamin E, SOD, GSH), recovery cardiac function (MAP, HR, dp/dt)	[263]
Polyphenolic compounds					
Quercetin	rat	22 min Ischaemia/ 30 min Reperfusion *in vitro*	day -4 to -1 oral	decreased impairment of cardiac function (developed pressure, diastolic function, reduced vascular resistance), protection of mitochondrial function (respiratory parameters)	[264]

(continued)

Antioxidant	Species	Model	Time/ Route	Effects	Ref
1/Rhamnoside -quercetin 2/ Flavones	rat	30 min Ischaemia /30- 40 min Reperfusion in vitro	right before Ischaemia (for 15 min)	improved recovery of left ventricular (end-diastolic) pressure	[265]
Baicalein	chicken	A/ 1 h Ischaemia B/ 1 h Ischaemia / 30 min Reperfusion embryonic cardiomyocytes	A/ during Ischaemia B/ during Reperfusion	attenuation of oxidative stress during Ischaemia and IR, reduced cell death and improved recovery of cardiac function during IR (contractility)	[266]
Purpurogallin	rabbit	1 h Ischaemia/ 3 h Reperfusion *in vivo*	just before Reperfusion i.v.	reduction of IS/AAR, reduction of IS compared with Trolox (vitamin E-analogue)	[267]
Resveratrol	rat	30 or 5 min Ischaemia/ 30 min Reperfusion *in vivo*	bolus 15 min before Ischaemia i.v.	free radical scavenging, no effect on ischaemia induced arrhythmias, reduction of mortality, ventricular tachycardia and fibrillation during reperfusion, reduced tissue damage (LDH release)	[268]
trans-resveratrol	rat	30 min Ischaemia/ 2 h Reperfusion *in vitro*	before Ischaemia (for 15 min)	improved recovery of post-ischaemic ventricular function (developed pressure,aortic flow), reduced lipid peroxidation (MDA), reduced IS/LV and IS/AAR	[269]
Proantho-cyanidin	rat	30 min Ischaemia/ 2 h Reperfusion *in vitro*	3 weeks before Ischaemia for 3 weeks oral	reduced IS/AAR, improved recovery of post-ischaemic contractile functions (developed pressure,+dp/dt,aortic flow), early reduction in lipid peroxidation (MDA), scavenger for peroxyl and hydroxyl radicals	[270]
Proantho-cyanidin extract	rat	30 min Ischaemia/ 2 h Reperfusion *in vitro*	for 3 weeks oral	reduced number of apoptotic cells, reduced protein levels of JNK-1 and c-Jun, reduction of oxygen free radical production, improved functional recovery (DP, dp/dt, and aortic flow)	[271]
Astringinin	rat	A/ 30 min Ischaemia/ *in vivo* B/4h Ischaemia/ *in vivo* C/ 5 min Ischaemia/ 30 min Reperfusion/ *in vivo*	bolus 15 min before Ischaemia i.v.	decreased incidence and duration of ventricular tachycardia and fibrillation during Ischaemia and Reperfusion, increased plasma NO and reduced LDH release during Ischaemia and Reperfusion, reduced IS/AAR and IS/LV after 4 h Ischaemia	[272]

(continued)

Antioxidant	Species	Model	Time/ Route	Effects	Ref
Melatonin or structural analogues					
Melatonin	mouse rat	60 min Ischaemia/ 4 h Reperfusion *in vivo*	30 min before Ischaemia or 15 min before Reperfusion or during Reperfusion i.p.	similar effects in rats and mice, most effective dose: 150 µg/kg, reduction of IS (after 0.5 and 2 h but NOT after 4 and 24 h), melatonin i.p. during Reperfusion: no protective effect	[273]
Melatonin	rat	30 min Ischaemia/ 30 min Reperfusion *in vitro*	during Ischaemia and Reperfusion	dose dependent recovery in LV function (LVDP and dp/dt), reduced hydroxyl radical formation and lipid peroxidation (dose dependent), reduced incidence and duration of ventricular arrhythmia	[274]
Melatonin	rat	12.5 min Ischaemia (chemical)/1.5-15 min Reperfusion cardiomyocytes	during Ischaemia only or during Ischaemia and Reperfusion	during Ischaemia: only short term protective effect (morphological, intracellular Ca^{2+}) during Reperfusion: protective effect (morphological, ROS production, intracellular Ca^{2+})	[275]
1/ Melatonin 2/ 5-MCA-NAT	rat	5 min Ischaemia/ 30 min Reperfusion 30 min Ischaemia/ 120 min Reperfusion *in vitro*	*in vivo*, 30 min before excision of hearts i.p.	reduced duration of reperfusion arrhythmias, reduced IS/AAR	[276]
Cytochrome P450 inhibitors					
1/Chloramphe-nicol 2/Cimetidine 3/Sulfaphena-zole	rat rabbit	rat: 30 min Ischaemia / 2 h Reperfusion rabbit: 30 min Ischaemia/ 4 h Reperfusion rat: *in vitro* rabbit: *in vivo*	for rats: during whole experiment or only during Reperfusion for rabbits: 30 min before Ischaemia; i.v.	rat model: reduced IS/AAR, reduced CK release (not in treatment during Reperfusion group), restored coronary flow (not in treatment during Reperfusion group), reduced superoxide generation (only tested for chloramphenicol administered before Ischaemia) rabbit model: reduced IS/LV (only tested for chloramphenicol and when administered 30 min before Ischaemia)	[277]

(continued)

Antioxidant	Species	Model	Time/ Route	Effects	Ref
Lipid peroxidation inhibitor					
U-74389G (21-amino-steroid)	rat	transplantation model (2 h Ischaemia/ 30 min Reperfusion) *in vivo*	10 min prior to explant and at beginning of Reperfusion i.v.	less severe oedema, milder changes (swelling, disappearance of cristae) in mitochondrial structure and maintained functionality, preserved structure of the vascular endothelium, maintenance of CP and ATP levels, lower lipid peroxidation	[278]
U-74006F (21-amino-steroid)	dog	2 h Ischaemia/ 6 h Reperfusion *in vivo*	1 h before Reperfusion (for 7 h) i.v.	reduced lipid peroxidation (production of conjugated dienes), no reduction in IS/AAR and IS/LV (after 2 h and 6 h), no reduction in inflammatory response (neutrophil infiltration)	[279]
U-74006F (21-amino-steroid)	rabbit	30 min Ischaemia/ 30 min Reperfusion *in vitro*	30 min before heart excision (for 30 min) i.v.	retention of U-74006F in myocardial tissue, reduced creatine phosphokinase release, improved LV systolic pressure (LVSP,+dp/dt) and LV diastolic pressure (LVDP,-dp/dt)	[280]
Indenoindole H290/51	pig	45 min Ischaemia/ 4 h Reperfusion *in vivo*	started 5 min prior to Reperfusion coronary vein (infusion for 30 min)	immediate and gradual recovery of the ischaemic left ventricular wall segment shortening versus no recovery in the vehicle group, reduction in IS/AAR and IS/LV	[281]
Xanthine oxidase inhibitor					
Allopurinol	rat	30 min Ischaemia/ 30-40 min Reperfusion *in vitro*	right before Ischaemia (for 15 min)	improved recovery of left ventricular (end-diastolic) pressure	[265]
Allopurinol	rat	5 or 30 min Ischaemia/ 10 min Reperfusion in vivo	oral: 24 h before Ischaemia and i.v.: 15 min before Ischaemia	during Ischaemia: reduced incidence of ventricular tachycardia during Reperfusion: reduced incidence and duration of ventricular fibrillation, reduced duration of tachycardia	[282]
Allopurinol	rat	25 min Ischaemia/ 30 min Reperfusion *in vitro*	perfusion for 10 min before Ischaemia and continuously for 30 min of Reperfusion	improved functional recovery (LVP_{max}, dp/dt_{max}, $-dp/dt_{min}$, and LVEDP), decreased tissue damage (LDH release), reduced oxidative stress (inhibition of xanthine oxidase activity, reduced lipid peroxidation, reduced generation of hydroxyl radical)	[283]

(continued)

Antioxidant	Species	Model	Time/ Route	Effects	Ref
Oxypurinol	dog	90 min Ischaemia/ 4 days Reperfusion in vivo	25 min before Reperfusion (for 2 min)/ i.v.	no reduction in IS/LV or IS/AAR	[216]
Glutathione analogues					
N-2-mercapto-propionyl-glycine	dog	90 min Ischaemia/ 4 h Reperfusion *in vivo*	15 min before Reperfusion and throughout Reperfusion/ i.v.	high plasma uptake, improved blood flow after reperfusion; no reduction of IS/AAR or IS/LV	[284]
N-2-mercapto-propionyl-glycine	dog	90 min Ischaemia/ 6 h Reperfusion *in vivo*	15 min before Reperfusion (for 75 min)/ intra-atrial	no reduction of IS/AAR; increased contraction band necrosis as a percentage of total infarct	[285]
N-2-mercapto-propionyl-glycine	dog PMN-de-pleted	90 min Ischaemia/ 6 h Reperfusion *in vivo*	15 min before Reperfusion (for 60 min) intra-atrial	reduction in IS/AAR	[104]
N-2-mercapto-propionyl-glycine	dog	90 min Ischaemia/ 6 h Reperfusion *in vivo*	A/ 15 min before Ischaemia (for 2 h); B/ 15 min before Reperfusion (for 1 h); C/ 45 min after Reperfusion (for 1 h)/ intra-atrial	A/, B/: reduction in IS/AAR C/ no reduction in IS/AAR	[286]
N-2-mercapto-propionyl-glycine	rabbit	A/ 30 min Ischaemia/ 3 h Reperfusion B/ 30 min Ischaemia/ 72 h Reperfusion in vivo	A/ starting 15 min before Reperfusion until 1h after onset of Reperfusion B/ same as 1 but until the end of Reperfusion i.v. infusion	lowered MAP during reperfusion; only significant reduction of IS/AAR after 3 h Reperfusion and NOT after 72 h Reperfusion and only when treatment lasts till end of reperfusion	[287]

(continued)

Antioxidant	Species	Model	Time/ Route	Effects	Ref
N-2-mercapto-propionyl-glycine	dog	15 min Ischaemia/ 4 h Reperfusion *in vivo*	A/ 15 min before Ischaemia (for 2.5h); B/ 1 min before Reperfusion (for 2h); C/ 1 min after Reperfusion (for 135 min)/ intra-coronary	A/, B/: greater recovery of systolic thickening fraction C/ no recovery of systolic thickening fraction (ischaemic myocardium: dyskinetic) B/ reduced release of oxygen free radicals compared to control and group C C/ reduced release of oxygen free radicals compared to control	[288]
N-2-mercapto-propionyl-glycine	dog	90 min Ischaemia/ 48 h Reperfusion *in vivo*	A/ 15 min before Reperfusion (for 4 h 15 min); B/ 30 min after onset Reperfusion (for 3 h 30 min); C/ 15 min before Ischaemia (for 1 h 15 min)/ i.v.	A/, B/ reduced IS/AAR C/ no reduction in IS/AAR scavenger of hydrogen peroxide but not of superoxide radical	[289]
1/ N-2-mercapto-propionyl-glycine 2/Deferoxamine 3/ Dimethyl-thiourea	dog	A/ 15 min Ischaemia/ 24 h Reperfusion B/ 30 min Ischaemia/ 24 h Reperfusion *in vivo*	15 min before Ischaemia (till 1.5 h into Reperfusion) Route: ?	2/,3/: protective effect in A and B (reduced coronary vascular permeability, free radical formation, myocardial edema, leukocyte uptake) 1/: no protective effect in A and B	[290]
Derivative of thiourea and pyruvate					
dimethylthiourea	mouse	4 weeks Ischaemia *in vivo*	starting 6 h after induction of Ischaemia, daily for 4 weeks/ i.p.	reduced hydroxyl radical formation, better LV contractile function, smaller increases in LV chamber size and hypertrophy, attenuated collagen volume fraction and reduced MMP-2 activity in noninfarcted myocardium, no reduction in IS	[291]
dimethylthiourea	dog	90 min Ischaemia/ 48 h Reperfusion *in vivo*	15 min before Reperfusion (for 30 min)/ i.v.	reduced IS/AAR	[292]

(continued)

Antioxidant	Species	Model	Time/ Route	Effects	Ref
ethylpyruvate	rat	30 min Ischaemia/30 min Reperfusion/ *in vivo*	just before Ischaemia and Reperfusion i.v.	increased levels of ATP in ischaemic myocardial extract, reduced lipid peroxidation, reduced IS/AAR, improved restoration of myocardial function (dp/dt,ejection fraction, cardiac output)	[293]
Miscellaneous					
Metoprolol	guinea -pig	45 min Ischaemia/15 min Reperfus/*in vitro*	perfusion 15 min before Ischaemia and during Reperfusion	lower oxidative damage (MDA and GSH levels), reduced heart rate, reduced impairment of developed pressure and dp/dt	[294]
Magnolol	rat	45 min Ischaemia/1 h Reperfus/*in vivo*	10 min before Ischaemia i.v. bolus	suppressed ventricular arrhythmias, reduced superoxide production and MPO activity, reduced IS/AAR, reduced mortality	[295]
Magnolol	rat	A/ 30 min Ischaemia/ 10 min Reperfusion B/ 4 h Ischaemia *in vivo*	15 min before Ischaemia i.v.	suppression of incidence and duration of ischaemia-induced arrhythmias (dose-dependent) and reperfusion-induced arrhythmias (at all doses), reduced IS/LV and IS/AAR ratio (dose-dependent)	[296]
WS® 1442	rat	4 h Ischaemia/ 15 min Reperfusion *in vivo*	day -7 to 1 h before anaesthesia/ oral	attenuation of ST-segment elevation, reduced incidence of ventricular fibrillations, reduced mortality rate, reduced IS/AAR and IS/LV	[297]
EGb 761	rat	30 min Ischaemia/ 2 h Reperfusion *in vitro*	day -10 to -1 oral	no significant reduction in arrhythmias, no improvement in cardiac function (LVDP,dp/dt_{max})	[298]
Caffeic acid Phenethyl-ester	rat	30 min Ischaemia/ 120 min Reperfusion *in vivo*	started 10 min before Ischaemia and continued during Ischaemia i.v. infusion	reduced IS/AAR, cardiac arrhythmias after coronary artery occlusion in all treated and control animals	[299]
AMP 579	chicken	60 min Ischaemia/ 15 min Reperfusion or 3 h Reperfusion embryonic chick cardiomyocytes	started 10 min before Reperfusion	reduction of ROS generation, reduced cell death	[300]

Derivative of thiourea and pyruvate

Dimethylthiourea (DMTU) is a low molecular weight agent which is highly diffusible, has a long half-life, and is an effective scavenger of hydrogen peroxide, hydroxyl radical, and hypochlorous acid [314]. DMTU reduces infarct size in an *in vivo* dog model of IR [292]. In addition, daily treatment with DMTU prevented left ventricular remodelling (myocardial dilatation and hypertrophy, interstitial fibrosis) in an *in vivo* model of myocardial infarction [291]. This suggests a role for ROS in ventricular remodelling after myocardial infarction [291].
Ethyl pyruvate, a commercial food additive, is a lipophilic ester derivative of pyruvate with improved stability compared to pyruvate [293]. It was shown that ethylpyruvate attenuated myocardial oxidative injury, decreased infarct size, and preserved cardiac function after IR [293].

Miscellaneous

Metoprolol
β-adrenergic blocking drugs are known to exert negative inotropic and chronotropic effects by reducing cardiac sympathetic nerve activity [294]. They are therefore used in the treatment after myocardial infarction to reduce myocardial energy demand and arrhythmias. Kalaycioglu *et al.* [315] showed that metoprolol also prevents myocardial IR injury by reducing oxidative stress and prevention of lipid peroxidation. However, if this lipid peroxidation reducing effect is due to an intrinsic antioxidant effect of metoprolol or an indirect effect due to the reduction of sympathetic nerve activity is not clear [315].

Extracts from Chinese medicinal herbs, trees or plants
This group includes magnolol which is an active component extracted from the Chinese medicinal herb *Magnolia officinalis*; WS®1442, an extract from the Hawthorn *Crataegus*; EGb 761, extracted from the tree *Ginkgo biloba*, and finally caffeic acid phenethyl ester which is derived from honeybee propolis. Protective effects of these extracts in the setting of cardiac IR are not clear. Magnolol [295, 296] and WS®1442 [297] reduced arrhythymias and infarct size in an *in vivo* rat model of IR. In contrast EGb 761 [298] could not reduce arrhythmia or improve cardiac function during *in vitro* IR. Caffeic acid phenethyl ester [299] could reduce infarct size but not the *in vivo* cardiac arrhythmias.

AMP 579
The rate at which isolated chick cardiomyocytes die following a period of simulated ischaemia was attenuated by the adenosine A_1/A_2 receptor agonist AMP 579 given just before reperfusion [300]. AMP 579 decreases the burst of reactive oxygen seen at reoxygenation. This effect was dependent on adenosine A2 receptor binding. However, adenosine could not duplicate these effects, indicating that AMP 579 has protective actions apart from its effect on adenosine receptors.

2.7. Antioxidants in clinical trials of reperfusion therapy

Numerous studies have evaluated the influence of superoxide dismutase, vitamin C, vitamin E, and thiol compounds alone or in various combinations on IR injury in patients undergoing reperfusion therapy after myocardial infarction. However, despite many research efforts and a wide availability of antioxidant agents, there is at the moment no clinical evidence for the routine use of antioxidants in the clinical setting of ischaemia and reperfusion.

Recombinant human superoxide dismutase

Recombinant h-SOD has been tested in two clinical trials of patients undergoing thrombolysis [316] or coronary angioplasty [317] for acute myocardial infarction. In the first trial in 34 patients with acute anterior myocardial infarction receiving thrombolytic agents, h-SOD was randomly administered just before reperfusion [316]. Although a significant reduction in the total number of ventricular premature complexes was observed during the first 15 minutes of reperfusion, SOD treatment failed to significantly improve left ventricular regional ejection fraction [316]. Subsequently, a multicenter, randomized, placebo-controlled clinical trial with 120 patients was designed to test the hypothesis that free radical-mediated reperfusion injury could be reduced by intravenous administration of h-SOD, administered before PTCA, in patients with acute transmural myocardial infarction [317]. The results of this clinical trial failed to demonstrate a beneficial effect of h-SOD on global or regional left ventricular functions in patients who underwent successful PTCA [317]. The authors don't have a clear explanation for these disappointing results. They mentioned that a clinically significant benefit might have been missed with such a small sample size because of the heterogeneity of intercoronary collaterals, vascular risk regions, and other important uncontrolled variables. They also indicate that the mean time to reperfusion was 4 hours after the onset of chest pain, a period sufficient to induce irreversible damage, without potential to recover [317].

Vitamin C

Results of the clinical studies of oral supplementation with vitamin C are rather contradictory. While most of the studies utilizing variable doses and regimens of vitamin supplementation achieved reduction in biochemical indices of reperfusion injury, this correction did not universally convert into better functional recovery and significant clinical benefit [318-320]. In the studies of Dingchao *et al.* protective effects of high-dose vitamin C on the myocardium were observed in patients undergoing cardiopulmonary bypass [321]. They observed that postoperative cardiac index was higher in vitamin C-treated patients than in their controls. This effect was associated with shorter intensive care and hospital stay.
In contrast, when vitamin C was infused intravenously prior to PTCA after acute myocardial infarction there was no lowering of the urine level of 8-epi prostaglandin

F2α, an indicator of oxidative stress [322]. No functional cardiac parameters were tested in this study.

Vitamin E

The data obtained with vitamin E supplementation are also variable. Studies with oral vitamin E intake face the difficulty of achieving increased tissue concentrations of vitamin E. This problem is demonstrated in the studies of Mickle *et al.* where different doses administered the night before cardiac surgery or a 3 day course did not increase myocardial vitamin E concentrations [323]. They observed that 2 week oral therapy was required to double the myocardial vitamin E concentration. In the studies of Yau *et al.* [324] vitamin E had a small but significant metabolic and functional effect after elective coronary bypass operations in low-risk patients. Sisto *et al.* [325] investigated higher risk patients and reported that the treated group had a reduced number of perioperative ischaemic events, myocardial infarctions, and arrhythmias. However, since vitamin E treatment was combined with vitamin C and allopurinol, the individual contribution of the vitamin E treatment cannot be determined. In contrast to the above studies showing clinical benefit, another clinical study, pretreating patients undergoing coronary artery bypass grafting with oral vitamin E for 7-10 days and oral vitamin C for 12 h, provided no measurable reduction in myocardial injury despite prevention of the depletion of vitamin E in plasma [318]. Finally, in a study by Lassnigg *et al.* normalization of plasma vitamin E concentrations with parenteral vitamin E emulsion did not affect biochemical markers of myocardial injury and clinical outcome after cardiac surgery [326].

Thiol compounds

Attempts to enhance intracellular glutathione, frequently utilized N-acetylcysteine (NAC), a membrane permeable precursor of GSH synthesis. Ferrari *et al.* reported beneficial effects in patients where the degree of oxidative stress following reperfusion was reduced and recovery of cardiac function improved [327]. Arstall *et al.* [328] explored the safety of NAC in combination with nitroglycerin and streptokinase for the treatment of evolving myocardial infarction. NAC administration appeared to be safe and was associated with significantly less oxidative stress, a trend toward more rapid reperfusion, and better preservation of ventricular function. The ISLAND (Infarct Size Limitation: Acute N-acetylcysteine Defense) trial was a randomized, angiography-, and echocardiography-controlled study [329]. In patients with successful reperfusion induced by a combination therapy including streptokinase and NAC, there was a reduction in infarct size associated with improved LV function when compared to patients with reperfusion induced by streptokinase alone or compared to patients with failed reperfusion. Despite these promising small-scale trials, no large-scale studies have been conducted uptill now, to confirm a clear benefit of NAC in reducing reperfusion injury in the treatment of acute myocardial infarction or surgically induced IR during cardiac surgery [329].

2.8. Conclusion

Reactive oxygen species are generated at an accelerated level in the postischaemic myocardium and contribute to modifications of several biomolecules leading to myocardial tissue injury. Multiple enzymes and subcellular structures contribute to enhanced ROS production and oxidative stress associated with ischaemia and reperfusion. Despite many research efforts and a wide availability of antioxidant agents results are conflicting and disappointing. A better understanding of the action of antioxidants in the setting of IR is needed before the therapeutic potential of free radical-directed drugs can be fully realized in a clinical setting.

3. Proteomics in cardiovascular disease

3.1. Introduction

Proteomics is the study of the "proteome" or the entire protein complement of a genome, a term first coined in 1995 by Marc Wilkins [330, 331]. The proteome is far more complex than previously suggested by the one-gene, one-protein theory. The proteome consists of all proteins present in a cell, tissue or organism at a given time, including not only those translated directly from genetic material but also the variety of modified proteins arising from alternative splicing of transcripts, from extensive co- and posttranslational processing, or from a combination of these. These protein modifications have the potential to alter protein structure and/or function.
Since proteins are involved in virtually every cellular function and in every regulatory mechanism, the proteome dictates the phenotype of the cell and, collectively, the tissue or organ that the cells comprise. This phenotype varies under normal conditions, such as cell cycle stage, differentiation, function, and ageing, or as a result of the onset of interventions or in response to acute injury or chronic diseases. In the acute phase, rapid posttranslational modifications of proteins occur, whereas in chronic disease or treatment states, co- and posttranslational protein modifications occur in concert with altered gene expression, leading to a wide variation in protein levels and modifications. For specific proteins, disease-induced modifications will substantially affect function, which in turn has the potential to affect the action of other proteins. The result is a dynamic, ongoing process of protein expression and modifications. Proteomics is aimed at identifying and characterizing these protein changes for example in relation to certain pathologies or drug therapy.

In the next sections we will explain the traditional technique of 2-D gel electrophoresis and mass spectrometry employed to characterize changes in the proteome (section 3.2). A complete overview of the results achieved in cardiovascular research by the use of this technique is given in section 3.3. Post-translational modifications and the advantages and usefulness of subcellular proteomics are included in the latter section. In section 3.4, the results, (dis)advantages of transcriptomic (RNA) and proteomic (protein) analysis in the field of cardiovascular research are compared. We will finalize this chapter with an explanation about functional proteomics and illustrate it with the functional proteomic analysis of the PKCε complex.

3.2. Two-D gel electrophoresis combined with mass spectrometry

Two-dimensional gel electrophoresis has been the primary tool for obtaining a global picture of the expression levels of proteins in the total proteome of cells or tissue, under various conditions [332]. By this technique a protein mixture is separated by making use of two intrinsic protein characteristics, i.e. net charge and molecular mass.

The first stage involves isoelectric focusing (IEF), where proteins are separated according to their isoelectric point (pI), using immobilised pH gradients (IPG). Proteins applied to these IPG strips migrate in an electric field and stop

migrating through the pH gradient when their net charge is neutral. These IPG strips are widely available in various formats, from wide range covering many pH units, to narrow pH ranges covering just one or two pH units. Narrow range strips provide much greater resolution and can be overlapped to overspan the desired pH range [333-335].

After completion of the first dimension separation by pI, proteins are separated by molecular weight in polyacrylamide gels containing sodium dodecyl sulphate (SDS). SDS is an anionic detergent which denatures the proteins, converting them to a linear molecule by relaxing their secondary structure. Because of its anionic nature it gives proteins a net negative charge and proteins are therefore exclusively separated by molecular mass.

Once the protein spots are separated they can be visualized on the gels using a variety of stains such as coomassie brilliant blue stain, which will detect proteins present in amounts between 10-40 ng. The sensitivity can be enhanced by silver staining, which can detect proteins in the 2-5 ng range [336]. However, with silver staining it is important to avoid cross-linking reagents such as glutaraldehyde, as the use of aldehydes makes the protein less susceptible to protease digestion and reduces therefore the efficiency of subsequent mass spectrometry [337]. Recently, developments in fluorescence technologies have led to the production of fluorescent protein dyes such as Sypro Ruby® and CyDyes® with sensitivity similar to silver stains. The advantages of protein detection with Sypro Ruby are that it is technically simple to use, its high sensitivity (1-10 ng), its linearity over 3 orders of magnitude and its compatibility with downstream analysis including mass spectrometry (see further) and Edman sequencing (N-terminal residue identification) [338, 339]. CyDyes are used in fluorescence 2D difference gel electrophoresis (DIGE), where up to three different samples are separated on a single gel, because these samples have each been labelled before 2D electrophoresis with a different fluorescent cyanine dye (Cy2, Cy3, Cy5). Each dye can then be visualized under a different wavelength and the images overlaid, giving a combined image that can be analyzed with high reliability [340].

After separation and detection, proteins of interest must be identified. For this, the most significant breakthrough in the evolution of proteomics is the development of mass spectrometry (MS) for protein identification [341]. Protein identification is based on the analysis of peptides generated by proteolytic digestion (for example trypsin digestion). In all mass spectrometers, peptides are ionized from the sample. This is achieved either by matrix-assisted laser desorption/ionization (MALDI) of a solid-state sample or by electrospray ionization (ESI) directly from the liquid phase. Ionized peptides are separated on the basis of their mass-to-charge ratio (m/z) and identified according to their time-of-flight (TOF) distribution or analyzed by quadrupole mass filters. In tandem MS/MS, an ionized peptide of interest is selected by the first MS and fragmented by collision with inert gas. The resulting fragments are then analyzed in the second MS. Modern ESI-based MS/MS may use liquid chromatography (LC) systems such as capillary zone electrophoresis or very low flow-rate reversed-phase high performance-LC (HPLC) before ionization, in order to fractionate complex mixtures. MS provides precise peptide masses for protein characterization, whereas more sophisticated instruments (particularly tandem MS)

also allow peptide sequence determination to identify the protein. More recently, mass analyzers have been combined to create tandem mass spectrometers (TOF-TOF). In this instrument, m/z values are selected by their time-of-flight and all others are deflected from the flight path. The ions then pass into a collision cell and undergo high-energy collisions with an inert gas such as helium, causing fragmentation of the ions which is referred to as collision-induced dissociation (CID). The additionally obtained masses of these peptide fragments, allow more reliable characterization of the protein.

3.3. Application of proteomics to cardiovascular research

3.3.1. Heart 2-DE protein databases

Proteomics of the heart started in the 1990s with the creation of 2-DE protein databases. Pioneering proteomic work by the laboratories of Michael J. Dunn (United Kingdom) and Peter Jungblut (Germany) led to the creation of several online 2-DE databases of human, dog, rat and mouse atrial and ventricular myocardial proteins [342-345]. The four main databases are HSC-2DPAGE, HEART-2D-PAGE, HP-2D-PAGE and RAT HEART-2DPAGE and conform to the rules for federated 2-DE protein databases [346]. Pleißner and co-workers have included a link to heart proteins associated with dilated cardiomyopathy in their database [347].

3.3.2. Proteomics of dilated cardiomyopathy

Until November 2004, in the area of cardiovascular research, the technique of proteomics has been predominantly applied to dilated cardiomyopathy (DCM) and is therefore discussed in more detail in this section.
Dilated cardiomyopathy in humans is a severe disease of the heart characterized by *impaired systolic function* with reduced ejection fraction, increased end systolic blood volume and dilatation of the ventricles [348]. The pathophysiology of DCM is less clear and genetic factors, myocarditis from infectious agents, autoimmune mechanisms, cytokine activation, toxic damage like alcohol abuse and hormonal or metabolic influences can play a role [348].

Two-dimensional gel electrophoresis has been applied to identify alterations in the myocardial protein pattern that characterize dilated cardiomyopathy. Subsequent identification of specific pathology-associated proteins has been achieved by visual comparison with database images, N-terminal protein microsequencing, and MS. Cardiac tissue (ventricular and atrial) from patients suffering from DCM [349-351] and animal models representative for human DCM, i.e. bovine hereditary DCM [352, 353] and a canine model of pacing-induced heart failure [352, 354] have been analyzed. As table 6 shows, more than 50 cardiac proteins have been identified that significantly alter their expression level in DCM [349, 351, 355-357].
Results of proteomic studies of cardiac tissue from the three species (human, canine and bovine) are very similar, i.e. the majority of these proteins being less abundant in the diseased heart (table 6) [349, 351, 355-357].

These proteins have been classified into three broad functional classes i.e. 1/ cytoskeletal and myofibrillar proteins, 2/ proteins associated with mitochondria and energy production and 3/ proteins associated with stress responses (table 6).
The most significant DCM-related change was a 7- fold increase in ubiquitin carboxyl-terminal hydrolase (UCH) in bovine [353]. UCH is a deubiquitinating enzyme responsible for maintaining the cytoplasmic pool of free ubiquitin. In contrast to the other identified proteins, the possible consequences for the change in expression level of this enzyme have been investigated in more detail [349, 359, 360]. Therefore we further limit ourselves to this protein.
It was reasoned that an increase in the abundance of UCH during DCM, could increase the intracellular concentration of ubiquitin and thereby facilitate increased protein ubiquitination in the disease state, leading to proteolysis of the targeted proteins via the 26S proteasome pathway [359]. In relation to this, inappropriate ubiquitin conjugation has already been proposed to contribute to heart failure [359]. A follow-up study showed that UCH is also more than 8-fold elevated at the protein level and more than 5-fold elevated at the mRNA level in human DCM hearts [360]. As shown with immunohistochemistry, the increased expression of UCH was present in human DCM cardiomyocytes and not in control hearts [360]. The incease in UCH level in human DCM hearts was associated with a 5-fold increase in overall protein ubiquitination relative to control hearts [360].
Using a selective affinity purification method enhanced ubiquitination of a specific set of proteins has been demonstrated in these human DCM hearts [360]. These proteins have been subsequently identified by mass spectrometry. Some of these proteins were reduced in abundance in bovine DCM [349] and are marked in grey in table 6. It was hypothesized that these data add support to the theory that inappropriate ubiquitination and proteolysis of a specific set of proteins occurs in DCM and that this contributes to cardiac dysfunction in the diseased heart [360].

3.3.3. Proteomics of ischaemia and ischaemia-reperfusion

Two-dimensional gel electrophoresis combined with mass spectrometry has also been applied to identify proteins that changed in expression level following myocardial ischaemia and IR. The technique has been applied in an *in vivo* rabbit [361] and canine [362] model of IR as well as in an *in vitro* rat model of ischaemia and IR [363].

Firstly, in an *in vivo* rabbit model of cardiac IR, Schwertz *et al.* [361] found 10 protein spots that were differentially expressed. Two could be characterized as superoxide dismutase precursor and αB-crystallin and were both decreased in expression after IR. Secondly, Sawicki *et al.* [362] found in an *in vivo* canine model of myocardial IR regional changes in the level of metabolic enzymes, with increased levels of NAD^+-isocitrate dehydrogenase, α-subunit and mitochondrial ATP synthase D chain, and decreased levels of the precursor of the α-subunit of ATP synthase. Additionally they found creatine kinase M and the contractile protein ventricular myosin light chain 1 to be decreased after IR.

Table 6: Myocardial protein changes found in proteomic studies of human DCM and animal models of DCM (modified from McGregor *et al.* [358]). The name of the protein and if this protein is up (↑)- or down (↓)- regulated in DCM, together with the species used for study is indicated. Proteins marked in grey, are proteins found to be ubiquitinated (see text).

Protein identification	↓ / ↑	Species	Ref
Cytoskeletal and myofibrillar proteins			
Sarcoplasmic reticulum Ca-ATPase (SERCA2a)	↓	Canine	[354]
Actin	↑	Canine	[352]
	↓	Human	[349]
Alpha-actin, cardiac	↓	Human	[349]
Desmin	↓, intact protein ↑, in low M_r	Canine	[354]
	↑	Bovine	[353]
	↓, intact protein	Human	[349]
MCL2 (ventricular isoforms)	↑	Human	[347,349, 350,357]
MLC1 (atrial isoform)	Variable	Human	[357]
MLC1 (ventricular isoform)	↓	Human	[349]
Vimentin	↑	Human	[349]
Proteins associated with mitochondria and energy production			
ATPase δ chain, ATP synthetase	↓	Canine	[354]
	variable	Human	[349,350]
Cytochrome c oxidase polypeptide VA	↓	Canine	[352]
	↓	Bovine	[353]
Cytochrome b_5	↓	Canine	[352]
Fatty acid-binding protein	↓	Canine	[354]
	↓	Bovine	[353]
3,2-*trans*-Enoyl-CoA-isomerase	↓	Canine	[352]
Dihydrolipoamide dehydrogenase	↓	Canine	[354]
	↓	Human	[349]
Isocitrate dehydrogenase	↓	Bovine	[353]
Creatine kinase M-chain	minor ↓	Canine	[352,354]
	↓	Human	[349]
Hydroxymethyl glutaryl CoA synthase	Variable ↓	Canine	[352]
Ubiquinol cytochrome c reductase core protein 1	↓	Bovine	[353]
Pyruvate dehydrogenase (E1 component)	↑	Canine	[354]
Triosephospate isomerase	↑/↓	Canine	[352,354]
	↓	Human	[349]
Phosphoglycerate mutase (muscle isoform)	↑	Canine	[352]
Isocitrate dehydrogenase (mitochondrial subunit A)	↓	Canine	[354]
Elongation factor Tu (mitochondrial preP43)	Not present	Canine	[354]
Mitochondrial thioredoxin-dependent peroxide reductase	↓	Bovine	[353]
Aconitate hydratase	↓	Human	[349]
Lactate dehydrogenase	↓	Human	[349]
Phosphofructokinase	↓	Human	[349]
Dihydrofolate reductase	↑	Human	[349]
Proteins associated with stress responses			
HSP 70 (inducible)	↓	Canine	[354]
	↓	Human	[349]

Protein identification	↓ / ↑	Species	Ref
HSP 70 (constitutive)	↓	Human	[349]
Mitochondrial HSP 70 precursor	↓	Bovine	[353]
Mitochondrial stress protein (HSP 70-related)	↑	Canine	[352]
HSP 60	↓	Canine	[354]
	↓	Human	[349]
HSP 27	↓	Human	[347,351]
	↑	Human	[350,351]
αB-crystallin	Variable	Human/ Canine	[349] [350,354]
Other proteins			
Farnesyl diphosphate farnesyl transferase	Variable ↓	Canine	[352]
α_1-antiproteinase precursor	↑/↓	Bovine	[353]
Galactoside 3(4)-L-fucosyltransferase	↓	Canine	[352]
IGG Fc receptor II	↑	Canine	[352]
Isovaleryl CoA dehydrogenase	↓	Bovine	[353]
Ras-related protein	↑	Canine	[352]
Syndecan-2	↓	Canine	[352]
Major allergen CAN F1	↓	Canine	[352]
Cystatin c	↓	Canine	[352]
Ubiquitin carboxyl terminal hydrolase	↑	Bovine	[353]
Inosine 5'-monophosphate dehydrogenase	↓	Canine	[352]
Myoglobin	↓	Canine	[352]
Salivary gland plasminogen activator β-precursor	↓	Canine	[352]
Haemoglobin α-chain	↓	Canine	[352]
Haptoglobin	↓	Human	[349]
Serum albumin, N-terminal fragment	↓	Human	[349]
Transferrin	↓	Human	[349]
Apolipoprotein A1	↓	Human	[349]
Carbonic anhydrase	↓	Human	[349]
Phenylalanine-4-hydroxylase	↓	Human	[349]

Lastly, Sakai *et al.* [363] found in an *in vitro* rat model, 8 protein spots with altered expression after cardiac ischaemia or IR. Five protein spots were identified as the endoplasmatic reticulum enzyme protein disulfide isomerase A3 precursor, one as 60 kDa heat shock protein and two as mitochondrial elongation factor Tu. They also suggest that protein disulfide isomerase A3 underwent dephosphorylation during ischaemia and IR.

These data indicate that the individual proteins that are differentially expressed after myocardial infarction vary considerably between studies and can be classified to a number of functional groups, i.e. contractile proteins, antioxidant precursors, heat shock proteins, metabolism-related proteins and RNA translation-related proteins.

The fact that different species were used and myocardial tissue was harvested at different time points, i.e. differences in the duration of ischaemia (range: 40 min [363]-90 min [362]) and in the duration of reperfusion (range 20 min [363] to 180 min [361]), possibly contributes to this phenomenon and shows the complexity of investigating changes in the proteome.

3.3.4. Post-translational modifications

Through genome sequencing no information can be gained on post-translational modifications of proteins. Hence, detection and characterization of PTMs are a major task in the research field of proteomics. For example protein phosphorylation is a key PTM, crucial in the control of numerous regulatory pathways, enzyme activities, and degradation of proteins, whereas glycosylation is associated with biochemical alterations, developmental changes and pathogenesis. One of the strenghts of 2-DE is its capability to readily localize post-translationally modified proteins, as they frequently appear as distinct rows of spots in the horizontal and/or vertical axis of the 2-DE gel. The number of studies in cardiovascular research concerning these modifications is relatively scarce. The PTMs of troponin and HSP-27 are most intensively investigated and will therefore be described separately in the next paragraphs.

Modification of troponin I and T

Cardiac troponin I (cTnI), an important filament regulatory protein of the myocardium, is extensively modified post-translationally during acute injuries such as myocardial stunning, ischaemia, and IR. In the serum of patients with acute myocardial infarction, both a cTnI degradation pattern as well as the existence of phosphorylated cTnI have been documented [364]. In these studies, myofilament proteins were subfractionated and separated either by SDS-PAGE or HPLC, followed by MS analysis, as an alternative method to 2-DE. Proteolysis products of cTnI were also found in myocardial biopsies of patients who underwent coronary artery by-pass surgery [365]. Based on studies in animal models, it has been suggested that specific troponin I degradation is caused by the activation of proteases, such as calpain I, triggered by intracellular calcium overload [366-369]. The main proteolysis product in this regard is a fragment, $TnI_{1\text{-}193}$ from the C-terminus [370]. In addition, calcium activates transglutaminases, which form covalent complexes with the troponin degradation products [370].

Post-translational modification, most notably proteolysis, of cardiac troponin I (cTnI) may represent the underlying molecular lesion responsible for the post-ischaemic stunned myocardium [365, 366, 369-372]. Discrepant results, however, have been obtained [368, 373-376], leading to the speculation that the relationship between myocardial stunning and degradation of cTnI may be model- and species dependent [366, 367]. In addition, Colantonio *et al.* proved recently that stunned, but viable peri-infarct canine myocardium is not characterized by degradation of troponin I but by a degradation of troponin T [377]. However, the dissociation between cTnT degradation and myocardial wall thickening argues against a direct, 'cause-and-effect' relationship between proteolysis of cTnT and acute, post-ischaemic contractile dysfunction of stunned peri-infarct myocardium [377]. The discrepancy in results indicates that the relation between troponin modifications during cardiac diseases and cardiac dysfunction needs further investigation [377].

Modification of heat shock protein- 27

Heat shock proteins are considered as "molecular chaperones", the expression of which increases by cellular stress [378]. HSP-27 acts as a protective agent against hypoxic injury in cultured adult rat [379] and canine cardiomyocytes [380].
Two-DE investigation of human myocardial samples from the right ventricle revealed that HSP-27 appears as a huge family of protein species. Using immunostaining, 34 protein spots [350] or even 59 protein spots [351, 381] reacted with an antibody against human HSP-27. However, the character of these modifications could not be described, despite immunostaining with anti-phospho-antibodies, periodate-glycostaining assays and biotinylation screening [381].
Differences of spot intensity within the HSP-27 spots between DCM and controls have been first described by Otto *et al.* [382]. Knowlton *et al.* detected a two-fold increase of HSP-27 protein concentration in DCM and also a significant increase in ischaemic heart failure [383].
A thorough comparison by 2-DE and immunostaining of the HSP-27 protein species pattern in human left ventricular tissue obtained from normal, DCM and ischaemic failing hearts revealed an increase of HSP-27 protein species at a molecular mass of 22-27 kDa and a decrease of some HSP-27 spots at 28 kDa, suggesting an enhanced HSP-27 degradation in heart failure [351].
A down-regulation of HSP-27 actually might be of functional relevance, since it belongs to the group of heat shock proteins acting as molecular chaperones, which are up-regulated in a number of cardiac diseases [378].

3.3.5. Proteomic analysis of cardiac subproteomes: subcellular proteomics

As described in section 3.2., the original approach of proteomics is characterized by a one-step sample preparation from a crude homogenate, followed by 2-D electrophoretic protein separation in order to display the whole body of expressed proteins under the given physiological or pathological condition. Despite the analytic power of this approach, systematic limitations of the approach became apparent.
First of all, there are certain classes of proteins, such as integral transmembrane proteins, that are difficult to extract and consequently not easily visible on the gel [384]. Furthermore, the analysis of post-translational modifications like protein phosphorylation and glycosylation [385, 386], oxidation of proteins [387] or the detection of intermolecular protein disulfide formation [388] requires a complex repertoire of additional analytical tools [389]. Moreover, there are also limitations with respect to the dynamic range of proteins that can be displayed on a gel compared with the dynamic range of protein abundance within cells which has been estimated to be as high as 10^7 [390]. This problem increases with sample complexity because high-abundant proteins muffle low-abundant proteins on the gel. The original approach may therefore fail in the discovery of gene products that are major proteins of particular subcellular compartments, but are minor proteins of the whole crude homogenate. Additionally, this original approach remains blind towards the dynamic changes at the subcellular level, e.g. protein translocation events between cell

compartments, and therefore inevitably will miss significant alterations in the proteome.

Subcellular proteomics, i.e. the combination of classic biochemical fractionation techniques (fractionation by differential centrifugation and/or affinity purification) for the enrichment of particular subcellular structures, combined with 2-DE and MS therefore provides the opportunity to deal with some of these problems. For that reason we further describe some advantages for the use of subcellular proteomics. This is illustrated with applications in the field of cardiovascular research.

A first line of information which can be provided by subcellular proteomics is the characterization of subcellular structures based on the entire protein population they contain. In addition to known physical and biochemical properties of these structures this offers a better understanding into the critical role of an organelle in the function of the cell. In relation to this, Taylor *et al.* have compiled an extensive catalogue of the mitochondrial proteome using highly purified mitochondria from normal human heart tissue [391]. This analysis identified a total of 615 distinct proteins which are involved in signaling, RNA-, DNA-, and protein- synthesis, ion transport, and lipid metabolism (see online http://www.mitokor.com/files/) [391]. The authors reported that the database of proteins provides a comprehensive resource for the discovery of novel mitochondrial functions and pathways [391]. Additional related examples in the field of cardiovascular research are the analysis of the mitochondrial proteome from mouse hearts deficient in creatine kinase [392], the nuclear membrane proteins in failing human dilated cardiomyopathy [393], myofilament protein enriched extract from failing swine heart [394], and sarcoplasmic reticulum and sarcolemmal proteins from rat heart [395].

A second line of information is provided by the fact that the subcellular localization of a protein is a characteristic that may provide an interesting hint to the function of that protein. For example, analysis of subcellular fractions of rat heart demonstrated that HSP-20, αB-crystallin, and myotonic dystrophy kinase binding protein were predominantly present in cytosolic fractions [396]. Moreover, immunofluorescence microscopy demonstrated that HSP-20 and αB-crystallin localize to distinct patterns as sarcomeric actin, which indicate that they might be involved in modulating cytoskeletal or contractile dynamics of cardiac myocytes [396]. A follow up study proved that phosphorylated HSP-20 increases myocyte shortening rate through increases in calcium uptake and more rapid relaxation of the cardiomyocytes [396].

A third line of information is that the analysis of proteins at the subcellular level can be used to monitor dynamic changes in the proteome such as protein translocations, e.g. between the cytoplasm and nucleus.

Fourth, it provides opportunities for the identification of previously unknown gene products. In regard to this, a comparative study of human endothelial cell caveolae and rafts, using two different fractionation techniques combined with 2-DE and MS, identified several novel proteins that, until then, were only predicted from their DNA sequences [397]. Thus, subcellular proteomics is a promising technique that may advance our knowledge on these four mentioned research fields.

3.4. Transcriptomics and proteomics in cardiac diseases

This section contains an overview of the findings from microarray studies in the field of cardiovascular research (section 3.4.1.). We further describe the advantages and disadvantages related to transcriptomic and proteomic studies (section 3.4.2.).
As an introductory remark, however, we have to mention that transcriptomics (RNA) and proteomics (proteins) would not be possible without the previous achievements of genomics (DNA) which provided the 'blueprint' of possible gene products, the focal point of transcriptomics and proteomics. A description of the findings in genomics is beyond the scope of this chapter. Therefore we want to refer to two elegant reviews from Gibbons *et al.* [398] and Yoshioka *et al.* [399], describing the findings in the field of cardiovascular genomics and genetic markers, respectively.

3.4.1. Microarrays for large-scale gene expression profiling in cardiac diseases

The evolution of methods that enable large-scale gene expression analysis, like serial analysis of gene expression, in silico analysis of expressed sequence tag databases, cDNA microarrays, and oligonucleotide microarrays, allows researchers to establish organ-or pathology-specific transcriptional profiles.
Using both human tissue and animal disease models, initial cardiovascular microarray studies identified transcriptional changes associated with myocardial infarction [400-403], cardiac hypertrophy [404-406], and human heart failure [407-413].

The effect of myocardial infarction on gene expression levels has been studied in mouse models [400] and rat models [401-403] by using microarrays. These studies are mainly restricted to a search for all the genes differently expressed after myocardial infarction without further unravelling possible functional consequences. For example, Stanton *et al.* found that more than 200 of 4000 genes related to metabolism, cell signaling, defence and structure were differentially expressed 2 and 16 weeks after myocardial infarction in rats [402]. Sehl *et al.* used microarrays and identified 14 different genes associated with stress and wound healing with elevated expression at one or more time points as long as 2 weeks after myocardial infarction in rats [401]. Lyn *et al.* used a mouse model of myocardial infarction and found that decreased levels of cell cycle regulators and the oxidative responsive gene glutathione S-transferase were accompanied by an upregulation of the genes associated with cardiac muscle development i.e. α- myosin heavy chain, fetal myosin alkali light chain and Egr-1 and Egr-3 transcription factors [400]. These findings indicate that expression of genes associated with a fetal transcription program may be involved with the post-ischaemic remodelling process in heart ventricles [400].

Similar techniques have been used by Jin *et al.* to identify new therapeutic drug targets [403]. They evaluated the effects of the ACE-inhibitor captopril treatment on myocardial remodelling eight weeks after myocardial infarction in rats [403]. The results of these experiments showed 37 differentially expressed genes after myocardial infarction which could be clustered into 11 functional groups. Captopril, partially or completely, inhibited changes in 10 of these genes and six of the functional gene clusters contained one or more genes affected by the treatment. Because mortality and

morbidity from heart failure after myocardial infarction remain high despite optimal ACE inhibitor therapy, the authors suggest that the genes whose expression was not affected by captopril, i.e. mediators of inflammation, enzymes involved in energetics or ion and water channels, may provide clues to new treatment strategies [403].

Gene arrays were furthermore used for gene expression profiling in mouse models of hypertrophy, either pharmacologically induced [405] or by transverse aortic constriction (TAC) [404, 406]. Friddle *et al.* found 55 genes out of an array of 4000 genes that show reproducible changes in expression level during the time course of induction and regression of hypertrophy; 32 genes were altered only during induction, and 8 were altered only during regression [405]. This demonstrates that cardiac remodelling during regression utilizes a set of genes that are distinct from those used during induction of hypertrophy [405].

Zhao *et al.* found an upregulation of 38 genes (48 hours), 269 genes (10 days) and 203 genes (3 weeks) and downregulation of 15 genes (48 hours), 160 genes (10 days) and 124 genes (3 weeks) after TAC [406]. These differentially expressed transcripts were categorized into 12 functional groups, and revealed the presence of several transcripts as cell proliferation-related Ki-67 and several apoptosis-related genes [406].

In humans, differential gene expression associated with heart failure has been studied using oligonucleotide microarrays containing ≈ 7000 genes [407, 410] and by using cDNA microarrays, containing up to 12000 genes [408, 409, 411, 412]. Barrans *et al.* constructed the first human cardiovascular cDNA microarray containing 10368 genes and selected 38 genes from failing hearts [408]. Using a human cardiovascular based cDNA microarray, a molecular profile of dilated cardiomyopathy was also obtained [410-412]. Heart failure resulting from dilated cardiomyopathy or hypertrophic cardiomyopathy appears to develop through different remodelling and molecular pathways. Microarrays of RNA samples of left ventricular tissue from patients with dilated cardiomyopathy and hypertrophic cardiomyopathy were hybridized against normal adult heart. The result showed more than 100 genes which were highly expressed in both dilated cardiomyopathy and hypertrophic cardiomyopathy, and several genes were differentially expressed comparing both pathologies [411]. In contrast, Steenman *et al.* [409] found 95 genes differentially expressed between failing and nonfailing hearts samples although no genes were found to be differentially expressed between failing dilated cardiomyopathy and failing ischaemic cardiomyopathy left ventricular tissue samples.

The published transcriptomic studies of heart failure have been carried out on tissue samples from relatively small numbers of human patients and these samples are often pooled. An added degree of biological variability occurs in human heart failure studies of mixed aetiology. In regard to this, Boheler *et al.* [413] found that most heart failure-candidate genes demonstrated significant changes in gene expression; however, the majority of differences among samples depended on variables such as age and/or sex, and not on heart failure alone.

Therefore, Tan *et al.* correctly suggest that large numbers of samples, that take into account absolute expression levels, need to be included in statistical analysis to generate unique profiles of a particular disease aetiology [410]. These data illustrate the necessity to establish sound statistical protocols for human transcriptomic studies in

order to identify differentially expressed genes from large samples and which are able to distinguish gene fingerprints between the different aetiologies of a disease.

3.4.2. Transcriptomics versus proteomics

The availability of cDNA and oligonucleotide microarrays for several thousands genes from the human and other mammalian genomes has made it possible to perform mRNA expression profiling on a truly global scale. Currently these microarrays allow the analysis of up to 12.000 human transcripts simultaneously. Therefore, it is clear that transcriptomic approaches allow a far greater coverage of the estimated 22.000 expressed genes in the human genome at the level of mRNA than is currently possible at the level of proteins [414, 415].

However, analysis at the protein level still has the distinctive advantage of analyzing the relative abundance of functional proteins that may not correlate with the levels of the corresponding mRNAs. Current data show that the transcriptome obtained with mRNA profiling for the characterization of cellular phenotypes, does not faithfully represent the proteome because the mRNA content seems to be a poor indicator of the corresponding protein levels [416-420]. Direct comparison of mRNA and protein levels in mammalian cells either for several genes in one tissue or for one gene product in many cell types reveals only poor correlations (0.5 or lower). For example, a correlation coefficient of 0.48 was obtained between mRNA and protein abundances in human liver [417]. Similar low values can be expected for correlations in protein and mRNA levels caused by a disease process or treatment [416, 417, 420-424].

In addition proteomic analysis facilitates the analysis of co-and post-translational modifications that are not apparent at the mRNA level. Proteomic studies of heart disease so far have concentrated predominantly on comparing the relative abundance of proteins. However, it is certain that post-translational modifications, without concomitant changes in protein abundance, are involved in pathological consequences at the molecular level (see section 3.3.4).

Some other properties also favour the importance of directly studying proteins: mRNA is a disposable message with the function to serve temporarily for the transport of one piece of information from one place to another. Therefore, mRNA is much more labile than proteins, resulting in spontaneous chemical degradation and to degradation by enzymes. Furthermore, degradation may be dependent on specific sequences, resulting in non-uniform degradation of RNA. This may introduce quantitative biases related to the time of tissue sampling and processing. In contrast, proteins are generally more stable, and exhibit slower turnover rates in most tissues. Certain high-turnover protein modifications (e.g. phosphorylation) and short half-life proteins can occur during tissue processing, although these changes are more restricted than effects on mRNA.

In the field of cardiac diseases, the number of gene products screened as mRNA by transcriptomic studies (typically up to 12.000) is higher than those that have been screened as proteins by proteomics (typically up to 3000). However, differentially expressed genes fall into similar functional classes to those reported at

the protein level by proteomics, i.e. genes encoding a) cytoskeletal and myofibrillar proteins, b) proteins associated with energy metabolism and mitochondria, c) proteins associated with stress responses, d) proteins involved in protein synthesis, and e) proteins associated with protein degradation and disassembly. Despite a higher sensitivity of microarray analysis, the current generation of proteomic technologies also yielded reports on differential changes in the expression of less abundant gene products associated with a) cell signalling, b) cell division and c) apoptosis [410-413].

The success of genomic microarrays for high-throughput analysis of transcriptional profiles has prompted analogous proteomic approaches. In the past few years, numerous articles have been published, detailing different approaches to protein chip technology. Most of these studies involve the application of proteins or antibodies in arrays on glass slides or membranes [425-429]. The technology is still in its infancy but has the potential to allow the analysis and characterization of thousands of proteins and their interactions in a single experiment. This would be a tremendous advantage for simultaneously screening large numbers of samples. The drawbacks of current methods are that post-translational modifications, which are known to be instrumental in the development of many diseases, will be difficult or impossible to track by these techniques. In an innovative departure from the traditional concept of protein chips, some researchers are implementing the microfluidic printing of arrayed chemistries on individual protein spots blotted onto membranes [430]. This technique will effectively allow each spot on a 2-D gel blot to act as a protein chip.

3.5. Functional proteomics

3.5.1. General

Transcriptomic and proteomic approaches are in general still descriptive, providing inventories of genes and proteins associated with heart disease. Many of these changes in expression level are compatible with the known pathophysiology of the disease processes involved. However, in some cases they are giving new insights into cellular processes that might be involved in cardiac dysfunction in a disease state.

A major challenge will be to investigate the detailed functional implications of these changes. Therefore, continuing technological developments and introduction of new approaches are leading to functional proteomic studies: conjunction of functional data from established biochemical and physiological methods with proteome information of the cellular or organ phenotype. Any phenotype is the sum of the contribution of all proteins present in the cell and a single observed phenotype may arise from multiple pathways. For that reason understanding of the precise role of each individual protein modification requires detailed physiological analysis. These analyses may range from *in vitro* biochemical studies to the use of drugs and transgenic animals. To completely understand how every change in protein expression level and/or modification either contributes to or plays a role in an observed phenotype, it is important to delineate the exact sequence of events that occur. A time course of protein change with measured alterations in physiological and biochemical parameters allows a reconstruction of the events leading up to and/or resulting from an altered

phenotype. As a result, it may be possible to determine exact functional changes arising from specific protein modifications. Under these conditions, functional proteomics may reveal whether a protein modification is the cause or the result of a particular disease process.

3.5.2. Functional proteomic analysis of protein kinase Cε signalling complexes

It has become increasingly clear that the molecular infrastructure supporting cellular function is composed of discrete multi-protein complexes that assemble and/or dissociate at given subcellular locations in order to accomplish specific tasks [431-447]. Moreover it has been suggested that many organ phenotypes, including those associated with ischaemic heart disease, occur as a direct result of alterations in the formation of subcellular, multiprotein complexes [431, 432, 439-441, 443, 444]. Therefore, to understand organ phenotypes in health and disease, one must understand the nature of these subcellular complexes.
Functional proteomic strategies are amongst others aimed at obtaining information regarding the expression profile of all proteins as well as the protein interactions within a signalling complex, thereby providing a holistic portrait of the entire signalling network.

In the field of cardiovascular research, the group of Ping *et al.* was, to our knowledge, the only one who applied this approach in their research. They used an approach of functional proteomics to determine whether the cardioprotective protein kinase Cε (PKCε) forms signaling complexes in the mouse heart and to identify the components of these complexes [431, 443]. By using monoclonal antibody-based immunoprecipitation combined with 2-DE, 1-DE SDS-PAGE and solution trypsin digestion followed by identification with mass spectrometry they found that PKCε co-localizes with various signalling molecules at a number of subcellular locations (see http://www.mcponline.org) [431, 443]. These PKCε-associated proteins can be classified into five functional groups, including 24 structural proteins (e.g. α myosin heavy chain, TnC, vimentin), 21 signaling molecules (e.g. Src and Lck tyrosine kinases and JNK1), 11 stress-activated proteins (e.g. iNOS, HSP-27, COX-2), 15 metabolism-related proteins (GAPDH, enolase, succinate dehydrogenase), 17 transcription- and translation-related proteins (elongation factor Tu, histone H4 and hnRNP K), and five proteins of unknown function.
Proteomic analysis additionally revealed that PKCε-mediated cardioprotection was related with associations and dissociations of these proteins into the signalling complex. Also posttranslational modifications occurred, as determined by a shift in pI in the 2-DE and/or MALDI analysis [431].
By this technique of functional proteomics, PKCε complexes have been found to contain at least four nonreceptor tyrosine kinases: PYK2, Bmx, Lck and Src [431]. Further studies specifically characterized the roles of Src, Lck and Bmx in cardiac protective phenotypes. The degree to which these molecules associate with the PKCε complex was found to increase significantly in distinct forms of cardiac protection, including ischaemic preconditioning (for LcK [440]), PKCε-mediated cardiac protection (for Lck [440]; for Src [448]), and nitric oxide donor-induced

preconditioning (for Src [444]; for Bmx [449]). This suggests that the presence of the tyrosine kinases Src, Lck and Bmx in the PKCε complex may have distinctive consequences for the protective phenotype regulated by this complex. In support of this, post-translational modification of Src, Lck and Bmx in the PKCε complex, and altered enzymatic activities of these kinases were observed, indicating that association of Src, Lck and Bmx with the PKCε complex results in signal transduction [431]. In the case of Lck, this signal transduction was found to involve the specific task of NFκB activation, a transcription factor known to participate necessarily in cardiac protection [440]. Importantly, these complexes formed between PKCε and nonreceptor tyrosine kinases appear to be essential for cardiac protection because their disruption (genetic or pharmacologic) results in a loss of the protective phenotype.

The information obtained with this proteomic analysis will expedite the understanding of PKC-ε dependent cardioprotection and signaling. In addition, the understanding gained from these studies lays the groundwork for molecular drugs to enhance the assembly of beneficial protein complexes and thereby reducing ischaemic cell death in the heart.

3.6. Conclusion

It can be concluded that proteomic technologies allow for the nonbiased large-scale analysis of protein expression levels and their post-translational modifications, with regard to the description of a cell phenotype, pharmacological interventions or during pathological situations. By the application of subcellular and functional proteomics, it also empowers the investigator to conduct possible hypothesis-driven research, and to gain definitive answers concerning the specific roles played by individual proteins of interest under certain conditions.

4. Aims and outline of the thesis

The first goal of this thesis was to investigate the potential cardioprotective effects of the antioxidant 7-monohydroxyethylrutoside (monoHER) in an *in vivo* mouse model of cardiac ischaemia-reperfusion (IR). The second goal was to determine the early alterations in cardiac protein expression in this IR model in order to delineate the mechanisms of action of monoHER in this setting. The background for these studies is outlined in the next paragraph.

The *in vivo* mouse model of cardiac IR was first described by Michael *et al.* in 1995 [450]. Following transient occlusion of the left anterior descending coronary artery they described the histological appearance of leukocytes and contraction bands in the ischaemic region of the heart up to 24 hours after reperfusion. From that moment on, the murine model of IR has been frequently used to study the pathogenic mechanism of cardiac reperfusion injury or as a model to evaluate the efficiency of potential therapies. However, most of these studies have focused on the short-term consequences of reperfusion, using myocardial infarct size or neutrophil influx as parameters to describe the progression of cardiac tissue damage in the time frame of a few hours up to one or a few days after the initiation of reperfusion. The long-term effects of IR injury, in terms of weeks or months, are less well examined in this mouse model. However, this is a relevant aspect for extrapolation to the clinical setting. It may be that the outcome of interventions that are beneficial shortly after initiation of reperfusion is different when the evaluation takes place at later stages. To examine such aspects we investigated the long-term morphological and functional consequences of cardiac IR in an *in vivo* mouse model (**chapter 2**). As a validation we compared the effects of IR with the effects of permanent ischaemia on these morphological and functional parameters. This was important as these models were the study objects for the next chapters in which potential protective effects of an antioxidant were evaluated and alterations in the cardiac proteome were investigated.

As illustrated previously, potential protective effects of exogenously administered antioxidants on reperfusion injury have already extensively been described in literature. However, as described in chapter 1, the beneficial effects of antioxidant treatment in these models remain controversial. Moreover, most of these studies only investigated potential short-term protective effects after initiation of reperfusion and did not examine sustained protective effects. Therefore in **chapter 3,** we investigated potential short- and long-term protective effects of the antioxidant monoHER after cardiac ischaemia-reperfusion. In this study monoHER was administered one hour before ischaemia. MonoHER was chosen for this study because it has strong radical scavenging and iron chelating properties. This capacity makes it a potential drug for the prevention of oxidative stress-related reperfusion injury. In addition, monoHER protects against doxorubicin-induced cardiotoxicity *in vivo* in mice.

In the prevention of "reperfusion injury", administering an antioxidant as a protective drug before the onset of ischaemia has less clinical relevance. In addition, recent pharmacokinetic data revealed that following intravenous injection of

monoHER in mice, maximal myocardial tissue concentrations of the drug are reached almost immediately. For that reason, in **chapter 4** we examined whether monoHER also acts cardioprotective when administered right before reperfusion of an ischaemic mouse heart.

To our knowledge, only three studies have applied 2-D gel electrophoresis to identify changes in protein levels after myocardial infarction i.e. in an *in vivo* canine [362] and rabbit model [361] of myocardial ischaemia-reperfusion and in an *in vitro* rat model [361] of cardiac ischaemia or ischaemia-reperfusion. The classes of proteins that are differentially expressed after myocardial infarction vary considerably between these studies. To date, two-dimensional gel electrophoresis combined with mass spectrometry has not been applied to identify alterations in protein expression in myocardial tissue after *in vivo* myocardial infarction in mice. In addition, only one study compared changes in protein expression after both ischaemia and ischaemia-reperfusion, although they used an *in vitro* rat model and no *in vivo* model. Therefore, the goal of the study described in **chapter 5** was to identify changes in cardiac protein expression after *in vivo* myocardial infarction in the mouse. Our mouse models of permanent myocardial infarction and ischaemia-reperfusion were used to identify and distinguish common and specific changes in protein expression in these models. We studied early changes in protein expression in order to identify potential new targets for cardioprotection that are beneficial in the first few hours of myocardial infarction. In addition, by separately analyzing the soluble cytosolic fraction and the membrane fraction we investigated potential pathology-related protein translocations.

To explain the discrepancy in results obtained with the two time points of monoHER administration, i.e. before ischaemia versus right before reperfusion, we hypothesized that monoHER has an influence on a signal transduction pathway that might be associated to its protective mechanism of action. Consequently in **chapter 6** we used this proteomics approach in order to find related changes in protein expression or post-translational modifications of certain proteins specifically influenced by monoHER therapy.

In **chapter 7**, a summary with conclusion and implications is represented.

References

1. Janssen B, De Celle T, Paquay J, Smits J, Blankesteijn M. Structural and Functional Adaptations of the Heart after Coronary Artery Ligation in the Mouse. In: Ince C, ed. The Physiological Genomics of the Critically Ill Mouse. Vol. 16. Boston/Dordrecht/London: Kluwer Academic Publishers; 2003: 211.
2. Redfield MM. Heart failure--an epidemic of uncertain proportions. N Engl J Med. 2002; 347: 1442.
3. Bayat H, Swaney JS, *et al.* Progressive heart failure after myocardial infarction in mice. Basic Res Cardiol. 2002; 97: 206.
4. Kanno S, Lerner DL, *et al.* Echocardiographic evaluation of ventricular remodeling in a mouse model of myocardial infarction. J Am Soc Echocardiogr. 2002; 15: 601.
5. Liao Y, Ishikura F, *et al.* Echocardiographic assessment of LV hypertrophy and function in aortic-banded mice: necropsy validation. Am J Physiol Heart Circ Physiol. 2002; 282: H1703.
6. Manning WJ, Wei JY, *et al.* Echocardiographically detected myocardial infarction in the mouse. Lab Anim Sci. 1993; 43: 583.
7. Patten RD, Aronovitz MJ, *et al.* Ventricular remodeling in a mouse model of myocardial infarction. Am J Physiol. 1998; 274: H1812.
8. Scherrer-Crosbie M, Steudel W, *et al.* Three-dimensional echocardiographic assessment of left ventricular wall motion abnormalities in mouse myocardial infarction. J Am Soc Echocardiogr. 1999; 12: 834.
9. Scherrer-Crosbie M, Steudel W, *et al.* Echocardiographic determination of risk area size in a murine model of myocardial ischemia. Am J Physiol. 1999; 277: H986.
10. Yang XP, Liu YH, *et al.* Echocardiographic assessment of cardiac function in conscious and anesthetized mice. Am J Physiol. 1999; 277: H1967.
11. Ross AJ, Yang Z, *et al.* Serial MRI evaluation of cardiac structure and function in mice after reperfused myocardial infarction. Magn Reson Med. 2002; 47: 1158.
12. Wiesmann F, Frydrychowicz A, *et al.* Analysis of right ventricular function in healthy mice and a murine model of heart failure by in vivo MRI. Am J Physiol Heart Circ Physiol. 2002; 283: H1065.
13. Takemura G, Fujiwara H, *et al.* High frequency of spontaneous acute myocardial infarction due to small coronary artery disease in dead (NZWxBXSB)F1 male mice. Am J Pathol. 1989; 135: 989.
14. Yoshida H, Fujiwara H, *et al.* Quantitative analysis of myocardial infarction in (NZW x BXSB)F1 hybrid mice with systemic lupus erythematosus and small coronary artery disease. Am J Pathol. 1987; 129: 477.
15. Antos CL, McKinsey TA, *et al.* Activated glycogen synthase-3 beta suppresses cardiac hypertrophy in vivo. Proc Natl Acad Sci U S A. 2002; 99: 907.
16. van Acker SA, Kramer K, *et al.* Monohydroxyethylrutoside as protector against chronic doxorubicin- induced cardiotoxicity. Br J Pharmacol. 1995; 115: 1260.
17. Yoshida A, Kand T, *et al.* Interleukin-18 reduces expression of cardiac tumor necrosis factor-alpha and atrial natriuretic peptide in a murine model of viral myocarditis. Life Sci. 2002; 70: 1225.
18. Lutgens E, Daemen MJ, *et al.* Chronic myocardial infarction in the mouse: cardiac structural and functional changes. Cardiovasc Res. 1999; 41: 586.
19. Blankesteijn WM, Creemers E, *et al.* Dynamics of cardiac wound healing following myocardial infarction: observations in genetically altered mice. Acta Physiol Scand. 2001; 173: 75.

20. Creemers EE, Davis JN, *et al.* Deficiency of Tissue Inhibitor of Matrix Metalloproteinase-1 Exacerbates LV Remodeling Following Myocardial Infarction in Mice. Am J Physiol Heart Circ Physiol. 2002; 26: 26.
21. Tall AR. MIghty mouse. Circ Res. 2002; 90: 244.
22. Eren M, Painter CA, *et al.* Age-dependent spontaneous coronary arterial thrombosis in transgenic mice that express a stable form of human plasminogen activator inhibitor-1. Circulation. 2002; 106: 491.
23. Aartsen WM, Schuijt MP, *et al.* The role of locally expressed angiotensin converting enzyme in cardiac remodeling after myocardial infarction in mice. Cardiovasc Res. 2002; 56: 205.
24. Creemers EE, Cleutjens JP, *et al.* Matrix metalloproteinase inhibition after myocardial infarction: a new approach to prevent heart failure? Circ Res. 2001; 89: 201.
25. Kogan ME, Belov LN, *et al.* [Modeling of myocardial pathology in mice with the surgical methods]. Kardiologiia. 1977; 17: 125.
26. Janssen B, Debets J, *et al.* Chronic measurement of cardiac output in conscious mice. Am J Physiol Regul Integr Comp Physiol. 2002; 282: R928.
27. De Celle T, Heeringa P, *et al.* 7-Monohydroxyethylrutoside, a semisynthetic flavonoid, prevents deterioration of cardiac function in a mouse model of myocardial-ischemia. Hypertension. 2002; 40: 568 (abstract).
28. Chien GL, Wolff RA, *et al.* "Normothermic range" temperature affects myocardial infarct size. Cardiovasc Res. 1994; 28: 1014.
29. Guo Y, Wu WJ, *et al.* Demonstration of an early and a late phase of ischemic preconditioning in mice. Am J Physiol. 1998; 275: H1375.
30. Dumont EA, Hofstra L, *et al.* Cardiomyocyte death induced by myocardial ischemia and reperfusion: measurement with recombinant human annexin-V in a mouse model. Circulation. 2000; 102: 1564.
31. Willems IE, Havenith MG, *et al.* The alpha-smooth muscle actin-positive cells in healing human myocardial scars. Am J Pathol. 1994; 145: 868.
32. Michael LH, Ballantyne CM, *et al.* Myocardial infarction and remodeling in mice: effect of reperfusion. Am J Physiol. 1999; 277: H660.
33. Gao XM, Dart AM, *et al.* Serial echocardiographic assessment of left ventricular dimensions and function after myocardial infarction in mice. Cardiovasc Res. 2000; 45: 330.
34. Xu J, Carretero OA, *et al.* Role of AT2 receptors in the cardioprotective effect of AT1 antagonists in mice. Hypertension. 2002; 40: 244.
35. Creemers E, Cleutjens J, *et al.* Disruption of the plasminogen gene in mice abolishes wound healing after myocardial infarction. Am J Pathol. 2000; 156: 1865.
36. Heymans S, Luttun A, *et al.* Inhibition of plasminogen activators or matrix metalloproteinases prevents cardiac rupture but impairs therapeutic angiogenesis and causes cardiac failure. Nat Med. 1999; 5: 1135.
37. Blankesteijn WM, Essers-Janssen YP, *et al.* A homologue of Drosophila tissue polarity gene frizzled is expressed in migrating myofibroblasts in the infarcted rat heart. Nat Med. 1997; 3: 541.
38. Gijn Mv, Eftekhari P, *et al.* Immunization of mice with a fragment of the frizzled 2 protein attenuates wound healing after myocardial infarction. Circulation. 2001; 104: II.
39. Barandon L, Couffinhal T, *et al.* FrzA overexpression in transgenic mouse reduces infarct size and modifies infarct healing. Circulation. 2002; 106: II.
40. Blankesteijn WM, van Gijn ME, *et al.* Beta-catenin, an inducer of uncontrolled cell proliferation and migration in malignancies, is localized in the cytoplasm of vascular endothelium during neovascularization after myocardial infarction. Am J Pathol. 2000; 157: 877.
41. Hoffmeyer MR, Jones SP, *et al.* Myocardial ischemia/reperfusion injury in NADPH oxidase-deficient mice. Circ Res. 2000; 87: 812.

42. Yang Z, Bove CM, *et al.* Angiotensin II type 2 receptor overexpression preserves left ventricular function after myocardial infarction. Circulation. 2002; 106: 106.
43. Shusterman V, Usiene I, *et al.* Strain-specific patterns of autonomic nervous system activity and heart failure susceptibility in mice. Am J Physiol Heart Circ Physiol. 2002; 282: H2076.
44. Gould KE, Taffet GE, *et al.* Heart failure and greater infarct expansion in middle-aged mice: a relevant model for postinfarction failure. Am J Physiol Heart Circ Physiol. 2002; 282: H615.
45. Nemoto S, DeFreitas G, *et al.* Effects of changes in left ventricular contractility on indexes of contractility in mice. Am J Physiol Heart Circ Physiol. 2002; 283: H2504.
46. Janssen BJ, Smits JF. Autonomic control of blood pressure in mice: basic physiology and effects of genetic modification. Am J Physiol Regul Integr Comp Physiol. 2002; 282: R1545.
47. Georgakopoulos D, Kass D. Minimal force-frequency modulation of inotropy and relaxation of in situ murine heart. J Physiol. 2001; 534: 535.
48. Williams TD, Chambers JB, *et al.* Cardiovascular responses to caloric restriction and thermoneutrality in C57BL/6J mice. Am J Physiol Regul Integr Comp Physiol. 2002; 282: R1459.
49. Janssen BJ, Leenders PJ, *et al.* Short-term and long-term blood pressure and heart rate variability in the mouse. Am J Physiol Regul Integr Comp Physiol. 2000; 278: R215.
50. Just A, Faulhaber J, *et al.* Autonomic cardiovascular control in conscious mice. Am J Physiol Regul Integr Comp Physiol. 2000; 279: R2214.
51. Radaelli A, Perlangeli S, *et al.* Altered blood pressure variability in patients with congestive heart failure. J Hypertens. 1999; 17: 1905.
52. Stassen FR, Fazzi GE, *et al.* Coronary arterial hyperreactivity and mesenteric arterial hyporeactivity after myocardial infarction in the rat. J Cardiovasc Pharmacol. 1997; 29: 780.
53. Koren G, Weiss AT, *et al.* Prevention of myocardial damage in acute myocardial ischemia by early treatment with intravenous streptokinase. N Engl J Med. 1985; 313: 1384.
54. Braunwald E, Kloner RA. Myocardial reperfusion: a double-edged sword? J Clin Invest. 1985; 76: 1713.
55. Simpson PJ, Lucchesi BR. Free radicals and myocardial ischemia and reperfusion injury. J Lab Clin Med. 1987; 110: 13.
56. Hansen PR. Role of neutrophils in myocardial ischemia and reperfusion. Circulation. 1995; 91: 1872.
57. Ma XL, Weyrich AS, *et al.* Diminished basal nitric oxide release after myocardial ischemia and reperfusion promotes neutrophil adherence to coronary endothelium. Circ Res. 1993; 72: 403.
58. Arroyo CM, Kramer JH, *et al.* Identification of free radicals in myocardial ischemia/reperfusion by spin trapping with nitrone DMPO. FEBS Lett. 1987; 221: 101.
59. Arroyo CM, Kramer JH, *et al.* Spin trapping of oxygen and carbon-centered free radicals in ischemic canine myocardium. Free Radic Biol Med. 1987; 3: 313.
60. Kramer JH, Arroyo CM, *et al.* Spin-trapping evidence that graded myocardial ischemia alters post-ischemic superoxide production. Free Radic Biol Med. 1987; 3: 153.
61. Godin DV, Garnett ME. Altered antioxidant status in the ischemic/reperfused rabbit myocardium: effects of allopurinol. Can J Cardiol. 1989; 5: 365.
62. Chatham JC, Seymour AL, *et al.* Depletion of myocardial glutathione: its effects on heart function and metabolism during ischaemia and reperfusion. Cardiovasc Res. 1988; 22: 833.
63. Leichtweis S, Ji LL. Glutathione deficiency intensifies ischaemia-reperfusion induced cardiac dysfunction and oxidative stress. Acta Physiol Scand. 2001; 172: 1.
64. Pyles LA, Fortney JE, *et al.* Plasma antioxidant depletion after cardiopulmonary bypass in operations for congenital heart disease. J Thorac Cardiovasc Surg. 1995; 110: 165.
65. Pietri S, Culcasi M, *et al.* Ascorbyl free radical as a reliable indicator of free-radical-mediated myocardial ischemic and post-ischemic injury. A real-time continuous-flow ESR study. Eur J Biochem. 1990; 193: 845.

66. Ko KM, Garnett ME, *et al.* Altered antioxidant status in ischemic/reperfused rabbit myocardium: reperfusion time-course study. Can J Cardiol. 1990; 6: 299.
67. Bolli R. Mechanism of myocardial "stunning". Circulation. 1990; 82: 723.
68. Jennings RB, Ganote CE. Mitochondrial structure and function in acute myocardial ischemic injury. Circ Res. 1976; 38: 180.
69. Moncada S, Palmer RM, *et al.* Biosynthesis of nitric oxide from L-arginine. A pathway for the regulation of cell function and communication. Biochem Pharmacol. 1989; 38: 1709.
70. Sadek HA, Nulton-Persson AC, *et al.* Cardiac ischemia/reperfusion, aging, and redox-dependent alterations in mitochondrial function. Arch Biochem Biophys. 2003; 420: 201.
71. Chance B, Williams GR. The respiratory chain and oxidative phosphorylation. Adv Enzymol Relat Subj Biochem. 1956; 17: 65.
72. Cadenas E, Davies KJ. Mitochondrial free radical generation, oxidative stress, and aging. Free Radic Biol Med. 2000; 29: 222.
73. Cadenas E, Boveris A, *et al.* Production of superoxide radicals and hydrogen peroxide by NADH-ubiquinone reductase and ubiquinol-cytochrome c reductase from beef-heart mitochondria. Arch Biochem Biophys. 1977; 180: 248.
74. Cadenas E, Boveris A. Enhancement of hydrogen peroxide formation by protophores and ionophores in antimycin-supplemented mitochondria. Biochem J. 1980; 188: 31.
75. Turrens JF, Boveris A. Generation of superoxide anion by the NADH dehydrogenase of bovine heart mitochondria. Biochem J. 1980; 191: 421.
76. Nohl H, Breuninger V, *et al.* Influence of mitochondrial radical formation on energy-linked respiration. Eur J Biochem. 1978; 90: 385.
77. Nohl H, Hegner D. Do mitochondria produce oxygen radicals in vivo? Eur J Biochem. 1978; 82: 563.
78. Boveris A, Chance B. The mitochondrial generation of hydrogen peroxide. General properties and effect of hyperbaric oxygen. Biochem J. 1973; 134: 707.
79. Boveris A, Cadenas E. Mitochondrial production of superoxide anions and its relationship to the antimycin insensitive respiration. FEBS Lett. 1975; 54: 311.
80. Loschen G, Azzi A, *et al.* Mitochondrial H2O2 formation: relationship with energy conservation. FEBS Lett. 1973; 33: 84.
81. Boveris A. Determination of the production of superoxide radicals and hydrogen peroxide in mitochondria. Methods Enzymol. 1984; 105: 429.
82. Duan J, Karmazyn M. Relationship between oxidative phosphorylation and adenine nucleotide translocase activity of two populations of cardiac mitochondria and mechanical recovery of ischemic hearts following reperfusion. Can J Physiol Pharmacol. 1989; 67: 704.
83. Hardy L, Clark JB, *et al.* Reoxygenation-dependent decrease in mitochondrial NADH: CoQ reductase (Complex I) activity in the hypoxic/reoxygenated rat heart. Biochem J. 1991; 274 (Pt 1): 133.
84. Lesnefsky EJ, Tandler B, *et al.* Myocardial ischemia decreases oxidative phosphorylation through cytochrome oxidase in subsarcolemmal mitochondria. Am J Physiol. 1997; 273: H1544.
85. Veitch K, Hombroeckx A, *et al.* Global ischaemia induces a biphasic response of the mitochondrial respiratory chain. Anoxic pre-perfusion protects against ischaemic damage. Biochem J. 1992; 281 (Pt 3): 709.
86. Vuorinen K, Ylitalo K, *et al.* Mechanisms of ischemic preconditioning in rat myocardium. Roles of adenosine, cellular energy state, and mitochondrial F1F0-ATPase. Circulation. 1995; 91: 2810.
87. Rouslin W. Mitochondrial complexes I, II, III, IV, and V in myocardial ischemia and autolysis. Am J Physiol. 1983; 244: H743.

88. Chen J, Henderson GI, *et al.* Role of 4-hydroxynonenal in modification of cytochrome c oxidase in ischemia/reperfused rat heart. J Mol Cell Cardiol. 2001; 33: 1919.
89. Vander Heide RS, Hill ML, *et al.* Effect of reversible ischemia on the activity of the mitochondrial ATPase: relationship to ischemic preconditioning. J Mol Cell Cardiol. 1996; 28: 103.
90. Granger DN, Rutili G, *et al.* Superoxide radicals in feline intestinal ischemia. Gastroenterology. 1981; 81: 22.
91. Berry CE, Hare JM. Xanthine oxidoreductase and cardiovascular disease: molecular mechanisms and pathophysiological implications. J Physiol. 2004; 555: 589.
92. Parks DA, Granger DN. Xanthine oxidase: biochemistry, distribution and physiology. Acta Physiol Scand Suppl. 1986; 548: 87.
93. Jarasch ED, Bruder G, *et al.* Significance of xanthine oxidase in capillary endothelial cells. Acta Physiol Scand Suppl. 1986; 548: 39.
94. de Jong JW, van der Meer P, *et al.* Xanthine oxidoreductase activity in perfused hearts of various species, including humans. Circ Res. 1990; 67: 770.
95. Muxfeldt M, Schaper W. The activity of xanthine oxidase in heart of pigs, guinea pigs, rabbits, rats, and humans. Basic Res Cardiol. 1987; 82: 486.
96. Linder N, Rapola J, *et al.* Cellular expression of xanthine oxidoreductase protein in normal human tissues. Lab Invest. 1999; 79: 967.
97. Jarasch ED, Grund C, *et al.* Localization of xanthine oxidase in mammary-gland epithelium and capillary endothelium. Cell. 1981; 25: 67.
98. Bruder G, Jarasch ED, *et al.* High concentrations of antibodies to xanthine oxidase in human and animal sera. Molecular characterization. J Clin Invest. 1984; 74: 783.
99. Abadeh S, Case PC, *et al.* Purification of xanthine oxidase from human heart. Biochem Soc Trans. 1993; 21: 99S.
100. Cappola TP, Kass DA, *et al.* Allopurinol improves myocardial efficiency in patients with idiopathic dilated cardiomyopathy. Circulation. 2001; 104: 2407.
101. Vickers S, Schiller HJ, *et al.* Immunoaffinity localization of the enzyme xanthine oxidase on the outside surface of the endothelial cell plasma membrane. Surgery. 1998; 124: 551.
102. Eddy LJ, Stewart JR, *et al.* Free radical-producing enzyme, xanthine oxidase, is undetectable in human hearts. Am J Physiol. 1987; 253: H709.
103. Rouquette M, Page S, *et al.* Xanthine oxidoreductase is asymmetrically localised on the outer surface of human endothelial and epithelial cells in culture. FEBS Lett. 1998; 426: 397.
104. Mitsos SE, Askew TE, *et al.* Protective effects of N-2-mercaptopropionyl glycine against myocardial reperfusion injury after neutrophil depletion in the dog: evidence for the role of intracellular-derived free radicals. Circulation. 1986; 73: 1077.
105. Duilio C, Ambrosio G, *et al.* Neutrophils are primary source of O2 radicals during reperfusion after prolonged myocardial ischemia. Am J Physiol Heart Circ Physiol. 2001; 280: H2649.
106. Rossi F. The O2- -forming NADPH oxidase of the phagocytes: nature, mechanisms of activation and function. Biochim Biophys Acta. 1986; 853: 65.
107. Taniyama Y, Griendling KK. Reactive oxygen species in the vasculature: molecular and cellular mechanisms. Hypertension. 2003; 42: 1075.
108. Nathan C. Inducible nitric oxide synthase: what difference does it make? J Clin Invest. 1997; 100: 2417.
109. Bates TE, Loesch A, *et al.* Immunocytochemical evidence for a mitochondrially located nitric oxide synthase in brain and liver. Biochem Biophys Res Commun. 1995; 213: 896.
110. Bates TE, Loesch A, *et al.* Mitochondrial nitric oxide synthase: a ubiquitous regulator of oxidative phosphorylation? Biochem Biophys Res Commun. 1996; 218: 40.
111. Bringold U, Ghafourifar P, *et al.* Peroxynitrite formed by mitochondrial NO synthase promotes mitochondrial Ca2+ release. Free Radic Biol Med. 2000; 29: 343.

112. Packer MA, Porteous CM, *et al.* Superoxide production by mitochondria in the presence of nitric oxide forms peroxynitrite. Biochem Mol Biol Int. 1996; 40: 527.
113. Groves JT, Wang CC. Nitric oxide synthase: models and mechanisms. Curr Opin Chem Biol. 2000; 4: 687.
114. Aust SD, Roerig DL, *et al.* Evidence for superoxide generation by NADPH-cytochrome c reductase of rat liver microsomes. Biochem Biophys Res Commun. 1972; 47: 1133.
115. Capdevila J, Parkhill L, *et al.* The oxidative metabolism of arachidonic acid by purified cytochromes P-450. Biochem Biophys Res Commun. 1981; 101: 1357.
116. Freeman BA, Crapo JD. Biology of disease: free radicals and tissue injury. Lab Invest. 1982; 47: 412.
117. Halliwell B, Gutteridge. Free Radicals in Biology and Medecine: Oxford Univesrity Press; 1989: 22.
118. Boveris A, Oshino N, *et al.* The cellular production of hydrogen peroxide. Biochem J. 1972; 128: 617.
119. Tolbert NE, Essner E. Microbodies: peroxisomes and glyoxysomes. J Cell Biol. 1981; 91: 271s.
120. Baud L, Ardaillou R. Reactive oxygen species: production and role in the kidney. Am J Physiol. 1986; 251: F765.
121. Lim LK, Hunt NH, *et al.* Reactive oxygen production, arachidonate metabolism and cyclic AMP in macrophages. Biochem Biophys Res Commun. 1983; 114: 549.
122. Nakamura Y, Colburn NH, *et al.* Role of reactive oxygen in tumor promotion: implication of superoxide anion in promotion of neoplastic transformation in JB-6 cells by TPA. Carcinogenesis. 1985; 6: 229.
123. Singh D, Greenwald JE, *et al.* Evidence for the generation of hydroxyl radical during arachidonic acid metabolism by human platelets. Am J Hematol. 1981; 11: 233.
124. Garlick PB, Davies MJ, *et al.* Direct detection of free radicals in the reperfused rat heart using electron spin resonance spectroscopy. Circ Res. 1987; 61: 757.
125. Zweier JL, Flaherty JT, *et al.* Direct measurement of free radical generation following reperfusion of ischemic myocardium. Proc Natl Acad Sci U S A. 1987; 84: 1404.
126. Zweier JL. Measurement of superoxide-derived free radicals in the reperfused heart. Evidence for a free radical mechanism of reperfusion injury. J Biol Chem. 1988; 263: 1353.
127. Bolli R, Patel BS, *et al.* Demonstration of free radical generation in "stunned" myocardium of intact dogs with the use of the spin trap alpha-phenyl N-tert-butyl nitrone. J Clin Invest. 1988; 82: 476.
128. Flaherty JT, Weisfeldt ML. Reperfusion injury. Free Radic Biol Med. 1988; 5: 409.
129. McCord JM. Free radicals and myocardial ischemia: overview and outlook. Free Radic Biol Med. 1988; 4: 9.
130. Ambrosio G, Zweier JL, *et al.* The relationship between oxygen radical generation and impairment of myocardial energy metabolism following post-ischemic reperfusion. J Mol Cell Cardiol. 1991; 23: 1359.
131. Xia Y, Khatchikian G, *et al.* Adenosine deaminase inhibition prevents free radical-mediated injury in the postischemic heart. J Biol Chem. 1996; 271: 10096.
132. Kuzuya T, Hoshida S, *et al.* Detection of oxygen-derived free radical generation in the canine postischemic heart during late phase of reperfusion. Circ Res. 1990; 66: 1160.
133. Berlett BS, Stadtman ER. Protein oxidation in aging, disease, and oxidative stress. J Biol Chem. 1997; 272: 20313.
134. Kaplan P, Matejovicova M, *et al.* Effect of myocardial stunning on thiol status, myofibrillar ATPase and troponin I proteolysis. Mol Cell Biochem. 2002; 233: 145.
135. Eaton P, Wright N, *et al.* Glyceraldehyde phosphate dehydrogenase oxidation during cardiac ischemia and reperfusion. J Mol Cell Cardiol. 2002; 34: 1549.

136. Eaton P, Byers HL, *et al.* Detection, quantitation, purification, and identification of cardiac proteins S-thiolated during ischemia and reperfusion. J Biol Chem. 2002; 277: 9806.
137. Esterbauer H, Schaur RJ, *et al.* Chemistry and biochemistry of 4-hydroxynonenal, malonaldehyde and related aldehydes. Free Radic Biol Med. 1991; 11: 81.
138. Uchida K, Stadtman ER. Covalent attachment of 4-hydroxynonenal to glyceraldehyde-3-phosphate dehydrogenase. A possible involvement of intra- and intermolecular cross-linking reaction. J Biol Chem. 1993; 268: 6388.
139. Kristal BS, Yu BP. An emerging hypothesis: synergistic induction of aging by free radicals and Maillard reactions. J Gerontol. 1992; 47: B107.
140. Levine RL, Williams JA, *et al.* Carbonyl assays for determination of oxidatively modified proteins. Methods Enzymol. 1994; 233: 346.
141. Powell SR, Gurzenda EM, *et al.* Actin is oxidized during myocardial ischemia. Free Radic Biol Med. 2001; 30: 1171.
142. Canton M, Neverova I, *et al.* Evidence of myofibrillar protein oxidation induced by postischemic reperfusion in isolated rat hearts. Am J Physiol Heart Circ Physiol. 2004; 286: H870.
143. White MY, Cordwell SJ, *et al.* Modifications of myosin-regulatory light chain correlate with function of stunned myocardium. J Mol Cell Cardiol. 2003; 35: 833.
144. Grune T, Merker K, *et al.* Selective degradation of oxidatively modified protein substrates by the proteasome. Biochem Biophys Res Commun. 2003; 305: 709.
145. Bulteau AL, Lundberg KC, *et al.* Oxidative modification and inactivation of the proteasome during coronary occlusion/reperfusion. J Biol Chem. 2001; 276: 30057.
146. Eaton P, Hearse DJ, *et al.* Lipid hydroperoxide modification of proteins during myocardial ischaemia. Cardiovasc Res. 2001; 51: 294.
147. Koller PT, Bergmann SR. Reduction of lipid peroxidation in reperfused isolated rabbit hearts by diltiazem. Circ Res. 1989; 65: 838.
148. Ambrosio G, Flaherty JT, *et al.* Oxygen radicals generated at reflow induce peroxidation of membrane lipids in reperfused hearts. J Clin Invest. 1991; 87: 2056.
149. Tavazzi B, Lazzarino G, *et al.* Malondialdehyde production and ascorbate decrease are associated to the reperfusion of the isolated postischemic rat heart. Free Radic Biol Med. 1992; 13: 75.
150. Kramer JH, Misik V, *et al.* Lipid peroxidation-derived free radical production and postischemic myocardial reperfusion injury. Ann N Y Acad Sci. 1994; 723: 180.
151. Blasig IE, Grune T, *et al.* 4-Hydroxynonenal, a novel indicator of lipid peroxidation for reperfusion injury of the myocardium. Am J Physiol. 1995; 269: H14.
152. Cordis GA, Maulik N, *et al.* Detection of oxidative stress in heart by estimating the dinitrophenylhydrazine derivative of malonaldehyde. J Mol Cell Cardiol. 1995; 27: 1645.
153. Pucheu S, Coudray C, *et al.* Assessment of radical activity during the acute phase of myocardial infarction following fibrinolysis: utility of assaying plasma malondialdehyde. Free Radic Biol Med. 1995; 19: 873.
154. Friguet B, Stadtman ER, *et al.* Modification of glucose-6-phosphate dehydrogenase by 4-hydroxy-2-nonenal. Formation of cross-linked protein that inhibits the multicatalytic protease. J Biol Chem. 1994; 269: 21639.
155. Nadkarni DV, Sayre LM. Structural definition of early lysine and histidine adduction chemistry of 4-hydroxynonenal. Chem Res Toxicol. 1995; 8: 284.
156. Tsai L, Sokoloski EA. The reaction of 4-hydroxy-2-nonenal with N alpha-acetyl-L-histidine. Free Radic Biol Med. 1995; 19: 39.
157. Cohn JA, Tsai L, *et al.* Chemical characterization of a protein-4-hydroxy-2-nonenal cross-link: immunochemical detection in mitochondria exposed to oxidative stress. Arch Biochem Biophys. 1996; 328: 158.

158. Szweda LI, Uchida K, *et al.* Inactivation of glucose-6-phosphate dehydrogenase by 4-hydroxy-2-nonenal. Selective modification of an active-site lysine. J Biol Chem. 1993; 268: 3342.
159. Chen JJ, Bertrand H, *et al.* Inhibition of adenine nucleotide translocator by lipid peroxidation products. Free Radic Biol Med. 1995; 19: 583.
160. Eaton P, Li JM, *et al.* Formation of 4-hydroxy-2-nonenal-modified proteins in ischemic rat heart. Am J Physiol. 1999; 276: H935.
161. Das DK, George A, *et al.* Detection of hydroxyl radical in the mitochondria of ischemic-reperfused myocardium by trapping with salicylate. Biochem Biophys Res Commun. 1989; 165: 1004.
162. Ambrosio G, Zweier JL, *et al.* Evidence that mitochondrial respiration is a source of potentially toxic oxygen free radicals in intact rabbit hearts subjected to ischemia and reflow. J Biol Chem. 1993; 268: 18532.
163. Lucas DT, Szweda LI. Cardiac reperfusion injury: aging, lipid peroxidation, and mitochondrial dysfunction. Proc Natl Acad Sci U S A. 1998; 95: 510.
164. Humphries KM, Yoo Y, *et al.* Inhibition of NADH-linked mitochondrial respiration by 4-hydroxy-2-nonenal. Biochemistry. 1998; 37: 552.
165. Lucas DT, Szweda LI. Declines in mitochondrial respiration during cardiac reperfusion: age-dependent inactivation of alpha-ketoglutarate dehydrogenase. Proc Natl Acad Sci U S A. 1999; 96: 6689.
166. Haenen GR, Plug HJ, *et al.* Contribution of 4-hydroxy-2,3-trans-nonenal to the reduction of beta-adrenoceptor function in the heart by oxidative stress. Life Sci. 1989; 45: 71.
167. Kasai H. Analysis of a form of oxidative DNA damage, 8-hydroxy-2'-deoxyguanosine, as a marker of cellular oxidative stress during carcinogenesis. Mutat Res. 1997; 387: 147.
168. Maki H, Sekiguchi M. MutT protein specifically hydrolyses a potent mutagenic substrate for DNA synthesis. Nature. 1992; 355: 273.
169. Hayakawa M, Hattori K, *et al.* Age-associated oxygen damage and mutations in mitochondrial DNA in human hearts. Biochem Biophys Res Commun. 1992; 189: 979.
170. Melov S, Coskun P, *et al.* Mitochondrial disease in superoxide dismutase 2 mutant mice. Proc Natl Acad Sci U S A. 1999; 96: 846.
171. Ide T, Tsutsui H, *et al.* Mitochondrial DNA damage and dysfunction associated with oxidative stress in failing hearts after myocardial infarction. Circ Res. 2001; 88: 529.
172. Tsutsui H, Ide T, *et al.* 8-oxo-dGTPase, which prevents oxidative stress-induced DNA damage, increases in the mitochondria from failing hearts. Circulation. 2001; 104: 2883.
173. Gilad E, Zingarelli B, *et al.* Protection by inhibition of poly (ADP-ribose) synthetase against oxidant injury in cardiac myoblasts In vitro. J Mol Cell Cardiol. 1997; 29: 2585.
174. Grupp IL, Jackson TM, *et al.* Protection against hypoxia-reoxygenation in the absence of poly (ADP-ribose) synthetase in isolated working hearts. J Mol Cell Cardiol. 1999; 31: 297.
175. Jacobson MK, Jacobson EL. Discovering new ADP-ribose polymer cycles: protecting the genome and more. Trends Biochem Sci. 1999; 24: 415.
176. Lindahl T, Satoh MS, *et al.* Post-translational modification of poly(ADP-ribose) polymerase induced by DNA strand breaks. Trends Biochem Sci. 1995; 20: 405.
177. Radons J, Heller B, *et al.* Nitric oxide toxicity in islet cells involves poly(ADP-ribose) polymerase activation and concomitant NAD+ depletion. Biochem Biophys Res Commun. 1994; 199: 1270.
178. Szabados E, Fischer GM, *et al.* Role of reactive oxygen species and poly-ADP-ribose polymerase in the development of AZT-induced cardiomyopathy in rat. Free Radic Biol Med. 1999; 26: 309.
179. Szabo G, Bahrle S, *et al.* Poly(ADP-Ribose) polymerase inhibition reduces reperfusion injury after heart transplantation. Circ Res. 2002; 90: 100.

180. Szabados E, Literati-Nagy P, *et al.* BGP-15, a nicotinic amidoxime derivate protecting heart from ischemia reperfusion injury through modulation of poly(ADP-ribose) polymerase. Biochem Pharmacol. 2000; 59: 937.
181. Halmosi R, Berente Z, *et al.* Effect of poly(ADP-ribose) polymerase inhibitors on the ischemia-reperfusion-induced oxidative cell damage and mitochondrial metabolism in Langendorff heart perfusion system. Mol Pharmacol. 2001; 59: 1497.
182. Faro R, Toyoda Y, *et al.* Myocardial protection by PJ34, a novel potent poly (ADP-ribose) synthetase inhibitor. Ann Thorac Surg. 2002; 73: 575.
183. Thiemermann C, Bowes J, *et al.* Inhibition of the activity of poly(ADP ribose) synthetase reduces ischemia-reperfusion injury in the heart and skeletal muscle. Proc Natl Acad Sci U S A. 1997; 94: 679.
184. Bowes J, Ruetten H, *et al.* Reduction of myocardial reperfusion injury by an inhibitor of poly (ADP-ribose) synthetase in the pig. Eur J Pharmacol. 1998; 359: 143.
185. Dhalla NS, Elmoselhi AB, *et al.* Status of myocardial antioxidants in ischemia-reperfusion injury. Cardiovasc Res. 2000; 47: 446.
186. Guarnieri C, Flamigni F, *et al.* Glutathione peroxidase activity and release of glutathione from oxygen-deficient perfused rat heart. Biochem Biophys Res Commun. 1979; 89: 678.
187. Ferrari R, Ceconi C, *et al.* Oxygen-mediated myocardial damage during ischaemia and reperfusion: role of the cellular defences against oxygen toxicity. J Mol Cell Cardiol. 1985; 17: 937.
188. Peterson DA, Asinger RW, *et al.* Reactive oxygen species may cause myocardial reperfusion injury. Biochem Biophys Res Commun. 1985; 127: 87.
189. Shlafer M, Myers CL, *et al.* Mitochondrial hydrogen peroxide generation and activities of glutathione peroxidase and superoxide dismutase following global ischemia. J Mol Cell Cardiol. 1987; 19: 1195.
190. Arduini A, Mezzetti A, *et al.* Effect of ischemia and reperfusion on antioxidant enzymes and mitochondrial inner membrane proteins in perfused rat heart. Biochim Biophys Acta. 1988; 970: 113.
191. Barsacchi R, Coassin M, *et al.* Increased ultra weak chemiluminescence emission from rat heart at postischemic reoxygenation: protective role of vitamin E. Free Radic Biol Med. 1989; 6: 573.
192. Coudray C, Pucheu S, *et al.* Ischemia and reperfusion injury in isolated rat heart: effect of reperfusion duration on xanthine oxidase, lipid peroxidation, and enzyme antioxidant systems in myocardium. Basic Res Cardiol. 1992; 87: 478.
193. Porreca E, Del Boccio G, *et al.* Myocardial antioxidant defense mechanisms: time related changes after reperfusion of the ischemic rat heart. Free Radic Res. 1994; 20: 171.
194. Engelman DT, Watanabe M, *et al.* Hypoxic preconditioning preserves antioxidant reserve in the working rat heart. Cardiovasc Res. 1995; 29: 133.
195. Haramaki N, Stewart DB, *et al.* Networking antioxidants in the isolated rat heart are selectively depleted by ischemia-reperfusion. Free Radic Biol Med. 1998; 25: 329.
196. Mezzetti A, Lapenna D, *et al.* Myocardial antioxidant defenses during cardiopulmonary bypass. J Card Surg. 1993; 8: 167.
197. Barsacchi R, Pelosi G, *et al.* Myocardial vitamin E is consumed during cardiopulmonary bypass: indirect evidence of free radical generation in human ischemic heart. Int J Cardiol. 1992; 37: 339.
198. England MD, Cavarocchi NC, *et al.* Influence of antioxidants (mannitol and allopurinol) on oxygen free radical generation during and after cardiopulmonary bypass. Circulation. 1986; 74: III134.
199. Coghlan JG, Flitter WD, *et al.* Allopurinol pretreatment improves postoperative recovery and reduces lipid peroxidation in patients undergoing coronary artery bypass grafting. J Thorac Cardiovasc Surg. 1994; 107: 248.

200. Coghlan JG, Flitter WD, *et al.* Lipid peroxidation and changes in vitamin E levels during coronary artery bypass grafting. J Thorac Cardiovasc Surg. 1993; 106: 268.
201. Pantke U, Volk T, *et al.* Oxidized proteins as a marker of oxidative stress during coronary heart surgery. Free Radic Biol Med. 1999; 27: 1080.
202. De Vecchi E, Pala MG, *et al.* Relation between left ventricular function and oxidative stress in patients undergoing bypass surgery. Heart. 1998; 79: 242.
203. Starkopf J, Zilmer K, *et al.* Time course of oxidative stress during open-heart surgery. Scand J Thorac Cardiovasc Surg. 1995; 29: 181.
204. Ferrari R, Ceconi C, *et al.* Myocardial damage during ischaemia and reperfusion. Eur Heart J. 1993; 14 Suppl G: 25.
205. Ferrari R, Alfieri O, *et al.* Occurrence of oxidative stress during reperfusion of the human heart. Circulation. 1990; 81: 201.
206. Buffon A, Santini SA, *et al.* Large, sustained cardiac lipid peroxidation and reduced antioxidant capacity in the coronary circulation after brief episodes of myocardial ischemia. J Am Coll Cardiol. 2000; 35: 633.
207. Rigattieri S, Buffon A, *et al.* Oxidative stress in ischemia-reperfusion injury: assessment by three independent biochemical markers. Ital Heart J. 2000; 1: 68.
208. Tomasetti M, Alleva R, *et al.* Evaluation of ischemia-reperfusion damage during coronary angioplasty. Electrocardiographic assessment and biochemical modifications in blood from the coronary sinus. Ital Heart J. 2000; 1: 216.
209. Jolly SR, Kane WJ, *et al.* Canine myocardial reperfusion injury. Its reduction by the combined a dministration of superoxide dismutase and catalase. Circ Res. 1984; 54: 277.
210. Galang N, Sasaki H, *et al.* Apoptotic cell death during ischemia/reperfusion and its attenuation by antioxidant therapy. Toxicology. 2000; 148: 111.
211. Naslund U, Haggmark S, *et al.* Limitation of myocardial infarct size by superoxide dismutase as an adjunct to reperfusion after different durations of coronary occlusion in the pig. Circ Res. 1990; 66: 1294.
212. Przyklenk K, Kloner RA. Effect of oxygen-derived free radical scavengers on infarct size following six hours of permanent coronary artery occlusion: salvage or delay of myocyte necrosis? Basic Res Cardiol. 1987; 82: 146.
213. Nejima J, Knight DR, *et al.* Superoxide dismutase reduces reperfusion arrhythmias but fails to salvage regional function or myocardium at risk in conscious dogs. Circulation. 1989; 79: 143.
214. Watanabe BI, Premaratne S, *et al.* High- and low-dose superoxide dismutase plus catalase does not reduce myocardial infarct size in a subhuman primate model. Am Heart J. 1993; 126: 840.
215. Tanaka M, Richard VJ, *et al.* Superoxide dismutase plus catalase therapy delays neither cell death nor the loss of the TTC reaction in experimental myocardial infarction in dogs. J Mol Cell Cardiol. 1993; 25: 367.
216. Richard VJ, Murry CE, *et al.* Therapy to reduce free radicals during early reperfusion does not limit the size of myocardial infarcts caused by 90 minutes of ischemia in dogs. Circulation. 1988; 78: 473.
217. Mehta JL, Nichols WW, *et al.* Superoxide dismutase decreases reperfusion arrhythmias and preserves myocardial function during thrombolysis with tissue plasminogen activator. J Cardiovasc Pharmacol. 1990; 16: 112.
218. Qian ZM, Xu MF, *et al.* Superoxide dismutase does protect the cultured rat cardiac myocytes against hypoxia/reoxygenation injury. Free Radic Res. 1997; 27: 13.
219. Burton KP. Superoxide dismutase enhances recovery following myocardial ischemia. Am J Physiol. 1985; 248: H637.
220. Werns SW, Simpson PJ, *et al.* Sustained limitation by superoxide dismutase of canine myocardial injury due to regional ischemia followed by reperfusion. J Cardiovasc Pharmacol. 1988; 11: 36.

221. Hatori N, Tadokoro H, *et al.* Beneficial effects of coronary venous retroinfusion but not left atrial administration of superoxide dismutase on myocardial necrosis in pigs. Eur Heart J. 1991; 12: 442.

222. Ambrosio G, Becker LC, *et al.* Reduction in experimental infarct size by recombinant human superoxide dismutase: insights into the pathophysiology of reperfusion injury. Circulation. 1986; 74: 1424.

223. Ambrosio G, Zweier JL, *et al.* Apoptosis is prevented by administration of superoxide dismutase in dogs with reperfused myocardial infarction. Basic Res Cardiol. 1998; 93: 94.

224. Werns SW, Shea MJ, *et al.* The independent effects of oxygen radical scavengers on canine infarct size. Reduction by superoxide dismutase but not catalase. Circ Res. 1985; 56: 895.

225. Nakajima H, Hangaishi M, *et al.* Lecithinized copper, zinc-superoxide dismutase ameliorates ischemia-induced myocardial damage. Life Sci. 2001; 69: 935.

226. Nakajima H, Ishizaka N, *et al.* Lecithinized copper, zinc-superoxide dismutase ameliorates prolonged hypoxia-induced injury of cardiomyocytes. Free Radic Biol Med. 2000; 29: 34.

227. Tanaka M, Fujiwara H, *et al.* Superoxide dismutase and N-2-mercaptopropionyl glycine attenuate infarct size limitation effect of ischaemic preconditioning in the rabbit. Cardiovasc Res. 1994; 28: 980.

228. Uraizee A, Reimer KA, *et al.* Failure of superoxide dismutase to limit size of myocardial infarction after 40 minutes of ischemia and 4 days of reperfusion in dogs. Circulation. 1987; 75: 1237.

229. Patel BS, Jeroudi MO, *et al.* Effect of human recombinant superoxide dismutase on canine myocardial infarction. Am J Physiol. 1990; 258: H369.

230. Gallagher KP, Buda AJ, *et al.* Failure of superoxide dismutase and catalase to alter size of infarction in conscious dogs after 3 hours of occlusion followed by reperfusion. Circulation. 1986; 73: 1065.

231. Naslund U, Haggmark S, *et al.* Superoxide dismutase and catalase reduce infarct size in a porcine myocardial occlusion-reperfusion model. J Mol Cell Cardiol. 1986; 18: 1077.

232. Tamura Y, Chi LG, *et al.* Superoxide dismutase conjugated to polyethylene glycol provides sustained protection against myocardial ischemia/reperfusion injury in canine heart. Circ Res. 1988; 63: 944.

233. Tanaka M, Stoler RC, *et al.* Evidence against the "early protection-delayed death" hypothesis of superoxide dismutase therapy in experimental myocardial infarction. Polyethylene glycol-superoxide dismutase plus catalase does not limit myocardial infarct size in dogs. Circ Res. 1990; 67: 636.

234. Hangaishi M, Nakajima H, *et al.* Lecithinized Cu, Zn-superoxide dismutase limits the infarct size following ischemia-reperfusion injury in rat hearts in vivo. Biochem Biophys Res Commun. 2001; 285: 1220.

235. Masini E, Cuzzocrea S, *et al.* Protective effects of M40403, a selective superoxide dismutase mimetic, in myocardial ischaemia and reperfusion injury in vivo. Br J Pharmacol. 2002; 136: 905.

236. Kilgore KS, Friedrichs GS, *et al.* Protective effects of the SOD-mimetic SC-52608 against ischemia/reperfusion damage in the rabbit isolated heart. J Mol Cell Cardiol. 1994; 26: 995.

237. Li Q, Bolli R, *et al.* Gene therapy with extracellular superoxide dismutase protects conscious rabbits against myocardial infarction. Circulation. 2001; 103: 1893.

238. Woo YJ, Zhang JC, *et al.* Recombinant adenovirus-mediated cardiac gene transfer of superoxide dismutase and catalase attenuates postischemic contractile dysfunction. Circulation. 1998; 98: II255.

239. Chen Z, Siu B, *et al.* Overexpression of MnSOD protects against myocardial ischemia/reperfusion injury in transgenic mice. J Mol Cell Cardiol. 1998; 30: 2281.

240. Dewald O, Frangogiannis NG, *et al.* Development of murine ischemic cardiomyopathy is associated with a transient inflammatory reaction and depends on reactive oxygen species. Proc Natl Acad Sci U S A. 2003; 100: 2700.
241. Wang P, Chen H, *et al.* Overexpression of human copper, zinc-superoxide dismutase (SOD1) prevents postischemic injury. Proc Natl Acad Sci U S A. 1998; 95: 4556.
242. Chen Z, Oberley TD, *et al.* Overexpression of CuZnSOD in coronary vascular cells attenuates myocardial ischemia/reperfusion injury. Free Radic Biol Med. 2000; 29: 589.
243. Yoshida T, Maulik N, *et al.* Targeted disruption of the mouse Sod 1 gene makes the hearts vulnerable to ischemic reperfusion injury. Circ Res. 2000; 86: 264.
244. Jones SP, Hoffmeyer MR, *et al.* Role of intracellular antioxidant enzymes after in vivo myocardial ischemia and reperfusion. Am J Physiol Heart Circ Physiol. 2003; 284: H277.
245. Asimakis GK, Lick S, *et al.* Postischemic recovery of contractile function is impaired in SOD2(+/-) but not SOD1(+/-) mouse hearts. Circulation. 2002; 105: 981.
246. Vulapalli SR, Chen Z, *et al.* Cardioselective overexpression of HO-1 prevents I/R-induced cardiac dysfunction and apoptosis. Am J Physiol Heart Circ Physiol. 2002; 283: H688.
247. Yet SF, Tian R, *et al.* Cardiac-specific expression of heme oxygenase-1 protects against ischemia and reperfusion injury in transgenic mice. Circ Res. 2001; 89: 168.
248. Yoshida T, Watanabe M, *et al.* Transgenic mice overexpressing glutathione peroxidase are resistant to myocardial ischemia reperfusion injury. J Mol Cell Cardiol. 1996; 28: 1759.
249. Yoshida T, Maulik N, *et al.* Glutathione peroxidase knockout mice are susceptible to myocardial ischemia reperfusion injury. Circulation. 1997; 96: II.
250. Tappel AL. Vitamin E and free radical peroxidation of lipids. Ann N Y Acad Sci. 1972; 203: 12.
251. Guarnieri C, Ferrari R, *et al.* Effect of alpha-tocopherol on hypoxic-perfused and reoxygenated rabbit heart muscle. J Mol Cell Cardiol. 1978; 10: 893.
252. Massey KD, Burton KP. alpha-Tocopherol attenuates myocardial membrane-related alterations resulting from ischemia and reperfusion. Am J Physiol. 1989; 256: H1192.
253. Chen H, Li D, *et al.* Mixed tocopherol preparation is superior to alpha-tocopherol alone against hypoxia-reoxygenation injury. Biochem Biophys Res Commun. 2002; 291: 349.
254. Axford-Gatley RA, Wilson GJ. Reduction of experimental myocardial infarct size by oral administration of alpha tocopherol. Cardiovasc Res. 1991; 25: 89.
255. Klein HH, Pich S, *et al.* Failure of chronic, high-dose, oral vitamin E treatment to protect the ischemic, reperfused porcine heart. J Mol Cell Cardiol. 1993; 25: 103.
256. Ooiwa H, Janero DR, *et al.* Examination of two small-molecule antiperoxidative agents in a rabbit model of postischemic myocardial infarction. J Cardiovasc Pharmacol. 1991; 17: 761.
257. Klein HH, Pich S, *et al.* Combined treatment with vitamins E and C in experimental myocardial infarction in pigs. Am Heart J. 1989; 118: 667.
258. Altavilla D, Deodato B, *et al.* IRFI 042, a novel dual vitamin E-like antioxidant, inhibits activation of nuclear factor-kappaB and reduces the inflammatory response in myocardial ischemia-reperfusion injury. Cardiovasc Res. 2000; 47: 515.
259. Lukovic L, Petty MA, *et al.* Protection of infarcted, chronically reperfused hearts by an alpha-tocopherol analogue. Eur J Pharmacol. 1993; 233: 63.
260. Petty MA, Grisar JM, *et al.* Protective effects of an alpha-tocopherol analogue against myocardial reperfusion injury in rats. Eur J Pharmacol. 1992; 210: 85.
261. Petty M, Grisar JM, *et al.* Effects of an alpha-tocopherol analogue on myocardial ischaemia and reperfusion injury in rats. Eur J Pharmacol. 1990; 179: 241.
262. Petty MA, Dow J, *et al.* Effect of a cardioselective alpha-tocopherol analogue on reperfusion injury in rats induced by myocardial ischaemia. Eur J Pharmacol. 1991; 192: 383.
263. Campo GM, Squadrito F, *et al.* Beneficial effect of raxofelast, an hydrophilic vitamin E analogue, in the rat heart after ischemia and reperfusion injury. J Mol Cell Cardiol. 1998; 30: 1493.

264. Brookes PS, Digerness SB, *et al.* Mitochondrial function in response to cardiac ischemia-reperfusion after oral treatment with quercetin. Free Radic Biol Med. 2002; 32: 1220.

265. Lebeau J, Neviere R, *et al.* Beneficial effects of different flavonoids, on functional recovery after ischemia and reperfusion in isolated rat heart. Bioorg Med Chem Lett. 2001; 11: 23.

266. Shao ZH, Vanden Hoek TL, *et al.* Baicalein attenuates oxidant stress in cardiomyocytes. Am J Physiol Heart Circ Physiol. 2002; 282: H999.

267. Wu TW, Wu J, *et al.* Purpurogallin: in vivo evidence of a novel and effective cardioprotector. Life Sci. 1994; 54: PL23.

268. Hung LM, Chen JK, *et al.* Cardioprotective effect of resveratrol, a natural antioxidant derived from grapes. Cardiovasc Res. 2000; 47: 549.

269. Ray PS, Maulik G, *et al.* The red wine antioxidant resveratrol protects isolated rat hearts from ischemia reperfusion injury. Free Radic Biol Med. 1999; 27: 160.

270. Sato M, Maulik G, *et al.* Cardioprotective effects of grape seed proanthocyanidin against ischemic reperfusion injury. J Mol Cell Cardiol. 1999; 31: 1289.

271. Sato M, Bagchi D, *et al.* Grape seed proanthocyanidin reduces cardiomyocyte apoptosis by inhibiting ischemia/reperfusion-induced activation of JNK-1 and C-JUN. Free Radic Biol Med. 2001; 31: 729.

272. Hung LM, Chen JK, *et al.* Beneficial effects of astringinin, a resveratrol analogue, on the ischemia and reperfusion damage in rat heart. Free Radic Biol Med. 2001; 30: 877.

273. Chen Z, Chua CC, *et al.* Protective effect of melatonin on myocardial infarction. Am J Physiol Heart Circ Physiol. 2003; 284: H1618.

274. Kaneko S, Okumura K, *et al.* Melatonin scavenges hydroxyl radical and protects isolated rat hearts from ischemic reperfusion injury. Life Sci. 2000; 67: 101.

275. Salie R, Harper I, *et al.* Melatonin protects against ischaemic-reperfusion myocardial damage. J Mol Cell Cardiol. 2001; 33: 343.

276. Lagneux C, Joyeux M, *et al.* Protective effects of melatonin against ischemia-reperfusion injury in the isolated rat heart. Life Sci. 2000; 66: 503.

277. Granville DJ, Tashakkor B, *et al.* Reduction of ischemia and reperfusion-induced myocardial damage by cytochrome P450 inhibitors. Proc Natl Acad Sci U S A. 2004; 101: 1321.

278. Perna AM, Liguori P, *et al.* Protection of rat heart from ischaemia-reperfusion injury by the 21-aminosteroid U-74389G. Pharmacol Res. 1996; 34: 25.

279. Ovize M, de Lorgeril M, *et al.* U74006F, a novel 21-aminosteroid, inhibits in vivo lipid peroxidation but fails to limit infarct size in a canine model of myocardial ischemia reperfusion. Am Heart J. 1991; 122: 681.

280. Carrea FP, Lesnefsky EJ, *et al.* The lazaroid U74006F, a 21-aminosteroid inhibitor of lipid peroxidation, attenuates myocardial injury from ischemia and reperfusion. J Cardiovasc Pharmacol. 1992; 20: 230.

281. Shimizu M, Wang QD, *et al.* The lipid peroxidation inhibitor indenoindole H290/51 protects myocardium at risk of injury induced by ischemia-reperfusion. Free Radic Biol Med. 1998; 24: 726.

282. Manning AS, Coltart DJ, *et al.* Ischemia and reperfusion-induced arrhythmias in the rat. Effects of xanthine oxidase inhibition with allopurinol. Circ Res. 1984; 55: 545.

283. Kinugasa Y, Ogino K, *et al.* Allopurinol improves cardiac dysfunction after ischemia-reperfusion via reduction of oxidative stress in isolated perfused rat hearts. Circ J. 2003; 67: 781.

284. Venturini CM, Flickinger AG, *et al.* The Antioxidant, N-(2-mercaptopropionyl)-glycine (MPG), Does Not Reduce Myocardial Infarct Size in an Acute Canine Model of Myocardial Ischemia and Reperfusion. J Thromb Thrombolysis. 1998; 5: 135.

285. Widman SC, Liang CS, *et al.* Contraction band necrosis: its modification by the free radical scavenger N-2-mercaptopropionyl glycine. J Cardiovasc Pharmacol. 1994; 24: 694.

286. Mitsos SE, Fantone JC, *et al.* Canine myocardial reperfusion injury: protection by a free radical scavenger, N-2-mercaptopropionyl glycine. J Cardiovasc Pharmacol. 1986; 8: 978.
287. Miki T, Cohen MV, *et al.* Failure of N-2-mercaptopropionyl glycine to reduce myocardial infarction after 3 days of reperfusion in rabbits. Basic Res Cardiol. 1999; 94: 180.
288. Bolli R, Jeroudi MO, *et al.* Marked reduction of free radical generation and contractile dysfunction by antioxidant therapy begun at the time of reperfusion. Evidence that myocardial "stunning" is a manifestation of reperfusion injury. Circ Res. 1989; 65: 607.
289. Horwitz LD, Fennessey PV, *et al.* Marked reduction in myocardial infarct size due to prolonged infusion of an antioxidant during reperfusion. Circulation. 1994; 89: 1792.
290. Patterson E. Coronary vascular injury following transient coronary artery occlusion: prevention by pretreatment with deferoxamine, dimethylthiourea and N-2-mercaptoproprionyl glycine. J Pharmacol Exp Ther. 1993; 266: 1528.
291. Kinugawa S, Tsutsui H, *et al.* Treatment with dimethylthiourea prevents left ventricular remodeling and failure after experimental myocardial infarction in mice: role of oxidative stress. Circ Res. 2000; 87: 392.
292. Carrea FP, Lesnefsky EJ, *et al.* Reduction of canine myocardial infarct size by a diffusible reactive oxygen metabolite scavenger. Efficacy of dimethylthiourea given at the onset of reperfusion. Circ Res. 1991; 68: 1652.
293. Woo YJ, Taylor MD, *et al.* Ethyl pyruvate preserves cardiac function and attenuates oxidative injury after prolonged myocardial ischemia. J Thorac Cardiovasc Surg. 2004; 127: 1262.
294. Liu XK, Engelman RM, *et al.* Preservation of membrane phospholipids by propranolol, pindolol, and metoprolol: a novel mechanism of action of beta-blockers. J Mol Cell Cardiol. 1991; 23: 1091.
295. Lee YM, Hsiao G, *et al.* Magnolol reduces myocardial ischemia/reperfusion injury via neutrophil inhibition in rats. Eur J Pharmacol. 2001; 422: 159.
296. Hong CY, Huang SS, *et al.* Magnolol reduces infarct size and suppresses ventricular arrhythmia in rats subjected to coronary ligation. Clin Exp Pharmacol Physiol. 1996; 23: 660.
297. Veveris M, Koch E, *et al.* Crataegus special extract WS 1442 improves cardiac function and reduces infarct size in a rat model of prolonged coronary ischemia and reperfusion. Life Sci. 2004; 74: 1945.
298. Haines DD, Bak I, *et al.* Cardioprotective effects of the calcineurin inhibitor FK506 and the PAF receptor antagonist and free radical scavenger, EGb 761, in isolated ischemic/reperfused rat hearts. J Cardiovasc Pharmacol. 2000; 35: 37.
299. Ozer MK, Parlakpinar H, *et al.* Reduction of ischemia--reperfusion induced myocardial infarct size in rats by caffeic acid phenethyl ester (CAPE). Clin Biochem. 2004; 37: 702.
300. Xu Z, Cohen MV, *et al.* Attenuation of oxidant stress during reoxygenation by AMP 579 in cardiomyocytes. Am J Physiol Heart Circ Physiol. 2001; 281: H2585.
301. Rimm EB, Giovannucci EL, *et al.* Prospective study of alcohol consumption and risk of coronary disease in men. Lancet. 1991; 338: 464.
302. St Leger AS, Cochrane AL, *et al.* Factors associated with cardiac mortality in developed countries with particular reference to the consumption of wine. Lancet. 1979; 1: 1017.
303. Hertog MG, Feskens EJ, *et al.* Antioxidant flavonols and coronary heart disease risk. Lancet. 1997; 349: 699.
304. Soleas GJ, Diamandis EP, *et al.* Wine as a biological fluid: history, production, and role in disease prevention. J Clin Lab Anal. 1997; 11: 287.
305. Salah N, Miller NJ, *et al.* Polyphenolic flavanols as scavengers of aqueous phase radicals and as chain-breaking antioxidants. Arch Biochem Biophys. 1995; 322: 339.
306. Reiter RJ, Melchiorri D, *et al.* A review of the evidence supporting melatonin's role as an antioxidant. J Pineal Res. 1995; 18: 1.

307. Reiter R, Tang L, *et al.* Pharmacological actions of melatonin in oxygen radical pathophysiology. Life Sci. 1997; 60: 2255.
308. Raynaud F, Mauviard F, *et al.* Plasma 6-hydroxymelatonin, 6-sulfatoxymelatonin and melatonin kinetics after melatonin administration to rats. Biol Signals. 1993; 2: 358.
309. Schaper J, Mulch J, *et al.* Ultrastructural, functional, and biochemical criteria for estimation of reversibility of ischemic injury: a study on the effects of global ischemia on the isolated dog heart. J Mol Cell Cardiol. 1979; 11: 521.
310. Freedman AM, Kramer JH, *et al.* Propranolol preserves ultrastructure in adult cardiocytes exposed to anoxia/reoxygenation: a morphometric analysis. Free Radic Biol Med. 1991; 11: 197.
311. Taylor IM, Shaikh NA, *et al.* Ultrastructural changes of ischemic injury due to coronary artery occlusion in the porcine heart. J Mol Cell Cardiol. 1984; 16: 79.
312. Braughler JM, Pregenzer JF, *et al.* Novel 21-amino steroids as potent inhibitors of iron-dependent lipid peroxidation. J Biol Chem. 1987; 262: 10438.
313. Braughler JM, Chase RL, *et al.* A new 21-aminosteroid antioxidant lacking glucocorticoid activity stimulates adrenocorticotropin secretion and blocks arachidonic acid release from mouse pituitary tumor (AtT-20) cells. J Pharmacol Exp Ther. 1988; 244: 423.
314. Fox RB. Prevention of granulocyte-mediated oxidant lung injury in rats by a hydroxyl radical scavenger, dimethylthiourea. J Clin Invest. 1984; 74: 1456.
315. Kalaycioglu S, Sinci V, *et al.* Metoprolol prevents ischemia-reperfusion injury by reducing lipid peroxidation. Jpn Circ J. 1999; 63: 718.
316. Murohara Y, Yui Y, *et al.* Effects of superoxide dismutase on reperfusion arrhythmias and left ventricular function in patients undergoing thrombolysis for anterior wall acute myocardial infarction. Am J Cardiol. 1991; 67: 765.
317. Flaherty JT, Pitt B, *et al.* Recombinant human superoxide dismutase (h-SOD) fails to improve recovery of ventricular function in patients undergoing coronary angioplasty for acute myocardial infarction. Circulation. 1994; 89: 1982.
318. Westhuyzen J, Cochrane AD, *et al.* Effect of preoperative supplementation with alpha-tocopherol and ascorbic acid on myocardial injury in patients undergoing cardiac operations. J Thorac Cardiovasc Surg. 1997; 113: 942.
319. Demirag K, Askar FZ, *et al.* The protective effects of high dose ascorbic acid and diltiazem on myocardial ischaemia-reperfusion injury. Middle East J Anesthesiol. 2001; 16: 67.
320. Barta E, Pechan I, *et al.* Protective effect of alpha-tocopherol and L-ascorbic acid against the ischemic-reperfusion injury in patients during open-heart surgery. Bratisl Lek Listy. 1991; 92: 174.
321. Dingchao H, Zhiduan Q, *et al.* The protective effects of high-dose ascorbic acid on myocardium against reperfusion injury during and after cardiopulmonary bypass. Thorac Cardiovasc Surg. 1994; 42: 276.
322. Guan W, Osanai T, *et al.* Time course of free radical production after primary coronary angioplasty for acute myocardial infarction and the effect of vitamin C. Jpn Circ J. 1999; 63: 924.
323. Mickle DA, Weisel RD, *et al.* Effect of orally administered alpha-tocopheryl acetate on human myocardial alpha-tocopherol levels. Cardiovasc Drugs Ther. 1991; 5 Suppl 2: 309.
324. Yau TM, Weisel RD, *et al.* Vitamin E for coronary bypass operations. A prospective, double-blind, randomized trial. J Thorac Cardiovasc Surg. 1994; 108: 302.
325. Sisto T, Paajanen H, *et al.* Pretreatment with antioxidants and allopurinol diminishes cardiac onset events in coronary artery bypass grafting. Ann Thorac Surg. 1995; 59: 1519.
326. Lassnigg A, Punz A, *et al.* Influence of intravenous vitamin E supplementation in cardiac surgery on oxidative stress: a double-blinded, randomized, controlled study. Br J Anaesth. 2003; 90: 148.

327. Ferrari R, Ceconi C, *et al.* Oxygen free radicals and myocardial damage: protective role of thiol-containing agents. Am J Med. 1991; 91: 95S.
328. Arstall MA, Yang J, *et al.* N-acetylcysteine in combination with nitroglycerin and streptokinase for the treatment of evolving acute myocardial infarction. Safety and biochemical effects. Circulation. 1995; 92: 2855.
329. Sochman J. N-acetylcysteine in acute cardiology: 10 years later: what do we know and what would we like to know?! J Am Coll Cardiol. 2002; 39: 1422.
330. Wasinger VC, Cordwell SJ, *et al.* Progress with gene-product mapping of the Mollicutes: Mycoplasma genitalium. Electrophoresis. 1995; 16: 1090.
331. Wilkins MR, Sanchez JC, *et al.* Progress with proteome projects: why all proteins expressed by a genome should be identified and how to do it. Biotechnol Genet Eng Rev. 1996; 13: 19.
332. Rabilloud T. Two-dimensional gel electrophoresis in proteomics: old, old fashioned, but it still climbs up the mountains. Proteomics. 2002; 2: 3.
333. Hoving S, Gerrits B, *et al.* Preparative two-dimensional gel electrophoresis at alkaline pH using narrow range immobilized pH gradients. Proteomics. 2002; 2:127.
334. Westbrook JA, Yan JX, *et al.* Zooming-in on the proteome: very narrow-range immobilised pH gradients reveal more protein species and isoforms. Electrophoresis. 2001; 22: 2865.
335. Hoving S, Voshol H, *et al.* Towards high performance two-dimensional gel electrophoresis using ultrazoom gels. Electrophoresis. 2000; 21: 2617.
336. Humphery-Smith I, Cordwell SJ, *et al.* Proteome research: complementarity and limitations with respect to the RNA and DNA worlds. Electrophoresis. 1997; 18: 1217.
337. Shevchenko A, Wilm M, *et al.* Mass spectrometric sequencing of proteins silver-stained polyacrylamide gels. Anal Chem. 1996; 68: 850.
338. Lopez MF, Berggren K, *et al.* A comparison of silver stain and SYPRO Ruby Protein Gel Stain with respect to protein detection in two-dimensional gels and identification by peptide mass profiling. Electrophoresis. 2000; 21: 3673.
339. Patton WF. A thousand points of light: the application of fluorescence detection technologies to two-dimensional gel electrophoresis and proteomics. Electrophoresis. 2000; 21: 1123.
340. Tonge R, Shaw J, *et al.* Validation and development of fluorescence two-dimensional differential gel electrophoresis proteomics technology. Proteomics. 2001; 1: 377.
341. Lahm HW, Langen H. Mass spectrometry: a tool for the identification of proteins separated by gels. Electrophoresis. 2000; 21: 2105.
342. Jungblut P, Otto A, *et al.* Identification of human myocard proteins separated by two-dimensional electrophoresis. Electrophoresis. 1992; 13: 739.
343. Jungblut P, Otto A, *et al.* Protein composition of the human heart: the construction of a myocardial two-dimensional electrophoresis database. Electrophoresis. 1994; 15: 685.
344. Baker CS, Corbett JM, *et al.* A human myocardial two-dimensional electrophoresis database: protein characterisation by microsequencing and immunoblotting. Electrophoresis. 1992; 13: 723.
345. Corbett JM, Wheeler CH, *et al.* The human myocardial two-dimensional gel protein database: update 1994. Electrophoresis. 1994; 15: 1459.
346. Li XP, Pleissner KP, *et al.* A two-dimensional electrophoresis database of rat heart proteins. Electrophoresis. 1999; 20: 891.
347. Pleissner KP, Soding P, *et al.* Dilated cardiomyopathy-associated proteins and their presentation in a WWW-accessible two-dimensional gel protein database. Electrophoresis. 1997; 18: 802.
348. O'Grady MR, O'Sullivan ML. Dilated cardiomyopathy: an update. Vet Clin North Am Small Anim Pract. 2004; 34: 1187.
349. Corbett JM, Why HJ, *et al.* Cardiac protein abnormalities in dilated cardiomyopathy detected by two-dimensional polyacrylamide gel electrophoresis. Electrophoresis. 1998; 19: 2031.

350. Thiede B, Otto A, *et al.* Identification of human myocardial proteins separated by two-dimensional electrophoresis with matrix-assisted laser desorption/ionization mass spectrometry. Electrophoresis. 1996; 17: 588.
351. Scheler C, Li XP, *et al.* Comparison of two-dimensional electrophoresis patterns of heat shock protein Hsp27 species in normal and cardiomyopathic hearts. Electrophoresis. 1999; 20: 3623.
352. Heinke MY, Wheeler CH, *et al.* Changes in myocardial protein expression in pacing-induced canine heart failure. Electrophoresis. 1999; 20: 2086.
353. Weekes J, Wheeler CH, *et al.* Bovine dilated cardiomyopathy: proteomic analysis of an animal model of human dilated cardiomyopathy. Electrophoresis. 1999; 20: 898.
354. Heinke MY, Wheeler CH, *et al.* Protein changes observed in pacing-induced heart failure using two-dimensional electrophoresis. Electrophoresis. 1998; 19: 2021.
355. Knecht M, Regitz-Zagrosek V, *et al.* Dilated cardiomyopathy: computer-assisted analysis of endomyocardial biopsy protein patterns by two-dimensional gel electrophoresis. Eur J Clin Chem Clin Biochem. 1994; 32: 615.
356. Knecht M, Regitz-Zagrosek V, *et al.* Characterization of myocardial protein composition in dilated cardiomyopathy by two-dimensional gel electrophoresis. Eur Heart J. 1994; 15 Suppl D: 37.
357. Pleissner KP, Regitz-Zagrosek V, *et al.* Chamber-specific expression of human myocardial proteins detected by two-dimensional gel electrophoresis. Electrophoresis. 1995; 16: 841.
358. McGregor E, Dunn MJ. Proteomics of heart disease. Hum Mol Genet. 2003; 12 Spec No 2: R135.
359. Field ML, Clark JF. Inappropriate ubiquitin conjugation: a proposed mechanism contributing to heart failure. Cardiovasc Res. 1997; 33: 8.
360. Weekes J, Morrison K, *et al.* Hyperubiquitination of proteins in dilated cardiomyopathy. Proteomics. 2003; 3: 208.
361. Schwertz H, Langin T, *et al.* Two-dimensional analysis of myocardial protein expression following myocardial ischemia and reperfusion in rabbits. Proteomics. 2002; 2: 988.
362. Sawicki G, Jugdutt BI. Detection of regional changes in protein levels in the in vivo canine model of acute heart failure following ischemia-reperfusion injury: functional proteomics studies. Proteomics. 2004; 4: 2195.
363. Sakai J, Ishikawa H, *et al.* Proteomic analysis of rat heart in ischemia and ischemia-reperfusion using fluorescence two-dimensional difference gel electrophoresis. Proteomics. 2003; 3: 1318.
364. Labugger R, Organ L, *et al.* Extensive troponin I and T modification detected in serum from patients with acute myocardial infarction. Circulation. 2000; 102: 1221.
365. McDonough JL, Labugger R, *et al.* Cardiac troponin I is modified in the myocardium of bypass patients. Circulation. 2001; 103: 58.
366. Van Eyk JE, Murphy AM. The role of troponin abnormalities as a cause for stunned myocardium. Coron Artery Dis. 2001; 12: 343.
367. Canty JM, Lee TC. Troponin I Proteolysis and Myocardial Stunning. J Mol Cell Cardiol. 2002; 34: 375.
368. Feng J, Schaus BJ, *et al.* Preload induces troponin I degradation independently of myocardial ischemia. Circulation. 2001; 103: 2035.
369. Gao WD, Atar D, *et al.* Role of troponin I proteolysis in the pathogenesis of stunned myocardium. Circ Res. 1997; 80: 393.
370. McDonough JL, Arrell DK, *et al.* Troponin I degradation and covalent complex formation accompanies myocardial ischemia/reperfusion injury. Circ Res. 1999; 84: 9.
371. Van Eyk JE, Powers F, *et al.* Breakdown and release of myofilament proteins during ischemia and ischemia/reperfusion in rat hearts: identification of degradation products and effects on the pCa-force relation. Circ Res. 1998; 82: 261.

372. Murphy AM, Kogler H, *et al.* Transgenic mouse model of stunned myocardium. Science. 2000; 287: 488.
373. Thomas SA, Fallavollita JA, *et al.* Absence of troponin I degradation or altered sarcoplasmic reticulum uptake protein expression after reversible ischemia in swine. Circ Res. 1999; 85: 446.
374. Sherman AJ, Klocke FJ, *et al.* Myofibrillar disruption in hypocontractile myocardium showing perfusion-contraction matches and mismatches. Am J Physiol Heart Circ Physiol. 2000; 278: H1320.
375. Kim SJ, Kudej RK, *et al.* A novel mechanism for myocardial stunning involving impaired Ca(2+) handling. Circ Res. 2001; 89: 831.
376. Prasan AM, McCarron HC, *et al.* Effect of treatment on ventricular function and troponin I proteolysis in reperfused myocardium. J Mol Cell Cardiol. 2002; 34: 401.
377. Colantonio DA, Van Eyk JE, *et al.* Stunned peri-infarct canine myocardium is characterized by degradation of troponin T, not troponin I. Cardiovasc Res. 2004; 63: 217.
378. Knowlton AA. The role of heat shock proteins in the heart. J Mol Cell Cardiol. 1995; 27: 121.
379. Martin JL, Mestril R, *et al.* Small heat shock proteins and protection against ischemic injury in cardiac myocytes. Circulation. 1997; 96: 4343.
380. Vander Heide RS. Increased expression of HSP27 protects canine myocytes from simulated ischemia-reperfusion injury. Am J Physiol Heart Circ Physiol. 2002; 282: H935.
381. Scheler C, Muller EC, *et al.* Identification and characterization of heat shock protein 27 protein species in human myocardial two-dimensional electrophoresis patterns. Electrophoresis. 1997; 18: 2823.
382. Otto A, Thiede B, *et al.* Identification of human myocardial proteins separated by two-dimensional electrophoresis using an effective sample preparation for mass spectrometry. Electrophoresis. 1996; 17: 1643.
383. Knowlton AA, Kapadia S, *et al.* Differential expression of heat shock proteins in normal and failing human hearts. J Mol Cell Cardiol. 1998; 30: 811.
384. Stanley BA, Neverova I, *et al.* Optimizing protein solubility for two-dimensional gel electrophoresis analysis of human myocardium. Proteomics. 2003; 3: 815.
385. Chu G, Egnaczyk GF, *et al.* Phosphoproteome analysis of cardiomyocytes subjected to beta-adrenergic stimulation: identification and characterization of a cardiac heat shock protein p20. Circ Res. 2004; 94: 184.
386. Whelan SA, Hart GW. Proteomic approaches to analyze the dynamic relationships between nucleocytoplasmic protein glycosylation and phosphorylation. Circ Res. 2003; 93: 1047.
387. Ghezzi P, Bonetto V. Redox proteomics: identification of oxidatively modified proteins. Proteomics. 2003; 3: 1145.
388. Brennan JP, Wait R, *et al.* Detection and mapping of widespread intermolecular protein disulfide formation during cardiac oxidative stress using proteomics with diagonal electrophoresis. J Biol Chem. 2004; 279: 41352.
389. Mann M, Ong SE, *et al.* Analysis of protein phosphorylation using mass spectrometry: deciphering the phosphoproteome. Trends Biotechnol. 2002; 20: 261.
390. Gygi SP, Corthals GL, *et al.* Evaluation of two-dimensional gel electrophoresis-based proteome analysis technology. Proc Natl Acad Sci U S A. 2000; 97: 9390.
391. Taylor SW, Fahy E, *et al.* Characterization of the human heart mitochondrial proteome. Nat Biotechnol. 2003; 21: 281.
392. Kernec F, Unlu M, *et al.* Changes in the mitochondrial proteome from mouse hearts deficient in creatine kinase. Physiol Genomics. 2001; 6: 117.
393. Berry DA, Keogh A, *et al.* Nuclear membrane proteins in failing human dilated cardiomyopathy. Proteomics. 2001; 1: 1507.
394. Neverova I, Van Eyk JE. Application of reversed phase high performance liquid chromatography for subproteomic analysis of cardiac muscle. Proteomics. 2002; 2: 22.

395. Macri J, McGee B, *et al.* Cardiac sarcoplasmic reticulum and sarcolemmal proteins separated by two-dimensional electrophoresis: surfactant effects on membrane solubilization. Electrophoresis. 2000; 21: 1685.
396. Pipkin W, Johnson JA, *et al.* Localization, macromolecular associations, and function of the small heat shock-related protein HSP20 in rat heart. Circulation. 2003; 107: 469.
397. Sprenger RR, Speijer D, *et al.* Comparative proteomics of human endothelial cell caveolae and rafts using two-dimensional gel electrophoresis and mass spectrometry. Electrophoresis. 2004; 25: 156.
398. Gibbons GH, Liew CC, *et al.* Genetic markers: progress and potential for cardiovascular disease. Circulation. 2004; 109: IV47.
399. Yoshioka J, Lee RT. Cardiovascular genomics. Cardiovasc Pathol. 2003; 12: 249.
400. Lyn D, Liu X, *et al.* Gene expression profile in mouse myocardium after ischemia. Physiol Genomics. 2000; 2: 93.
401. Sehl PD, Tai JT, *et al.* Application of cDNA microarrays in determining molecular phenotype in cardiac growth, development, and response to injury. Circulation. 2000; 101: 1990.
402. Stanton LW, Garrard LJ, *et al.* Altered patterns of gene expression in response to myocardial infarction. Circ Res. 2000; 86: 939.
403. Jin H, Yang R, *et al.* Effects of early angiotensin-converting enzyme inhibition on cardiac gene expression after acute myocardial infarction. Circulation. 2001; 103: 736.
404. Weinberg EO, Mirotsou M, *et al.* Sex dependence and temporal dependence of the left ventricular genomic response to pressure overload. Physiol Genomics. 2003; 12: 113.
405. Friddle CJ, Koga T, *et al.* Expression profiling reveals distinct sets of genes altered during induction and regression of cardiac hypertrophy. Proc Natl Acad Sci U S A. 2000; 97: 6745.
406. Zhao M, Chow A, *et al.* Microarray analysis of gene expression after transverse aortic constriction in mice. Physiol Genomics. 2004; 19: 93.
407. Yang J, Moravec CS, *et al.* Decreased SLIM1 expression and increased gelsolin expression in failing human hearts measured by high-density oligonucleotide arrays. Circulation. 2000; 102: 3046.
408. Barrans JD, Stamatiou D, *et al.* Construction of a human cardiovascular cDNA microarray: portrait of the failing heart. Biochem Biophys Res Commun. 2001; 280: 964.
409. Steenman M, Chen YW, *et al.* Transcriptomal analysis of failing and nonfailing human hearts. Physiol Genomics. 2003; 12: 97.
410. Tan FL, Moravec CS, *et al.* The gene expression fingerprint of human heart failure. Proc Natl Acad Sci U S A. 2002; 99: 11387.
411. Hwang JJ, Allen PD, *et al.* Microarray gene expression profiles in dilated and hypertrophic cardiomyopathic end-stage heart failure. Physiol Genomics. 2002; 10: 31.
412. Barrans JD, Allen PD, *et al.* Global gene expression profiling of end-stage dilated cardiomyopathy using a human cardiovascular-based cDNA microarray. Am J Pathol. 2002; 160: 2035.
413. Boheler KR, Volkova M, *et al.* Sex- and age-dependent human transcriptome variability: implications for chronic heart failure. Proc Natl Acad Sci U S A. 2003; 100: 2754.
414. Lander ES, Linton LM, *et al.* Initial sequencing and analysis of the human genome. Nature. 2001; 409: 860.
415. Venter JC, Adams MD, *et al.* The sequence of the human genome. Science. 2001; 291: 1304.
416. Tew KD, Monks A, *et al.* Glutathione-associated enzymes in the human cell lines of the National Cancer Institute Drug Screening Program. Mol Pharmacol. 1996; 50: 149.
417. Anderson L, Seilhamer J. A comparison of selected mRNA and protein abundances in human liver. Electrophoresis. 1997; 18: 533.
418. Gygi SP, Rist B, *et al.* Quantitative analysis of complex protein mixtures using isotope-coded affinity tags. Nat Biotechnol. 1999; 17: 994.

419. Futcher B, Latter GI, *et al.* A sampling of the yeast proteome. Mol Cell Biol. 1999; 19: 7357.
420. Hoogeveen RC, Reaves SK, *et al.* Copper deficiency increases hepatic apolipoprotein A-I synthesis and secretion but does not alter hepatic total cellular apolipoprotein A-I mRNA abundance in rats. J Nutr. 1995; 125: 2935.
421. Skidmore AF, Beebee TJ. Rat lactate dehydrogenase A and B subunit concentrations are not regulated by mRNA abundance in liver and heart. FEBS Lett. 1990; 270: 67.
422. Le Naour F, Hohenkirk L, *et al.* Profiling changes in gene expression during differentiation and maturation of monocyte-derived dendritic cells using both oligonucleotide microarrays and proteomics. J Biol Chem. 2001; 276: 17920.
423. dos Remedios CG, Berry DA, *et al.* Different electrophoretic techniques produce conflicting data in the analysis of myocardial samples from dilated cardiomyopathy patients: protein levels do not necessarily reflect mRNA levels. Electrophoresis. 1996; 17: 235.
424. Chen G, Gharib TG, *et al.* Discordant protein and mRNA expression in lung adenocarcinomas. Mol Cell Proteomics. 2002; 1: 304.
425. Haab BB, Dunham MJ, *et al.* Protein microarrays for highly parallel detection and quantitation of specific proteins and antibodies in complex solutions. Genome Biol. 2001; 2(2): 1.
426. Cahill DJ. Protein and antibody arrays and their medical applications. J Immunol Methods. 2001; 250: 81.
427. Bashir R, Gomez R, *et al.* Adsorption of avidin on microfabricated surfaces for protein biochip applications. Biotechnol Bioeng. 2001; 73: 324.
428. Williams DM, Cole PA. Kinase chips hit the proteomics era. Trends Biochem Sci. 2001; 26: 271.
429. Zhu H, Bilgin M, *et al.* Global analysis of protein activities using proteome chips. Science. 2001; 293: 2101.
430. Herbert BR, Harry JL, *et al.* What place for polyacrylamide in proteomics? Trends Biotechnol. 2001; 19: S3.
431. Ping P, Zhang J, *et al.* Functional proteomic analysis of protein kinase C epsilon signaling complexes in the normal heart and during cardioprotection. Circ Res. 2001; 88: 59.
432. Vondriska TM, Klein JB, *et al.* Use of functional proteomics to investigate PKC epsilon-mediated cardioprotection: the signaling module hypothesis. Am J Physiol Heart Circ Physiol. 2001; 280: H1434.
433. Liu Y, Ranish JA, *et al.* Yeast nuclear extract contains two major forms of RNA polymerase II mediator complexes. J Biol Chem. 2001; 276: 7169.
434. Neubauer G, King A, *et al.* Mass spectrometry and EST-database searching allows characterization of the multi-protein spliceosome complex. Nat Genet. 1998; 20: 46.
435. Jordan JD, Landau EM, *et al.* Signaling networks: the origins of cellular multitasking. Cell. 2000; 103: 193.
436. Diviani D, Scott JD. AKAP signaling complexes at the cytoskeleton. J Cell Sci. 2001; 114: 1431.
437. Gavin AC, Bosche M, *et al.* Functional organization of the yeast proteome by systematic analysis of protein complexes. Nature. 2002; 415: 141.
438. Ho Y, Gruhler A, *et al.* Systematic identification of protein complexes in Saccharomyces cerevisiae by mass spectrometry. Nature. 2002; 415: 180.
439. Husi H, Ward MA, *et al.* Proteomic analysis of NMDA receptor-adhesion protein signaling complexes. Nat Neurosci. 2000; 3: 661.
440. Ping P, Song C, *et al.* Formation of protein kinase C(epsilon)-Lck signaling modules confers cardioprotection. J Clin Invest. 2002; 109: 499.
441. Baines CP, Zhang J, *et al.* Mitochondrial PKCepsilon and MAPK form signaling modules in the murine heart: enhanced mitochondrial PKCepsilon-MAPK interactions and differential MAPK activation in PKCepsilon-induced cardioprotection. Circ Res. 2002; 90: 390.

442. Soskic V, Gorlach M, *et al.* Functional proteomics analysis of signal transduction pathways of the platelet-derived growth factor beta receptor. Biochemistry. 1999; 38: 1757.
443. Edmondson RD, Vondriska TM, *et al.* Protein kinase C epsilon signaling complexes include metabolism- and transcription/translation-related proteins: complimentary separation techniques with LC/MS/MS. Mol Cell Proteomics. 2002; 1: 421.
444. Vondriska TM, Zhang J, *et al.* Protein kinase C epsilon-Src modules direct signal transduction in nitric oxide-induced cardioprotection: complex formation as a means for cardioprotective signaling. Circ Res. 2001; 88: 1306.
445. Nedelkov D, Nelson RW. Delineation of in vivo assembled multiprotein complexes via biomolecular interaction analysis mass spectrometry. Proteomics. 2001; 1: 1441.
446. Ohi MD, Link AJ, *et al.* Proteomics analysis reveals stable multiprotein complexes in both fission and budding yeasts containing Myb-related Cdc5p/Cef1p, novel pre-mRNA splicing factors, and snRNAs. Mol Cell Biol. 2002; 22: 2011.
447. Allen NP, Huang L, *et al.* Proteomic analysis of nucleoporin interacting proteins. J Biol Chem. 2001; 276: 29268.
448. Song C, Vondriska TM, *et al.* Molecular conformation dictates signaling module formation: example of PKCepsilon and Src tyrosine kinase. Am J Physiol Heart Circ Physiol. 2002; 282: H1166.
449. Zhang J, Ping P, *et al.* Bmx, a member of the Tec family of non-receptor tyrosine kinases, is a novel participant in pharmacological cardioprotection. Am J Physiol Heart Circ Physiol. 2004.
450. Michael LH, Entman ML, *et al.* Myocardial ischemia and reperfusion: a murine model. Am J Physiol.1995; 269: H2147.

Chapter 2

Long-term structural and functional consequences of cardiac ischaemia-reperfusion injury *in vivo* in mice

Tijl De Celle[1], Jack P. Cleutjens[2], W. Matthijs Blankesteijn[1], Jacques J. Debets[1], Jos F. Smits[1] & Ben J. Janssen[1]

Experimental Physiology; 2004; 89(5): 605-615

Departments of Pharmacology & Toxicology[1] and Pathology[2], Cardiovascular Research Institute Maastricht, Universiteit Maastricht, The Netherlands

Abstract

The short-term (< 24 h) consequences of oxidative stress induced by ischaemia-reperfusion (IR) have been studied extensively in the mouse heart. However, much less is known about the long-term effects inflicted by a brief ischaemic period on the murine heart.

We therefore examined the structural and functional consequences of a 30-min ischaemic period after 2 and 8 weeks of reperfusion and compared these to the effects of permanent ischaemia induced by permanent occlusion of the left anterior descending coronary artery (LAD).

The latter procedure resulted in transmural myocardial infarcts of about 52 % of the left ventricle. In contrast, the single 30-min ischaemic period led to infarct sizes of about 13 % of the left ventricle (range 4-23 %) at 2 and 8 weeks after reperfusion. Maximal cardiac contractility responses (+dp/dt) to dobutamine infusion and volume loading were depressed at 2 weeks, but not at 8 weeks after IR. The restoration of cardiac contractility at 8 weeks after IR was associated with a significant 20 % enlargement of the end-diastolic volume and 16 % increase of the left ventricular wall thickness. These changes in cardiac geometry were less pronounced at 2 weeks after IR.

Histological examination revealed that the IR injury was associated with prominent calcification. At 2 and at 8 weeks after IR, 25±5 % and 38±5 % of the injured area was calcified as observed in 69 % and 73 % of the animals, respectively. After permanent occlusion of the LAD, calcification was not observed and wound healing was characterized by thinning and dilatation of the infarcted myocardium.

These data indicate that, in mice, a single 30-min period of ischaemia reduced ventricular contractility up to at least 2 weeks after IR. However, 8 weeks after IR, cardiac function was restored by eccentric hypertrophy associated with calcification of the injured ventricular wall.

Introduction

Cardiac reperfusion injury is a clinical problem associated with revascularization therapy as thrombolytic therapy, coronary artery bypass grafting and percutaneous transluminal coronary angioplasty [1]. Although these therapies are successfully used to restore blood flow to the previously ischaemic myocardium after myocardial infarction, reperfusion induces a complex cascade of events that can result in myocardial stunning, myocyte damage, microvascular and endothelial injury, and necrosis [2]. The destructive effects of reperfusion arise mainly from the acute generation of extremely reactive oxygen species (ROS), which are reduced oxygen species including superoxide anion ($O_2^{\cdot}$), hydrogen peroxide (H_2O_2) and hydroxyl radicals ($OH^{\cdot}$). These ROS cause direct tissue damage through interaction with proteins, carbohydrates, lipids and nucleic acids leading to an inflammatory reaction and further damage [3].

The *in vivo* mouse model of cardiac ischaemia-reperfusion (IR) was first published by Michael *et al.* in 1995 [4]. Following transient occlusion of the left anterior descending coronary artery (LAD) they described the histological appearance of leukocytes and contraction bands in the ischaemic region of the heart up to 24 h after reperfusion.

It should be noted that in this model infarct size is dependent on the duration of the ischaemic period. Infarct size is smaller after 30 min than after 60 min of ischaemia. However, when the ischaemic period is extended up to 2 h, infarct size is comparable to those resulting from permanent occlusion of the LAD [5].

The murine model of IR has been frequently used to study the molecular mechanism of cardiac reperfusion injury or to evaluate potential therapies [6-9]. Most of these studies have focused on the short-term consequences of reperfusion with myocardial infarct size or neutrophil influx as parameters to describe the progression of cardiac tissue damage in the time frame of a few hours [10-12], 1 day [13-16] or 3 days [17, 18] after the initiation of reperfusion.

The long-term effects of IR injury, in terms of weeks or months, are less well examined in this mouse model. However, this is relevant for extrapolation to the clinical setting. The outcome of interventions that are beneficial shortly after initiation of reperfusion may be different when the evaluation takes place at later stages. For example, a study by Metzler *et al.* [19], showed that genetic disruption of intercellular adhesion molecule-1 was associated with a beneficial effect and reduced influx of neutrophils in the heart in the early phase following IR. However, at 3 weeks following IR, left ventricular scar size did not differ compared to values obtained in wild-type mice.

In addition, long-term adaptations to IR may differ from those induced by permanent occlusion of the LAD. As described by Michael *et al.* (1999) the degree of septal hypertrophy was smaller after IR than after permanent occlusion of the LAD, despite a comparable infarct size [5].

The goal of the present study was to characterize the long-term functional and morphological consequences of cardiac IR in the *in vivo* mouse model. The ischaemic period was set to 30 min because this interval is most commonly used in

literature. We examined cardiac function by direct ventricular pressure measurements and cardiac geometry by echocardiography at three time points after IR (1 day, 2 weeks, and 8 weeks). In addition standard histological techniques were applied to describe the morphological adaptations of the injured heart over time. We noticed that the long-term histological adaptations to IR were associated with prominent calcification. To evaluate whether this latter effect was specific for the IR process, data were compared to those obtained in mice subjected to permanent ischaemia (PI).

Methods

Animals

Male outbred Swiss mice (8-11 weeks old, body weight of 35-40 g) were purchased from Charles River (Someren, The Netherlands). Experiments were performed according to the guidelines of the University of Maastricht and were approved by the institutional animal ethics committee. The animals were kept on a 12 h light-12-h dark cycle in a temperature-controlled (21±2 °C) room. After surgery, animals were housed individually with *ad libitum* access to standard food pellets (type Ssniff, Soest, Germany) and water.

In vivo ischaemia-reperfusion and permanent ischaemia

Mice were anaesthetized with ketamine (100 mg/kg i.m.) and xylazine (5 mg/kg s.c.). Body temperature was monitored with a rectal probe and maintained at 37 °C using a warming pad and heating lamp. The trachea of each mouse was intubated perorally with a stainless-steel tube connected to a respirator (Hugo Sachs Electronic rodent ventilator type 845, March-Hugstetten, Germany) set at a stroke volume of 250 µL and a rate of 210 strokes/min. After left thoracotomy and exposure of the heart, the LAD was ligated with 6-0 polypropylene suture (Surgipro, Connecticut, USA) just proximal to its main branching point. The suture was tied around a 3-mm long polyethylene tube (PE-10) to induce ischaemia. In the IR group, blood flow was re-established after 30 min of ischaemia by removal of the tube and suture. The occurrence of reperfusion was assessed by the observation of blood flow in the epicardial coronary arteries through a surgical microscope.

In the PI group, the suture was tied permanently. Sham procedures were identical, with the exception of the actual tying of the polypropylene suture. The chest was closed with 5-0 silk sutures. The animals were then weaned from the respirator, and the intratracheal tube was removed once they were breathing spontaneously. Then 0.2 mg/kg body weight buprenorphine hydrochloride (Buprenex; Reckitt and Colman Pharmaceuticals, Richmond, VA, US) was injected s.c. as an analgaesic.

Echocardiography

Echocardiographic measurements were performed under light isoflurane anaesthesia. One recording was taken prior to surgical procedures (week 0) and two recordings were taken at 2 and 8 weeks thereafter. The *in vivo* transthoracic echocardiography of the left ventricle (LV) was performed using a Hewlett-Packard 15-MHz linear array transducer (15-6L) interfaced with a Sonos 5500 echocardiography system (Philips,

Eindhoven, The Netherlands). Two-dimensional B-Mode echocardiograms were captured at a rate of 90-120 Hz from parasternal long-axis views as well as from mid-papillary short-axis views of the left ventricle. The spatial resolution in the B-Mode is 5 times higher than in the M-Mode. Data were obtained from at least 3 different images taken in end-diastole and systole using EnConcert software (Agilent Technologies, Andover, MA, USA). Representative examples of these images are given in figure 2 (control). From the long-axis B-mode echocardiograms, the LVAd and LVAs, (the LV area in diastole and systole, respectively), as well as the LVLd and LVLs (the length of the LV lumen from base to apex in diastole and systole, respectively) were determined. The end-diastolic volume (EDV) and end-systolic volume (ESV) were calculated from area and length measurements as 8 $(LVAd)^2/3\ \pi$ LVLd and 8 $(LVAs)^2/3\ \pi$ LVLs, respectively. Stroke volume was determined as EDV-ESV and the ejection fraction was defined as 100 (EDV-ESV)/EDV. From the short-axis B-mode echocardiograms we determined the left ventricular wall thickness at two sites. Given the anatomical location of the coronary arteries in a mouse heart [20], the anterior wall contains the ischaemia-associated lesion, while the posterior wall represents the non-ischaemic part of the LV wall. In addition to wall thickness, LV internal chamber diameters were determined in diastole (LVIDd) and systole (LVIDs). The LV percent fractional shortening (FS) was calculated according to the following equation: 100 (LVIDd – LVIDs)/LVIDd.

Evaluation of left ventricular contractility

Left ventricular contractility was evaluated at 1 day as well as 2 and 8 weeks after IR. For this purpose mice were anaesthetized with urethane (2.5 mg/g body weight i.p., Sigma). Body temperature and respiration were controlled as described above. A high-fidelity catheter tip micromanometer (Mikro-tip, 1.4F, SPR-671; Millar Instruments, Houston, TX, USA) was inserted through the right carotid artery into the left ventricular cavity. Ventricular pressure was measured and sampled at a rate of 2 kHz. Maximal positive pressure development (+dp/dt) and heart rate were determined on a beat to beat basis and one-second averages were stored on disk. The heart was then stimulated by an i.v. ramp-infusion of dobutamine (Sigma) using a microinjection pump (Model 200 Series, KdScientific, Boston, MA, USA). The infusion rate of dobutamine was increased every 2 min by 0.5 ng/g/min (last step=5 ng/g/min). Following recovery from dobutamine infusion (taking 10-20 min and assessed by restoration of +dp/dt and heart rate to around baseline levels), hearts were additionally stressed by loading the circulation with an i.v. infusion of warmed (37 °C) Ringer's solution for 1 min at a rate of 2.5 ml/min. Maximal values of +dp/dt were recorded and the changes of +dp/dt value from baseline were calculated. At the end of the experiment ventricles and lungs were excised, washed with isotonic saline and weighed. Ventricles were further incubated for 24 h in formalin and embedded into paraffin for histochemical staining and evaluation of infarct size as described below.

Evaluation of ischaemic area at risk and infarct size

Twenty-four hours after IR, the infarcted area was measured on triphenyltetrazoliumchloride (TTC)- stained tissue sections [4]. In short, mice were

anaesthetized with pentobarbital (120 mg/kg), the jugular vein was canulated and the thorax was reopened, the LAD was re-occluded and 500 µL of 2.5 % trypan blue was injected into the jugular vein to delineate the non-ischaemic tissue and to quantify the area at risk (AAR). The heart was then excised, briefly washed with isotonic saline and cut into 2 parts: along the frontal plane and centrally through the ventricles. These parts were incubated for 20 min at 37°C in 5 ml of 1 % 2, 3, 5-triphenyltetrazolium chloride solution (TTC, Sigma Chemicals Co., St. Louis, MO, USA). Viable myocardium is stained red by TTC while the necrotic, infarcted area remains unstained [21]. Surface of the left ventricle (LV), the AAR as well as the infarcted area (infarct) were measured in both parts of the heart. The percentages AAR/LV, infarct/AAR and infarct/LV were calculated and expressed as the mean of both parts. To determine infarct size 2 and 8 weeks after IR or PI, mice were anaesthetized with pentobarbital (120 mg/kg), hearts were excised, washed with isotonic saline, cut into 2 parts as described above and embedded in paraffin. One section (5 µm) from each of the two parts of the heart was stained with AZAN [22]. The surface of the blue stained parts and the surface of the left ventricle were measured on both sections and the percentage infarct/LV was calculated and expressed as the mean of both sections. All measurements were done using a computerized morphometry system (Quantimet 570C, Leica, Cambridge, UK) [23].

Histochemistry

For histological examination, tissue sections were deparaffinized and stained with hematoxylin-eosin (HE staining). To localize calcium phosphate crystals, sections were stained using von Kossa staining [24]. The same computerized morphometry system was used to measure the relative surface area of the calcified regions to the infarcted area.

Statistical analysis

All parameters are expressed as mean ±S.E.M. Infarct sizes and maximal changes in +dp/dt evoked by dobutamine and volume loading were evaluated using a Student's t-test. The dose response curves for dobutamine were compared using a two-way analysis of variance (ANOVA) and a post-hoc Bonferonni t-test. Parameters serially obtained by echocardiography were compared using an ANOVA for repeated measures and a post-hoc Fishers t-test to identify the time-related and between-group differences. *P*-values ≤0.05 were regarded as statistically significant.

Results

General

A total of 102 animals was used for this study of which 82 (~80 %) survived the entire protocol. Nine animals died during or shortly after sham, IR or PI surgery because of complications due to anaesthesia, arrhythmia or bleeding. Six animals died between 3 and 7 days after surgery of which 2 PI animals had a ruptured heart and the other 4 (1 sham, 3 IR) died for unknown reasons. Five animals died between 2 and 8 weeks after IR or PI (2 sham, 2 IR, 1 PI). A total of 70 animals were used for the cardiac contractility experiments, 7 animals of which were excluded because of difficulties in passing the aortic valves with the catheter tip, and 2 animals because they had died just before measurement due to complications with anaesthesia (1 sham, 1 IR).

Morphometric characteristics

Table 1 summarizes morphometric characteristics of the different groups of mice at the different time points in this study. Body weight was slightly decreased 1 day after surgery, but was increased in all groups (sham, IR and PI) at later time points. Ventricular weight and ventricular weight/body weight ratio were slightly, but insignificantly increased 2 weeks after IR compared to sham at that time point.

A significant positive correlation between infarct size and ventricular weight (R=+0.72) was found 2 weeks after IR. At 8 weeks after IR the increase in ventricular weight was much more pronounced ($P<0.01$) compared to sham at that time point and comparable to changes observed in the PI group. Also at this time point a significant positive correlation between infarct size and ventricular weight (R=+0.69) was found. Lung weights and lung weight/body weight ratios were significantly increased 8 weeks after PI ($P<0.05$ compared to sham at that time point), but not after IR.

Table 1: Myocardial infarct size and morphometric characteristics at three different time points after sham surgery (sham), ischaemia-reperfusion (IR) or permanent ischaemia (PI).

	1 day		2 weeks		8 weeks		
	sham (N=10)	**IR** (N=10)	**sham** (N=10)	**IR** (N=13)	**sham** (N=11)	**IR** (N=11)	**PI** (N=7)
Age (weeks)	11.0±0.5	10.3±0.5	8.1±0.2	8.7±0.1	9.1±0.2	8.6±0.2	8.2±0.1
BW1 (g)	39.9±1.0	39.8±1.1	36.7±0.6	38.4±0.8	37.1±0.7	36.7±0.1	38.4±1.0
BW2 (g)	37.3±1.0	37.1±0.9	39.2±0.6	38.9±1.1	42.3±0.8	42.0±0.6	43.0±1.2
VW (g)	0.17±0.01	0.17±0.01	0.18±0.00	0.19±0.01	0.18±0.00	0.22±0.01 *	0.22±0.01 *
LW (g)	0.23±0.01	0.24±0.01	0.23±0.01	0.24±0.01	0.25±0.02	0.25±0.02	0.33±0.03 #
VW/BW2 (%)	0.45±0.01	0.46±0.01	0.45±0.01	0.49±0.02	0.41±0.01	0.52±0.02 *	0.51±0.03 *
LW/BW2 (%)	0.63±0.03	0.64±0.02	0.59±0.01	0.59±0.03	0.57±0.04	0.58±0.04	0.80±0.06 #
Infarct/LV (%)	0	21.2±3.5	0	12.9±1.8	0	12.3±1.9	52.0±2.5

Abbreviations: BW1: body weight before sham-surgery, IR or PI; BW2: body weight before sacrifice; VW: ventricular weight; LW: lung weight; VW/BW2: percentage of VW relative to BW2; LW/BW2: percentage of LW relative to BW2; Infarct/LV: percentage of infarct size relative to left ventricular area. *$P<0.01$, #$P<0.05$ between sham and IR or PI. (mean ±S.E.M.)

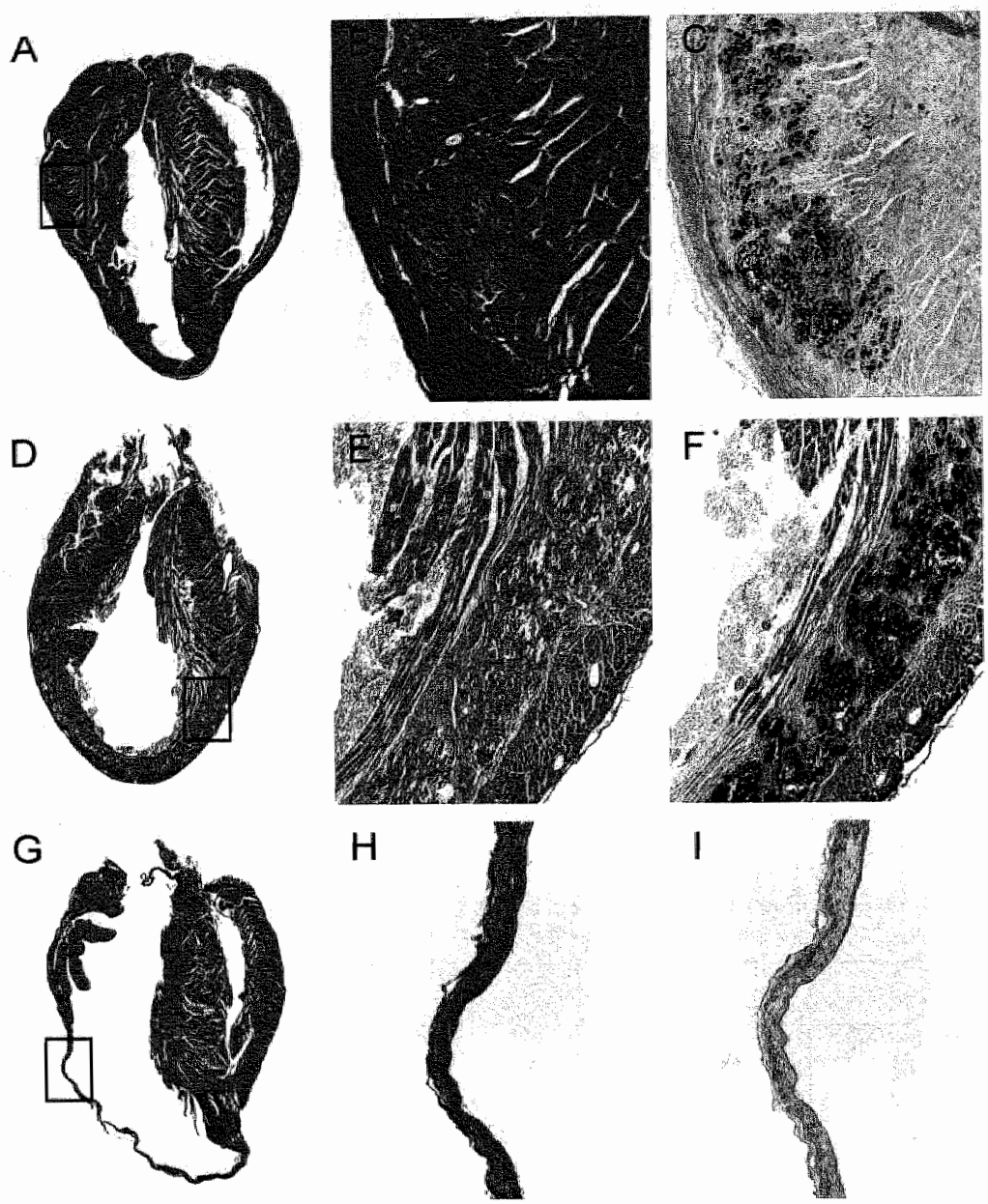

Figure 1: Photomicrograph of AZAN stained longitudinal heart sections of a 2 week IR animal (A), an 8 week IR animal (D) and an 8 week PI animal (G) (magnification 16x). Detailed images focusing on an injured part of the left ventricle of these AZAN stained sections are shown in B, E, and H (magnification 100x). Note the transmural infarct and the pronounced infarct thinning and dilatation in the 8 week PI animal compared to the IR animals. C, F, I are images of the same region stained by von Kossa staining (magnification 100x). Note that calcium deposits stained black in the IR animals and no calcification was observed in the PI group.

Myocardial infarct size

One day after IR the AAR was 47±2 % of the left ventricular area. 51±8 % of the AAR was identified as infarcted area, meaning that 21±4 % of the left ventricle was infarcted area (table 1). The magnitude of infarcted area/left ventricle ratio did not differ at 2 and 8 weeks after IR, but was considerably less than in the PI group. As shown by the AZAN staining in figure 1 A, B, D, E, the ventricular wall of mice subjected to the IR protocol consisted of viable endo- and epicardial layers of myocytes and patchy distributed scar tissue. In contrast, 8 weeks after PI, the infarcted wall of the left ventricle was thinned with an almost transmural appearance of granulation tissue (figure 1 G, H).

Calcification

In the majority of animals subjected to IR a process of calcification occurred in the infarcted area of the ventricular wall. Calcium deposits were macroscopically observed as fine, white granules or clumps. By HE staining they appeared as basophilic, clumped and amorphous granules lying in a pattern of previous cardiomyocytes and encircled by fibrous tissue. The calcium crystals were stained black by the von Kossa staining (figure 1 C, F) and appeared in a frequency of 9/13 animals (69 %) in the 2 week reperfusion group and 8/11 animals (73 %) in the 8 week IR group.

In the calcified hearts, the size of the calcified area was 25±5 % of the infarcted area in the 2-week IR group and 38±5 % of the infarcted area in the 8-week IR group. The calcification of the wound healing area was specific for the IR protocol because no calcification was observed in mice subjected to PI (figure 1 I).

Table 2: Comparison of echocardiographic parameters in mice subjected to the 30 min ischaemia-reperfusion (IR) procedure, permanent ischaemia (PI) or sham-procedure. Data were obtained before (0 weeks time point) as well as 2 and 8 weeks after the surgical interventions. For the PI group only data at week 0 and 8 are shown.

Parameter	0 weeks Sham	0 weeks IR	0 weeks PI	2 weeks Sham	2 weeks IR	8 weeks Sham	8 weeks IR	8 weeks PI
N	9	9	7	7	6	9	9	7
Long-axis derived parameters								
EDV (µl)	65±3	65±3	84±5 $^{\#}$	77±6	83±10 *	78±4	87±8 *	281±47 *$^{\#}$
ESV (µl)	31±3	31±2	43±4 $^{\#}$	36±3	36±6	40±4	44±5 *	258±44 *$^{\#}$
SV (µl)	34±4	34±2	41±4	41±4	46±7	39±3	43±5	30±6 *$^{\#}$
EF (%)	52±5	51±3	49±3	54±3	56±6	50±4	49±3	10±3 *$^{\#}$
Short-axis derived parameters								
AWTd (mm)	1.00±0.02	1.07±0.04	0.89±0.03	1.03±0.08	1.24±0.08	1.12±0.04*	1.14±0.05	0.51±0.08 *$^{\#}$
PWTd (mm)	1.01±0.03	1.08±0.02	0.98±0.05	1.12±0.08	1.18±0.06	1.14±0.04*	1.31±0.08 *$^{\$}$	1.09±0.15
AWTs (mm)	1.27±0.06	1.33±0.07	1.11±0.04	1.24±0.10	1.54±0.10 *	1.42±0.06	1.54±0.04 *	0.53±0.06 *$^{\#}$
PWTs (mm)	1.26±0.03	1.33±0.04	1.20±0.05	1.33±0.08	1.44±0.08	1.38±0.04	1.55±0.06 *$^{\$}$	1.55±0.20 *
LVIDd (mm)	4.16±0.09	4.22±0.12	4.51±0.10	4.50±0.15	4.61±0.17 *	4.32±0.13	4.68±0.13 *	7.26±0.41 *$^{\#}$
LVIDs (mm)	3.09±0.15	3.20±0.14	3.53±0.17	3.49±0.17	3.59±0.19	3.28±0.17	3.59±0.17	7.04±0.44 *$^{\#}$
FS (%)	26±3	24±3	22±3	23±2	22±2	24±4	23±3	3±1 *$^{\#}$

Abbreviations: EDV, ESV: end diastolic and end systolic left ventricular volume; SV: stroke volume; EF: ejection fraction; AWTd, PWTd, AWTs, PWTs: anterior wall and posterior wall thickness in diastole and systole, respectively; LVIDd, LVIDs: left ventricular internal cavity diameter in diastole and systole, respectively; FS: fractional shortening. *$P<0.05$: different from control at week 0; $^{\$}P<0.05$: between sham and IR; $^{\#}P<0.05$: between IR and PI. (mean ±S.E.M.)

Echocardiography

The results of the *in vivo* echocardiographic measurements are given in table 2. The comparison of the echocardiographic parameters at week 0 indicates that baseline values of end diastolic volume (EDV) and end systolic volume (ESV) were somewhat greater in the PI group than in the sham or IR group. This is probably due to normal time-dependent biological variation given the fact that the mice used for the PI series of experiments were not simultaneously purchased.

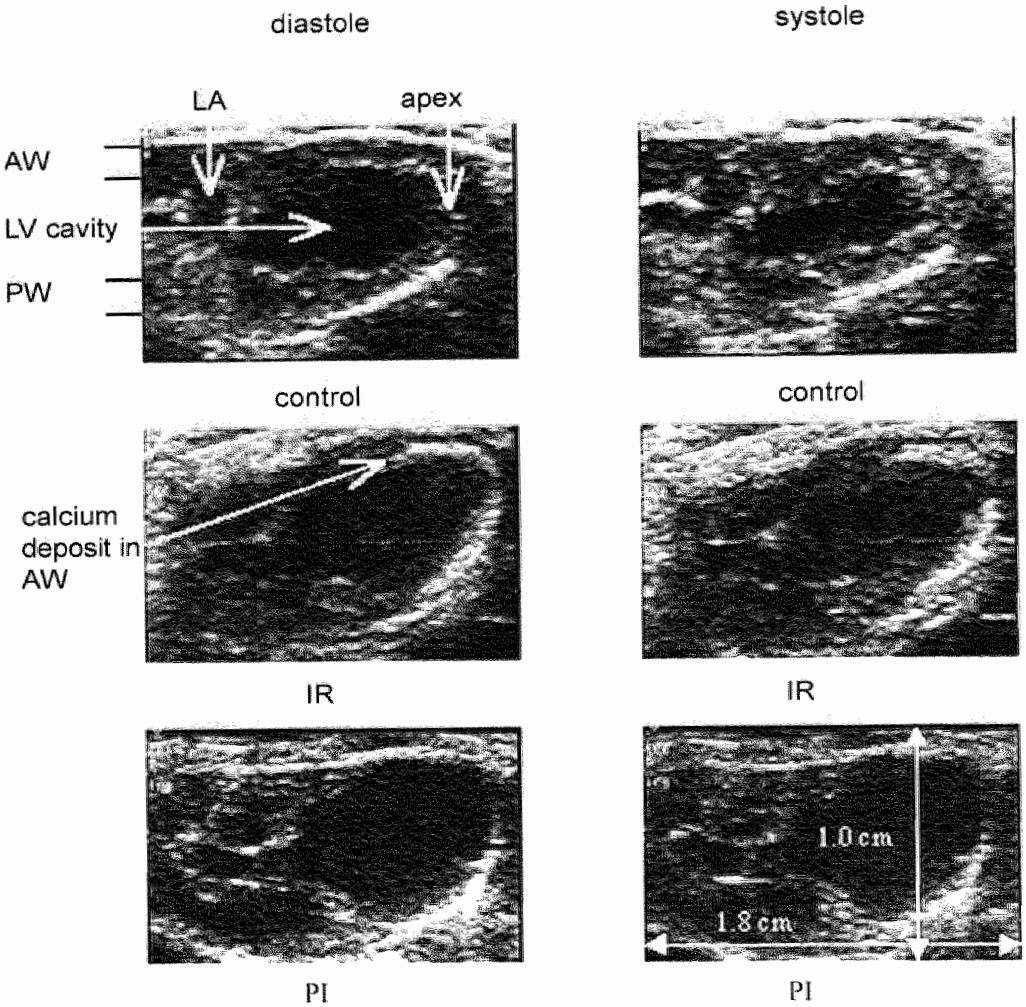

Figure 2: Long-axis echocardiographic images of the heart taken 8 weeks after mice were subjected to sham-surgery, ischaemia-reperfusion (IR) or permanent ischaemia (PI). Note the extreme dilatation in the PI model and occurrence of a white area within the AW of the IR heart, histologically confirmed as a calcium deposit. Abbreviations; LA=left atrium, LV=left ventricle, AW=anterior wall, PW=posterior wall.

Compared to the baseline value, the EDV was significantly increased at 2 and 8 weeks after IR while this was not the case in the sham-operated mice. However, when compared to the PI group, the dilatory remodeling response to the IR injury was relatively small (40±15 % for IR versus 250±70 % for PI, figure 2). The time-dependent changes in EDV 8 weeks after IR were paralleled by those in ESV. However, cardiac function, as assessed by stroke volume (SV), ejection fraction (EF) and fractional shortening (FS), was not significantly altered at 2 and 8 weeks after IR. In contrast, the geometrical changes in the PI group had significant functional consequences for SV, EF, and FS (figure 2).
The echocardiographic measurements also identified a small but significant thickening of the anterior wall (AW) at 2 and 8 weeks after IR, especially during systole. At 8 weeks after IR the posterior wall (PW) thickness was significantly increased as well. After PI the affected AW became very thin whereas the PW showed a comparable hypertrophic response as observed 8 weeks after IR.

Ventricular contractility
Figure 3 presents LV function as evaluated in sham, IR and PI groups at the different time points by measuring the rate of left ventricular pressure development (+dp/dt) and heart rate (HR). Under basal conditions, +dp/dt did not differ between sham, IR, or PI. Also systolic blood pressures did not differ at baseline between sham, IR or PI (74±2 mmHg, 71±2 mmHg, 72±2 respectively; data not shown). Baseline HR values were significantly ($P<0.01$) higher in the IR group than in sham-operated mice 1 day after reperfusion. When hearts were stimulated with dobutamine, +dp/dt levels increased dose-dependently in sham-operated animals, whereas the increase was blunted in IR animals at 1 day and 2 weeks after reperfusion (figure 3A). Dose response curves for heart rate were comparable between groups. One day after IR, the increase in +dp/dt was significantly smaller (2456±475 mmHg/s) when compared to increments observed in the sham group (5939±928 mmHg/s; $P=0.004$). The blunted response was still present 2 weeks after IR (IR: 3174±1066 mmHg/s versus sham: 7487±1209 mmHg/s; $P=0.01$). In contrast, 8 weeks after IR, the contractility response to dobutamine was nearly restored to control levels (5828±735 mmHg/s in IR versus 6620±735 mmHg/s in sham-operated mice). At this time point, the contractile response to dobutamine in the PI group was significantly blunted.
Figure 3 B shows that comparable results were obtained with volume loading. The increase of +dp/dt at 2 weeks after IR (1758±991 mmHg/s) was significantly smaller than in the sham group (6129±1247 mmHg/s; $P=0.02$). At 8 weeks after IR the increase in +dp/dt following volume loading (5149±820 mmHg/s) did not differ from values observed in the sham group (4669±466 mmHg/s). In the PI group the response was significantly reduced (2245±665 mmHg/s; $P<0.03$).

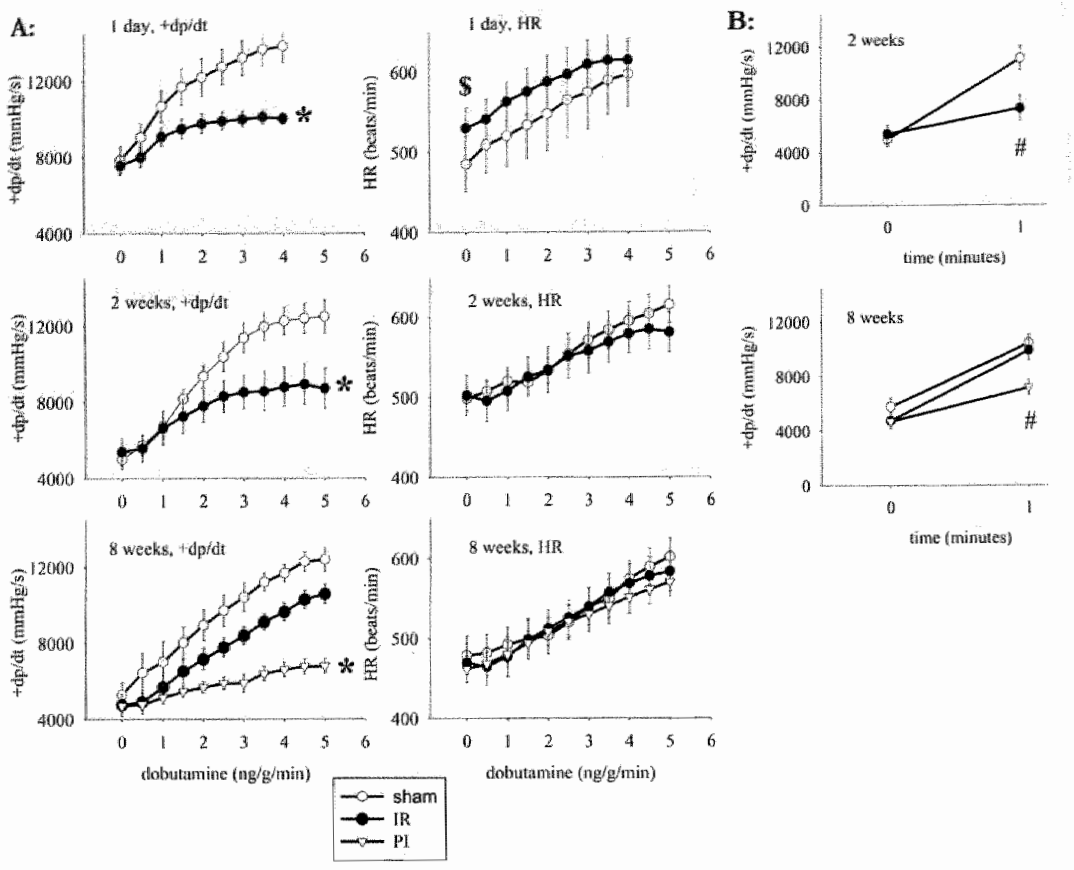

Figure 3: *In vivo* assessment of left ventricular contractility.

A: Change in cardiac contractility (+dp/dt) and heart rate (HR) during dobutamine stimulation (0-5 ng/g/min) in sham groups, IR groups and PI group at 1 day, 2 weeks and 8 weeks (N=7-10 per group). $^{*}P<0.01$, $^{\$}P<0.01$. (Results are expressed as means ±S.E.M.)

B: Change in cardiac contractility (+dp/dt) under volume loading (2.5 ml/min Ringer solution) in sham groups, IR groups and PI group at 2 weeks and 8 weeks (N=7 to 10 per group). $^{\#}P<0.05$. (Results are expressed as means ±S.E.M.)

To examine whether the amount of calcification was associated with deficits in cardiac function, infarct size was plotted against the maximal +dp/dt responses to dobutamine in the 2 and 8 week IR groups (figure 4). The subgroup of mice with the largest calcified LV areas is separately indicated in this figure. The figure shows that although the mice with the largest amount of calcification were among those with the largest infarct size, no obvious relation to cardiac contractility was observed.

Discussion

The present study shows that a single 30-min ischaemia-reperfusion protocol has long-term consequences for cardiac morphometry and function in mice.

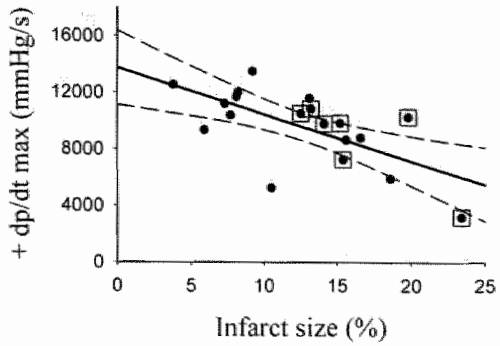

Figure 4: Linear correlation (R=-0.64, N=19, $P<0.01$) between infarct size and maximal left ventricular pressure development ($+dp/dt_{max}$) following dobutamine in mice at 2 weeks and 8 weeks after IR. The subgroup of mice with the largest calcified left ventricular area is indicated by squares.

Left ventricular contractility was depressed up to 2 weeks after IR, but was restored 8 weeks after the intervention. The recovery of cardiac contractility was associated with left ventricular dilatation and hypertrophy. Remarkably, in the IR model, but not in the PI model, the long-term repair mechanisms were associated with considerable calcification.

The degree of cardiac injury and survival rate is related to the duration of the ischaemic stimulus. In the present study, we chose a commonly used time frame of 30 min of ischaemia and the survival rate was more than 80 % at 8 weeks after IR.

In a study by Michael *et al.* [5] it has been described that following a 2 h ischaemic period the survival rate was 60 % after 24 h and only 45 % several weeks after reperfusion. In that study, left ventricular infarct size was about 30 % and did not differ from infarct sizes found after permanent ischaemia. In the present study, following the shorter 30 min ischaemic period, left ventricular infarct size was 21 % at 1 day after IR. Two and 8 weeks after IR the LV infarct size was smaller (about 13 %). This time-related difference in infarct size is most likely a consequence of the technique used to assess infarct size. Staining by TTC is based on the ability of living cells to reduce TTC to an insoluble red pigment. It cannot be excluded that 24-h after IR, part of the cardiomyocytes, were unable to metabolize TTC because they were in a hibernating state. Later on in the process these cells may have regenerated to vital cardiomyocytes which may explain the reduced infarct size measured at 2 and 8 weeks after IR [25, 26].

As shown in figure 1, permanent occlusion of the LAD in the PI model resulted in large transmural infarcts with thinning of the left ventricular wall and did not involve the septum and right ventricle. In contrast, in the IR model, infarcts were never transmural, but characterized by a patchy distribution of granulation and scar tissue localized between an endo- and epicardial layer of vital cardiomyocytes.

At 2 and 8 weeks after IR we observed in about 70 % of the animals pronounced calcified regions in the left ventricular wall that were surrounded by granulation and fibrous scar tissue. This phenomenon was completely absent in the PI animals.

Dystrophic calcium deposition appears in many pathological conditions due to passive precipitation of calcium and phosphates. In cardiovascular diseases this process is

mostly described in atherosclerosis in which arterial plaque calcification occurs and in degenerative diseases of heart valves [27, 28]. To our knowledge only two reports are published about calcification in relation to reperfusion. A case study of Tseng *et al.* [29] reported acute calcification following transient ligation of the rodent middle cerebral artery, while Jennische [30] showed post-ischaemic calcification in skeletal muscle of the rat. However, following myocardial ischaemia-reperfusion, tissue calcification is not documented. Lipids, apoptotic bodies and necrotic debris in the wound-healing area may play a role in the nucleation of calcium hydroxyapatite crystals [31]. When blood flow is restored after ischaemia, debris of death cells may accumulate with calcium and phosphates from the blood before the inflammatory cells infiltrate the damaged tissue. After permanent occlusion of the area at risk, blood flow is not restored and hence the deposition of calcium crystals is prevented, enabling the inflammatory cells to clear the necrotic debris. The present study was not designed to clarify the mechanisms of this aspect of wound healing. We observed that the animals with the largest area of calcification were among those that had the largest infarct size (figure 4). However, the calcification process did not seem to have a negative impact on cardiac function because it returned to normal 8 weeks after IR. Further studies are necessary to investigate this issue in more depth.

Cardiac contractility was measured in order to characterize the evolution of cardiac function over time after ischaemia-reperfusion. Baseline heart rates were slightly elevated 24 h after IR compared to sham-operated animals. This was probably due to neurohumoral compensation following the acute IR injury. Baseline heart rates did not differ between sham-operated and IR mice at 2 and 8 weeks after surgery, suggesting a normalization of this response.

Baseline +dp/dt levels were not different between the IR and sham-operated mice at any time point. Also, baseline +dp/dt values obtained 8 weeks after PI were not different from those found in the sham group, despite the increase in lung weights, which suggest signs of congestive heart failure. In contrast, other studies have reported decreased +dp/dt values after PI at baseline conditions [32, 33]. Differences in anaesthetic regimens and other experimental circumstances may explain these discrepancies. To obtain a better insight into the physiological consequences of IR injury, contractility changes were measured while the heart was stressed with dobutamine or a volume load. In comparison to sham-operated mice, cardiac contractility responses to dobutamine were reduced 1 day and 2 weeks after IR. At 8 weeks after IR, but not after PI, responses to dobutamine and volume loading were nearly restored.

The recovery of cardiac contractility at 8 weeks after IR occurred simultaneously with morphological adaptations as determined by echocardiography and was paralleled by a significant increase in ventricular weight. Part of this hypertrophic response is due to normal physiological growth. However, the enlargement of the end-diastolic volume (40 % in IR versus 20 % in sham-operated mice) and thickening of the posterial wall (23 % in IR versus 13 % in sham-operated mice) suggest an eccentric hypertrophic response to IR injury. Early signs of this process were detected already at 2 weeks after IR, as suggested by the positive correlation between infarct size and ventricular weight. The remodeling response may

be too small at that time point to compensate for the reduced cardiac contractility response.
The process of dilatation was much smaller after IR than after PI. Eight weeks after PI the end-diastolic volume was increased by a factor 2.5. Despite the enlargement of the ventricular cavity, stroke volume and ejection fraction were significantly reduced because the infarcted and thinned myocardial wall remained fully akinetic. These functional impairments as detected by echocardiography are in agreement with those obtained before by direct ascending aortic blood flow measurements in this model [34].

We conclude that in our mouse model, long-term cardiac consequences following ischaemia-reperfusion are different from those observed after permanent ischaemia. Contractility of the heart was depressed for at least 2 weeks after IR, but was restored after 8 weeks. Given the significant negative correlation between infarct size and cardiac contractility the functional differences between the IR model and the PI model are most likely of a quantitative nature. After reoxygenation of the ischaemic heart, calcification, hypertrophy and minor dilatation characterized the wound healing process. However, the gross architecture of the ventricular wall was preserved. This aspect differed qualitatively from the permanent ischaemia model. When reperfusion was not established, the ischaemic area was not calcified, but completely replaced by connective tissue. In addition, the ventricular wall was severely dilated and loss of cardiac function was permanent.

References

1. Kaminski KA, Bonda TA, *et al.* Oxidative stress and neutrophil activation--the two keystones of ischemia/reperfusion injury. Int J Cardiol. 2002; 86: 41.
2. Verma S, Fedak PW, *et al.* Fundamentals of reperfusion injury for the clinical cardiologist. Circulation. 2002; 105: 2332.
3. Li C, Jackson RM. Reactive species mechanisms of cellular hypoxia-reoxygenation injury. Am J Physiol Cell Physiol. 2002; 282: C227.
4. Michael LH, Entman ML, *et al.* Myocardial ischemia and reperfusion: a murine model. Am J Physiol. 1995; 269: H2147.
5. Michael LH, Ballantyne CM, *et al.* Myocardial infarction and remodeling in mice: effect of reperfusion. Am J Physiol. 1999; 277: H660.
6. Chen Z, Chua CC, *et al.* Protective effect of melatonin on myocardial infarction. Am J Physiol Heart Circ Physiol. 2003; 284: H1618.
7. Jones SP, Lefer DJ. Myocardial Reperfusion Injury: Insights Gained from Gene-Targeted Mice. News Physiol Sci. 2000; 15: 303.
8. Jones SP, Hoffmeyer MR, *et al.* Role of intracellular antioxidant enzymes after in vivo myocardial ischemia and reperfusion. Am J Physiol Heart Circ Physiol. 2003; 284: H277.
9. Yet SF, Tian R, *et al.* Cardiac-specific expression of heme oxygenase-1 protects against ischemia and reperfusion injury in transgenic mice. Circ Res. 2001; 89: 168.
10. Girod WG, Jones SP, *et al.* Effects of hypercholesterolemia on myocardial ischemia-reperfusion injury in LDL receptor-deficient mice. Arterioscler Thromb Vasc Biol. 1999; 19: 2776.
11. Jones SP, Girod WG, *et al.* Reperfusion injury is not affected by blockade of P-selectin in the diabetic mouse heart. Am J Physiol. 1999; 277: H763.

12. Palazzo AJ, Jones SP, *et al.* Myocardial ischemia-reperfusion injury in CD18- and ICAM-1-deficient mice. Am J Physiol. 1998; 275: H2300.
13. Scalia R, Gooszen ME, *et al.* Simvastatin exerts both anti-inflammatory and cardioprotective effects in apolipoprotein E-deficient mice. Circulation. 2001; 103: 2598.
14. Jones SP, Trocha SD, *et al.* Cardioprotective actions of endogenous IL-10 are independent of iNOS. Am J Physiol Heart Circ Physiol. 2001; 281: H48.
15. Jones SP, Gibson MF, *et al.* Direct vascular and cardioprotective effects of rosuvastatin, a new HMG-CoA reductase inhibitor. J Am Coll Cardiol. 2002; 40: 1172.
16. Hoffmeyer MR, Scalia R, *et al.* PR-39, a potent neutrophil inhibitor, attenuates myocardial ischemia-reperfusion injury in mice. Am J Physiol Heart Circ Physiol. 2000; 279: H2824.
17. Briaud SA, Ding ZM, *et al.* Leukocyte trafficking and myocardial reperfusion injury in ICAM-1/P-selectin-knockout mice. Am J Physiol Heart Circ Physiol. 2001; 280: H60.
18. Yang J, Jones SP, *et al.* Endothelial cell overexpression of fas ligand attenuates ischemia-reperfusion injury in the heart. J Biol Chem. 2003; 278: 15185.
19. Metzler B, Mair J, *et al.* Mouse model of myocardial remodelling after ischemia: role of intercellular adhesion molecule-1. Cardiovasc Res. 2001; 49: 399.
20. Janssen B, De Celle T, Paquay J, Smits J, Blankesteijn M. Structural and Functional Adaptations of the Heart after Coronary Artery Ligation in the Mouse. In: Ince C, ed. The Physiological Genomics of the Critically Ill Mouse. Vol. 16. Boston/Dordrecht/London: Kluwer Academic Publishers; 2003: 211.
21. Vivaldi MT, Kloner RA, *et al.* Triphenyltetrazolium staining of irreversible ischemic injury following coronary artery occlusion in rats. Am J Pathol. 1985; 121: 522.
22. Cleutjens JP, Verluyten MJ, *et al.* Collagen remodeling after myocardial infarction in the rat heart. Am J Pathol. 1995; 147: 325.
23. Smits JF, van Krimpen C, *et al.* Angiotensin II receptor blockade after myocardial infarction in rats: effects on hemodynamics, myocardial DNA synthesis, and interstitial collagen content. J Cardiovasc Pharmacol. 1992; 20: 772.
24. Bills CE, Eisenberg H, *et al.* Complexes of organic acids with calcium phosphate: the Von Kossa stain as a clue to the composition of bone mineral. Johns Hopkins Med J. 1974; 128: 194.
25. Vanoverschelde JL, Melin JA. The pathophysiology of myocardial hibernation: current controversies and future directions. Prog Cardiovasc Dis. 2001; 43: 387.
26. Ausma J, Cleutjens J, *et al.* Chronic hibernating myocardium: interstitial changes. Mol Cell Biochem. 1995; 147: 35.
27. Doherty TM, Asotra K, *et al.* Calcification in atherosclerosis: bone biology and chronic inflammation at the arterial crossroads. Proc Natl Acad Sci U S A. 2003; 100: 11201.
28. David TE, Ivanov J. Is degenerative calcification of the native aortic valve similar to calcification of bioprosthetic heart valves? J Thorac Cardiovasc Surg. 2003; 126: 939.
29. Tseng MT, Chan SA, *et al.* A case study of ligation induced calcification in middle cerebral artery in rat. Histol Histopathol. 2000; 15: 483.
30. Jennische E. Post-ischemic calcification in skeletal muscle. A light microscopic study in the rat. Acta Pathol Microbiol Immunol Scand [A]. 1984; 92: 139.
31. Proudfoot D, Skepper JN, *et al.* Apoptosis regulates human vascular calcification in vitro: evidence for initiation of vascular calcification by apoptotic bodies. Circ Res. 2000; 87: 1055.
32. Lutgens E, Daemen MJ, *et al.* Chronic myocardial infarction in the mouse: cardiac structural and functional changes. Cardiovasc Res. 1999; 41: 586.
33. Patten RD, Aronovitz MJ, *et al.* Ventricular remodeling in a mouse model of myocardial infarction. Am J Physiol. 1998; 274: H1812.
34. Janssen B, Debets J, *et al.* Chronic measurement of cardiac output in conscious mice. Am J Physiol Regul Integr Comp Physiol. 2002; 282: R928.

Chapter 3

Sustained protective effects of 7-monohydroxyethylrutoside in an *in vivo* model of cardiac ischaemia-reperfusion

Tijl De Celle[1], Peter Heeringa[2], Agnieska E. Strzelecka[1], Aalt Bast[1], Jos F. Smits[1] & Ben J. Janssen[1]

European Journal of Pharmacology; 2004; 494: 205-212

Departments of Pharmacology & Toxicology[1] and Clinical & Experimental Immunology[2], Cardiovascular Research Institute Maastricht, Universiteit Maastricht, The Netherlands

Abstract

Earlier studies have shown that 7-monohydroxyethylrutoside (monoHER), an antioxidant flavonoid, protects against doxorubicin-induced cardiotoxicity. In this study we investigated potential sustained cardioprotective effects of monoHER in a model of ischaemia-reperfusion (IR) in mice.

Ischaemia was induced for 30 min by ligating the left anterior descending coronary artery. Afterwards the ligature was removed and reperfusion allowed for 6 h, 24 h or 2 weeks. MonoHER (500 mg/kg) or saline was given intraperitoneally, 1 h before ischaemia.

Treatment with monoHER significantly attenuated myocardial neutrophil influx both at 6 h and 24 h after reperfusion by 77 % and 76 %, respectively. Infarct size was also significantly reduced, 24 h and 2 weeks after reperfusion by 58 % and 49 %, respectively. Whereas IR had no influence on basal levels of cardiac contractility (+dp/dt), responses to dobutamine were blunted 24 h and 2 weeks after reperfusion. In mice treated with monoHER, cardiac contractility response was significantly restored.

These results indicate that monoHER exerts a sustained cardioprotective effect on IR injury and prevents deterioration of cardiac contractility.

Introduction

Myocardial reperfusion through thrombolysis, percutaneous transluminal coronary angioplasty or coronary artery bypass grafting, is standard treatment in acute myocardial infarction. However, these revascularization therapies initiate a second phase of myocardial injury either by acceleration of detrimental processes initiated during ischaemia, or by inducing additional pathological processes following reperfusion [1, 2].

Many studies support a role of "reactive oxygen species" (ROS) in myocardial ischaemia-reperfusion (IR) injury [2, 3]. The mechanism implicates the sequential reduction of molecular oxygen into these ROS, including superoxide anion ($O_2^{\cdot}$), hydrogen peroxide (H_2O_2), and hydroxyl radicals ($OH^{\cdot}$) in an amount that overwhelms the scavenging capacity of endogenous antioxidants in the heart. The interaction of these ROS with cell membrane lipids and essential proteins contributes to myocardial cell damage, leading to inflammatory reactions, irreversible tissue injury and, consequently, to impaired cardiac function [4]. Reperfusion injury triggers an acute inflammatory response in which polymorphonuclear neutrophils infiltrate the myocardium, under the influence of chemotactic attraction and activation of the complement cascade [5, 6]. Although essential in wound healing, these neutrophils may have detrimental effects by producing additional ROS and proteolytic enzymes [4, 6, 7].

Flavonoids are a group of naturally occurring polyphenolic compounds with excellent iron chelating as well as radical scavenging properties [8]. The semisynthetic flavonoid, 7-monohydroxyethylrutoside (monoHER), has been shown to protect *in vivo* against chronic doxorubicin-induced cardiotoxicity in mice [9, 10] and is now being tested in a phase II clinical trial.

Potential protective effects of exogenously administered antioxidants on reperfusion injury have already been described in literature, but the results are controversial [3]. Moreover, most of these studies only investigated possible short-term protective effects after initiation of reperfusion (range 1-24 h) and did not prove sustained protective effects.

In the present study we investigated potential short- (6, 24 h) and long-term (2 weeks) protective effects of monoHER after *in vivo* cardiac IR in mice. We did this by examining neutrophil tissue infiltration, infarct size and cardiac contractility. Possible dose-dependent effects of monoHER on mean arterial pressure and heart rate were examined in a separate set of experiments.

Materials and Methods

Animals

Male outbred Swiss mice (8-11 week old, weighing 35-40 g) were used. The mice were purchased from Charles River (The Netherlands). Experiments were performed according to the guidelines of the Universiteit Maastricht and were approved by the institutional animal ethics committee. The animals were kept on a 12 h light-12 h dark cycle in a temperature-controlled (21±2 °C) room. After surgery, animals were housed

individually with *ad libitum* access to standard food pellets (type Ssniff, Soest, Germany) and water.

Measurement of blood pressure and heart rate in conscious animals
A catheter was implanted in the femoral artery and in the jugular vein under isoflurane anaesthesia (1.5-2.5 %), as described in detail [11]. The arterial catheter was connected to a pressure transducer (micro-switch, model 156PC 156WL, Honeywell, Amsterdam, The Netherlands) and to an amplifier that delivered a high-voltage signal to an analog-to-digital converter board (model 2814, Data Translation, CN Rood, Rijswijk, the Netherlands) mounted in an IBM 486-compatible computer. The blood pressure signal was sampled at 2,000 Hz (~200 data samples/beat). Beat-to-beat values of mean arterial pressure were calculated as the area under the curve of each pressure wave using the end-diastolic value to determine the heart rate. Animals were allowed to recover from surgery for 2 days and on the 3rd day blood pressure and heart rate were measured continuously in the conscious state after i.v. administration of monoHER (pH: 7.9-8.1) in a dose range from 1-100 mg/kg with an interval of 15 min between each dose.

Ischaemia-reperfusion of the murine heart in vivo
Mice were anaesthetized with ketamine (100 mg/kg i.m.) and xylazine (5 mg/kg s.c.). Body temperature was monitored with a rectal probe and maintained at 37 °C using a warming pad and heating lamp.
The trachea of each mouse was intubated perorally with a stainless-steel tube connected to a respirator (Hugo Sachs Elektronic rodent ventilator type 845, March-Hugstetten, Germany) set at a stroke volume of 250 µl and a rate of 210 strokes/min. After left thoracotomy and exposure of the heart, the left anterior descending coronary artery (LAD) was ligated with 6-0 polypropylene (Surgipro, Connecticut, USA) just proximal to its main branching point. The suture was tied over a 3-mm long polyethylene tube (PE-10) that was left in place for 30 min. Blood flow was then re-established by removal of the tube. The occurrence of reperfusion was assessed by the observation of blood flow in the epicardial coronary arteries through a surgical microscope.
Sham procedures were identical, with the exception of the actual tying of the polypropylene suture. The chest was closed with 5-0 silk sutures. The animals were then weaned from the respirator, and the intratracheal tube was removed once they were breathing spontaneously. Afterwards, 0.2 mg/kg buprenorphine was given s.c. as an analgaesic.

Treatment
MonoHER (7-monohydroxyethylrutoside, molecular weight 654.6, figure 1) was kindly donated by Zyma S.A. (Nyon, Switzerland). Before injection, monoHER was dissolved in 36 mM NaOH in sterile water, in a final concentration of 20 mg/ml (pH=7.9-8.1). Based upon its proven efficacy in earlier studies, monoHER was given i.p. in a dose of 500 mg/kg, 1 hour before induction of ischaemia [9]. Control mice were given 25 µl/g, 0.9 % NaCl solution (same pH) i.p., 1 hour before ischaemia. In

our study four groups were compared: sham saline, sham monoHER, IR saline and IR monoHER.

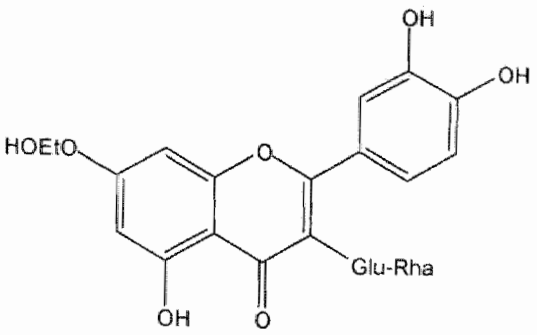

Figure 1: Basic structure of the semisynthetic flavonoid 7-monohydroxyethylrutoside

Evaluation of ischaemic area at risk and infarct size

Depending on the time point of reperfusion (24 h or 2 weeks), infarct size was measured on triphenyltetrazolium chloride (TTC)-stained [12] or AZAN-stained tissue sections with the use of a computerized morphometry system (Quantimet 570, Leica, Cambridge, UK). Briefly we describe these methods.

In the 24 h IR group, mice were anaesthetized with pentobarbital (120 mg/kg, i.p.), the jugular vein was canulated and the thorax was reopened, the LAD reoccluded, and 500 µl of 2.5 % trypan blue was injected into the jugular vein to delineate the non-ischaemic tissue and to quantify the area at risk (AAR). The heart was then excised, briefly washed with isotonic saline, and cut into 2 parts in the frontal plane, central through the ventricles. These parts were then incubated for 20 min at 37 °C with 5 ml of 1 % 2, 3, 5-triphenyltetrazolium chloride solution (TTC, Sigma Chemicals Co., St. Louis, MO, USA). Viable myocardium is stained red by TTC and the necrotic, infarcted area remains unstained [13]. The surface of the left ventricle (LV), the AAR and the infarcted area was measured on both parts of the heart. The percentage AAR/LV, infarct/AAR and infarct/LV was calculated and expressed as the mean of both parts.

For the 2 week IR group, mice were also anaesthetized under pentobarbital (120 mg/kg, i.p.), hearts were excised, washed with isotonic saline and cut into 2 parts in the frontal plane, central through the ventricles, and embedded in paraffin. From each part, one slide (5 µm) was taken and stained with AZAN. The surface of the infarct and the left ventricle were measured on both slides and the percentage infarct/LV was calculated and expressed as the mean of both slides.

Evaluation of ventricular function

Mice were anaesthetized with urethane (2.5 mg/g body weight, i.p., Sigma). Body temperature and respiration were controlled as described before.

A high-fidelity catheter tip micromanometer (Mikro-tip, 1.4F, SPR-671; Millar Instruments, Houston, TX, USA) was inserted through the right carotid artery into the left ventricular cavity. Ventricular pressure was measured and sampled at a rate of 2 kHz. Maximal positive pressure development (+dp/dt) and heart rate were determined on a beat to beat basis and one-second averages were stored on disk.
The heart was then stimulated by an i.v. ramp-infusion of dobutamine (Sigma) using a microinjection pump (Model 200 Series, KdScientific, Boston, MA, USA). The infusion rate of dobutamine was increased every 2 min by 0.5 ng/g/min (last step=5 ng/g/min). In the 2 week IR group, following recovery from dobutamine infusion (taking 10-20 min and assessed by restoration of +dp/dt and heart rate to around baseline levels), hearts were additionally stressed by loading the circulation with an i.v. infusion of warmed (37 °C) Ringer's solution for 1 min at a rate of 2.5 ml/min.
Maximal values for +dp/dt were recorded and the difference between the maximal value and the value at baseline was calculated. At the end of the experiment, hearts were excised, washed with isotonic saline and ventricular weights were determined.

Immunohistochemistry
To determine the number of infiltrating polymorphonuclear neutrophils (PMNs), heart specimens were immediately frozen and stored at –80 ^{0}C. Frozen sections (6 μm) were stained for neutrophils with a rat anti-mouse neutrophil specific antibody, NIMP-R14 [14] using peroxidase-labelled rabbit anti-rat immunoglobulin (Ig) as the secondary mAb and 3-amino-9-ethylcarbazole as a chromogen followed by a hematoxylin counterstain. The numbers of PMNs per grid (0.25 mm^2) were counted under a high-power microscope field (x 200) in a blinded fashion. Average numbers of PMNs were obtained by counting 9 grids per slide in 8 apical slides per heart and compared between saline and monoHER-treated animals at both 6 h and 24 h reperfusion.

Statistical analysis
All parameters are expressed as mean ±S.E.M. Numbers of neutrophils, infarct size and increase in +dp/dt by dobutamine and volume loading were evaluated using Student's t-test.
Dose response curves for dobutamine were compared using a two-way analysis of variance (ANOVA) and a post-hoc Bonferonni test. *P*-values <0.05 were regarded as statistically significant.

Results

General
A total of 50 animals were subjected to sham surgery or IR, and studied for ventricular contractility after 24 h reperfusion. Six of these animals died prematurely because of complications due to anaesthesia, arrhythmia or bleeding. In 5 animals we could not measure contractility because of difficulties in passing the cardiac valves with the catheter tip.

Table 1: Biometric data of mice subjected to sham surgery and ischaemia-reperfusion.

Time	Group		N	Age (weeks)	BW (g)	VW/BW (%)
24 h	Sham	Saline	10	11.0±0.5	37.3±1.0	0.44±0.01
		MonoHER	10	10.7±0.5	38.0±1.1	0.45±0.01
	IR	Saline	10	10.3±0.5	37.1±0.9	0.44±0.02
		MonoHER	9	10.4±0.4	37.7±0.7	0.40±0.05
2 weeks	Sham	Saline	9	10.1±0.3	39.2±0.8	0.45±0.01
		MonoHER	7	11.0±0.3	38.3±0.7	0.44±0.01
	IR	Saline	10	10.7±0.3	40.0±1.6	0.49±0.02
		MonoHER	9	11.1±0.2	39.1±0.9	0.44±0.05

Abbreviations: BW=body weight; VW=ventricular weight.

For the 2 week IR group, 43 animals were subjected to surgery. Two animals died during or shortly after surgery, 2 animals died between 3 and 7 days after reperfusion and 1 animal died after 12 days, for unknown reason. In 3 animals we could not measure contractility due to technical complications as mentioned above.
Table 1 summarizes age and body weights of mice in the different groups used for evaluation of cardiac contractility. There were no significant differences between groups in any of the parameters. The ventricular weight/body weight ratio (VW/BW) was slightly increased in the 2 week saline IR group compared to the sham groups and the monoHER-treated IR group at that time point.

Blood pressure and heart rate
Figure 2 shows mean arterial pressure and heart rate in conscious mice (N=4) measured under control conditions (marker C) and after i.v. administration of cumulative amounts of monoHER. MonoHER was found to have no acute influence on blood pressure and heart rate.

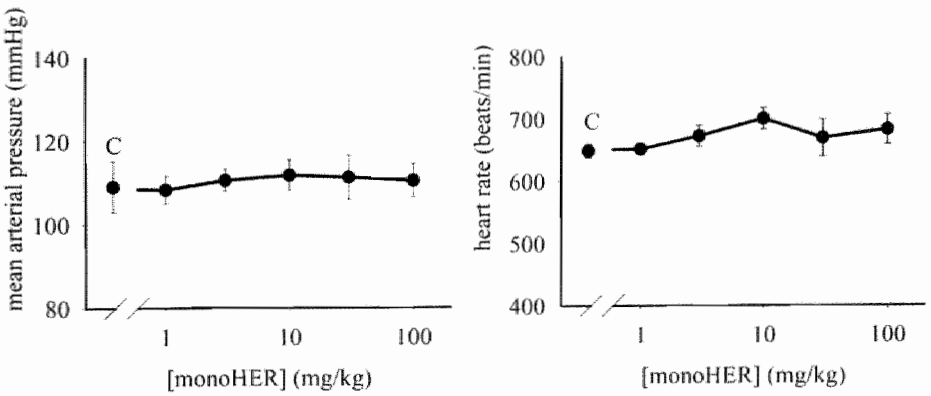

Figure 2: Mean arterial pressure and heart rate measured in conscious mice (N=4) under control conditions (marker C) and after i.v. administration of monoHER in a cumulative fashion from 1-100 mg/kg. Data points represent the mean values obtained from 5-15 min after injection.

Neutrophil infiltration

Figure 3 illustrates the inflammatory response following IR as evidenced by neutrophil infiltration within the injured tissue. In the saline group, the amount of neutrophils in cardiac tissue was more than doubled from 6 to 24 h after reperfusion. The number of neutrophils was significantly lower in the monoHER-treated group, 6 h after reperfusion (saline: 22±5, monoHER: 5±1; P=0.006) and 24 h after reperfusion (saline: 51±11, monoHER: 12±3; P=0.007). In the sham groups, no neutrophils were detected in cardiac tissue.

A:

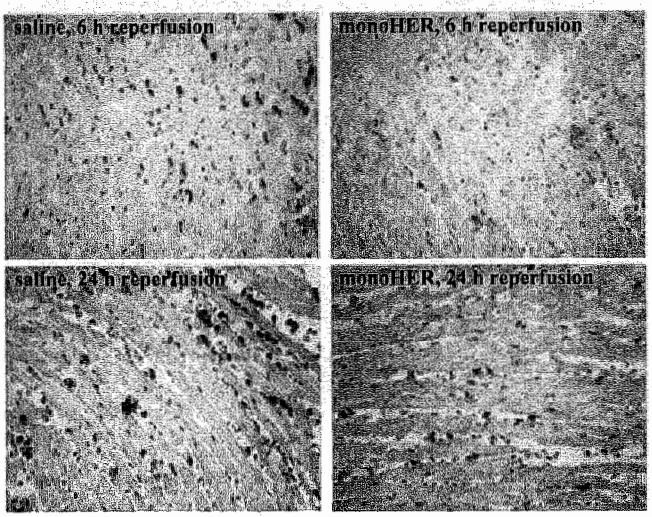

B:

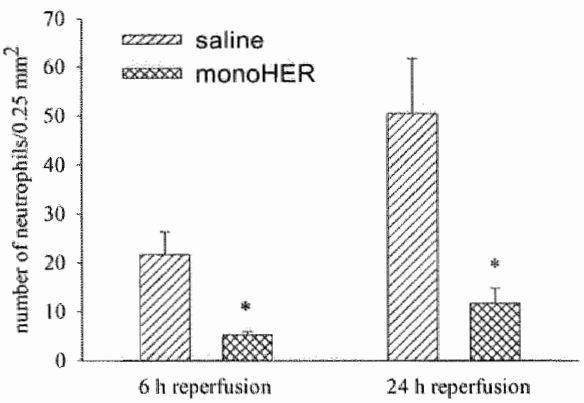

Figure 3: Neutrophil infiltration in the ischaemic heart after 6 h and 24 h of reperfusion (N=10 per group). **A:** Cardiac tissue sections with NIMP-R14 positive cells (brown), representing neutrophils.
B: Average number of infiltrating neutrophils per grid (magnification x200).
At both 6 h and 24 h of reperfusion, neutrophil numbers were significantly lower (*P<0.01) in monoHER-treated mice than in time-matched saline groups.

Myocardial infarct size

Twenty-four hours after reperfusion the AAR of the left ventricle was comparable in the saline group and the monoHER-treated group (47±2 % and 50±7 %, respectively), indicating that the ligation was placed reproducibly (figure 4B).

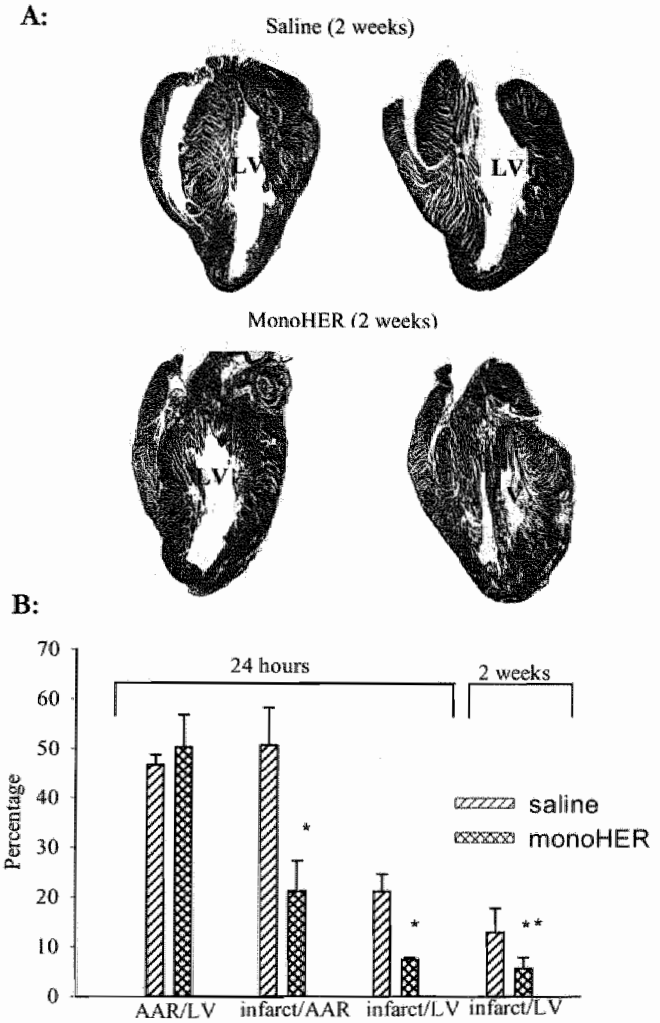

Figure 4: Evaluation of area at risk (AAR) and infarct size (infarct) after 24 h and 2 weeks of reperfusion.
A: AZAN stained heart tissue sections of animals after 2 weeks of IR. Infarcted area (blue) in the wall of the left ventricle (indicated as LV) versus non-infarcted area (red). Note the reduced infarcted area in the monoHER-treated animal.
B: There was no significant difference in myocardial AAR/LV ratios in monoHER-treated mice and mice from the saline group at 24 h of reperfusion. Infarct/AAR and infarct/LV ratios were significantly smaller in monoHER-treated mice than in mice from the saline group after 24 h (*P<0.01) and 2 weeks (**P=0.014) of reperfusion.

However, the infarct/AAR ratio was significantly smaller in the monoHER-treated group than in the saline group (saline: 51±8 %, monoHER: 21±6 %; *P*=0.009; N=13 per group). The infarct/LV ratio was also significantly smaller in the monoHER-treated group than in the saline group (saline: 21±4 %, monoHER: 9±4 %; *P*=0.005). Figure 4A represents 2 sections of a heart from the saline group versus 2 sections of the heart of a monoHER-treated animal 2 weeks after reperfusion. Infarct size 2 weeks after reperfusion was significantly smaller in the monoHER-treated group than in the saline group (figure 4B; saline: 13±4 %, monoHER: 7±2 %; *P*=0.014; N=10 per group).

Ventricular contractility

Cardiac function was evaluated 24 h and 2 weeks after reperfusion by measuring heart rate and the rate of left ventricular pressure development (+dp/dt). Under basal conditions +dp/dt and heart rate did not differ between sham and IR groups. Basal heart rate was significantly higher in the saline IR group compared to the saline sham group (*P*<0.01) after 24 h. When the heart was stimulated with an increasing dose of dobutamine (i.v.), +dp/dt levels increased dose-dependently in the sham animals whereas the increase was significantly blunted in the saline IR animals (figure 5A).

The increase of +dp/dt was significantly restored in the monoHER-treated IR group at both time points (24 h and 2 weeks after reperfusion). Dose response curves for heart rate were comparable between groups (figure 5B). In the 24 h IR saline group, increase in +dp/dt was significantly smaller (+2456±475 mmHg/s) than in the sham saline group (+5939±928 mmHg/s; *P*=0.004) and the IR monoHER-treated group (+5515±928 mmHg/s; *P*=0.0003). Similar effects were seen in the 2 week IR saline group where the increase in +dp/dt (+3174±1066 mmHg/s) was significantly lower than in the sham saline group (+7487±1209 mmHg/s; *P*=0.01) and the monoHER-treated IR group (+7274±687 mmHg/s; *P*=0.005). Comparable results were obtained following volume loading (figure 5C). The increase of +dp/dt in the 2 week IR saline group (+1758±991 mmHg/s) was significantly smaller than in the sham saline group (+6129±1247 mmHg/s; *P*=0.02) and the monoHER-treated IR group (+5723±575 mmHg/s; *P*=0.006).

Discussion

The results of this study show that 7-monohydroxyethylrutoside (monoHER), when administered i.p. one hour before ischaemia, exerts a significant cardioprotective effect after IR in mouse hearts and that this effect is sustained.

MonoHER was chosen for this study because it has strong radical scavenging and iron chelating properties [15]. This capacity makes it a potential drug for the prevention of oxidative stress-related reperfusion injury. In addition monoHER protects against doxorubicin-induced cardiotoxicity *in vivo* [9, 10].

Flavonoids have effects on a variety of inflammatory responses and immune function [16]. An *in vitro* study showed that monoHER has anti-inflammatory effects by reducing neutrophil adhesion through inhibition of doxorubicin-induced expression of vascular cell adhesion molecule (VCAM) and E-selectin [17].

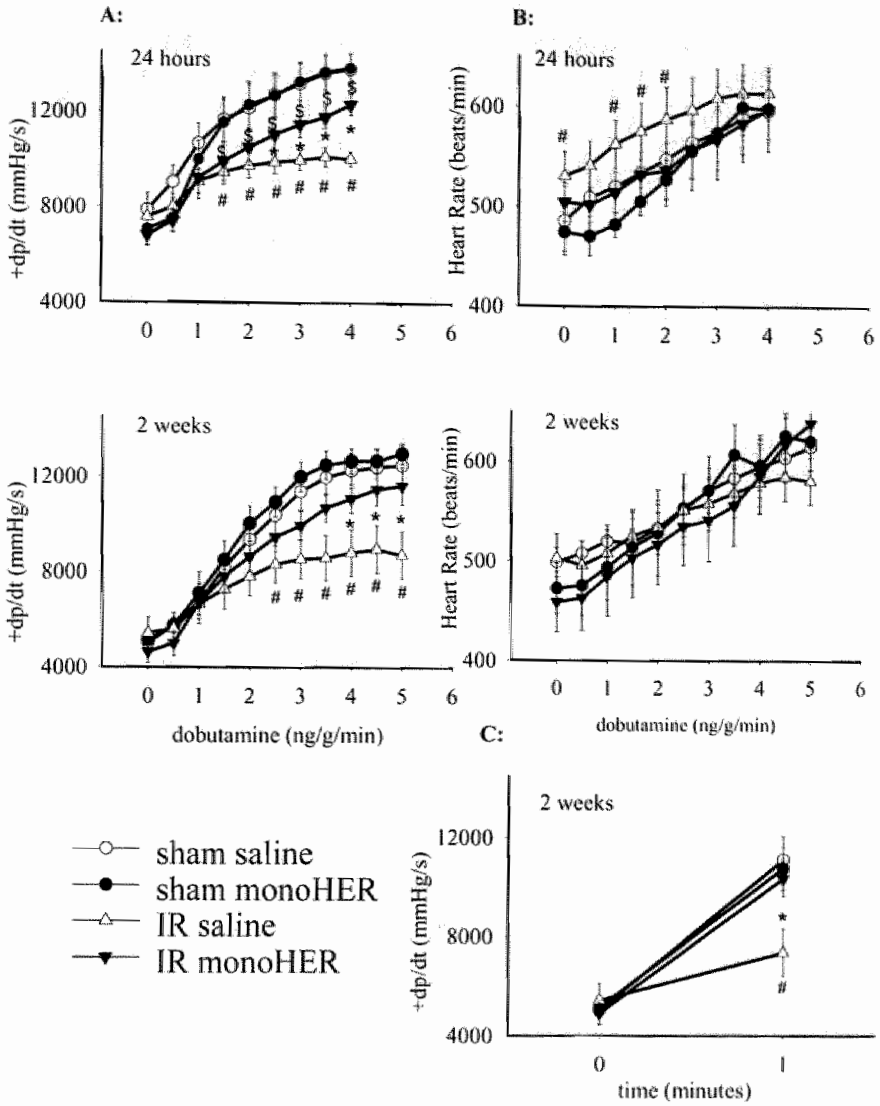

Figure 5: *In vivo* assessment of left ventricular contractility:

A: Cardiac contractility during dobutamine stimulation at 24 h and 2 weeks after reperfusion. $^{\#}P<0.01$: significantly different between non-treated IR (IR saline) and sham-operated controls (sham saline); $^{*}P<0.01$: significantly different between non-treated IR (IR saline) and monoHER-treated IR (IR monoHER); $^{\$}P<0.01$: significantly different between monoHER-treated IR (IR monoHER) and monoHER-treated sham (sham monoHER).

B: Increase in heart rate after dobutamine stimulation. At both time points, 24 h and 2 weeks after reperfusion, there was no significant difference between the groups. Basal heart rate in the saline IR group was significantly higher than in the saline sham group ($^{\#}P<0.01$).

C: Contractility (+dp/dt) measured before and after volume loading at 2 weeks of reperfusion. $^{*}P=0.006$: significantly different between IR saline and IR monoHER; $^{\#}P\leq0.02$: significantly different between non-treated IR (IR saline) and sham-operated controls (sham saline).

In the present study we showed that monoHER also reduces the inflammatory response *in vivo* by reducing influx of neutrophils in the infarcted area of the heart. The reason for this reduction in the number of neutrophils by monoHER in our model is probably dual. First, due to a reduction in tissue damage and therefore a reduced stimulus for an inflammatory response, and second, due to a direct anti-inflammatory effect of monoHER. However, the role of the reduction in neutrophils itself by monoHER treatment on the reduced infarct size 2 weeks after reperfusion is unknown. A direct causal association between the number of neutrophils and myocardial cell death is still under debate [18-23]. To our knowledge, there is only one *in vivo* study that has examined the effects of neutrophil depletion after a prolonged time (in terms of weeks) of reperfusion.

Metzler *et al.* (2001) demonstrated that in mice deficient in intercellular adhesion molecule-1 (ICAM-1), protection occurred in the early phase after reperfusion, but that at a later stage, 1 and 3 weeks after reperfusion, scar size in the ventricles was comparable between knock-out and wild-type mice. This suggests that neutrophil infiltration into the infarcted area may help promote repairing cardiac tissue, and consequently, the enhancement of leukocyte recruitment might be beneficial.

However, following monoHER treatment, infarct size remained significantly smaller 2 weeks after reperfusion, indicating that monoHER prevents, rather than delays myocardial IR injury. In contrast to the study of Metzler *et al.* (2001), monoHER treatment was applied to prevent the initial damage before the influx of neutrophils occurs. This means that the reduction in myocardial neutrophil influx and infarct size and the prevention of deterioration of cardiac contractility by monoHER was effective and that no significant additional damage occurred during the subsequent period of reperfusion. The present data therefore support the view that IR injury due to free radicals occurs in the initial phase after initiation of reperfusion [24-27] and effective antioxidant treatment must therefore be directed to this phase.

In the saline groups, infarct size/left ventricle ratio was higher at 24 h than at 2 weeks after reperfusion, most likely due to the different techniques that were required to measure infarct size. TTC staining is used to detect infarct size shortly after reperfusion, whereas AZAN staining is used after longer periods of reperfusion to detect the amount of granulation tissue. There is, however, a clear reduction in infarct size in the monoHER-treated reperfusion group compared to the saline reperfusion group at both time points.

MonoHER did not influence baseline levels of heart rate and mean arterial pressure in conscious mice. This finding excludes the notion that protective effects of monoHER are due to possible hemodynamic changes which can have preconditioning and therefore protective effects [28].

Baseline +dp/dt levels were not different between the IR and sham-operated mice at any time point. This is probably due to the fact that the infarct size is relatively small after cardiac IR in mice. Earlier experiments from our group showed a significantly reduced cardiac contractility at baseline in mice with permanent myocardial infarction and related larger infarcts of around 45 % of the left ventricle [29]. The significantly higher heart rate at basal level, 24 h after reperfusion in the saline group is probably due to neurohumoral compensation to maintain cardiac output after cardiac damage.

This phenomenon was not observed 2 weeks after reperfusion suggesting a normalization of this response. Stressing the heart by an infusion of dobutamine did reveal differences in cardiac contractility between groups. Ischaemia-reperfusion resulted in a blunted response to dobutamine. Treatment with monoHER improved the increase of cardiac contractility, both 24 h and 2 weeks after reperfusion. To examine if the blunted response to dobutamine was primarily due an impaired β-adrenergic effect we also stressed the heart by volume loading. Because the increase in contractility was comparable to the effects obtained by dobutamine stimulation, we can conclude that the improved cardiac response is due to a reduced infarct size rather than a change in β-adrenergic effectiveness.

Timing, route and amount of monoHER administration in this study were based on the design of the earlier *in vivo* studies in which monoHER was proven to act protective in a model of doxorubicin cardiotoxicity. For later clinical application of monoHER in the reduction of IR injury, further studies has to be done in which different time points of administration (as post-ischaemia) and lower amounts of monoHER should be tested.

In conclusion the present study shows that the antioxidant 7-monohydroxyethylrutoside strongly reduced myocardial neutrophil influx, infarct size and prevented deterioration of cardiac contractility in an *in vivo* mouse model of cardiac ischaemia-reperfusion. To our knowledge, this is the first time that sustained protective effects (in terms of weeks) of a flavonoid are demonstrated in a model of cardiac ischaemia-reperfusion.

References

1. Dhalla NS, Elmoselhi AB, *et al.* Status of myocardial antioxidants in ischemia-reperfusion injury. Cardiovasc Res. 2000; 47: 446.
2. Jolly SR, Kane WJ, *et al.* Canine myocardial reperfusion injury. Its reduction by the combined administration of superoxide dismutase and catalase. Circ Res. 1984; 54: 277.
3. Lefer DJ, Granger DN. Oxidative stress and cardiac disease. Am J Med. 2000; 109: 315.
4. Kaminski KA, Bonda TA, *et al.* Oxidative stress and neutrophil activation--the two keystones of ischemia/reperfusion injury. Int J Cardiol. 2002; 86: 41.
5. Frangogiannis NG, Smith CW, *et al.* The inflammatory response in myocardial infarction. Cardiovasc Res. 2002; 53: 31.
6. Jordan JE, Zhao ZQ, *et al.* The role of neutrophils in myocardial ischemia-reperfusion injury. Cardiovasc Res. 1999; 43: 860.
7. Duilio C, Ambrosio G, *et al.* Neutrophils are primary source of O2 radicals during reperfusion after prolonged myocardial ischemia. Am J Physiol Heart Circ Physiol. 2001; 280: H2649.
8. Rekka E, Kourounakis PN. Effect of hydroxyethyl rutosides and related compounds on lipid peroxidation and free radical scavenging activity. Some structural aspects. J Pharm Pharmacol. 1991; 43: 486.
9. van Acker SA, Kramer K, *et al.* Monohydroxyethylrutoside as protector against chronic doxorubicin-induced cardiotoxicity. Br J Pharmacol. 1995; 115: 1260.
10. van Acker FA, van Acker SA, *et al.* 7-monohydroxyethylrutoside protects against chronic doxorubicin-induced cardiotoxicity when administered only once per week. Clin Cancer Res. 2000; 6: 1337.

11. Janssen BJ, Leenders PJ, *et al.* Short-term and long-term blood pressure and heart rate variability in the mouse. Am J Physiol Regul Integr Comp Physiol. 2000; 278: R215.
12. Nachlas MM, Shnitka TK. Macroscopic identification of early myocardial infarcts by alterations in dehydrogenase activity. Am J Pathol. 1963; 42: 379.
13. Vivaldi MT, Kloner RA, *et al.* Triphenyltetrazolium staining of irreversible ischemic injury following coronary artery occlusion in rats. Am J Pathol. 1985; 121: 522.
14. McLaren DJ, Strath M, *et al.* Schistosoma mansoni: evidence that immunity in vaccinated and chronically infected CBA/Ca mice is sensitive to treatment with a monoclonal antibody that depletes cutaneous effector cells. Parasite Immunol. 1987; 9: 667.
15. van Acker FA, Hageman JA, *et al.* Synthesis of novel 3,7-substituted-2-(3',4'-dihydroxyphenyl)flavones with improved antioxidant activity. J Med Chem. 2000; 43: 3752.
16. Manthey JA. Biological properties of flavonoids pertaining to inflammation. Microcirculation. 2000; 7: S29.
17. Abou El Hassan MA, Verheul HM, *et al.* The new cardioprotector Monohydroxyethylrutoside protects against doxorubicin-induced inflammatory effects in vitro. Br J Cancer. 2003; 89: 357.
18. Baxter GF. The neutrophil as a mediator of myocardial ischemia-reperfusion injury: time to move on. Basic Res Cardiol. 2002; 97: 268.
19. Hoffmeyer MR, Scalia R, *et al.* PR-39, a potent neutrophil inhibitor, attenuates myocardial ischemia-reperfusion injury in mice. Am J Physiol Heart Circ Physiol. 2000; 279: H2824.
20. Metzler B, Mair J, *et al.* Mouse model of myocardial remodelling after ischemia: role of intercellular adhesion molecule-1. Cardiovasc Res. 2001; 49: 399.
21. Arai M, Lefer DJ, *et al.* An anti-CD18 antibody limits infarct size and preserves left ventricular function in dogs with ischemia and 48-h reperfusion. J Am Coll Cardiol. 1996; 27: 1278.
22. Birnbaum Y, Patterson M, *et al.* The effect of CY1503, a sialyl Lewisx analog blocker of the selectin adhesion molecules, on infarct size and "no-reflow" in the rabbit model of acute myocardial infarction/reperfusion. J Mol Cell Cardiol. 1997; 29: 2013.
23. Briaud SA, Ding ZM, *et al.* Leukocyte trafficking and myocardial reperfusion injury in ICAM-1/P-selectin-knockout mice. Am J Physiol Heart Circ Physiol. 2001; 280: H60.
24. Zweier JL, Flaherty JT, *et al.* Direct measurement of free radical generation following reperfusion of ischemic myocardium. Proc Natl Acad Sci U S A. 1987; 84: 1404.
25. Shao ZH, Vanden Hoek TL, *et al.* Baicalein attenuates oxidant stress in cardiomyocytes. Am J Physiol Heart Circ Physiol. 2002; 282: H999.
26. Bolli R, Jeroudi MO, *et al.* Direct evidence that oxygen-derived free radicals contribute to postischemic myocardial dysfunction in the intact dog. Proc Natl Acad Sci U S A. 1989; 86: 4695.
27. Wang P, Zweier JL. Measurement of nitric oxide and peroxynitrite generation in the postischemic heart. Evidence for peroxynitrite-mediated reperfusion injury. J Biol Chem. 1996; 271: 29223.
28. Thornton JD, Liu GS, *et al.* Intravenous pretreatment with A1-selective adenosine analogues protects the heart against infarction. Circulation. 1992; 85: 659.
29. Lutgens E, Daemen MJ, *et al.* Chronic myocardial infarction in the mouse: cardiac structural and functional changes. Cardiovasc Res. 1999; 41: 586.

Chapter 4

In vivo protective effects of 7-monohydroxyethylrutoside in a mouse model of cardiac ischaemia-reperfusion are dependent on the time point of administration

Tijl De Celle, Nicole Bitsch, Peter Leenders, Aalt Bast,
Jos F. Smits & Ben J. Janssen

Departments of Pharmacology & Toxicology, Cardiovascular Research Institute Maastricht, Universiteit Maastricht, The Netherlands

Abstract

Previously (chapter 3) we demonstrated that monoHER has strong and sustained cardioprotective effects in an *in vivo* mouse model of cardiac ischaemia-reperfusion when it was administered intraperitoneally, one hour before ischaemia.
The chosen route and timing of administration of monoHER were based on historic results. Recent pharmacokinetic data in mice revealed that following intravenous (i.v.) injection of monoHER, maximal myocardial tissue concentrations of the drug are reached almost immediately. Therefore, we set out a study to test if monoHER would be also effective when administered five min before reperfusion, a time point that has more clinical relevance.
Ischaemia was maintained for 30 min by ligation of the left anterior descending coronary artery. Then the ligature was removed and reperfusion allowed for 24 h. MonoHER (150 mg/kg) or saline was administered i.v. 5 min before reperfusion.
Treatment with monoHER at this time point did neither influence the influx of neutrophils in the injured tissue (IR, saline: 39±12 neutrophils/0.25 mm^2; IR, monoHER: 40±8 neutrophils/0.25 mm^2) nor the increase in cardiac contractility (+dp/dt) in response to dobutamine (IR, saline: +2509±567 mmHg/s; IR, monoHER: +2839±734 mmHg/s), 24 hours after reperfusion.
Based on these data we conclude that the time point of administration is crucial to elicit a cardioprotective effect with monoHER.
Among the explanations for the lack of a clear pharmacodynamic effect of monoHER in this setting are 1) the potential restriction in myocardial uptake in conditions of cardiac IR; 2) the necessity of formation of active metabolites of monoHER; and 3) the possibility that cardioprotective effects of monoHER are due to interference with specific signal transduction pathways during the ischaemic period. Further research is necessary to examine these hypotheses.

Introduction

Reintroduction of oxygen to ischaemic myocardium after myocardial infarction advances the damage caused by ischaemia. This phenomenon, termed the "oxygen paradox" is believed to result from the metabolites of oxygen produced in the reperfused ischaemic milieu [1]. These reactive oxygen species (ROS) are potent cytotoxic compounds capable of disrupting cellular structures and generating myocardial damage. Subsequently, neutrophils adhere to the endothelium and invade the myocardial tissue [2]. Although essential in wound healing, these neutrophils may turn injurious by producing additional ROS and proteolytic enzymes [3-5]. Therefore, the inflammatory response has been linked to lethal injury of myocardium during ischaemia and reperfusion [6].

As described in the general introduction (chapter 1), numerous studies have evaluated the influence of superoxide dismutase, vitamin C, vitamin E, and thiol compounds alone or in various combinations on oxidative stress injury in patients undergoing reperfusion therapy after myocardial infarction. Despite much research and the wide availability of antioxidant agents, there are, however, no clinical indications for the routine use of an antioxidant in the setting of ischaemia and reperfusion.

Flavonoids are a group of naturally occurring polyphenolic compounds with excellent iron chelating as well as radical scavenging properties [7]. In a previous study we demonstrated that the semi-synthetic flavonoid monoHER has potent cardioprotective effects in an *in vivo* mouse model of cardiac ischaemia-reperfusion when administered intraperitoneally (i.p.) one hour before ischaemia [8]. MonoHER treatment significantly reduced myocardial neutrophil influx and infarct size and strongly prevented deterioration of cardiac contractility [8]. These cardioprotective effects were still present two weeks after reperfusion when wound healing is completed. Therefore they can be regarded as being sustained [8].

The timing, route and dose of monoHER administration in that study were based on earlier *in vivo* mouse studies in which monoHER protected against doxorubicin-induced cardiotoxicity [9, 10]. In these studies monoHER was administered i.p. one hour before doxorubicin injection.
Obviously, to minimize damage evoked by chemotherapeutic agents such as doxorubicin it is logical to pre-treat patients with radical scavenging agents such as monoHER. However, when preventing "reperfusion injury", administering an antioxidant as a protective drug before the onset of ischaemia, has less clinical relevance. In addition, recent pharmacokinetic data revealed that following intravenous (i.v.) injection of monoHER, maximal myocardial tissue concentrations of the drug are reached almost immediately [11]. Therefore, we examined whether monoHER would also be cardioprotective if the drug is administered shortly before reperfusion of the ischaemic mouse heart.

Materials and Methods

Animals
Male Swiss mice weighting 35-40 g were used. The animals were purchased and housed as described in detail in chapter 3. The experimental protocol was approved by the animal ethics committee of the Universiteit Maastricht.

Ischaemia-reperfusion of the murine heart in vivo
Mouse hearts were subjected to a 30 min ischaemia and 24 h reperfusion procedure as described in detail in chapter 3. Two experimental groups were compared; one group treated with monoHER and one group in which saline was used as a placebo.
Before injection, monoHER (7-monohydroxyethylrutoside, molecular weight 654.6) was dissolved in 36 mM NaOH in sterile water, in a final concentration of 20 mg/ml (pH=7.9-8.1). MonoHER was given i.v. in a dose of 150 mg/kg, five min before reperfusion. In control mice 25 µl/g, 0.9 % NaCl solution (same pH) was injected i.v., five min before reperfusion.

Evaluation of ventricular function
Under urethane anaesthesia, a Millar pressure transducer was inserted into the left ventricle 24 h after reperfusion. Maximal positive pressure development (+dp/dt) and heart rate were determined in baseline conditions and during a ramp-infusion of i.v. dobutamine (0.5 to 5 ng/g/min) in both groups. For a detailed description the reader is referred to chapter 3.

Immunohistochemistry
At the end of the experiment the area at risk of the heart was excised and the numbers of infiltrating neutrophils were determined by immunocytochemistry as described in detail in chapter 3.

Statistical analysis
All parameters are expressed as mean ±S.E.M. Numbers of neutrophils and maximal increase in +dp/dt by dobutamine between monoHER and saline group were compared by Student's t-test. Dose response curves for dobutamine were compared using a two-way analysis of variance (ANOVA) and a post-hoc Bonferonni test. *P*-values ≤0.05 were considered to indicate statistical significance.

Results

Neutrophil infiltration

Figure 1 illustrates the inflammatory response following cardiac ischaemia-reperfusion as evidenced by neutrophil infiltration within the injured tissue. After 24 h of reperfusion, the number of neutrophils was comparable in the IR, saline group (39±12 neutrophils/0.25 mm²; N=7) and the IR, monoHER group (40±8 neutrophils/0.25 mm²; N=8).

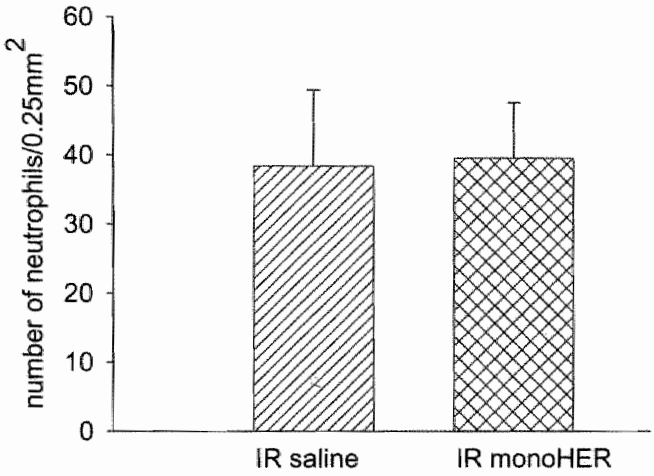

Figure 1: Quantification of the infiltration of neutrophils 24 h after initiation of reperfusion in the ischaemic heart tissue of mice from the IR, saline group and the IR, monoHER group. Average number of infiltrating neutrophils per grid (magnification x200). Neutrophil numbers were similar in the IR, monoHER group (N=8) and the IR, saline group (N=7).

Ventricular contractility

Cardiac function was evaluated 24 h after reperfusion by measuring heart rate and the rate of left ventricular pressure development (+dp/dt) in both the IR, saline group (N=7) and the IR, monoHER group (N=7). Baseline levels of +dp/dt and heart rate were comparable between both groups. During dobutamine stimulation, dose response curves for +dp/dt (figure 2A) and heart rate (figure 2B) were comparable in the IR, saline group and the IR, monoHER group. After 24h of reperfusion the increase in +dp/dt was similar in the IR, saline group (+2509±567 mmHg/s) compared to the IR, monoHER group (+2839±734 mmHg/s).

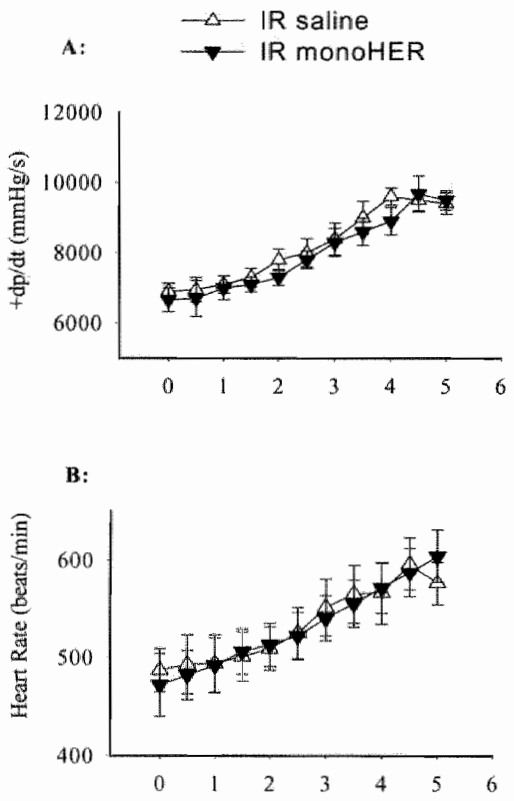

Figure 2: *In vivo* assessment of left ventricular contractility:

A: Cardiac contractility during dobutamine stimulation at 24 h of reperfusion. There was no significant difference between the IR, saline (N=7) and the IR, monoHER group (N=7) in the cardiac contractility response to dobutamine.

B: Increase in heart rate during dobutamine stimulation. Twenty-four hours after reperfusion there was no significant difference between the IR, saline and the IR, monoHER group in the heart rate response to dobutamine.

Discussion

This study indicates that the antioxidant 7-monohydroxyethylrutoside (monoHER) has no cardioprotective effects in our *in vivo* mouse model of myocardial ischaemia-reperfusion when administered i.v. five min before reperfusion. Administration of monoHER at this time point neither affects the influx of neutrophils in the injured tissue nor improved stimulated cardiac contractility, 24 h after reperfusion.
These results are in contrast with our previous study in the same animal model when monoHER was administered i.p. one hour before ischaemia and did reduce myocardial neutrophil influx and infarct size and strongly prevented deterioration of cardiac contractility [8].
This discrepancy in results suggests that the time point of monoHER administration is very crucial to obtain cardioprotective effects.
Abou El Hassan *et al.* showed that the peak concentration of monoHER in heart tissue of mice was reached almost immediately after i.v. administration [11]. This implies that in our current IR model the highest levels of monoHER in heart tissue are most likely reached very early (within one minute) after the initiation of reperfusion. Since this corresponds with the phase at which the production of reactive oxygen species is the highest [12, 13] it was expected that monoHER should have optimal beneficial effects under these conditions. However, it should be mentioned that these pharmacokinetic properties of monoHER were determined in healthy mice that did not undergo cardiac IR. It is possible that the occlusion of the LAD at the moment of monoHER administration prohibited the fast uptake of monoHER in the injured area so that the concentration of monoHER in the affected area was insufficient. In contrast, when monoHER was applied one hour before ischaemia there was no apparent restriction in uptake of monoHER in cardiac tissue. In parallel to these results it has recently been demonstrated that monoHER has also no cardioprotective effects when administered i.p., five min before doxorubicin treatment (unpublished observation, Aalt Bast). This is in contrast with the protective effects which have been demonstrated when monoHER was administered i.p. one hour before doxorubicin injection [9, 10].
In the doxorubicin model there is no restriction at all in the uptake of monoHER in cardiac tissue. Therefore it is doubtful that the limited uptake of monoHER in our cardiac IR model is a major cause for its failure when applied five min before reperfusion. However, tissue concentrations of monoHER should be determined in the area that undergoes IR to clarify this point.

A second explanation for the lack of effect is that not the parent compound but an active metabolite of monoHER is responsible for its beneficial effects. If this is true, five min before reperfusion may be too late to obtain a reasonable concentration of this metabolite and hence cardioprotection against "reperfusion injury". Except for the aglycones, no metabolites of monoHER have been described today [11]. Blood samples of patients treated with monoHER are currently sampled to investigate this possibility (personal communication, W.J.F. van der Vijgh, Amsterdam Free University).

The dominant concept of antioxidant therapy during cardiac IR is that it results in a reduction of the detrimental effects of oxidative stress and therefore a direct reduction of tissue damage and impairment of cardiac function. However, recent studies have shown that antioxidant therapy, as a side effect and independent of its antioxidant action, may induce specific signalling cascades [14]. Therefore, a third explanation can be that cardioprotection is not related to the antioxidant effect of monoHER only, but to an unknown side-effect of this compound, or one of its metabolites, on proteins critically involved in the determination of cellular fate, i.e. injury, death or adaptation during ischaemia. In this case it is clear that the time point of monoHER administration, i.e. before ischaemia versus right before reperfusion, may be very crucial.

Furthermore, in some reports it has been shown that production of ROS may occur during the period of ischaemia [15-18]. Specifically, when exposed to hypoxia, cardiomyocytes have been shown to increase production of ROS derived from the mitochondrial electron transport chain [19]. The general physiological consequences of hypoxic mitochondrial ROS production are not completely understood. Mitochondrial ROS may 1) promote the stabilization and activity of hypoxia inducible factor-1α (HIF-1α) transcription factor [20]; 2) alter cardiac myocyte contractility [19]; 3) modulate Na^+-K^+-ATPase activity [21]; or 4) influence mitochondrial depolarization [22]; and 5) mitogen-activated protein kinases [23].
These studies reveal that ROS, besides their direct detrimental effects on cellular structures, influence a variety of cellular signal transduction cascades during ischaemia. Therefore, our fourth explanation is that monoHER, by reducing ROS during ischaemia, may have an influence on such pathways.

We conclude that monoHER has potential strong and sustained cardioprotective properties in an *in vivo* mouse model of cardiac ischaemia-reperfusion. However, these protective effects of monoHER are highly dependent on the time point of administration. Future studies are necessary to determine the mechanisms of action of monoHER and the clinical efficiency of monoHER in the setting of cardiac ischaemia-reperfusion.

References

1. Hess ML, Manson NH. Molecular oxygen: friend and foe. The role of the oxygen free radical system in the calcium paradox, the oxygen paradox and ischemia/reperfusion injury. J Mol Cell Cardiol. 1984; 16: 969.
2. Entman ML, Michael L, *et al.* Inflammation in the course of early myocardial ischemia. Faseb J. 1991; 5: 2529.
3. Duilio C, Ambrosio G, *et al.* Neutrophils are primary source of O2 radicals during reperfusion after prolonged myocardial ischemia. Am J Physiol Heart Circ Physiol. 2001; 280: H2649.
4. Jordan JE, Zhao ZQ, *et al.* The role of neutrophils in myocardial ischemia-reperfusion injury. Cardiovasc Res. 1999; 43: 860.
5. Kaminski KA, Bonda TA, *et al.* Oxidative stress and neutrophil activation--the two keystones of ischemia/reperfusion injury. Int J Cardiol. 2002; 86: 41.
6. Hansen PR. Role of neutrophils in myocardial ischemia and reperfusion. Circulation. 1995; 91: 1872.

7. Rekka E, Kourounakis PN. Effect of hydroxyethyl rutosides and related compounds on lipid peroxidation and free radical scavenging activity. Some structural aspects. J Pharm Pharmacol. 1991; 43: 486.
8. De Celle T, Heeringa P, *et al.* Sustained protective effects of 7-monohydroxyethylrutoside in an in vivo model of cardiac ischemia-reperfusion. Eur J Pharmacol. 2004; 494: 205.
9. van Acker SA, Kramer K, *et al.* Monohydroxyethylrutoside as protector against chronic doxorubicin-induced cardiotoxicity. Br J Pharmacol. 1995; 115: 1260.
10. van Acker FA, van Acker SA, *et al.* 7-monohydroxyethylrutoside protects against chronic doxorubicin-induced cardiotoxicity when administered only once per week. Clin Cancer Res. 2000; 6: 1337.
11. Abou El Hassan MA, Kedde MA, *et al.* Bioavailability and pharmacokinetics of the cardioprotecting flavonoid 7-monohydroxyethylrutoside in mice. Cancer Chemother Pharmacol. 2003; 52: 371.
12. Bolli R, Jeroudi MO, *et al.* Marked reduction of free radical generation and contractile dysfunction by antioxidant therapy begun at the time of reperfusion. Evidence that myocardial "stunning" is a manifestation of reperfusion injury. Circ Res. 1989; 65: 607.
13. Mitsos SE, Fantone JC, *et al.* Canine myocardial reperfusion injury: protection by a free radical scavenger, N-2-mercaptopropionyl glycine. J Cardiovasc Pharmacol. 1986; 8: 978.
14. Marczin N, El-Habashi N, *et al.* Antioxidants in myocardial ischemia-reperfusion injury: therapeutic potential and basic mechanisms. Arch Biochem Biophys. 2003; 420: 222.
15. Vanden Hoek TL, Li C, *et al.* Significant levels of oxidants are generated by isolated cardiomyocytes during ischemia prior to reperfusion. J Mol Cell Cardiol. 1997; 29: 2571.
16. Przyklenk K, Kloner RA. Effect of oxygen-derived free radical scavengers on infarct size following six hours of permanent coronary artery occlusion: salvage or delay of myocyte necrosis? Basic Res Cardiol. 1987; 82: 146.
17. Kevin LG, Camara AK, *et al.* Ischemic preconditioning alters real-time measure of O2 radicals in intact hearts with ischemia and reperfusion. Am J Physiol Heart Circ Physiol. 2003; 284: H566.
18. Becker LB. New concepts in reactive oxygen species and cardiovascular reperfusion physiology. Cardiovasc Res. 2004; 61: 461.
19. Duranteau J, Chandel NS, *et al.* Intracellular signaling by reactive oxygen species during hypoxia in cardiomyocytes. J Biol Chem. 1998; 273: 11619.
20. Schroedl C, McClintock DS, *et al.* Hypoxic but not anoxic stabilization of HIF-1alpha requires mitochondrial reactive oxygen species. Am J Physiol Lung Cell Mol Physiol. 2002; 283: L922.
21. Dada LA, Chandel NS, *et al.* Hypoxia-induced endocytosis of Na,K-ATPase in alveolar epithelial cells is mediated by mitochondrial reactive oxygen species and PKC-zeta. J Clin Invest. 2003; 111: 1057.
22. Levraut J, Iwase H, *et al.* Cell death during ischemia: relationship to mitochondrial depolarization and ROS generation. Am J Physiol Heart Circ Physiol. 2003; 284: H549.
23. Kulisz A, Chen N, *et al.* Mitochondrial ROS initiate phosphorylation of p38 MAP kinase during hypoxia in cardiomyocytes. Am J Physiol Lung Cell Mol Physiol. 2002; 282: L1324.

Chapter 5

Alterations in mouse cardiac proteome after *in vivo* myocardial infarction: permanent ischaemia versus ischaemia-reperfusion

Tijl De Celle[1], Frank Vanrobaeys[3], Peter Lijnen[1], W. Matthijs Blankesteijn[1], Sylvia Heeneman[2], Jozef Van Beeumen[3], Bart Devreese[3], Jos F.M. Smits[1], Ben J.A. Janssen[1]

Experimental Physiology; 2005; 90 (4): 593-606

Departments of Pharmacology & Toxicology[1] and Pathology[2], Cardiovascular Research Institute Maastricht, Universiteit Maastricht, The Netherlands
Laboratory of Protein Biochemistry and Protein Engineering[3], Universiteit Gent, Belgium

Abstract

Mice are increasingly used to study the early molecular mechanisms inducing injury to the heart following myocardial infarction. To date, two-dimensional gel electrophoresis combined with mass spectrometry has not been applied to identify changes in protein expression in myocardial tissue of mice subjected *in vivo* to permanent ischaemia (PI) or ischaemia-reperfusion (IR).

In the PI group, ischaemia was induced for 210 min by ligation of the left anterior descending coronary artery while in the IR group, ischaemia was maintained for 30 min and reperfusion was allowed for 180 min. In both groups, the area at risk of the left ventricle was processed for 2-D gel electrophoresis.

By comparing protein density changes in cytosolic as well as membrane fractions, we found a total of thirty-two protein spots that were differentially expressed. Twenty spots changed in expression level after PI alone, four spots after IR alone, and eight spots changed in both models. Identified proteins with MALDI TOF-TOF and LC-MS/MS can be classified into functional groups being anticoagulant proteins, structural proteins, inflammatory-related proteins, transcription- and translation-related proteins, heat shock proteins (HSPs), metabolism-related proteins, and miscellaneous. A remarkable finding was the IR specific translocation of annexins (A3 & A5) from the cytosolic to the membrane compartment, a phenomenon that was verified by Western blotting. Four proteins were changed in expression level at multiple spot locations, characterized by a difference in isoelectric point. In the case of cardiac troponin T and HSP-20, these changes were also dependent on the model. In addition, one spot for the proteins adenylate kinase 1, cardiac troponin T and HSP-20 was uniquely present in the IR and/or PI groups and not in the respective sham groups.

The specific alterations in protein expression that took place after PI and IR may stimulate the search for new tools to diagnose myocardial infarction and to characterize specific pathology related changes in protein expression.

Introduction

Myocardial infarction is one of the most frequent cardiovascular events in the Western world. Current treatment of myocardial infarction is directed to restore blood flow to the ischaemic region by thrombolysis, coronary artery bypass surgery or percutaneous transluminal coronary angioplasty. Depending on the degree of success of the therapeutic intervention, the area at risk (AAR) remains either hypoxic or is fully salvaged. When the AAR remains hypoxic, the myocardial tissue loses its contractile function, becomes necrotic and a wound-healing process is initiated [1]. In contrast, when blood flow through the myocardium is re-established in time, hibernating myocardial tissue may regain its function but may also experience additional damage due to the reperfusion process itself. This reperfusion injury is mainly induced by the generation of reactive oxygen species [2, 3].

Proteomic studies of human heart tissue may provide new insights into the specific early molecular mechanisms that underlie the responses to ischaemia or ischaemia-reperfusion injury and therefore may have important implications for the specificity and efficacy of diagnosis and treatment. In relation to this, Van Eyk *et al.* have described a two-dimensional electrophoresis technique on myocardial biopsies from patients undergoing coronary artery bypass surgery [4]. However, these studies are complicated by factors such as small size of sample, availability, disease state, tissue heterogeneity, genetic variability, medical history, and therapeutic interventions [5].

Alternatively, standardized animal models of myocardial infarction and ischaemia-reperfusion are available [6, 7]. To our knowledge in three studies, 2-D gel electrophoresis was used to identify changes in protein levels after myocardial infarction [8-10]. Sawicki *et al.* [10] found, in an *in vivo* dog model of myocardial ischaemia-reperfusion, changes in the level of four metabolic enzymes (NAD^+-isocitrate dehydrogenase, α subunit; creatine kinase, chain M; α subunit ATP synthase isoforms precursor; ATP synthase D chain, mitochondrial) and a contractile protein (ventricular myosin light chain 1). Also, in an *in vivo* rabbit model of cardiac ischaemia-reperfusion, Schwertz *et al.* [8] found ten protein spots that were differentially expressed. Two could be characterized as the protective proteins superoxide dismutase and αB-crystallin. In addition, Sakai *et al.* [9] found in an *in vitro* rat model eight protein spots with altered expression after cardiac ischaemia or ischaemia-reperfusion. Five protein spots were identified as the endoplasmatic reticulum enzyme protein disulfide isomerase A3, one as 60 kDa heat shock protein and two as mitochondrial elongation factor Tu. These data indicate that the classes of proteins that are differentially expressed after myocardial infarction vary considerably between studies. The fact that different species were used and myocardial tissue was harvested at different time points (i.e. between 60 and 240 min after initiation of ischaemia) may contribute to this.

The mouse has been increasingly used to study the early molecular mechanisms inducing injury to the heart following myocardial infarction. To date two-dimensional gel electrophoresis combined with mass spectrometry has not been applied to identify alterations in protein expression in myocardial tissue after *in vivo*

myocardial infarction in mice. In addition, only the study of Sakai *et al.* [9] compared changes in protein expression after both ischaemia and ischaemia-reperfusion, although they used an *in vitro* rat model and no *in vivo* model.

Thus, the goal of the present study was to identify changes in cardiac protein expression after *in vivo* myocardial infarction in the mouse. A model of permanent ischaemia (PI) and a model of ischaemia-reperfusion (IR) were used to identify and distinguish between common and specific changes in protein expression induced by *in vivo* IR and PI. We studied early (210 min) changes in protein expression in order to identify potential new targets for cardioprotection that are beneficial in the first few hours of myocardial infarction. In addition, by separately analyzing the soluble cytosolic fraction and the membrane fraction we were not only able to increase the resolution but also to detect pathology-related protein translocations between both compartments.

Materials and methods

Animals

Male outbred Swiss mice (7-9 weeks old, body weight of 35-40 g) were purchased from Charles River (Maastricht, The Netherlands). Experiments were performed according to the guidelines of the University of Maastricht and were approved by the institutional animal ethics committee. The animals were kept on a 12 h light-12-h dark cycle in a temperature-controlled (21±2 °C) room. After surgery, animals were housed individually with *ad libitum* access to water and standard food pellets (type Ssniff, Soest, Germany).

In vivo ischaemia-reperfusion and permanent ischaemia

Mice were anaesthetized with ketamine (100 mg/kg i.m.) and xylazine (5 mg/kg s.c.). Body temperature was monitored with a rectal probe and maintained at 37 °C using a warming pad and heating lamp. The trachea of each mouse was intubated per orally with a stainless-steel tube connected to a respirator (Hugo Sachs Electronic rodent ventilator type 845, March-Hugstetten, Germany) set at a stroke volume of 250 µL and a rate of 210 strokes/min. After left thoracotomy and exposure of the heart, the LAD was ligated with a 6-0 polypropylene suture (Surgipro, Connecticut, USA) directly proximal to its main branching point. The suture was tied around a 3-mm long polyethylene tube (PE-10) to induce ischaemia.

After 30 min of ischaemia, in the IR group, the ligature around the LAD was removed and the occurrence of reperfusion was assessed by the observation of blood flow in the epicardial coronary arteries through a surgical microscope. The ischaemic myocardium was reperfused for 180 min. In the PI group, the suture was tied permanently for 210 min. Separate sham groups for both IR and PI models were made following an identical procedure but without the actual tying of the polypropylene suture. The chest was closed with 5-0 silk sutures. The animals were then weaned from the respirator, and the intratracheal tube was removed once they were breathing spontaneously.

Cardiac tissue was harvested 210 min after initiation of ischaemia. At this point, mice were re-anaesthetized with pentobarbital (120 mg/kg intraperitoneally) and the thorax was reopened. In the IR animals the LAD was re-occluded and 500 µL of 2.5 % trypan blue (Merck, Darmstadt, Germany) was injected into the jugular vein to delineate the non-ischaemic tissue from the ischaemic tissue. This ischaemic area is defined as the area at risk (AAR). Immediately afterwards the heart was excised and cleared from blood by rinsing in isotonic saline (0 °C). In the PI and IR group, the AAR was cut out whilst in the sham-operated animals the corresponding left ventricular region was taken. Only these tissue samples (AAR and corresponding region in the sham animals) were snap frozen in liquid nitrogen, stored at -80 °C and used whole for further study. As the AAR is not perfused with trypan blue, there can't be an influence of the dye on the proteome. The amount of myocardial necrosis and apoptosis in these *in vivo* mice models has previously been determined in our lab [7, 11].

Sample preparation

The frozen tissue samples were pulverized to fine powder under liquid nitrogen using a mortar and pestle and homogenized using a handheld homogenizer in 40 mM Tris buffer (pH=10.0) containing 300 U DNase and RNase and a protease inhibitor mix (Complete Mini®, Merck, Darmstadt, Germany). We used a technique of high-speed sedimentation/centrifugation that separates the total membrane fraction from all soluble cytosolic proteins as described by Pasquali *et al.* [12]. To assure the reliability, all samples from the IR group (or PI group) and its respective sham group were processed simultaneously. After 30 min on ice, cytosolic fractions were separated by centrifugation at 100.000 g for 60 min at 4°C and stored at -80 °C for further analysis. To avoid contamination with remaining cytosolic proteins, the 100.000 g pellet fraction was additionally dissolved in 40 mM Tris buffer and precipitated under the same conditions. After the supernatant was removed, the remaining membrane pellet was dissolved in 40 mM Tris buffer (pH=7.5) containing 7 M urea, 2 M thiourea, 1 % DTT, 1 % CHAPS and a protease inhibitor mix (Complete Mini®, Merck, Darmstadt, Germany) and stored at -80 °C. The final protein concentration of both homogeneous fractions was determined using a protein assay (BioRad, Veenendaal, The Netherlands).

Two-dimensional gel electrophoresis

For the cytosolic fraction as well as the membrane fraction, 400 µg of protein were dissolved in rehydration solution (8 M urea, 2 % CHAPS, 0.5 % IPG-buffer, pH 4-7 linear and a trace of coomassie brilliant blue) up to a volume of 450 µL. Only for the cytosolic fraction, a 2-D Clean-Up kit (Amersham Pharmacia, Uppsala, Sweden) was used in order to remove Tris buffer and to dissolve only the protein fraction in the rehydration solution (pH: 7.5). Immobiline DryStrips® (Amersham Pharmacia, Uppsala, Sweden), 24 cm, pH 4-7 linear, were allowed to rehydrate (14 h, 30 V) in the protein solution under low viscosity oil in strip holders. Then, isoelectrical focusing was performed at 200 V for 1h, 500 V for 1 h, 1000 V for 1 h and 8000 V for 16 h (approximately 128 kVh in total). The rehydration step and isoelectric focusing (IEF)

steps were accomplished using an IPGphor unit (Amersham Pharmacia, Freiburg, Germany) with the temperature being maintained at 20 °C.
After the first dimensional run, the individual strips were equilibrated by gently shaking twice for 15 min in a solution containing 50 mM Tris-HCl (pH 8.8), 6 M urea, 30 % v/v glycerol, 2 % SDS and a trace of coomassie brilliant blue. Additionally, the first equilibration step contained 1 % DTT and the second 2.5 % iodoacetamide.
After equilibration, the IPG strips were placed on top of a 12 % polyacrylamide gel (37:5:1) and proteins were then separated according to their molecular weight (M_r) using an electrophoresis system (Ettan Dalt, Amersham Pharmacia, Freiburg, Germany). The run was completed when the coomassie brilliant blue front reached the bottom of the gel.
We used 6 animals per group and the material from each animal corresponded with one gel for the cytosolic fraction and one gel for the membrane fraction. The system allowed a maximal run of 12 gels simultaneously. We therefore completed both the cytosolic and the membrane fraction separately using a run for the IR group with its respective sham group and a run for the PI group with its respective sham group. The gels were then washed for 1 h in a 10 % v/v methanol and 7 % v/v acetic acid solution and were stained overnight (12h) with Sypro Ruby fluorescent stain (Bio-Rad, Veenendaal, The Netherlands). Before scanning the gels, they were destained for 1 h in a 10 % v/v methanol and 7 % v/v acetic acid solution.

Spot detection and analysis
Gel images were scanned at a resolution of 100 µm (Molecular Imager FX, BioRad, Veenendaal, The Netherlands) and further analyzed using PDQuest 7.1 software (BioRad, Veenendaal, The Netherlands). The gels were ordered in the appropriate matchset and protein spots were manually matched according to the manufacturer's guidelines. Four different matchsets were used to compare separately the IR and PI group with their respective sham group for both the cytosolic fraction as well as the membrane fraction. The quantity of each spot was normalized by total quantity in valid spots using PDQuest 7.1. This normalized value was used to calculate the mean quantity of each spot per group. The fold change (density ratio) for a protein spot that was increased in quantity after IR (or PI) was calculated by dividing the mean quantitative value of that spot in the IR (or PI) group with the mean quantitative value of that spot in the respective sham group. For a protein spot that was decreased in quantity after IR (or PI) the inverse was taken. Using the PDQuest 7.1 software, a correlation coefficient was measured between the quantities of all spots in a gel and its quantities in another gel from the same matchset. The reproducibility of the 2-D gels was expressed as the mean correlation coefficient between all gels in a matchset.

Statistical analysis
A statistical comparison of the relative abundance of each matched protein spot between the IR group (N=6) or PI group (N=6) and their respective sham group (both N=6) was accomplished using a two-tailed t-test (PDQuest). Between groups, qualitative differences means that the spot is present in the samples from one of the groups (IR or PI) and not in its respective sham group or *vice versa*. Between group

quantitative or qualitative differences ≥ 1.6 times and a significant difference with *P*-value ≤ 0.05 were registered. All values are expressed as mean ± SD.

In-gel digestion

Protein spots of interest were excised from Sypro Ruby stained gels with an automatic spot cutter (Proteome Works Spot Cutter system, BioRad). Each spot was pooled out of 3-6 gels, washed twice with 200 mM ammonium bicarbonate in 50 % acetonitrile/water (20 min at 30 °C), and allowed to dry at room temperature. The tubes were then chilled on ice and 8 μL of digestion buffer (50 mM ammonium bicarbonate, pH 7.8) containing 150 ng modified trypsin (Promega, Madison, WI, USA) were added. The samples were incubated on ice for 45 min with 15 μL digestion buffer and afterwards incubated overnight at 37 °C. The supernatant was recovered, and the remaining peptides were extracted from the gel piece by washing twice with 60 % acetonitrile/0.1 % formic acid in water. The extracts were combined and the samples were dried in a Speedvac. The samples were resuspended in 10 μL of 0.1 % formic acid.

Protein identification-mass spectrometry

The peptide mixture was analyzed on a 4700 Proteomics Analyzer, a MALDI TOF-TOF mass spectrometer (Applied Biosystems, Framingham, CA, USA). We applied 1 μL of the digest mixture, mixed with 1 μL 100 mM α-cyano-4-hydroxycinnamic acid in 50 % acetonitrile and 0.1 % TFA onto a MALDI target plate. MS and MS/MS analysis of the peptides was performed. MS spectra were acquired after accumulation of 2000 consecutive laser shots and MS/MS spectra were obtained after 3000 laser shots and air used as collision gas (1.2×10^{-7} Torr). This approach could not unambiguously identify all protein spots. Thus, a second strategy was used to identify the remaining 2D-spots and to confirm the identification of the MALDI analysis. Hence, the samples were loaded on an automated nano-HPLC system (Dionex-LC Packings, Amsterdam, The Netherlands) and separated peptides were then detected on-line by an ESI-Q-TRAP mass spectrometer (Applied Biosystems, Framingham, CA, USA). In this method, an automated MS to MS/MS switching protocol was used for on-line LC-MS/MS analysis of the peptides [13]. For identification, MASCOT v1.9 was used for searching the MS and MS/MS data, obtained by either MALDI or LC-ESI analysis [14]. Searches were performed against the NCBI protein database. For the LC-MS/MS analyses, MASCOT was used with the following parameters: peptide tolerance 0.6 Da, fragment tolerance 0.8 Da, trypsin, specificity two possible missed cleavage sites, variable modifications carbamidomethylation and methionine oxidation and ESI-TRAP selected as the instrument.

Western blot analysis

Equal amounts of sample protein (10 μg) were separated by 10 % SDS-PAGE. After transfer to polyvinylidene difluoride membranes, they were blotted with rabbit anti-annexin 5 polyclonal (Hyphen BioMed, France) or rabbit anti-annexin 3 polyclonal (gift from F. Russo-Marie, Bionexus Pharmaceuticals SA, Gif sur Yvette, France) and

scanned. Densities were determined arbitrarily by ImageQuant (Molecular Dynamics, Sunnyvale, CA, USA).

Results

General

The average amount of ventricular tissue from the AAR, collected per animal was 54.0±6.6 mg and 50.0±11.5 mg after IR and PI respectively. The final protein fraction per amount of tissue was 4.2±0.6 % and 5.3±1.7 % for the cytosolic fractions and 8.9±2.2 % and 7.8±3.2 % for the membrane fractions of the IR and the PI group, respectively. Typical 2-DE spot patterns of both the cytosolic and membrane fraction, representative for the sham and PI group are shown in figure 1.

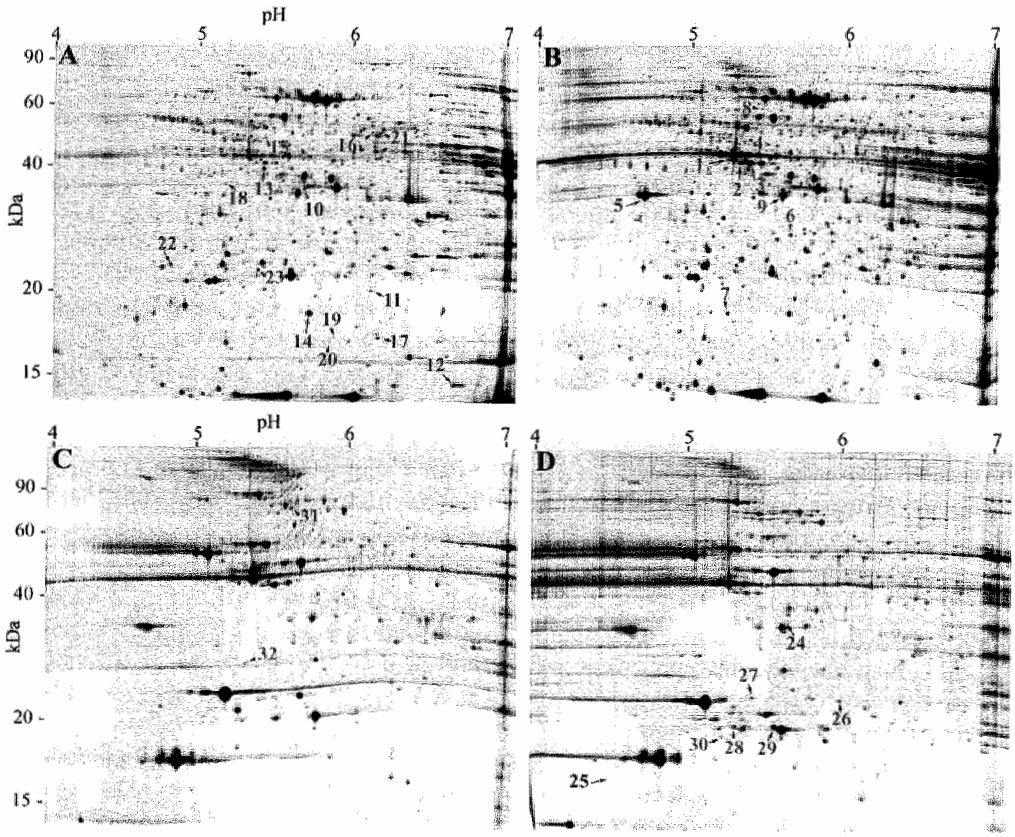

Figure 1. Sypro Ruby stained 2-DE gels of the cytosolic fraction (A, B) and the membrane fraction (C, D) from a sham animal (A, C) and a PI animal (B, D). Coloured numbers depict protein spots displaying significant quantitative or qualitative changes in expression level ($P \leq 0.05$ and density ratio ≥ 1.6). Protein spots changing in expression level after IR alone, after PI alone or after both IR and PI are numbered in blue, red and green, respectively. Spot numbers refer to the numbers given in table 1 (1A-1D).

Table 1: List of protein spots and their identification.

Spot no.[A]	Accession no. [B]	Protein ID	Mr (kDa) exp/ (thrt)[C]	pI exp/ (thrt)[C]	IR to sham (density ratio and P value) [D]	PI to sham (density ratio and P value) [D]	Sequence [E]	LC-MS/MS MASCOT score
1A.	**Cytosolic proteins displaying significantly increased abundance upon IR and/or PI compared to their respective sham group**							
1	1717770	Troponin T, cardiac muscle isoforms	42/ (35.8)	5.2/ (4.98)	qualitative ns	qualitative P=0.002	YEINVLR	55
							LFMPNLVPPK	
2	1717770	Troponin T, cardiac muscle isoforms	42/ (35.8)	5.3/ (4.98)	2.3x ns	5.4x P=0.01	YEINVLR	86
							LFMPNLVPPK	
							ALSNMMHFGGYIQK	
3	1717770	Troponin T, cardiac muscle isoforms	42/ (35.8)	5.4/ (4.98)	1.5x ns	2.8x P=0.02	YEINVLR	240
							LFMPNLVPPK	
							QQKYEINVLR	
							KKEEEELISLK	
							ALAIDHLNEDQLR	
							LFMPNLVPPKIPDGER	
4	1717770	Troponin T, cardiac muscle isoforms	42/ (35.8)	5.4/ (4.98)	1.3x ns	2.5x P=0.002	YEINVLR	96
							ALAIDHLNEDQLR	
							DLNELQTLIEAHFENR	
5	20522240	Tropomyosin 1 alpha chain (alpha-tropomyosin)	34/ (32.7)	4.7/ (4.69)	1.6x ns	4.6x *P*=0.006	CAELEEELK	574
							MEIQEIQLK	
							LVIIESDLER	
							IQLVEEELDR	
							QLEDELVSLQK	
							KLVIIESDLER	
							ATDAEADVASLNR	
							LATALQKLEEAEK	
							KATDAEADVASLNR	
							ATDAEADVASLNRR	
							SKQLEDELVSLQK	
							SIDDLEDELYAQK	
							KATDAEADVASLNRR	
							SKQLEDELVSLQKK	

(continued)

Spot no.[A]	Accession no.[B]	Protein ID	Mr (kDa) exp/ (thrt)[C]	pI exp/ (thrt)[C]	IR to sham (density ratio and P value)[D]	PI to sham (density ratio and P value)[D]	Sequence[E]	LC-MS/MS MASCOT score
							LVIIESDLERAEER	
							IQLVEEELDRAQER	
							AISEELDHALNDMTSI	
							CAELEEELKTVTNNLK	
							AQKDEEKMEIQEIQLK	
6	134198	Serum amyloid P-component precursor	30/ (26.2)	5.7/ (5.98)	1.1x ns	3.5x P=0.007	SQSLFSYSVK	56
							APPSIVLGQEQDNYGGGFQR	
7	20825064	Heat shock protein -20	18.5/ (17.5)	5.2/ (5.64)	5.7x P<0.001	2.3x P=0.001	HFLPEEISVK	84
							ASAPLPGFSAPGR	
							ASAPLPGFSAPGRLFDQR	
8	13384620	Heterogeneous nuclear ribonucleoprotein K	60/ (51.0)	5.4/ (5.39)	5.8x P<0.001	1.9x P=0.04	NLPLPPPPPPR	54
							IITITGTQDQIQNAQYLLQNSVK	
9	46396509	Pyruvate dehydrogenase E1-beta	34/ (38.9)	5.6/ (6.41)	1.6x P=0.04	1.8x P=0.02	VLEDNSVPQVK	264
							VVSPWNSEDAK	
							VTGADVPMPYAK	
							EGIECEVINLR	
							IMEGPAFNFLDAPAVR	
							TYYMSAGLQPVPIVFR	
1B.	**Cytosolic proteins displaying significantly reduced abundance upon IR and/or PI compared to their respective sham group**							
10	5902786	Annexin A3	35/ (36.4)	5.6/ (5.33)	0.25x P=0.003	0.9x ns	SLGDDISSETSGDFRK	49
11	20137946	Dual Specifity Phosphatase 3	20/ (20.5)	6.1/ (6.07)	0.45x P=0.04	0.67x ns	LGITHVLNAAEGR	85
							VYVGNASVAQDITQLQK	
12	2495231	Histidine triad nucleotide- binding protein 1	14/ (13.8)	6.6/ (6.36)	0.59x ns	0.53x P=0.006	CAADLGLKR	61
							AQVAQPGGDTIFGK	

(continued)

Spot no.[A]	Accession no.[B]	Protein ID	Mr (kDa) exp/ (thrt)[C]	pI exp/ (thrt)[C]	IR to sham (density ratio and P value)[D]	PI to sham (density ratio and P value)[D]	Sequence[E]	LC-MS/MS MASCOT score
13	21313356	Zn alcohol dehydrogenase-like protein	40/ (38.0)	5.4/ (5.27)	1.0x ns	0.63x P=0.009	AILDGNGLEK QIVCISEDSSL TLYLSVDPYMR	44
14	20825064	Heat shock protein-20	18.5/ (17.5)	5.7/ (5.64)	0.71x ns	0.38x P<0.001	HFLPEEISVK ASAPLPGFSAPGR	74
15	Not identified		50/ (?)	5.4/ (?)	1.0x ns	0.56x P=0.02		
16	Not identified		50/ (?)	6.1/ (?)	0.91x ns	0.42x P=0.002		
17	Not identified		16/ (?)	6.2/ (?)	0.91x ns	0.36x P=0.01		
18	Not identified		36/ (?)	5.1/ (?)	0.67x ns	0.48x P=0.009		
19	Not identified		16/ (?)	5.9/ (?)	0.83x ns	0.32x P=0.02		
20	Not identified		16/ (?)	5.8/ (?)	0.43x ns	0.43x P=0.02		
21	Not identified		50/ (?)	6.2/ (?)	0.63x ns	0.29x P=0.01		
22	Not identified		25/ (?)	4.8/ (?)	0.83x ns	0.28x P<0.001		
23	5921831	Catechol-O-methyltransferase	24/ (29.5)	5.3/ (5.52)	0.63x P=0.04	0.48x P=0.007	AVYQGPGSSPVKS	47
1C.	**Membrane proteins displaying significantly increased abundance upon IR and/or PI compared to their respective sham group**							
24	5902786	Annexin A3	35/ (36.4)	5.6/ (5.33)	5.8x P<0.001	0.63x ns	ALLTLADGR LTFDEYR	64

(continued)

Spot no.[A]	Accession no.[B]	Protein ID	Mr (kDa) exp/ (thrt)[C]	pI exp/ (thrt)[C]	IR to sham (density ratio and P value)[D]	PI to sham (density ratio and P value)[D]	Sequence[E]	LC-MS/MS MASCOT score
25	Not identified		17/ (?)	4.4/ (?)	qualitative P=0.01	qualitative ns		
26	547679	Heat shock protein-27	24/ (23.0)	6.0/ (6.12)	qualitative ns	qualitative P=0.01	RVPFSLLR	53
							LFDQAFGVPR	
27	547679	Heat shock protein-27	24/ (23.0)	5.4/ (6.12)	3.3x P=0.001	2.7x P=0.02	RVPFSLLR	110
							LFDQAFGVPR	
28	13959400	Adenylate kinase 1	21/ (21.5)	5.3/ (5.67)	qualitative P=0.007	qualitative P=0.007	IIFVVGGPGSGK	
							YGYTHLSTGDLLR	
29	13959400	Adenylate kinase 1	21/ (21.5)	5.5/ (5.67)	2.8x P=0.03	5.3x P=0.008	IIFVVGGPGSGK	289
							YGYTHLSTGDLLR	
							VDSSNGFLIDGYPR	
							IGQPTLLLYVDAGAETMTQR	
							LETYYNATEPVISFYDKR	
30	Not identified		19/ (?)	5.3/ (?)	qualitative P<0.001	qualitative P=0.01		
1D. Membrane proteins displaying significantly reduced abundance upon IR and/or PI compared to their respective sham group								
31	3024204	Myosin heavy chain-alpha isoform	75/ (223.5)	5.6/ (5.57)	0.63x ns	0.17x P=0.01	SLSTELFK	144
							LQDAEEAVEAVNAK	
							MVDSLQTSLDAETR	
							AQLEFNQIKAEIER	
							QAEEAEEQANTNLSKFR	
32	130020	Prohibitin	29/ (29.8)	5.2/ (5.57)	1.25x ns	0.24x P=0.003	FDAGELITQR	236
							DLQNVNITLR	
							VLPSITTEILK	
							ILFRPVASQLPR	
							IYTSIGEDYDER	
							FDAGELITQRELVSR	

A. Numbers refer to the spot numbers given in figure 1 and 4.

B. Protein entry code of the National Center for Biotechnology Information (NCBI): http://ncbi.nlm.nih.gov.

C. Mr and pI exp/thrt: experimental molecular weight and pI from the position on the 2-D gel/ theoretical molecular weight or pI calculated by the "Compute pI/Mw" tool provided by ExPasy: http://us.expasy.org.

D. 'Qualitative': no spot observed in the samples from one group compared to the other/ns: not significant

E. Peptide sequence corresponding to the appropriate peptide mass. Parts of the sequence, determined by LC-MS/MS, could indisputably confirm the peptide.

The digitized master gel was composed of a total of 12 gels in which the IR or PI group was compared with its respective sham group. The mean number of spots in each gel that matched with the master gel was 495±106 for the cytosolic fraction and 116±22 for the membrane fraction. The reproducibility of the 2-D gels was high. The mean correlation coefficient between all gels within the matchset of the IR group (and is respective sham group) was 0.83±0.04 (cytosolic fraction) and 0.84±0.07 (membrane fraction). The mean correlation coefficient between all gels within the matchset of the PI group (and its respective sham group) was 0.81±0.07 (cytosolic fraction) and 0.83±0.07 (membrane fraction).

Identification of protein spots changed in expression level after PI and IR

Figure 1 indicates the protein spots on the 2-DE spot patterns that significantly changed in expression level after IR and/or PI compared with their respective sham group. These protein spots are numbered in separate colours to distinguish between protein spots that changed significantly in expression level after IR alone (blue), after PI alone (red) or commonly after IR and PI (green). The spot numbers in this figure refer to the numbers in table 1 (1A-1D) which lists these protein spots and their protein identification. The experimental and theoretical mass and pI of the proteins and the density ratio (with *P* value) of expression level after IR and PI compared with the respective sham group are also listed in table 1.

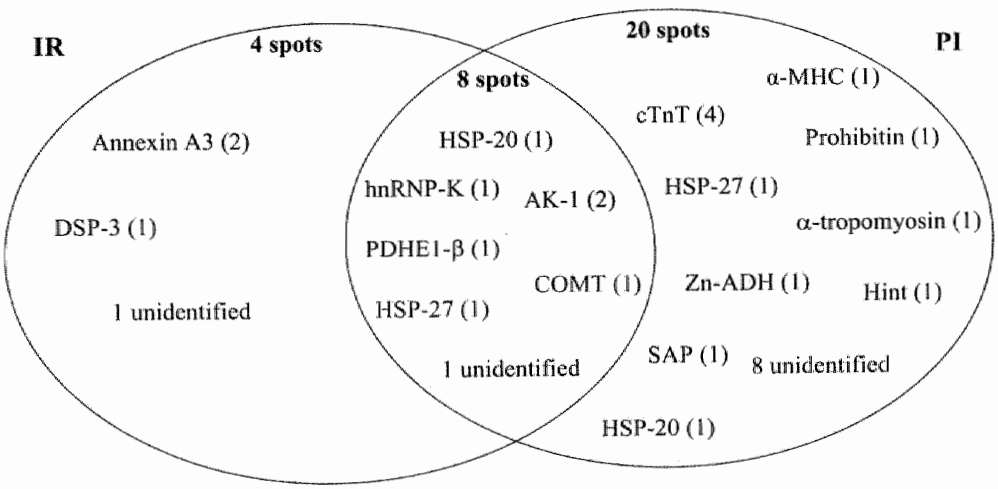

Figure 2. Venn diagram indicating the number of protein spots that changed significantly in expression level and the abbreviated names of the proteins they represent. The numbers of spot locations at which the identified proteins occur in each model (IR or PI) or both models are indicated between brackets. The amount of unidentified protein spots is also indicated. Four protein spots changed significantly in expression level after IR alone, 20 protein spots changed significantly in expression level after PI alone and 8 protein spots are commonly changed in both models compared to their respective sham group.

The Venn diagram (figure 2) gives an overview of the amount of spots significantly changed in expression level. Some proteins occur at one spot location while other proteins are present at several locations. The number of spot locations at which each protein occurred is indicated in the Venn diagram, within parentheses, after the abbreviated names of the proteins.
Four protein spots changed significantly in expression level after IR alone while 20 protein spots changed significantly in expression level after PI alone. Eight protein spots changed significantly in both models.
As indicated in this Venn diagram, 22 protein spots (3 spots after IR alone, 12 spots after PI alone, 7 spots after both PI and IR) could be identified by MS while 10 protein spots (1 spot after IR alone, 8 spots after PI alone, 1 spot after both PI and IR) could not. Thus about 70 % of the protein spots could be identified by mass spectrometry. In table 1, the MASCOT score of the identified peptides is given together with (parts of) the deduced amino acid sequences. The unidentified proteins were relatively low in abundance and probably fell, despite pooling, below the detection limit of the technique.
Protein spots present on the 2-D gels showing no significant change in expression level after IR or PI or with < 1.6-fold change were not identified by mass spectrometry.
As indicated in figure 2, proteins (or protein spots) that significantly changed in expression level after IR but not after PI were annexin-A3 (spot 10, 24) and dual specificity phosphatase-3 (DSP-3, spot 11). Proteins (or protein spots) that significantly changed in expression level after PI but not IR were cardiac troponin T (cTnT, spot 1-4), α-tropomyosin (spot 5), α-myosin heavy chain (α-MHC, spot 31), serum amyloid P-component precursor (SAP, spot 6), Zn-alcohol dehydrogenase (Zn-ADH, spot 13), prohibitin (spot 32), histidine triad nucleotide binding protein (Hint, spot 12), heat shock protein-27 (HSP-27, spot 26) and heat shock protein-20 (HSP-20, spot 14). The proteins (or protein spots) that significantly changed in expression level in both models were heterogeneous nuclear ribonucleoprotein-K (hnRNP-K, spot 8), pyruvate dehydrogenase E1-β (PDHE1-β, spot 9), catechol-O-methyltransferase (COMT, spot 23), adenylate kinase-1 (AK-1, spot 28, 29), HSP-20 (spot 7) and HSP-27 (spot 27). In general these identified proteins can be classified into functional groups i.e. anticoagulant proteins, structural proteins, inflammatory-related proteins, transcription- and translation-related proteins, heat shock proteins, metabolism-related proteins and miscellaneous.

Translocation of annexin A3 and annexin A5
2-DE analysis showed that the quantity of annexin A3 in the cytosolic fraction was 4 times lower (P=0.003) in the IR group than in the respective sham group. In contrast, in the membrane fraction of the IR group, the amount of annexin A3 was 5.8 times higher (P=0.001) than in the sham group. These findings were verified using Western blots for annexin A3 as well as annexin A5 (figure 3). Annexin A5 was significantly reduced in the cytosolic fraction (P<0.001) and significantly increased in the membrane fraction after IR (P<0.001). It is remarkable, that for both annexin A3 and annexin A5, such changes were specific for IR and did not occur after PI. As indicated

in the Venn diagram (figure 2), annexin A3 is significantly changed in expression level at two spot locations: one in the cytosolic fraction (decreased) and one in the membrane fraction (increased). Annexin A5 was not included in the Venn diagram (figure 2) because this protein was not found on the 2-DE gels.

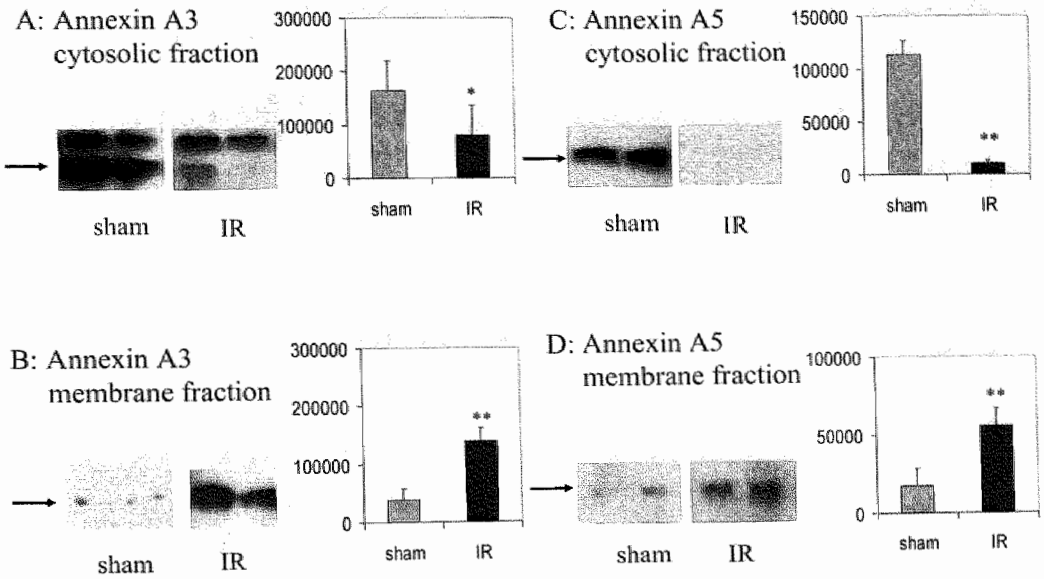

Figure 3. Western blot analysis for the cytosolic fraction **(A)** and membrane fraction **(B)** of annexin A3 and the cytosolic fraction **(C)** and the membrane fraction **(D)** of annexin A5 compared between sham and IR. The arrow indicates the position of the annexin band. Panels next to every Western blot picture show significant quantitative density differences between the IR group and their respective sham group (*P=0.017, **P<0.001, N=6 per group).

Post-translational modification of proteins

Four of the identified proteins that changed in expression level were found at multiple spot locations, characterized by a difference in isoelectric point (pI), on the gels (figure 2). This suggests that these are isoforms or proteins that underwent post-translational modifications under IR and/or PI. Mass spectrometry was not able to accurately distinguish between isoforms or to determine potential post-translational modifications. Figure 4 represents detailed 2-DE patterns of Sypro Ruby stained 2-DE gels showing these protein spots. In the cytosolic fraction of the PI group but not in the IR group, HSP-20 shifted to a lower pI with a difference in pI of approximately 0.43. Cardiac troponin T was identified at 4 spot locations of which 3 spots had the same apparent molecular weight but had a pI difference of approximately 0.07. These 4 spots were significantly up-regulated only in the PI group and not in the IR group. In the membrane fraction of the PI group, adenylate kinase 1 and HSP-27 were

significantly up-regulated at 2 spot locations separated by a pI range of 0.27 and 0.60, respectively.
For adenylate kinase 1, the spot at the lowest pI and for HSP-27, the spot at the highest pI were not present in the sham group. The same phenomenon was observed for the IR group although the HSP-27 spot at the highest pI was not significantly up-regulated compared to the respective sham group.

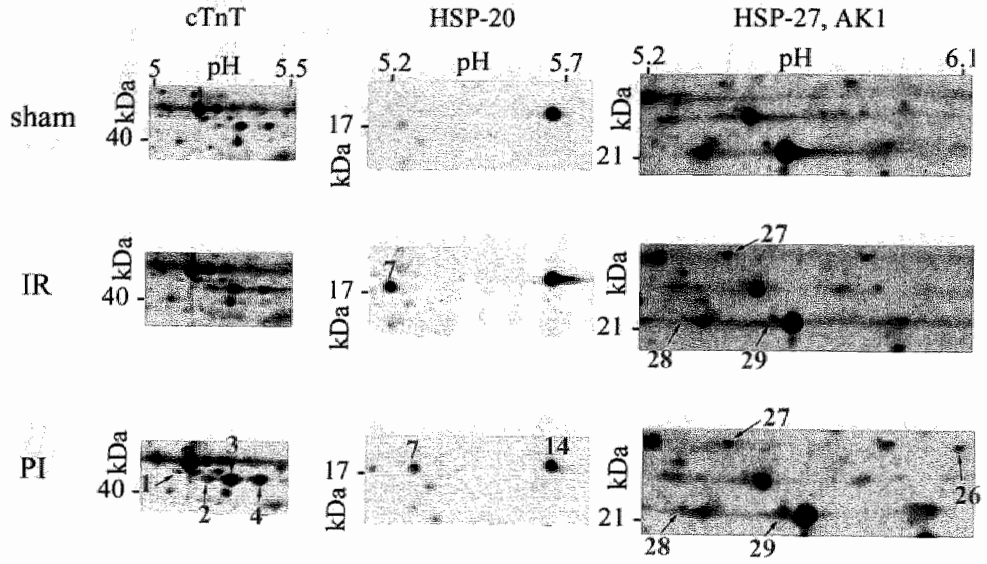

Figure 4. Detailed 2-DE pattern of the Sypro Ruby stained 2-DE gels showing identified proteins that are present at multiple spot locations. Different colours are used to indicate if these protein spots significantly changed in expression level after PI alone (red) or both after IR and PI (green). These proteins are cTnT (spot 1-4), HSP-20 (spot 7 and 14), HSP-27 (spot 26 and 27) and AK1 (spot 28 and 29) and they are shown for the sham group (upper panel), the IR group (middle panel) and the PI group (lower panel). Note that none of these protein spots changed significantly in expression level after IR alone. Spot numbers also refer to the numbers given in figure 1 and table 1.

Discussion

This study is the first to describe changes in cardiac protein expression by 2-DE in *in vivo* mouse models of myocardial infarction, i.e. a model of PI and a model of IR. Twenty protein spots changed significantly in expression level after PI alone, 4 protein spots changed significantly after IR alone, while 8 protein spots changed significantly in both models. We classified the identified proteins into functional groups: anticoagulant proteins, structural proteins, inflammatory-related proteins, transcription- and translation-related proteins, heat shock proteins, metabolism-related proteins and miscellaneous. We discuss their potential role in PI and IR in separate sections below. It is remarkably that none of the individual proteins we identified were differentially expressed in one of the three previous studies in this area. However, a few are functionally related as discussed below [8-10]. Moreover the number of

proteins that changed in expression level in our study was higher than in these previous studies. Several factors may account for this discrepancy. Firstly, we analyzed the cytosolic and membrane fraction separately to make low abundance proteins more easily detectable. Secondly, our study was conducted in the mouse while others used the dog [10], rabbit [8] and rat [9]. Thirdly, differences in the duration of ischaemia (range: 40 min [9]-90 min [10]) or in the duration of reperfusion (range 20 min [9] to 180 min [8]) could contribute to the differences in outcome.

Anticoagulant proteins

The significant decrease of annexin A3 in the cytosolic fraction and the significant increase in the membrane fraction was specific for the IR model. This was also verified by Western blot analysis and suggests translocation of annexin A3 to the membrane fraction triggered by reperfusion. This phenomenon was also observed for annexin A5, as verified by Western blot analysis and correlates with the fact that the C-terminal protein core, which is responsible for the calcium-mediated membrane recognition and binding, is highly conserved between annexins [15]. An explanation for the fact that annexin A5 was not detected on 2-D gels could be that other proteins masked the corresponding spot. *In vivo* functional properties for annexins are diverse and include membrane trafficking, endo- and exocytosis, membrane-cytoskeleton interactions, regulation of membrane protein activity, cell signalling, and roles in inflammatory and coagulation processes (see [16] for review). The fact that this phenomenon occurred after IR alone and not after PI suggests a specific related mechanism that triggers translocation of annexins to the membrane fraction during reperfusion. These findings may give new impetus for further studies in relation to annexins and early diagnosis of reperfusion injury in connection with earlier studies from our laboratory [17].

Structural proteins

Cardiac troponin T (cTnT) and another myofilament protein, α-tropomyosin, were significantly increased in the cytosolic fraction after PI but not after IR. cTnT is known as an α-tropomyosin binding protein, and both proteins are involved in the process of muscle contraction [18]. Several animal studies have shown that the appearance of cTnT in blood is a highly sensitive and specific marker for myocardial injury and is directly correlated with infarct size [19, 20]. We have recently described that in mice after PI, infarct size is almost 4 times greater than after IR [7]. With respect to this, the data suggest that the increased cytosolic levels of cTnT and α tropomyosin are markers for high breakdown of the contractile apparatus after PI compared to IR.

Inflammatory-related proteins

Myocardial infarction is associated with an early inflammatory response, which is a prerequisite for wound healing and scar formation (see [21] for a review).

In relation to this we observed that serum amyloid P-component precursor (SAP) was significantly increased in the cytosolic fraction after PI but not after IR. SAP is a precursor for serum amyloid P component which is an acute-phase reactant produced

by the liver and able to activate the complement system [22]. SAP does not only exist in plasma but also in peripheral tissues where it is associated with extra-cellular matrix proteins [23-27]. To our knowledge, this study is the first to describe SAP as a potential specific marker for hypoxic cardiac tissue after PI.

Transcription- and translation-related proteins

Prohibitin (membrane fraction) and histidine triad nucleotide binding protein 1 (cytosolic fraction) were both significantly reduced after PI but not after IR. Prohibitin is known to inhibit cell proliferation [28], to regulate transcriptional activity [29] and to stabilize mitochondrial proteins [30]. In addition, both proteins have been reported to function as tumour suppressers [31-33]. However at present, nothing is known about a functional role of these proteins in relation to cardiovascular diseases. In our study, heterogeneous nuclear ribonucleoprotein K (hnRNP K, cytosolic fraction) and in the study of Sakai *et al.* [9], elongation factor Tu showed increased expression after PI and IR. Both proteins are associated with serine/threonine protein kinase Cε, a protein complex with a critical role in protecting the myocardium against IR injury [34]. Elongation factor Tu promotes amino-acyl tRNA binding to the ribosome [35] and hnRNP is a nucleic acid binding protein involved in RNA processing [36], translocation [37], and translation [38]. The finding that proteins belonging to this functional group changed in expression level suggests possible extensive control over protein expression in part by regulation of mRNA. This partially depends on the model, PI or IR.

Heat shock proteins

In accordance with the previous studies by Schwertz *et al.* [8] and Sakai *et al.* [9], we observed a change in expression level of heat shock proteins (HSP) after myocardial infarction. These proteins are considered as "molecular chaperones", the expression of which increases by cellular stress [39]. HSP-27 (membrane fraction) and HSP-20 (cytosolic fraction) were increased both after PI and IR. Differential changes in HSP-27 levels have been described in rat [40] and human [41, 42] cardiac tissues exhibiting heart failure. HSP-27 acts as a protective agent against hypoxic injury in cultured adult rat [43] and canine cardiomyocytes [44]. However, this protective effect has not been shown in an *in vivo* animal model to date. Because of its increased expression level, our study suggests a possible role for HSP-27 in the cardioprotective mechanism after *in vivo* PI and IR.

HSP-20 was identified at two spot locations after myocardial infarction. The spot at the lowest pI increased in expression level after IR and PI, while the spot at the highest pI decreased after PI alone. Phospho-isoforms for HSP-20 have been described in literature [45] and additional research is necessary to investigate whether one or both of these spots in our models represents phospo-isoforms of HSP-20. Recently Chu *et al.* [46] showed in mouse cardiomyocytes that HSP-20 increases in expression and phosphorylation after prolonged activation of the β–adrenergic signalling pathway, which has consequences for the regulation of cardiac contractility and Ca^{2+} handling. The same group also suggested that HSP-20 and its phospho-isoform may provide cardioprotection against β-agonist-induced apoptosis [47].

Extrapolation of these results to our study could mean that HSP-20 may have a role in cardiac myocyte function and cell death after myocardial infarction in which β–adrenergic stimulation occurs to compensate for a reduced cardiac output.
Myocardial ischaemia is associated with a marked interstitial accumulation of catecholamines [48]. Under physiological conditions part of the catecholamines are broken down by catechol-O-methyltransferase (COMT) [49]. The finding that COMT levels were significantly decreased in the cytosolic fraction after PI and IR points to a myocardial adaptation of the metabolism of catecholamines or related substrates under these conditions [49, 50].

Metabolism-related proteins
Adenylate kinase 1 (AK1) in the membrane fraction and pyruvate dehydrogenase E1 component beta subunit (PDHE1-β) in the cytosolic fraction were both significantly increased after IR and PI. AK1 reversibly catalyses (high-energy) phosphotransfer between ADP, ATP, AMP and serves as an integral component of phosphotransfer networks [51]. During metabolic challenges, AK1 has been reported to be an essential enzyme in maintaining myocardial energy homeostasis [52, 53] and in metabolic signal transduction to ATP sensitive K^+ channels [54]. Deletion of the *AK1* gene revealed that adenylate kinase phosphotransfer supports myocardial function after initiation of ischaemic stress and safeguards intracellular nucleotide pools in post-ischaemic recovery [55]. Simultaneously PDHE1-β, which is a subunit of pyruvate dehydrogenase that largely controls the rate of entry of pyruvate into the Krebs cycle, was up-regulated. Both indicate a regulatory mechanism during IR and PI to achieve energy balance for the increased energy demands that occurs during these stress periods and to achieve cellular energetic economy and metabolic signal transduction. In relation to this, the previous study of Sawicki *et al.* [10] showed after IR an increase in isocitrate dehydrogenase, a key enzyme in the Krebs cycle.

Miscellaneous
At this moment it is not possible to formulate a hypothesis about the relevance of a few proteins i.e. "α-myosin heavy chain" (membrane fraction); "dual specificity phosphatase" (cytosolic fraction); and a protein "similar to Zn-alcohol dehydrogenase" (cytosolic fraction) which were differentially expressed after PI and/or IR.

Conclusion

This study demonstrates that mouse myocardial infarction models are suitable to study *in vivo* changes in the proteome early after induction of PI or IR. By analyzing selectively membrane and cytosolic fractions we were able to detect a substantial number of proteins that were differentially expressed in either compartment after PI, after IR or both. In addition, our approach allowed the identification of translocation of particular proteins such as annexins, from cytosolic to membrane compartments. Additional research is necessary to identify the functional relevance of these proteins in these pathologies and to determine the character of possible pathology related post-

translational modifications. The specific alterations in protein expression that took place after PI and IR may stimulate the search for new tools to diagnose myocardial infarction and to characterize specific pathology related changes in protein expression.

References

1. Cleutjens JP, Blankesteijn WM, *et al.* The infarcted myocardium: simply dead tissue, or a lively target for therapeutic interventions. Cardiovasc Res. 1999; 44: 232.
2. De Celle T, Heeringa P, *et al.* Sustained protective effects of 7-monohydroxyethylrutoside in an in vivo model of cardiac ischemia-reperfusion. Eur J Pharmacol. 2004; 494: 205.
3. Flaherty JT, Weisfeldt ML. Reperfusion injury. Free Radic Biol Med. 1988; 5: 409.
4. McDonough JL, Neverova I, *et al.* Proteomic analysis of human biopsy samples by single two-dimensional electrophoresis: Coomassie, silver, mass spectrometry, and Western blotting. Proteomics. 2002; 2: 978.
5. McGregor E, Dunn MJ. Proteomics of heart disease. Hum Mol Genet. 2003; 12 Spec No 2: R135.
6. Lutgens E, Daemen MJ, *et al.* Chronic myocardial infarction in the mouse: cardiac structural and functional changes. Cardiovasc Res. 1999; 41: 586.
7. De Celle T, Cleutjens J, *et al.* Long-Term Structural and Functional Consequences of Cardiac Ischemia/Reperfusion Injury in vivo in Mice. Exp Physiol. 2004.
8. Schwertz H, Langin T, *et al.* Two-dimensional analysis of myocardial protein expression following myocardial ischemia and reperfusion in rabbits. Proteomics. 2002; 2: 988.
9. Sakai J, Ishikawa H, *et al.* Proteomic analysis of rat heart in ischemia and ischemia-reperfusion using fluorescence two-dimensional difference gel electrophoresis. Proteomics. 2003; 3: 1318.
10. Sawicki G, Jugdutt BI. Detection of regional changes in protein levels in the in vivo canine model of acute heart failure following ischemia-reperfusion injury: functional proteomics studies. Proteomics. 2004; 4: 2195.
11. Dumont EA, Hofstra L, *et al.* Cardiomyocyte death induced by myocardial ischemia and reperfusion: measurement with recombinant human annexin-V in a mouse model. Circulation. 2000; 102: 1564.
12. Pasquali C, Fialka I, *et al.* Preparative two-dimensional gel electrophoresis of membrane proteins. Electrophoresis. 1997; 18: 2573.
13. Sule A, Vanrobaeys F, *et al.* Proteomic analysis of small heat shock protein isoforms in barley shoots. Phytochemistry. 2004; 65: 1853.
14. Perkins DN, Pappin DJ, *et al.* Probability-based protein identification by searching sequence databases using mass spectrometry data. Electrophoresis. 1999; 20: 3551.
15. Barton GJ, Newman RH, *et al.* Amino acid sequence analysis of the annexin super-gene family of proteins. Eur J Biochem. 1991; 198: 749.
16. Gerke V, Moss SE. Annexins: from structure to function. Physiol Rev. 2002; 82: 331.
17. Dumont EA, Reutelingsperger CP, *et al.* Real-time imaging of apoptotic cell-membrane changes at the single-cell level in the beating murine heart. Nat Med. 2001; 7: 1352.
18. Bacchiocchi C, Lehrer SS. Ca(2+)-induced movement of tropomyosin in skeletal muscle thin filaments observed by multi-site FRET. Biophys J. 2002; 82: 1524.
19. Metzler B, Hammerer-Lercher A, *et al.* Plasma cardiac troponin T closely correlates with infarct size in a mouse model of acute myocardial infarction. Clin Chim Acta. 2002; 325: 87.
20. Remppis A, Ehlermann P, *et al.* Cardiac troponin T levels at 96 hours reflect myocardial infarct size: a pathoanatomical study. Cardiology. 2000; 93: 249.
21. Frangogiannis NG, Smith CW, *et al.* The inflammatory response in myocardial infarction. Cardiovasc Res. 2002; 53: 31.

22. Steel DM, Whitehead AS. The major acute phase reactants: C-reactive protein, serum amyloid P component and serum amyloid A protein. Immunol Today. 1994; 15: 81.
23. Dyck RF, Evans DJ, *et al.* Amyloid P-component in human glomerular basement membrane. Abnormal patterns of immunofluorescent staining in glomerular disease. Lancet. 1980; 2: 606.
24. Breathnach SM, Melrose SM, *et al.* Amyloid P component is located on elastic fibre microfibrils in normal human tissue. Nature. 1981; 293: 652.
25. Breathnach SM, Melrose SM, *et al.* Immunohistochemical studies of amyloid P component distribution in normal human skin. J Invest Dermatol. 1983; 80: 86.
26. Zahedi K. Characterization of the binding of serum amyloid P to type IV collagen. J Biol Chem. 1996; 271: 14897.
27. Zahedi K. Characterization of the binding of serum amyloid P to laminin. J Biol Chem. 1997; 272: 2143.
28. Nuell MJ, Stewart DA, *et al.* Prohibitin, an evolutionarily conserved intracellular protein that blocks DNA synthesis in normal fibroblasts and HeLa cells. Mol Cell Biol. 1991; 11: 1372.
29. Fusaro G, Dasgupta P, *et al.* Prohibitin induces the transcriptional activity of p53 and is exported from the nucleus upon apoptotic signaling. J Biol Chem. 2003; 278: 47853.
30. Nijtmans LG, de Jong L, *et al.* Prohibitins act as a membrane-bound chaperone for the stabilization of mitochondrial proteins. Embo J. 2000; 19: 2444.
31. Fong LY, Fidanza V, *et al.* Muir-Torre-like syndrome in Fhit-deficient mice. Proc Natl Acad Sci U S A. 2000; 97: 4742.
32. Zanesi N, Fidanza V, *et al.* The tumor spectrum in FHIT-deficient mice. Proc Natl Acad Sci U S A. 2001; 98: 10250.
33. Manjeshwar S, Branam DE, *et al.* Tumor suppression by the prohibitin gene 3'untranslated region RNA in human breast cancer. Cancer Res. 2003; 63: 5251.
34. Edmondson RD, Vondriska TM, *et al.* Protein kinase C epsilon signaling complexes include metabolism- and transcription/translation-related proteins: complimentary separation techniques with LC/MS/MS. Mol Cell Proteomics. 2002; 1: 421.
35. Cai YC, Bullard JM, *et al.* Interaction of mitochondrial elongation factor Tu with aminoacyl-tRNA and elongation factor Ts. J Biol Chem. 2000; 275: 20308.
36. Shnyreva M, Schullery DS, *et al.* Interaction of two multifunctional proteins. Heterogeneous nuclear ribonucleoprotein K and Y-box-binding protein. J Biol Chem. 2000; 275: 15498.
37. Mattaj IW, Englmeier L. Nucleocytoplasmic transport: the soluble phase. Annu Rev Biochem. 1998; 67: 265.
38. Ostareck DH, Ostareck-Lederer A, *et al.* Lipoxygenase mRNA silencing in erythroid differentiation: The 3'UTR regulatory complex controls 60S ribosomal subunit joining. Cell. 2001; 104: 281.
39. Knowlton AA. The role of heat shock proteins in the heart. J Mol Cell Cardiol. 1995; 27: 121.
40. Tanonaka K, Yoshida H, *et al.* Myocardial heat shock proteins during the development of heart failure. Biochem Biophys Res Commun. 2001; 283: 520.
41. Knowlton AA, Kapadia S, *et al.* Differential expression of heat shock proteins in normal and failing human hearts. J Mol Cell Cardiol. 1998; 30: 811.
42. Scheler C, Li XP, *et al.* Comparison of two-dimensional electrophoresis patterns of heat shock protein Hsp27 species in normal and cardiomyopathic hearts. Electrophoresis. 1999; 20: 3623.
43. Martin JL, Mestril R, *et al.* Small heat shock proteins and protection against ischemic injury in cardiac myocytes. Circulation. 1997; 96: 4343.
44. Vander Heide RS. Increased expression of HSP27 protects canine myocytes from simulated ischemia-reperfusion injury. Am J Physiol Heart Circ Physiol. 2002; 282: H935.
45. Rembold CM, O'Connor M, *et al.* Selected contribution: HSP20 phosphorylation in nitroglycerin- and forskolin-induced sustained reductions in swine carotid media tone. J Appl Physiol. 2001; 91: 1460.

46. Chu G, Egnaczyk GF, *et al.* Phosphoproteome analysis of cardiomyocytes subjected to beta-adrenergic stimulation: identification and characterization of a cardiac heat shock protein p20. Circ Res. 2004; 94: 184.
47. Fan GC, Chu G, *et al.* Small heat-shock protein Hsp20 phosphorylation inhibits beta-agonist-induced cardiac apoptosis. Circ Res. 2004; 94: 1474.
48. Lameris TW, de Zeeuw S, *et al.* Time course and mechanism of myocardial catecholamine release during transient ischemia in vivo. Circulation. 2000; 101: 2645.
49. Mannisto PT, Kaakkola S. Catechol-O-methyltransferase (COMT): biochemistry, molecular biology, pharmacology, and clinical efficacy of the new selective COMT inhibitors. Pharmacol Rev. 1999; 51: 593.
50. Ball P, Knuppen R. Catecholoestrogens (2-and 4-hydroxyoestrogens): chemistry, biogenesis, metabolism, occurrence and physiological significance. Acta Endocrinol Suppl (Copenh). 1980; 232: 1.
51. Dzeja P, Kalvenas A, *et al.* The effect of adenylate kinase activity on the rate and efficiency of energy transport from mitochondria to hexokinase. Biochem Int. 1985; 10: 259.
52. Dzeja PP, Pucar D, *et al.* Reduced activity of enzymes coupling ATP-generating with ATP-consuming processes in the failing myocardium. Mol Cell Biochem. 1999; 201: 33.
53. Puçar D, Janssen E, *et al.* Compromised energetics in the adenylate kinase AK1 gene knockout heart under metabolic stress. J Biol Chem. 2000; 275: 41424.
54. Carrasco AJ, Dzeja PP, *et al.* Adenylate kinase phosphotransfer communicates cellular energetic signals to ATP-sensitive potassium channels. Proc Natl Acad Sci U S A. 2001; 98: 7623.
55. Pucar D, Bast P, *et al.* Adenylate kinase AK1 knockout heart: energetics and functional performance under ischemia-reperfusion. Am J Physiol Heart Circ Physiol. 2002; 283: H776.

Chapter 6

Lack of effect of 7-monohydroxyethylrutoside on cardiac protein expression in an *in vivo* mouse model of myocardial ischaemia-reperfusion as assessed by 2-D gel electrophoresis

Tijl De Celle[1], Bart Devreese[2], Jozef Van Beeumen[2], Aalt Bast[1], Jos F. M. Smits[1], Ben J.A. Janssen[1]

Departments of Pharmacology & Toxicology[1], Cardiovascular Research Institute Maastricht, Universiteit Maastricht, The Netherlands
Laboratory of Protein Biochemistry and Protein Engineering[2], Universiteit Gent, Belgium

Abstract

Previously we showed that the antioxidant monoHER protects in an *in vivo* mouse model of cardiac ischaemia-reperfusion when administered intraperitoneally (i.p.) one hour before ischaemia but it did not have a protective action when applied intravenously five min before reperfusion.
To explain this discrepancy we hypothesized that monoHER has an influence on a signal transduction pathway that might be associated to its protective mechanism of action.
Therefore we used a technique of 2-D gel electrophoresis combined with mass spectrometry in order to find related changes in protein expression or post-translational modifications of proteins.
Ischaemia was maintained for 30 min by ligation of the left anterior descending coronary artery. MonoHER (500 mg/kg) or saline was administered i.p. one hour before ischaemia. Reperfusion was allowed for three hours and the area at risk of the left ventricle was processed for 2-D gel electrophoresis.
In total twelve protein spots changed significantly in expression level after IR. Pretreatment with monoHER did not alter this protein expression profile. Ten of the twelve protein spots could be identified by mass spectrometry. In both monoHER-treated and non-treated mice these were: heat shock protein-20 and heat shock protein-27, heterogeneous nuclear ribonucleoprotein K, pyruvate dehydrogenase E1-β, annexin A3 (at 2 spot locations), dual specificity phosphatase-3, catechol-O-methyltransferase, and adenylate kinase 1 (at 2 spot locations).
We conclude that the strong and sustained cardioprotective effects of monoHER as evidenced on a histological and functional level were not associated with detectable early changes in the proteome. Whether the protective effects of monoHER during IR are related to alterations in expression level or post-translational modifications of low-abundance proteins or proteins at specific subcellular locations needs further research.

Introduction

Current treatment of myocardial infarction is directed at the restoration of coronary blood flow to the ischaemic region. However, during revascularization, the heart undergoes further damage which, to a large extent, is due to the generation of reactive oxygen species (ROS) [1].

In a previous study we demonstrated that the antioxidant monoHER has sustained cardioprotective effects in an *in vivo* mouse model of cardiac ischaemia-reperfusion when administered i.p. one hour before ischaemia [2]. MonoHER significantly reduced myocardial neutrophil influx and infarct size and strongly attenuated IR induced deterioration of cardiac contractility [2]. In a subsequent study we demonstrated that monoHER does, however, not exhibit these cardioprotective effects when administered i.v. five min before reperfusion, a time point more relevant for extrapolation to a clinical situation (chapter 4).
This was however not expected, based on its pharmacokinetic properties.

Among the explanations for the lack of a clear pharmacodynamic effect of monoHER in this setting are the potential restriction in myocardial uptake in conditions of cardiac ischaemia-reperfusion or the necessity of formation of metabolites of monoHER (chapter 4).
In addition we hypothesized that cardioprotection is not related to the antioxidant effect only but also to an unknown side-effect of monoHER (or one of its metabolites) on proteins influencing ischaemia-reperfusion injury (chapter 4).
Specifically, monoHER might interfere with a characteristic signal transduction pathway, critically involved in the determination of cellular fate, injury, death or adaptation during ischaemia. In relation to this, the time point of monoHER administration, i.e. before ischaemia versus before reperfusion, might be very crucial.
Proteomic techniques allow the identification of proteins that undergo changes in expression level, phosphorylation, oxidation-reduction or other post-translational modifications during *in vivo* cardiac ischaemia-reperfusion. For instance, Schwertz *et al.* applied proteomics to search for protein changes induced by the synthetic serine protease inhibitor FUT-175, an inhibitor of the complement pathway, in an *in vivo* rabbit model of ischaemia-reperfusion [3]. Using 2-D gel electrophoresis they found that treatment with FUT-175 resulted in preserved myocardial protein levels of superoxide dismutase and αB-crystallin, which suggests that this agent does not only affect the complement system, but also affects the protein expression of other cardioprotective targets.
Similarly, by using this technique, it might be possible to find alterations in the proteome that can be related to the mechanism of action of monoHER.
Furthermore, anti-oxidants might also interfere with the production of ROS during the period of ischaemia [4-7]. Specifically, when exposed to hypoxia, cardiomyocytes have been shown to increase production of ROS derived from the mitochondrial electron transport chain [8]. The general physiological consequences of hypoxic mitochondrial ROS production are not completely understood. Mitochondrial ROS may 1) promote the stabilization and activity of hypoxia inducible factor-1α (HIF-1α) transcription factor [9-12]; 2) alter cardiac myocyte contractility [8]; 3) modulate Na^+-

K^+-ATPase activity [13]; or 4) influence mitochondrial depolarization [14] and 5) mitogen-activated protein kinases [15]. These studies reveal that ROS, besides their direct detrimental effects on cellular structures, influence a variety of cellular signal transduction cascades during ischaemia. This implies that monoHER, by reducing ROS during ischaemia, may have an influence on such pathways.
Thus we hypothesize that monoHER treatment may affect the proteome during ischaemia through 2 mechanisms. Firstly through an, at the moment, unknown side-effect of monoHER or a metabolite or secondly through an indirect effect by reducing potential influences of ROS on a signal transduction pathway.

Consequently the goal of this study was to examine the effects of monoHER on changes in the proteome, 3 h after reperfusion, by using a technique of 2-D gel electrophoresis combined with mass spectrometry. We chose this early time point because we were primarily interested to find the reason for the protective effects of monoHER. Moreover, previous studies showed that by using this technique it is possible to detect early alterations in the proteome induced by IR [3, 16, 17]. This approach could provide more insight in the mechanism of action of monoHER in the setting of *in vivo* cardiac ischaemia-reperfusion.

Materials and methods

Animals
Male Swiss mice (7-9 weeks old, weighting 35-40 g) were used. The animals were purchased from Charles River (Maastricht, The Netherlands) and housed as described in detail in chapter 5. The experimental protocol was approved by the local animal ethics committee of the Universiteit Maastricht.

In vivo cardiac ischaemia-reperfusion
Mouse hearts were subjected to a 30 min ischaemia and 3 h reperfusion procedure as described in detail in chapter 5. Four experimental groups were compared; sham-saline, sham-monoHER, IR-saline and IR-monoHER. Before injection, monoHER (7-monohydroxyethylrutoside, molecular weight 654.6) was dissolved in 36 mM NaOH in sterile water, in a final concentration of 20 mg/ml (pH=7.9-8.1). MonoHER was given i.p. in a dose of 500 mg/kg, one hour before induction of ischaemia [18]. In control mice 25 µl/g, 0.9 % NaCl solution (same pH) was also injected i.p., one hour before ischaemia.

Sample preparation
For a description: see chapter 5

Two-dimensional gel electrophoresis
For a description: see chapter 5

Spot detection and analysis
Gel images were scanned and analyzed using PDQuest 7.1 software (BioRad). The gels were ordered in the appropriate matchset and protein spots were manually

matched according to the manufacturer's guidelines. Two different matchsets were used to compare separately the IR groups (saline and monoHER) with their respective sham group (saline and monoHER) for both the cytosolic fraction as well as the membrane fraction.
For a detailed description readers are referred to chapter 5.

Statistical analysis
A statistical comparison of the relative abundance of each matched protein spot between the IR group (saline or monoHER, both N=6) and their respective sham group (saline or monoHER, both N=6) was accomplished using a two-tailed t-test (PDQuest). A qualitative between group difference means that a spot is only present in samples from one particular group and lacking in another. Quantitative and qualitative between group differences were considered statistically significant when changes in protein expression were $\geq$ 1.6 times and a *P*-value $\leq$ 0.05. All values are expressed as mean $\pm$ SD.

In-gel digestion
For a description: see chapter 5

Protein identification-mass spectrometry
For a description: see chapter 5

Results

General
The average amount of ventricular tissue from the AAR, collected per animal was 54.0±5.8 mg and 51.0±9.5 mg for the IR-saline group and the IR-monoHER group, respectively. The final protein fraction per amount of tissue was 4.5±0.8 % and 4.7±2.9 % for the cytosolic fractions and 8.6±1.9 % and 7.1±2.8 % for the membrane fractions of the IR-saline and the IR-monoHER group, respectively. Typical 2-DE spot patterns of both the cytosolic and membrane fraction, representative for a sham and IR group are shown in figure 1. The digitised master gel was composed of a total of 24 gels in which the IR-saline and IR-monoHER group were compared with their respective sham groups. The mean number of spots in each gel that matched with the master gel was 512±119 for the cytosolic fraction and 127±24 for the membrane fraction. The reproducibility of the 2-D gels was high. The mean correlation coefficient between all gels within the matchset of the IR group (and its respective sham group) was 0.82±0.05 (cytosolic fraction) and 0.85±0.06 (membrane fraction).

Identification of protein spots changed in expression level
Figure 1 indicates the protein spots on the 2-DE spot pattern that significantly changed in expression level after IR. The spot numbers in this figure refer to the numbers in table 1 (1A-1C) which lists these protein spots and their protein identification.

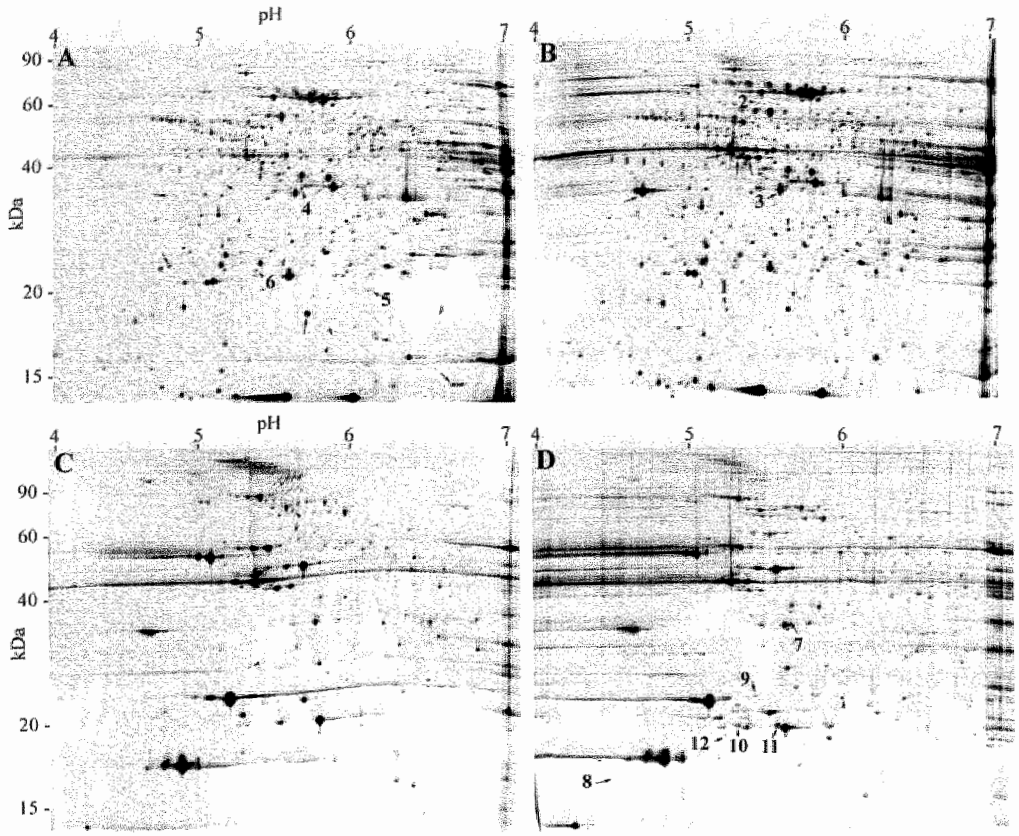

Figure 1: Sypro Ruby stained 2-DE gels identical to the one shown in chapter 5. In this case only protein spots displaying significant quantitative or qualitative changes in expression level ($P \leq 0.05$ and density ratio ≥ 1.6) after IR are depicted. These protein spots are the same in the IR, saline group and in the IR, monoHER group. Spot numbers refer to the numbers given in table 1 (1A-1D).

The experimental and theoretical mass and pI of the proteins and the density ratio (with *P* value) of expression level after IR (saline and monoHER) compared with the respective sham group (saline and monoHER) are also listed in table 1.
After IR there were significant changes in expression level in twelve protein spots. Ten of these protein spots (83 %) could be identified by mass spectrometry while 2 protein spots could not.
In table 1, the MASCOT score (chapter 5) of the identified peptides is given together with (parts of) the deduced amino acid sequences. The two unidentified proteins were relatively low in abundance and probably fell, despite pooling, below the detection limit of the technique.

Table 1: List of protein spots and their identification.

Spot no.[A]	Accession no.[B]	Protein ID	Mr (kDa) exp/ (thrt)[C]	pI exp/ (thrt)[C]	IR to sham SALINE (Density ratio and P value)[D]	IR to sham MONOHER (Density ratio and P value)[D]	Sequence[E]	LC_MS/MS MASCOT score
1A.	*Cytosolic proteins displaying significantly increased abundance upon IR and/or PI compared to their respective sham group*							
1	20825064	Heat shock protein -20	18.5/ (17.5)	5.2/ (5.64)	5.7x *P*<0.001	3.4x *P*<0.001	HFLPEEISVK	84
							ASAPLPGFSAPGR	
							ASAPLPGFSAPGRLFDQR	
2	13384620	Heterogeneous nuclear ribonucleoprotein K	60/ (51.0)	5.4/ (5.39)	5.8x *P*<0.001	6.7x *P*<0.001	NLPLPPPPPPR	54
							IITTTGTQDQIQNAQYLLQNSVK	
3	46396509	Pyruvate dehydrogenase E1-beta	34/ (38.9)	5.6/ (6.41)	1.6x *P*=0.04	1.4x *P*=0.01	VLEDNSVPQVK	264
							VVSPWNSEDAK	
							VTGADVPMPYAK	
							EGIECEVINLR	
							IMEGPAFNFLDAPAVR	
							TYYMSAGLQPVPIVFR	
1B.	*Cytosolic proteins displaying significantly reduced abundance upon IR and/or PI compared to their respective sham group*							
4	5902786	Annexin A3	35/ (36.4)	5.6/ (5.33)	0.25x *P*=0.003	0.17x *P*=0.001	SLGDDISSETSGDFRK	49
5	20137946	Dual Specifity Phosphatase 3	20/ (20.5)	6.1/ (6.07)	0.45x *P*=0.04	0.32x *P*=0.03	LGITHVLNAAEGR	85
							VYVGNASVAQDITQLQK	
6	5921831	Catechol-O-methyltransferase	24/ (29.5)	5.3/ (5.52)	0.63x *P*=0.04	0.56x *P*=0.03	AVYQGPGSSPVKS	47
1C.	*Membrane proteins displaying significantly increased abundance upon IR and/or PI compared to their respective sham group*							
7	5902786	Annexin A3	35/ (36.4)	5.6/ (5.33)	5.8x *P*<0.001	6.2x *P*=0.001	ALLTLADGR	64
							LTFDEYR	
8	Not identified		17/ (?)	4.4/ (?)	qualitative *P*=0.01	qualitative *P*=0.01		
9	547679	Heat shock protein-27	24/ (23.0)	5.4/ (6.12)	3.3x *P*=0.001	2.6x *P*=0.001	RVPFSLLR	110
							LFDQAFGVPR	

(continued)

Spot no.[A]	Accession no.[B]	Protein ID	Mr (kDa) exp/ (thrt)[C]	pI exp/ (thrt)[C]	IR to sham SALINE (Density ratio and P value)[D]	IR to sham MONOHER (Density ratio and P value)[D]	Sequence[E]	LC_MS/MS MASCOT score
10	13959400	Adenylate kinase 1	21/ (21.5)	5.3/ (5.67)	qualitative P=0.007	qualitative P=0.005	IIFVVGGPGSGK	
							YGYTHLSTGDLLR	
11	13959400	Adenylate kinase 1	21/ (21.5)	5.5/ (5.67)	2.8x P=0.03	2.2x P=0.04	IIFVVGGPGSGK	289
							YGYTHLSTGDLLR	
							VDSSNGFLIDGYPR	
							IGQPTLLLYVDAGAETMTQR	
							LETYYNATEPVISFYDKR	
12	Not identified		19/ (?)	5.3/ (?)	qualitative P<0.001	qualitative P=0.007		

A. Numbers refer to the spot numbers given in figure 1 and 4.
B. Protein entry code of the National Center for Biotechnology Information (NCBI): http://ncbi.nlm.nih.gov.
C. Mr and pI exp/thrt: experimental molecular weight and pI from the position on the 2-D gel/ theoretical molecular weight or pI calculated by the "Compute pI/Mw" tool provided by ExPasy: http://us.expasy.org.
D. 'Qualitative': no spot observed in the samples from one group compared to the other/ns: not significant
E. Peptide sequence corresponding to the appropriate peptide mass. Parts of the sequence, determined by LC-MS/MS, could indisputably confirm the peptide.

Identified proteins (or protein spots) that significantly changed in expression level after IR were heat shock protein-20 (spot 1), heterogeneous nuclear ribonucleoprotein K (spot 2), pyruvate dehydrogenase E1-β (spot 3), annexin A3 (spot 4 and spot 7), dual specificity phosphatase-3 (spot 5), catechol-O-methyltransferase (spot 6), heat shock protein-27 (spot 9) and adenylate kinase 1 (spot 10 and spot 11).
For both the cytosolic as well as the membrane fraction, protein spots that were significantly changed in expression level in the IR-saline group compared to the sham-saline group were also significantly changed in expression level in the IR-monoHER group compared to the sham-monoHER group and *vice versa*. In addition for both the cytosolic as well as the membrane fraction, none of the protein spots on the gels differed significantly in expression level between the IR-saline group and the IR-monoHER group.

Translocation of annexin A3
Two-DE analysis showed that the quantity of annexin A3 in the cytosolic fraction was 4 times lower (P=0.003) in the IR-saline group than in the sham-saline group. In contrast, in the membrane fraction of the IR-saline group, the amount of annexin A3 was 5.8 times higher (P=0.001) than in the sham-saline group.
The same phenomenon was observed in the monoHER groups. In the cytosolic fraction, the quantity of annexin A3 was around 6 times lower (P=0.001) in the IR-monoHER group than in the sham-monoHER group. The quantity in the membrane fraction of the IR-monoHER group was around 6 times higher (P=0.001) than in the sham-monoHER group.

Post-translational modification of adenylate kinase-1
Adenylate kinase-1 in the membrane fraction was significantly increased in expression level at two spot locations (spot 10 and spot 11) separated by a pI range of 0.27. This phenomenon was observed in both the IR-saline and the IR-monoHER group.

Discussion

The goal of this study was to test if 7-monohydroxyethylrutoside (monoHER) when administered i.p. one hour before ischaemia has an influence on changes in the cardiac proteome after ischaemia-reperfusion in an *in vivo* mouse model. In this way we hoped to gain insight into the molecular mechanism of action of monoHER during IR. However, we did not find significant differences in expression level of protein spots between the IR-saline and the IR-monoHER group. These results indicate that, contrary to expectations, the sustained protective effects of monoHER visible on histological and functional level [2] were not detected on proteome level by using a technique of 2-D gel electrophoresis combined with mass spectrometry.

In our *in vivo* ischaemia-reperfusion model, twelve protein spots changed significantly in expression level. These proteins can be classified into functional groups being anticoagulant protein (annexin A3), translation- related protein (hnRNP), heat shock proteins (HSP-20 and HSP-27), metabolism-related proteins

(AK-1 and COMT) and miscellaneous (DSP-3). Their potential role in cardiac ischaemia-reperfusion is discussed in chapter 5 (discussion section).
Additionally, two unidentified proteins (spot 8 and spot 12) changed in expression level but could not be characterized by mass spectrometry, probably due to the fact that their abundance fell below the detection limit of the technique.
The significant decrease in abundance of annexin A3 in the cytosolic fraction and the significant increase in the membrane fraction were observed in both the IR-saline group and the IR-monoHER group. Furthermore adenylate kinase-1, a phosphotransfer catalyzing enzyme (chapter 5), was significantly increased at two spot locations in both the IR-saline and the IR-monoHER group. In addition, there were also no other protein spots on the gels specifically affected by monoHER treatment.

Possible explanations for the discrepancy between findings on histological/functional level (chapter 2) and proteome level are three-fold.
Firstly, it is possible that monoHER did not affect changes in protein expression after cardiac ischaemia-reperfusion. This is not very likely in view of the very strong protective effects of monoHER observed on histological and functional level. The proteins that were differentially expressed after cardiac ischaemia-reperfusion can be regarded as being functionally related to the imposed stimulus. Therefore it is surprising that they were not affected by the monoHER treatment, at least at the time point under investigation in the present study.
We chose to study the alterations in protein expression at 3 hours after initiation of reperfusion because we reasoned that this period was necessary for the development of significant alterations in the proteome (f.i. protein synthesis) which could give a clue on the cause of protection of monoHER. However, the present results indicate that this is obviously not the case. The study should be repeated either at an earlier time point (f.i. 20-30 min after IR) with a focus on posttranslational modifications (see below) as well as at a later time point which may facilitate the identifications of other alterations in protein expression that might be influenced by monoHER.
Thirdly the technique we used in this study may not have been able to detect alterations in the proteome specifically triggered by monoHER. For example, we only analyzed proteins within a restricted isoelectric point (pI) range (between 4 and 7) and relatively low molecular weight (below 100 kDa). Additionally analyzing proteins within other pI and molecular weight ranges can resolve this possibility. Furthermore, despite the analytic power of the approach we used in this study, systematic limitations of the approach at the present state of the technology must be taken into consideration. There are certain classes of proteins, such as integral transmembrane proteins, that are difficult to extract and consequently not easily visible on the gel. Other extraction procedures with agents that disrupt membranes to separate these transmembrane proteins can possibly resolve this problem.
Furthermore, the analysis of post-translational modifications like protein phosphorylation and glycosylation [19, 20], oxidation of proteins [21] or the detection of intermolecular protein disulfide formation [22], which might be important in signal transduction, requires a complex repertoire of additional analytical tools [23]. There are also limitations with respect to the dynamic range of proteins that can be displayed on a gel compared with the dynamic range of protein abundance within the cardiac

cells which has been estimated to be as high as 10^7 [24]. This problem increases with sample complexity because high abundant proteins muffle low abundant proteins, like for example transcription factors, on the gel. Therefore the classical approach may fail in the discovery of gene products that are major proteins of particular subcellular compartments, but are minor proteins of the whole crude homogenate.
Although we separately analyzed the cytosolic and membrane fraction, the enrichment of particular subcellular structures as for example mitochondria or nuclei and specifically analyzing their protein constituents provides the opportunity to deal with these problems.

We conclude that by using a technique of 2-D gel electrophoresis combined with mass spectrometry we did not find alterations in the proteome specifically triggered by monoHER after *in vivo* cardiac ischaemia-reperfusion in a mouse model. These results signify that the strong protective effects of monoHER visible at a later time point on histological and functional level were not detected on proteome level at an early time point by using the current techniques. Therefore additional sophisticated tools must be applied to search for such molecular mediators.

References

1. Flaherty JT, Weisfeldt ML. Reperfusion injury. Free Radic Biol Med. 1988; 5: 409.
2. De Celle T, Heeringa P, *et al.* Sustained protective effects of 7-monohydroxyethylrutoside in an in vivo model of cardiac ischemia-reperfusion. Eur J Pharmacol. 2004; 494: 205.
3. Schwertz H, Langin T, *et al.* Two-dimensional analysis of myocardial protein expression following myocardial ischemia and reperfusion in rabbits. Proteomics. 2002; 2: 988.
4. Vanden Hoek TL, Li C, *et al.* Significant levels of oxidants are generated by isolated cardiomyocytes during ischemia prior to reperfusion. J Mol Cell Cardiol. 1997; 29: 2571.
5. Becker LB. New concepts in reactive oxygen species and cardiovascular reperfusion physiology. Cardiovasc Res. 2004; 61: 461.
6. Przyklenk K, Kloner RA. Effect of oxygen-derived free radical scavengers on infarct size following six hours of permanent coronary artery occlusion: salvage or delay of myocyte necrosis? Basic Res Cardiol. 1987; 82: 146.
7. Kevin LG, Camara AK, *et al.* Ischemic preconditioning alters real-time measure of O2 radicals in intact hearts with ischemia and reperfusion. Am J Physiol Heart Circ Physiol. 2003; 284: H566.
8. Duranteau J, Chandel NS, *et al.* Intracellular signaling by reactive oxygen species during hypoxia in cardiomyocytes. J Biol Chem. 1998; 273: 11619.
9. Schroedl C, McClintock DS, *et al.* Hypoxic but not anoxic stabilization of HIF-1alpha requires mitochondrial reactive oxygen species. Am J Physiol Lung Cell Mol Physiol. 2002; 283: L922.
10. Chandel NS, McClintock DS, *et al.* Reactive oxygen species generated at mitochondrial complex III stabilize hypoxia-inducible factor-1alpha during hypoxia: a mechanism of O2 sensing. J Biol Chem. 2000; 275: 25130.
11. Chandel NS, Maltepe E, *et al.* Mitochondrial reactive oxygen species trigger hypoxia-induced transcription. Proc Natl Acad Sci U S A. 1998; 95: 11715.
12. Agani FH, Pichiule P, *et al.* The role of mitochondria in the regulation of hypoxia-inducible factor 1 expression during hypoxia. J Biol Chem. 2000; 275: 35863.
13. Dada LA, Chandel NS, *et al.* Hypoxia-induced endocytosis of Na,K-ATPase in alveolar epithelial cells is mediated by mitochondrial reactive oxygen species and PKC-zeta. J Clin Invest. 2003; 111: 1057.

14. Levraut J, Iwase H, *et al.* Cell death during ischemia: relationship to mitochondrial depolarization and ROS generation. Am J Physiol Heart Circ Physiol. 2003; 284: H549.
15. Kulisz A, Chen N, *et al.* Mitochondrial ROS initiate phosphorylation of p38 MAP kinase during hypoxia in cardiomyocytes. Am J Physiol Lung Cell Mol Physiol. 2002; 282: L1324.
16. Sawicki G, Jugdutt BI. Detection of regional changes in protein levels in the in vivo canine model of acute heart failure following ischemia-reperfusion injury: functional proteomics studies. Proteomics. 2004; 4: 2195.
17. Sakai J, Ishikawa H, *et al.* Proteomic analysis of rat heart in ischemia and ischemia-reperfusion using fluorescence two-dimensional difference gel electrophoresis. Proteomics. 2003; 3: 1318.
18. van Acker SA, Kramer K, *et al.* Monohydroxyethylrutoside as protector against chronic doxorubicin-induced cardiotoxicity. Br J Pharmacol. 1995; 115: 1260.
19. Chu G, Egnaczyk GF, *et al.* Phosphoproteome analysis of cardiomyocytes subjected to beta-adrenergic stimulation: identification and characterization of a cardiac heat shock protein p20. Circ Res. 2004; 94: 184.
20. Whelan SA, Hart GW. Proteomic approaches to analyze the dynamic relationships between nucleocytoplasmic protein glycosylation and phosphorylation. Circ Res. 2003; 93: 1047.
21. Ghezzi P, Bonetto V. Redox proteomics: identification of oxidatively modified proteins. Proteomics. 2003; 3: 1145.
22. Brennan JP, Wait R, *et al.* Detection and mapping of widespread intermolecular protein disulfide formation during cardiac oxidative stress using proteomics with diagonal electrophoresis. J Biol Chem. 2004; 279: 41352.
23. Mann M, Ong SE, *et al.* Analysis of protein phosphorylation using mass spectrometry: deciphering the phosphoproteome. Trends Biotechnol. 2002; 20: 261.
24. Gygi SP, Corthals GL, *et al.* Evaluation of two-dimensional gel electrophoresis-based proteome analysis technology. Proc Natl Acad Sci U S A. 2000; 97: 9390.

Chapter 7

Summary and conclusions

Summary

The first goal of this thesis was to investigate the potential cardioprotective effects of the antioxidant 7-monohydroxyethylrutoside (monoHER) in an *in vivo* mouse model of cardiac ischaemia-reperfusion (IR). The second goal was to determine the early alterations in cardiac protein expression in this IR model in order to delineate the mechanisms of action of monoHER in this setting.

As the *in vivo* mouse model of cardiac IR was the study object of this thesis we compared in **chapter 2** the long-term structural and functional consequences of this myocardial infarction model to the ones induced by permanent ischaemia (PI).
The majority of studies on cardiac IR injury have focused on the short-term consequences of reperfusion. Using myocardial infarct size or neutrophil influx as parameters, the progression of cardiac tissue damage has been described in the time frame of a few hours up to one or a few days after the initiation of reperfusion. The long-term effects of IR injury, in terms of weeks or months, are less well examined in this *in vivo* mouse model. This is, however, a relevant aspect for extrapolation to the clinical setting as it may be that the outcome of interventions that are beneficial shortly after initiation of reperfusion is different when the evaluation takes place at later stages.
In chapter 2 we showed that the long-term structural and functional consequences following cardiac IR are different from those observed after PI. Contractility of the heart was depressed for at least 2 weeks after IR, but was nearly restored after 8 weeks of IR. After cardiac IR, the gross architecture of the ventricular wall was preserved and the wound healing process was characterized by extensive calcification, minor hypertrophy and minor dilatation. In the PI model, the ischaemic area was not calcified, but completely replaced by connective tissue. In addition, the ventricular wall was severely dilated, the remaining myocardial muscle was strongly hypertrophied and loss of cardiac function was permanent.

The potential protective effects of exogenously administered antioxidants on cardiac reperfusion injury have been studied extensively. However, as described in detail in **chapter 1**, the beneficial effects of antioxidant treatment in these models remain controversial and need further clarification. Moreover, most of these studies only investigated potential short-term protective effects after initiation of reperfusion and did not examine sustained protective effects.
In **chapter 3**, we evaluated the cardioprotective effects of the antioxidant flavonoid monoHER in the *in vivo* mouse model of cardiac IR up till two weeks after IR, a time point when wound healing processes are completed. There were three indications that monoHER might act protective against injury in this model. These were: 1/ strong radical scavenging and iron chelating properties of monoHER; 2/ proven protective effects of monoHER against doxorubicin-induced cardiotoxicity *in vivo* in mice; 3/ *in vitro* anti-inflammatory effects of monoHER by reducing neutrophil adhesion.
We showed that monoHER exerted a sustained cardioprotective effect in this *in vivo* mouse model of cardiac IR. This was demonstrated at two time points (24 hours and

2 weeks after IR) by the fact that monoHER significantly reduced myocardial neutrophil influx, infarct size and maintenance of cardiac contractile responses when the heart was stressed with dobutamine and volume loading.
To our knowledge, this was the first time that sustained protective effects (in terms of weeks) of a flavonoid are demonstrated in this cardiac IR model.
The timing, route and dose of monoHER administration in this study (chapter 3) were based on earlier *in vivo* mouse studies in which monoHER protected against doxorubicin-induced cardiotoxicity [1, 2]. In these studies monoHER was administered intraperitoneally one hour before doxorubicin injection.

Obviously, to minimize myocardial damage evoked by chemotherapeutic agents such as doxorubicin it is logical to pre-treat patients with radical scavenging agents such as monoHER. However, when preventing "reperfusion injury", administering an antioxidant as a protective drug before the onset of ischaemia, has less clinical relevance. In addition, recent pharmacokinetic data in mice revealed that following intravenous injection of monoHER maximal myocardial tissue concentrations of the drug were reached almost immediately [3].
Therefore, in **chapter 4** we set out a study to test if monoHER would also be effective when administered intravenously five minutes before reperfusion. Administration of monoHER at this time point neither affected the influx of neutrophils in the injured tissue nor improved stimulated cardiac contractility, 24 hours after reperfusion.
Thus monoHER protects in an *in vivo* mouse model of cardiac IR when administered intraperitoneally one hour before ischaemia but lacks these properties when applied intravenously five minutes before reperfusion.
This discrepancy in results (between chapter 3 and 4) indicates that the time point of monoHER administration is very crucial to obtain cardioprotective effects.
Among the explanations for the lack of a clear pharmacodynamic effect of monoHER in the latter study (chapter 4) are: 1) the potential restriction in myocardial uptake of monoHER in conditions of cardiac IR; 2) the necessity of formation of active metabolites of monoHER; and 3) the possibility that cardioprotective effects are, directly or otherwise indirectly via antioxidant effects, due to interference of monoHER with specific signal transduction pathways during the ischaemic period. Such signal transduction pathways might be associated to the protective mechanism of action of monoHER. As signalling pathways consist of proteins, it is essential to study changes in protein expression or post-translational modifications of proteins to verify this hypothesis.

To search for those, two sets of proteomic studies were performed in which we used a technique of 2-DE combined with mass spectrometry (MS). We studied early (210 min) changes in protein expression because we were primarily interested in finding the reason for the protective effects of monoHER. In addition we were interested in identifying potential new targets for cardioprotection that are beneficial in the first few hours of myocardial infarction. Previous studies showed that by using this technique

of 2-DE and MS it is possible to detect early alterations in the proteome induced by cardiac IR [4-6].
In **chapter 5** we compared protein density changes in the area at risk of the mouse heart following *in vivo* PI and IR. We analyzed cytosolic as well as membrane fractions and found a total of thirty-two protein spots (out of about 600 matched spots) that were differentially expressed. With this technique we were able to find twenty protein spots that were changed in expression level after PI alone, four protein spots that were changed in expression level after IR alone, and eight spots that changed commonly in both models. The results of this study are therefore a source for further studies in which the specific functional relevance of these proteins in models of myocardial infarction can be investigated.
Identified proteins (by MS) could be classified in seven functional groups being the 1/ anticoagulant proteins (Annexin A3 and Annexin A5), 2/ structural proteins (cardiac troponin T, α-tropomyosin and α-myosin heavy chain), 3/ inflammatory-related proteins (serum amyloid P-component precursor), 4/ transcription- and translation-related proteins (Prohibitin and Histidine Triad Nucleotide Binding Protein 1, Heterogeneous Nuclear Ribonucleoprotein K), 5/ heat shock proteins (Heat Shock Protein 20&27), 6/ metabolism-related proteins (Adenylate Kinase 1, Pyruvate Dehydrogenase E1 Component Beta Subunit, Catechol-O-Methyltransferase) and 7/ miscellaneous (dual specificity phosphatase, similar to Zn-alcohol dehydrogenase).
A remarkable finding was the IR specific translocation of annexins (A3 and A5) from the cytosolic to the membrane compartment, a phenomenon that was verified by Western blotting. The fact that this phenomenon occurred after reperfusion only and not after permanent ischaemia suggests a specific related mechanism that triggers translocation of annexins to the membrane fraction during reperfusion. These findings may give new impetus for further studies in relation to annexins and early diagnosis of reperfusion injury in connection with earlier studies from our laboratory [7].
Four proteins were changed in expression level at multiple spot locations, characterized by a difference in isoelectric point. In the case of cardiac troponin T and HSP-20, these changes were also dependent on the model. In addition, one spot for the proteins adenylate kinase 1, cardiac troponin T and HSP-20 was uniquely present in the IR and/or PI and not in the respective sham groups. Further research is necessary to determine the character of possible pathology related post-translational modifications.

A total of twelve protein spots changed significantly in expression level after cardiac IR (**chapter 6**). Ten of these protein spots could be characterized by MS. These were: Heat Shock Protein-20 and Heat Shock Protein 27, Heterogeneous Nuclear Ribonucleoprotein K, Pyruvate Dehydrogenase E1-β, Annexin A3 (at 2 spot locations), Dual Specificity Phosphatase-3, Catechol-O-Methyltransferase, and Adenylate Kinase 1 (at 2 spot locations).
Intraperitoneal administration of monoHER, one hour before ischaemia, did not alter this protein expression profile related to cardiac IR. This means that the proven cardioprotective effects of monoHER as evidenced at a later time point on

histological and functional level were not detected on proteome level at an early time point by using the current techniques.
The discrepancy between these two studies in chapters 3 and 6 may be explained by the possibility: 1/ that monoHER did not affect changes in protein expression after cardiac IR; 2/ this time point was not relevant to detect alterations caused by monoHER; 3/ the technique we used in this study may not have been able to detect alterations in the proteome specifically triggered by monoHER.

Conclusions and implications

The discrepancy in outcome with antioxidant treatment related to cardiac IR
As summarized in the general introduction to this thesis, numerous *in vitro* and *in vivo* studies have examined the role of antioxidant enzymes and less specific antioxidant interventions in reducing cardiac IR injury. The results of these studies are very conflicting since the number of studies in which protective effects were proven was comparable to the number that could not. Furthermore, it is reasonable to assume that numerous studies have been performed, that did not reach the stage of publication, because protective effects of the antioxidant under investigation was disputable or even could not be proven under certain conditions.
Although research on this topic started already in the early eighties, a clear explanation for this discrepancy is, up to now, not known. Among the experimental variables that have been postulated to explain these conflicting results are: 1/ animal species; 2/ general features of the experimental model (e.g. anaesthetized or awake model, open- or closed- chest model); 3/ the presence or absence of critical stenosis; 4/ duration of ischaemia; 5/ duration of reperfusion; 6/ pharmacokinetic considerations; 7/ methodology to quantify infarct size; and 8/ inclusion or omission of measurements to control for baseline predictors of infarct size (e.g. collateral blood flow). However, up to now, there is no study available in literature that really proved that one of these factors or a combination of them is the cause for this discrepancy.
Studies in transgenic mice with altered levels of antioxidant enzymes consistently yield results in support of a detrimental role for reactive oxygen species (ROS) in experimental myocardial IR injury (chapter 1). This means that the lack of effect of these exogenous antioxidants may be (in part) due to a restricted access to the sites of ROS generation. As the capacity of an antioxidant to gain entry to the target tissue and cells and the relevant ROS-producing intracellular compartments or sites is an important condition, this ability needs to be verified. It will not be surprising if therapies fail if they do not successfully enter these compartments.

Pharmacokinetic aspects (time point of delivery)
In addition to this explanation, our study with monoHER revealed that the time point of administration of the antioxidant, to act protective, might be very crucial. MonoHER exerted protective effects when it was administrated one hour before cardiac ischaemia. In contrast, no (protective) effect was found when it was applied intravenously right before reperfusion. This phenomenon has been observed also in the doxorubicin mouse model. MonoHER protected against the cardiotoxicity of

doxorubicin when it was administered one hour before doxorubicin treatment but not when it was applied five minutes before doxorubicin treatment (unpublished observation, Prof. Aalt Bast). The data suggest that this time-dependency may be a specific characteristic of monoHER. Studies with superoxide dismutase [8] and a glutathione analogue [9] in dogs, as well as an α-tocopherol analogue in rats [10] and melatonin in mice [11] demonstrated that the time point of antioxidant administration did not influence the protective capacity of these antioxidants in *in vivo* models of experimental cardiac IR. In addition, studies in which the time point of administration of the antioxidant was shown to be crucial for its protective effect are not available in literature. This means that the observation that the efficacy of antioxidant therapy is dependent on the time point of administration is not a general concept. Further research is therefore necessary to determine this specific mechanism of action of monoHER.

The dominant concept of antioxidant therapy during cardiac IR is that the antioxidant agent reduces the detrimental effects of oxidative stress specifically during the initial phase of reperfusion by scavenging ROS [9, 12]. Recent pharmacokinetic studies with monoHER showed that the peak concentration of monoHER in heart tissue of mice was reached almost immediately after intravenous administration [3]. This implies that also in our current cardiac IR model the highest cardiac tissue levels of monoHER, when administered intravenously, right before reperfusion, are reached very early (within one minute) after the initiation of reperfusion.
Since this corresponds with the phase at which the production of ROS is the highest [9, 13], it was very unexpected that monoHER treatment lacked any beneficial effects when administered right before reperfusion. At the moment we do not have a clear explanation for this. Analyzing the pharmacokinetics of monoHER specifically in our cardiac IR model and determining the correlation between cardiac tissue levels of monoHER and ROS during reperfusion gives the opportunity to test if the dominant concept (see above) applies for monoHER too. If this is not the case, a logic explanation may be that the antioxidant monoHER protects against detrimental effects during the period of ischaemia and not during the initial phase of reperfusion. In this case, it is also evident that there are doubts about the truth of this dominant concept that ROS act detrimental initially after reperfusion (see above).

Despite the dominant concept (ROS are produced primarily with the reintroduction of oxygen following reperfusion), several investigators have observed ROS generation during ischaemia [14]. In addition, the fact that our studies showed that monoHER acts protective when applied before ischaemia but not when applied right before reperfusion also indirectly indicate possible detrimental effects of ROS during the experimental ischaemic phase. In our view it is therefore essential to further determine to which extent and at which stage ROS act detrimental during cardiac IR injury in order to deliver the agents in a time-sensitive fashion.

Clinical implications
Several clinical studies have evaluated the influence of antioxidants alone or in various combinations on IR injury in patients undergoing reperfusion therapy after myocardial infarction. Despite many research efforts and a wide availability of antioxidant agents,

there is at the moment no clinical evidence for the routine use of antioxidants in the clinical setting of cardiac IR. With respect to the clinical relevance it is evident that antioxidants are administered right before reperfusion therapy. In relation to our findings with monoHER this pleads in favour of a more thorough and critical analysis of a specific antioxidant at several time points of administration in an experimental setting before specific clinical trials should be done. However, the fact that some antioxidants act protective in animal models when applied right before or during reperfusion and not in a clinical setting of cardiac IR makes an explanation even more complex. For example the free radical scavenger recombinant h-SOD when administered before [12] or at the moment of reperfusion [15] acted protective in an *in vivo* dog model of cardiac IR but not in patients who underwent PTCA [16].
Myocardial infarction related to ischaemia-reperfusion is not a homogenous insult as shown by the patchy distribution of granulation and scar tissue. It is possible that some antioxidant compounds have failed because they protect the most affected regions of the area at risk but also contributed to additional injury in the adjoining tissue, as the border zones. This nearby tissue may loose preconditioning effects by the (non-specific) addition of antioxidants that scavenge ROS and these antioxidants are therefore interfering in adaptive natural cardioprotection.

Pharmacodynamic aspects
In our opinion it is necessary to define in more detail the patho-mechanism specifically related to cardiac repefusion injury and to determine the influence of ROS and antioxidants on this mechanism. This underlines the need for studies in which the analysis of patho-mechanisms of permanent ischaemia and IR is compared next to each other in one study in order to determine targets specifically related to reperfusion injury.
The comparison of the effects of cardiac IR and permanent ischaemia (PI) on the proteome can provide a first view at this mechanism. Proteomic studies of human heart tissue are, however, complicated by factors such as small size of sample, availability, disease state, tissue heterogeneity, genetic variability, medical history, and therapeutic interventions [17].
Our proteomic study was set-up in order to resolve part of this mechanism of action of monoHER in an *in vivo* mouse model of cardiac IR.
Our study demonstrates that *in vivo* mouse myocardial infarction models are suitable to study *in vivo* changes in the proteome early after induction of PI or IR.
We were able to identify proteins that were changed in expression level specifically after IR or PI and proteins that were commonly changed in level in both models.
Three proteins, Annexin A3&A5 and dual specificity phosphatase were significantly changed in expression level after cardiac IR but not after PI. This means that the changes in expression level of these proteins are specifically triggered by the process of cardiac IR. Their functional significance needs to be investigated in order to determine their impact on IR injury or the contribution to its mechanism.
Twenty protein spots were significantly changed in expression level after PI alone and are therefore potential targets for further study specifically on ischaemic injury.

However, we showed that the infarct size is almost 4 times greater after cardiac PI compared to IR (chapter 2). This means that the affected area is possibly bigger after PI and alterations in proteome are consequently easier to intercept. To overcome this problem, more specific techniques, as for instance laser capture micro-dissection, will be necessary to select more specifically the affected area for analysis. This is mainly true for the IR model as the infarct is patchy distributed in the area at risk.
In addition it is difficult to distinguish between detrimental effects triggered by the ischaemic period, the reperfusion period or the combination ischaemia and reperfusion. Studying the changes in protein expression specifically triggered by IR with different time-combinations of ischaemia and reperfusion can reduce part of this problem.
The protective effects of monoHER visible on histological and functional level were not detected on proteome level by using a technique of 2-DE combined with mass spectrometry.
This implies that more specific tools as for example subcellular proteomics (chapter 1), the detection of oxidation of proteins [18] or of intermolecular protein disulfide formation [19] are necessary to determine changes in the proteome due to oxidative stress in order to determine parts of the mechanism of IR injury.
We conclude that the specific alterations in protein expression that take place after cardiac ischaemia-reperfusion and permanent ischaemia may stimulate the search for new tools to resolve specific mechanisms and to find specific targets for therapy for these pathologies.

References

1. van Acker FA, van Acker SA, *et al.* 7-monohydroxyethylrutoside protects against chronic doxorubicin-induced cardiotoxicity when administered only once per week. Clin Cancer Res. 2000; 6: 1337.
2. van Acker SA, Kramer K, *et al.* Monohydroxyethylrutoside as protector against chronic doxorubicin-induced cardiotoxicity. Br J Pharmacol. 1995; 115: 1260.
3. Abou El Hassan MA, Kedde MA, *et al.* Bioavailability and pharmacokinetics of the cardioprotecting flavonoid 7-monohydroxyethylrutoside in mice. Cancer Chemother Pharmacol. 2003; 52: 371.
4. Sakai J, Ishikawa H, *et al.* Proteomic analysis of rat heart in ischemia and ischemia-reperfusion using fluorescence two-dimensional difference gel electrophoresis. Proteomics. 2003; 3: 1318.
5. Sawicki G, Jugdutt BI. Detection of regional changes in protein levels in the in vivo canine model of acute heart failure following ischemia-reperfusion injury: functional proteomics studies. Proteomics. 2004; 4: 2195.
6. Schwertz H, Langin T, *et al.* Two-dimensional analysis of myocardial protein expression following myocardial ischemia and reperfusion in rabbits. Proteomics. 2002; 2: 988.
7. Dumont EA, Reutelingsperger CP, *et al.* Real-time imaging of apoptotic cell-membrane changes at the single-cell level in the beating murine heart. Nat Med. 2001; 7: 1352.
8. Tamura Y, Chi LG, *et al.* Superoxide dismutase conjugated to polyethylene glycol provides sustained protection against myocardial ischemia/reperfusion injury in canine heart. Circ Res. 1988; 63: 944.

9. Bolli R, Jeroudi MO, *et al.* Marked reduction of free radical generation and contractile dysfunction by antioxidant therapy begun at the time of reperfusion. Evidence that myocardial "stunning" is a manifestation of reperfusion injury. Circ Res. 1989; 65: 607.
10. Petty MA, Grisar JM, *et al.* Protective effects of an alpha-tocopherol analogue against myocardial reperfusion injury in rats. Eur J Pharmacol. 1992; 210: 85.
11. Chen Z, Chua CC, *et al.* Protective effect of melatonin on myocardial infarction. Am J Physiol Heart Circ Physiol. 2003; 284: H1618.
12. Jolly SR, Kane WJ, *et al.* Canine myocardial reperfusion injury. Its reduction by the combined administration of superoxide dismutase and catalase. Circ Res. 1984; 54: 277.
13. Mitsos SE, Fantone JC, *et al.* Canine myocardial reperfusion injury: protection by a free radical scavenger, N-2-mercaptopropionyl glycine. J Cardiovasc Pharmacol. 1986; 8: 978.
14. Becker LB. New concepts in reactive oxygen species and cardiovascular reperfusion physiology. Cardiovasc Res. 2004; 61: 461.
15. Ambrosio G, Becker LC, *et al.* Reduction in experimental infarct size by recombinant human superoxide dismutase: insights into the pathophysiology of reperfusion injury. Circulation. 1986; 74: 1424.
16. Flaherty JT, Pitt B, *et al.* Recombinant human superoxide dismutase (h-SOD) fails to improve recovery of ventricular function in patients undergoing coronary angioplasty for acute myocardial infarction. Circulation. 1994; 89: 1982.
17. McGregor E, Dunn MJ. Proteomics of heart disease. Hum Mol Genet. 2003; 12 Spec No 2: R135.
18. Ghezzi P, Bonetto V. Redox proteomics: identification of oxidatively modified proteins. Proteomics. 2003; 3: 1145.
19. Brennan JP, Wait R, *et al.* Detection and mapping of widespread intermolecular protein disulfide formation during cardiac oxidative stress using proteomics with diagonal electrophoresis. J Biol Chem. 2004; 279: 41352.

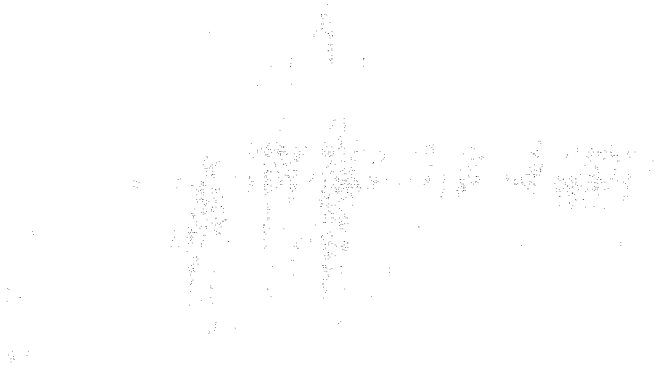

Chapter 7

Samenvatting

Het eerste doel van dit proefschrift was om in een *in vivo* muizenmodel van cardiale ischemie-reperfusie (IR) na te gaan of de antioxidante stof 7-monohydroxyethylrutoside (monoHER) een beschermende werking heeft op het muizenhart. Om het werkingsmechanisme van monoHER in dit IR model te analyseren, was het tweede doel de vroege veranderingen in proteïneëxpressie in het muizenhart te onderzoeken bij dit model.

Het *in vivo* muizenmodel van cardiale IR is het studieobject van deze thesis. Daarom vergeleken wij in **hoofdstuk 2** de structurele en functionele effecten van cardiale IR op het muizenhart, met deze geïnduceerd door permanente ischemie (PI).
Het merendeel van de studies met betrekking tot dit model hebben het accent gelegd op de kortetermijneffecten van reperfusie. Door gebruik te maken van parameters als oppervlakte van het infarct en neutrofielinfiltratie werd de vooruitgang van weefselschade beschreven binnen een tijdsbestek van een paar uren tot een paar dagen na de inductie van reperfusie. De langetermijneffecten van IR-schade, in termen van weken of maanden, werden slechts in beperkt mate onderzocht in dit *in vivo* muizenmodel. Echter, voor extrapolatie naar een klinische situatie is het nagaan van de effecten op lange termijn zeer relevant, aangezien deze kunnen verschillen van de effecten op korte termijn.
In hoofdstuk 2 toonden we aan dat de structurele en functionele effecten van cardiale IR op lange termijn, verschillen van deze bij cardiale PI. De contractiliteit van het hart was aanzienlijk verminderd gedurende minstens 2 weken na IR, maar was min of meer hersteld 8 weken na IR. Na cardiale IR was de algemene architectuur van de wand van het linker ventrikel intact gebleven en was het proces van wondheling gekarakteriseerd door uitgebreide calcificatie, beperkte hypertrofie en beperkte dilatatie.
In het PI model was de ischemische zone niet gecalcificeerd, maar volledig vervangen door bindweefsel. Bijkomend was het linker ventrikel, ten gevolge van PI, sterk gedilateerd, het resterende spierweefsel sterk gehypertrofieerd en het verlies van de hartfunctie permanent.

Het potentieel beschermend effect van exogeen toegediende antioxidanten op cardiale reperfusieschade zijn al uitgebreid bestudeerd. Echter, zoals in detail beschreven in hoofdstuk 1, blijken de effecten van behandeling met antioxidanten in deze modellen controversieel en moeten deze verder uitgeklaard worden. Bovendien, de meeste van deze studies hebben enkel kortetermijneffecten en geen langetermijneffecten van IR bestudeerd.
In **hoofdstuk 3** hebben we de beschermende werking van de antioxidante stof monoHER op het hart, in het *in vivo* muizenmodel van cardiale IR, geëvalueerd. Dit tot 2 weken na IR, het tijdstip waarop het wondhelingsproces vervolledigd is.
Er zijn drie redenen waarom we voorop stelden dat monoHER mogelijk beschermend werkt in dit cardiaal IR model. Deze zijn: 1/ sterke radicaal opvangende en ijzer-bindende eigenschappen van monoHER; 2/ de aangetoonde beschermende werking van monoHER tegen de cardiotoxiciteit geïnduceerd door doxorubicine; 3/ *in vitro* anti-inflammatoire effecten van monoHER door een vermindering van de neutrofieladhesie.

We toonden aan dat monoHER blijvende beschermende effecten heeft in dit *in vivo* muizenmodel van cardiale IR. We hebben op 2 tijdstippen (24 uur en 2 weken na IR) aangetoond dat een behandeling met monoHER de infiltratie van neutrofielen vermindert, de oppervlakte van het infarct reduceert en bijkomend zorgt voor een behoud van de contractiele eigenschappen van het hart bij zowel stimulatie door dobutamine als door volumebelasting.
Voor zover we weten is deze studie de eerste die blijvende beschermende effecten aantoont van een flavonoïd in dit muizenmodel van cardiale IR.
Het tijdstip, de route van toediening en de dosis van monoHER waar in deze studie (hoofdstuk 3) voor gekozen werd, zijn gebaseerd op voorgaande studies in dewelke aangetoond werd dat monoHER een beschermend effect heeft in het model van doxorubicine geïnduceerde cardiotoxiciteit [1, 2]. In deze studies werd monoHER intra-peritoneaal, één uur voor doxorubicine injectie, toegediend.

Om de oxidatieve schade op het hart, veroorzaakt door een chemotherapeutisch middel zoals doxorubicine, te verminderen, is het logisch om patiënten vooraf te behandelen met een antioxidante stof als monoHER. Echter, om "reperfusieschade" te verminderen is het toedienen van een antioxidante stof, vóór de ischemische fase, vanuit klinisch oogpunt, niet relevant. Bovendien tonen recente farmacokinetische studies in muizen aan dat de maximale weefselconcentratie van monoHER bijna onmiddellijk na intraveneuze toediening bereikt wordt [3].
In **hoofdstuk 4** onderzochten we daarom of monoHER tevens effectief was wanneer het intraveneus, vijf minuten vóór reperfusie, toegediend werd. Toediening van monoHER beïnvloedde de infiltratie van neutrofielen in het hartweefsel, noch had het een beschermend effect op de cardiale contractiliteit, 24 uur na reperfusie.
MonoHER heeft dus een beschermende werking in het *in vivo* muizenmodel van cardiale IR wanneer het intraperitoneaal, één uur vóór ischemie toegediend wordt, maar niet wanneer het intraveneus, vijf minuten vóór reperfusie toegediend wordt.
Deze discrepantie in resultaten (tussen hoofdstuk 3 en 4) toont aan dat het tijdstip van monoHER toediening zeer cruciaal is om een zijn beschermend effect te realiseren.
Mogelijke verklaringen voor het ontbreken van een farmacodynamisch effect van monoHER in deze laatste studie (hoofdstuk 4) zijn: 1/ de mogelijke beperking in de opname van monoHER door het hartweefsel in het model van cardiale IR; 2/ de noodzaak voor de vorming van actieve metabolieten van monoHER; en 3/ de kans dat beschermende effecten, enerzijds direct of anderzijds indirect via antioxidante effecten, te wijten zijn aan een wisselwerking van monoHER met specifieke signaaltransductiecascades gedurende de periode van ischemie. Deze signaaltransductiecascades zouden kunnen geassocieerd zijn aan de beschermende werking van monoHER.
Aangezien signaaltransductiecascades opgebouwd zijn uit proteïnen is het essentieel om, ten einde deze hypothese te verifiëren, veranderingen in proteïneëxpressie of post-translationele modificaties van proteïnen te bestuderen.

Daarom werden 2 reeksen 'proteomics' studies uitgevoerd d.m.v. de techniek van 2-D gelelectroforese gecombineerd met massaspectrometrie (MS) voor de karakterisatie van de proteïnen.
Aangezien we in eerste instantie geïnteresseerd waren in de oorzaak van de beschermende werking van monoHER, bestudeerden we vroege (na 210 minuten) veranderingen in proteïneëxpressie. Bijkomend waren we geïnteresseerd in het identificeren van potentieel onbekende 'protein targets' die een invloed hebben in de vroege fase na het ontstaan van een hartinfarct. Voorgaande studies van andere laboratoria toonden aan dat deze techniek in staat is om vroege veranderingen in het proteoom, geïnduceerd door cardiale IR, te detecteren [4-6].
In **hoofdstuk 5** vergeleken we de veranderingen in proteïnedensiteit in de 'area at risk' van het muizenhart bij *in vivo* PI en IR. We analyseerden zowel cytosolische als membraanfracties en vonden een totaal van 32 proteïnespots (uit ongeveer 600 'matched' spots) die differentieel tot expressie kwamen.
Met deze techniek waren we in staat om 20 proteïnespots te bepalen die enkel na PI veranderden in densiteit, 4 proteïnespots die enkel na IR veranderden in densiteit en tenslotte 8 proteïnespots die gemeenschappelijk in beide modellen veranderden in densiteit. De resultaten van deze studie zijn daarom een basis voor verdere studies in dewelke de specifieke functionele relevantie van deze proteïnen in modellen van hartinfarct onderzocht kunnen worden.
De geïdentificeerde proteïnen (door MS) kunnen worden geclassificeerd in zeven functionele groepen, met name: 1/ anticoagulante proteïnen (Annexin A3&A5), 2/ structurele proteïnen (cardiac troponin T, α-tropomyosin and α-myosin heavy chain), 3/ inflammatoir-gerelateerde proteïnen (serum amyloid P-component precursor), 4/ transcriptie- en translatie- gerelateerde proteïnen (Prohibitin and Histidine Triad Nucleotide Binding Protein 1, Heterogeneous Nuclear Ribonucleoprotein K), 5/ heat shock proteïnen (Heat Shock Protein 20 en Heat Shock Protein 27), 6/ metabolisme-gerelateerde proteïnen (Adenylate Kinase 1, Pyruvate Dehydrogenase E1 Component Beta Subunit, Catechol-O-Methyltransferase) en 7/ overige (dual specificity phosphatase, similar to Zn-alcohol dehydrogenase).
Een opmerkelijke bevinding was de translocatie van annexines (A3 en A5) van het cytosolische naar het membranaire celcompartiment, tijdens cardiale IR. Een bevinding die tevens bevestigd werd d.m.v. 'Western blotting'. Het feit dat dit fenomeen enkel optreedt na reperfusie en niet na permanente ischemie suggereert een specifiek mechanisme dat de translocatie van annexines induceert gedurende reperfusie. Deze bevindingen zijn een bijkomende stimulans voor verdere studies in relatie tot annexines en de vroege diagnose van reperfusieschade met betrekking tot voorgaande studies in ons laboratorium [7].
Vier proteïnen waren op meerdere spotlocaties veranderd in expressieniveau, gekarakteriseerd door een verschil in isoelectrisch punt. In het geval van troponine T en HSP-20 waren deze veranderingen ook afhankelijk van het model. Bijkomend, één spot voor de proteïnen adenylate kinase 1, troponine T en HSP-20 was uniek aanwezig in de IR en/of de PI groep en niet in de respectievelijke sham groepen. Voortgezet onderzoek is nodig voor het bepalen van pathologie gerelateerde post-translationele modificaties.

Een totaal van 12 proteïnespots veranderde in expressieniveau na cardiale IR (**hoofdstuk 6**). Tien van deze proteïnespots konden gekarakteriseerd worden met MS. Deze waren: Heat Shock Proteïne 20 en Heat Shock Proteïne 27, Heterogeneous Nuclear Ribonucleoprotein K, Pyruvate Dehydrogenase E1-β, Annexine A3 (op 2 spotlocaties), Dual Specificity Phosphatase-3, Catechol-O-Methyltransferase, and Adenylate Kinase 1 (op 2 spotlocaties).
De intraperitoneale toediening van monoHER, één uur vóór ischemie, had geen invloed op het profiel van proteïneëxpressie gerelateerd aan cardiale IR. Dit betekent dat de beschermende effecten van monoHER op lange-termijn, die aangetoond werden op histologisch en functioneel niveau, niet geassocieerd waren met detecteerbare vroege veranderingen in het proteoom, nagegaan met 2-D gel electroforese. Mogelijke verklaringen voor de discrepantie in resultaten tussen beide studies in hoofdstuk 3 en 6 zijn: 1/ monoHER heeft geen invloed op de veranderingen in proteïneëxpressie na cardiale IR; 2/ het gekozen tijdstip is niet relevant voor het detecteren van veranderingen in het proteoom veroorzaakt door monoHER; 3/ de techniek die we gebruikt hebben was niet in staat om veranderingen in het proteoom, specifiek veroorzaakt door monoHER, aan te tonen.
We concluderen dat de specifieke veranderingen in proteineëxpresssie die plaatsvinden na cardiale ischemie-reperfusie en permanente ischemie de zoektocht stimuleren naar middelen voor het ontrafelen van specifieke mechanismen en het vinden van specifieke 'targets' die als therapie kunnen gebruikt worden.

Referenties

1. van Acker FA, van Acker SA, *et al.* 7-monohydroxyethylrutoside protects against chronic doxorubicin-induced cardiotoxicity when administered only once per week. Clin Cancer Res. 2000; 6: 1337.
2. van Acker SA, Kramer K, *et al.* Monohydroxyethylrutoside as protector against chronic doxorubicin-induced cardiotoxicity. Br J Pharmacol. 1995; 115: 1260.
3. Abou El Hassan MA, Kedde MA, *et al.* Bioavailability and pharmacokinetics of the cardioprotecting flavonoid 7-monohydroxyethylrutoside in mice. Cancer Chemother Pharmacol. 2003; 52: 371.
4. Sakai J, Ishikawa H, *et al.* Proteomic analysis of rat heart in ischemia and ischemia-reperfusion using fluorescence two-dimensional difference gel electrophoresis. Proteomics. 2003; 3: 1318.
5. Sawicki G, Jugdutt BI. Detection of regional changes in protein levels in the in vivo canine model of acute heart failure following ischemia-reperfusion injury: functional proteomics studies. Proteomics. 2004; 4: 2195.
6. Schwertz H, Langin T, *et al.* Two-dimensional analysis of myocardial protein expression following myocardial ischemia and reperfusion in rabbits. Proteomics. 2002; 2: 988.
7. Dumont EA, Reutelingsperger CP, *et al.* Real-time imaging of apoptotic cell-membrane changes at the single-cell level in the beating murine heart. Nat Med. 2001; 7: 135.

Dankwoord

De charme van promoveren is volhouden, lopen op de lijn tussen pressie en passie, tussen doorzetten en toegeven, tussen de juiste en de verkeerde beslissingen, tussen succes en teleurstellingen en het feit dat je daarin niet alleen staat. Tegen iedereen die ik tijdens mijn doctoraat heb mogen ervaren als een steun en hulp zal ik wel eens één of meerdere malen een 'bedankt' hebben gezegd. Weet dan dat dit oprecht en welgemeend was, ook als je je naam in de rest van dit dankwoord niet tegenkomt.

Allereerst wil ik natuurlijk mijn promotor Prof. Jos Smits en co-promotor dr. Ben Janssen bedanken. Jos, ik kan mij nog herinneren dat ik u in mijn eerste werkweek op Farmacologie & Toxicologie, als pas afgestudeerde student uit België, aansprak met Professor. Onmiddellijk wees u mij terecht dat voor mij de aanspreektitel niet Professor Smits was, maar wel Jos. Deze gezellige en vriendschappelijke sfeer met u en de andere collega's heb ik tot op het einde van mijn promotieschap mogen ervaren. Ik wil u bedanken voor het vertrouwen en de kans die u mij gaf om, in overleg, aan mijn eigen onderzoekswegen te bouwen. Jos, bedankt voor alle adviezen, boeiende discussies en hulp bij oa. het schrijven van de artikels en mijn proefschrift.
Ben, mijn directe en dagelijkse begeleider. Jou heb ik mogen ervaren als een enthousiast, betrokken en inspiratievol begeleider. Met jou had ik steeds een zeer open bespreking over oa. de keuze van de te volgen onderzoeksweg, de bepaling van de beste onderzoeksstrategie en het verwoorden van de discussies bij de artikels. In mijn enthousiasme, ambitie en overtuiging kon dit overleg er dan ook soms heftig aan toe gaan. Maar, ik ben er zeker van dat we samen de juiste beslissingen genomen hebben en dat je tevreden bent met het resultaat. Hartelijk bedankt voor alles!

Prof. Aalt Bast, Prof. Wim van der Vijgh, Prof. Jo De Mey en Prof. Harry Struijcker-Boudier wil ik tevens bedanken. Aalt, dankzij u kreeg ik de kans om monoHER te testen op het model van cardiale ischemie-reperfusie, wat de basis vormde van mijn eerste artikel. Prof. van der Vijgh, bedankt voor het kritisch nalezen van het monoHER artikel. Jo, spijtig dat het model van darm ischemie-reperfusie bij de muis niet consistent was, anders was ik ervan overtuigd dat, samenwerking met u, geleid had tot een gemeenschappelijk artikel. Uw adviezen waren waardevol. Harry, met u had ik een interessant gesprek over de post-doc mogelijkheden na mijn AIO-schap.

De leden van de beoordelingscommissie onder leiding van Prof. dr. E. Mariman, die mijn proefschrift beoordeeld hebben, wil ik hartelijk bedanken voor de tijd die ze geïnvesteerd hebben in het lezen van mijn proefschrift.

Mijn oprechte dank gaat uit naar de mensen van het dierenlab. Jacques, Agnieszka, Peter Leenders, Helma en Nicole. Van jullie heb ik de techniek geleerd om muizen en ratten op de correcte manier te opereren. Bedankt hiervoor, voor de hulp en de prettige sfeer die er meestal op het lab heerste. Peter Lijnen, Gregorio, Ger en de andere (ex-)analisten wil ik bedanken voor de hulp, de tips en de gezelligheid.

De mensen van het CPV wil ik bedanken voor het goed verzorgen van de proefdieren.

Ik wil de U(H)D-ers van Farmaco/Toxico bedanken voor de adviezen en de discussies. Rob Hermans wil ik hierbij nogmaals bedanken voor zijn doordachte adviezen en steun bij onze vele gesprekken (meestal in de late avonduurtjes op het

lab). Alle AIOs en post-docs wil ik tevens bedanken voor de gezellige babbel en het meeleven. Verder nog veel succes!

Els, Mia en Marielle van het secretariaat Farmaco/Toxico wil ik bedanken voor de onmisbare en sympathieke assistentie bij alle administratieve activiteiten.

Peter Heeringa van het laboratorium voor Experimentele Immunologie en Bart de Vries van het laboratorium voor Experimentele Heelkunde wil ik hartelijk bedanken voor hun hulp en adviezen bij mijn eerste project met monoHER. Peter, jij bracht mij in contact met dr. J. Schanstra. Joost, met een beetje meer geluk was het Marie-Curie project aanvaard geworden. Toch bedankt voor de kans die je me bood.

De mensen op het laboratorium voor Pathologie wil ik hartelijk bedanken. Hier heb ik vele weken, weekeinden, avond en zelfs nachtelijke uurtjes gesleten bij het uitvoeren van de proteomics experimenten. Ik wens Prof. dr. Mat Daemen te bedanken voor het mij ter beschikking stellen van het excellente materiaal voor het uitvoeren van deze experimenten. Marjo, Sylvia en Moniek jullie hebben mij op een efficiënte manier deze techniek aangeleerd en waren steeds bereid mij hierbij te helpen. Kitty, bedankt voor het verbeteren van de Engelse schrijfstijl van mijn publicaties. Jack, bedankt voor al jouw deskundige adviezen i.v.m histologie. De analisten wil ik bedanken voor de tips.

Het Maastrichts Proteomics platform wil ik bedanken voor het ter beschikking stellen van het materiaal en de adviezen.

Prof. dr. Bart Devreese, Prof dr. Jos Van Beeumen en Frank Vanrobaeys van de Universiteit Gent wil ik bedanken voor het uitvoeren van de massaspectrometrische bepalingen. Jullie deskundige adviezen bij mijn proteomics experimenten, schrijven van het artikel en beantwoorden van de vragen van de reviewers waren essentieel. Kelly Tilleman, bedankt voor het mij wegwijs maken in PDQuest en andere proteomics tips.

Ik wil mijn collega's bij Pfizer bedanken voor de kansen die ze mij bieden, voor de gezellige sfeer en voor de financiële steun voor de drukkosten van dit boekje. Bruno, bedankt voor het advies bij de lay-out en het ontwerpen van de cover van dit boekje.

Mijn paranimfen, Tom en Henny, jullie ben ik alvast wat verschuldigd nu jullie in het 'uur van de waarheid' naast mij willen staan. Tom, als broer leef jij steeds met mij mee. Ik ben fier op jou als bekwame kinesitherapeut en goede vader. Henny, jij hebt de Bourgondische keuken in Maastricht geïntroduceerd. Jouw spaghettisaus is nog steeds mijn stokpaardje.

Ik wil de mensen bedanken die mij het nauwst aan het hart liggen en waar ik steeds gehoor vind. Kaat, Siebe, Emma, mijn petekind Wout, mijn meter en de andere familieleden. Wim V, Wim VV, Steve en Els, Filip, Youri, Willem en Magali, Leo en Josian. Jan zou fier zijn! Linda bedankt voor de steun, het geduld, de leuke momenten en zoveel meer.
Mijn ouders bedank ik voor alle kansen die ze mij gaven en die steeds mijn grootste supporters zullen zijn. Jullie hebben mij in al mijn beslissingen gesteund en mij steeds met alle mogelijke middelen geholpen. Jullie weten dat ik dat nooit zal vergeten en dat ik jullie ontzettend dankbaar ben voor alles.

Curriculum vitae

The author of this thesis was born on May 16th, 1974 in Asse, Belgium. He attended high school, with natural science as main subject, at the Sint-Jozefsinstituut in Ternat, Belgium from 1986 to 1992. In October 1992 he started studying Master in Physical Therapy at the Faculty of Medicine at the Free University of Brussels, Belgium. The last year of this study he worked on a thesis entitled: "Comparative Study of the Registration of Spine Movements Measured with a Back Tracker System® and an Inclinometer" under the supervision of Prof. dr. P. Van Roy, at the Laboratory of Experimental Anatomy. He obtained his Master degree in Physical Therapy July 5th, 1996. In October 1996 he started studying Master in Biochemistry at the Faculty of Science at the University of Ghent. The last year of his biochemical training he worked on a thesis entitled "Gene Characterization and Overexpression Analysis of Cytochrome b-558 of the Purple Bacterium *Ectothiorhodospira vacuolata*", under the supervision of Prof. dr. J. Van Beeumen at the Laboratory of Protein Biochemistry and Protein Engineering. He obtained his Master degree in Biochemistry on July 7th, 1999. In November 1999 he moved to Maastricht, The Netherlands where he was a PhD. student at the Laboratory of Pharmacology & Toxicology (head Prof. dr. J. Smits) until November 2004. During this period the work that is contained in this thesis was accomplished under the supervision of dr. Ben Janssen and Prof. dr. Jos Smits on a project entitled "Experimental Myocardial Infarction: A Proteomics Point of View". Since April 2005 he has been working at Pfizer (in Brussels) at the Medical Department as Medical Advisor/Medinfo.

List of publications

Abstracts

Ben JA Janssen, Tijl De Celle, Ulf Gerhardt, Jos FM Smits; Control of Blood Pressure and Heart Rate after Myocardial Infarction in Mice; Hypertension, 2000; 36:4, 655

Ben JA Janssen, Tijl De Celle, Jos FM Smits:
Impaired Pressor Response to L-NAME in Mice with Heart Failure is due to Sympathetic Hypo responsiveness; The Faseb Journal, 2001

Tijl De Celle, Peter Leenders, Jos Smits, Ben Janssen; Effects of Fluoxetine on Cardiac Function after Myocardial Infarction in Mice; The Faseb Journal, 2001

Tijl De Celle, Peter Heeringa, Aalt Bast, Jos Smits, Ben Janssen; Effects of the Antioxidant monoHER on the Neutrophil Influx after Myocardial Ischemia-Reperfusion in Mice; Nederlandse Farmacologiedagen, 2002

Tijl De Celle, Peter Heeringa, W. Matthijs Blankesteijn, Aalt Bast, Jos Smits, Ben Janssen; 7-monohydroxyethylrutoside, a Semisynthetic Flavonoid, Prevents Deterioration of Cardiac Function in a Mouse Model of Myocardial Ischemia-Reperfusion; The Faseb Journal, 2003 and Hypertension, 2002, Vol. 40 (No 4): p 575

Book chapter

Ben Janssen, Tijl De Celle, Jos Paquay, Jos Smits and Matthijs Blankesteijn
Structural and Functional Adaptations of the Heart after Coronary Artery Ligation in the Mouse;The Physiological Genomics of the Critically Ill Mouse. Edited by Can Ince; Basic Science for the Cardiologist; Kluwer Academic Publishers Boston/Dordrecht/London; Chapter 16, page 211-224, 2003

Articles

Tijl De Celle, Peter Heeringa, Agnieska Strzelecka, Aalt Bast, Jos Smits, Ben Janssen; Sustained Protective Effects of 7- Monohydroxyethylrutoside in an *in vivo* model of Cardiac Ischemia-Reperfusion; European Journal of Pharmacology; 2004, 494(2-3): 205-212

Tijl De Celle, Jack P. Cleutjens, W. Matthijs Blankesteijn, Jacques J. Debets, Jos F. Smits & Ben J. Janssen; Long- term Structural and Functional Consequences of Cardiac Ischemia/Reperfusion Injury *in vivo* in Mice; Experimental Physiology; 2004, 89(5): 605-615

Tijl De Celle, Frank Vanrobaeys, Peter Lijnen, Matthijs Blankesteijn, Jozef Van Beeumen, Bart Devreese, Jos Smits, Ben Janssen; Alterations in Mouse Myocardial; Proteome after *in vivo* Myocardial Infarction: Ischaemia versus Ischaemia-reperfusion; Experimental Physiology; 2005,

Ben J.A. Janssen, Tijl De Celle, Jacques J.M. Debets, Agnieszka E. Brouns, Michael F. Callahan and Thomas L. Smith; Effects of Anesthetics on Systemic Hemodynamics in Mice; Am. J. Physiol. Heart Circ. Physiol. 2004 Oct;287(4):H1618-24

Jos B.G. Paquay, Tijl De Celle, Gregorio E. Fazzi, Jack P.M. Cleutjens, Hans Duimel, Ben J.A. Janssen, Jo G.R. De Mey, Jos F.M. Smits and W. Matthijs Blankesteijn; Inverse Relation between Contractile Properties and Dilatation of Myocardial Infarct Tissue (in preparation)